Investigating ineffective erythropoiesis in sickle cell disease and its impact on the erythroid niche

Auria Godard

Université Paris Cité

Université Paris Cité

École doctorale Bio Sorbonne Paris Cité – ED 562

UMR 7268 Anthropologie bio-culturelle, droit, éthique et santé

Investigating ineffective erythropoiesis in sickle cell disease and its impact on the erythroid niche

Par Auria GODARD

Thèse de doctorat de Physiologie et Physiopathologie

Dirigée par Dr. Wassim EL NEMER

Présentée et soutenue publiquement à Marseille le 20 décembre 2023

Devant un jury composé de :

Dr. Wassim EL NEMER, DR, Université d'Aix Marseille	**Directeur de thèse**
Dr. Frédérique VERDIER, DR, Université Paris Cité	**Présidente**
Dr. Sandrina KINET, DR, Université de Montpellier	**Rapportrice**
Dr. Emile VAN DEN AKKER, PI, Lecturer, Université d'Amsterdam	**Rapporteur**
Dr. Thiago TROVATI MACIEL, CR-HDR, Université Paris Cité	**Examinateur**
Dr. Benoît FAUCHER, Docteur en Médecine, PhD, APHM	**Examinateur**

ACKNOWLEDGMENTS

Tout d'abord, je tiens à exprimer ma gratitude envers le Dr. **Wassim El Nemer** pour m'avoir offert l'opportunité de réaliser ma thèse au sein de son (ses ?) équipe(s). **Wassim**, entre la thèse, la pandémie et le déménagement à Marseille, les quatre dernières années ont été très mouvementées. Ta présence en tant que directeur de thèse a été d'une aide inestimable, et je suis extrêmement reconnaissante pour ton soutien constant, ta positivité inébranlable, ton grand enthousiasme, et ton accent « marseillais ».

J'aimerais également remercier Dr. **Jacques Chiaroni** de m'avoir accueillie au sein de l'EFS et de l'unité UMR 7268. Rejoindre ADES a été pour moi une expérience très enrichissante.

Je tiens également à remercier Dr. **Sandrina Kinet** et Dr. **Emile Van den Akker** d'avoir accepté d'être rapporteurs de mes travaux de thèse. Je remercie également le Dr. **Frédérique Verdier**, Dr. **Thiago Trovati Maciel**, et Dr. **Benoît Faucher** de participer à ma thèse en tant qu'examinateurs. Je suis honorée de votre présence dans mon jury de thèse, merci de tous participer à cette aventure.

Je souhaite également remercier le Dr. **Sara El Hoss**. **Sara**, merci pour ta supervision durant mon M2 et au début de ma thèse. Tu as fait preuve d'une grande patience et de gentillesse pendant notre temps ensemble, et je t'en suis extrêmement reconnaissante. Je te souhaite beaucoup de succès dans la suite de ta carrière.

Ayant débuté ma thèse à Paris, je tiens à remercier toutes les personnes de l'unité Inserm 1134 pour leur soutien durant cette période de mon doctorat. **Margaux**, **Clara**, **Alice T.**, **Alice D.**, et **Sarah**, les pizzas pendant les nuits au laboratoire, ainsi que les discussions sur les films de Noël lors des déjeuners, m'ont énormément manqué depuis mon départ de Paris. **Arnaud**, je te remercie pour les nombreux conseils que tu m'as donnés au début de ma thèse, ainsi que de ta participation à mon CSI. **Sandrine**, c'était un plaisir de travailler avec toi, tu avais le don de tout rendre amusant lorsque j'étais encore à Paris. Un grand merci également à la 'team Wassim' originelle, **Maria Lizzaralde Iragorri**, **Ralf Buks**, et **Sylvie Cochet**. Vous avez embelli le début de mon doctorat.

Il est important pour moi de remercier l'ensemble de l'équipe EFS de l'UMR 7268. Je vous remercie sincèrement de m'avoir accueillie parmi vous, malgré le fais que je sois parisienne.

Alex, merci, tu as toujours été un excellent soutien, et je sais que je peux toujours compter sur toi quand la RTM me laisse tomber. **Audrey**, tu es toujours une personne positive au labo. Je te remercie de m'avoir appris tant de nouvelles manières à communiquer avec des gestes. **Barbara**, merci pour les bonnes ondes que tu apportes au labo. J'espère qu'un jour nous aurons l'occasion de grimper

ensemble. **Cathy**, tu es la personne qui m'a appris que les sanglochons existent et pour ça je te remercie. **Cécile**, merci pour tous les déjeuners, dîners et cafés que nous avons partagés. Je m'excuse pour le manque de temps que j'ai eu récemment. J'espère que nous aurons plus d'opportunités l'année prochaine. **Joël** et **Fanny**, mes compagnons de bureau, même si nous n'avons pas eu beaucoup de temps pour discuter jusqu'à présent, j'espère qu'après ma thèse, on en aura plus l'occasion. François, je te remercie de toujours amener du rosé quand l'occasion est à la fête. **Julien**, depuis que je t'ai rencontré j'ai appris tant de choses sur des sujets souvent très obscurs. Ton savoir sur toutes sorte de sujets divers et ta capacité à en discuter pendant des heures m'impressionnent constamment. Collaborer avec toi est un réel plaisir, et est toujours très marrant. **Soraya** et **Jonatane**, je vous remercie d'avoir apporté votre soutien à mon projet. **Maria**, merci de toujours garder le sourire, même lorsque je mets du lait dans mon café. **Marie-Laurence**, sans toi, on aurait sûrement plus aucun appareil qui fonctionne correctement dans le laboratoire. Merci pour tout le travail que tu accomplis pour maintenir le laboratoire en bon état de marche. **Valérie**, merci de ta patience à chaque fois que je rajoute un produit au dernier moment sur le tableau des commandes. **Sophie**, travailler avec toi fut un plaisir, j'espère que tu vas te rétablir très rapidement ! **Sylvie**, merci pour la gentillesse et la bienveillance dont tu as fait preuve tout au long de ma thèse. **Thomas**, merci d'avoir appris le français à Robert quand j'étais trop occupée pour le faire**. Jonathan**, thank you for your constant positive vibes during your stay in the lab. We miss you here ! **Stéphane** et **Léa**, je vous remercie pour votre soutien et votre patience avec l'AMNIS.

J'aimerai également remercier le personnel de l'hôpital Necker à Paris, Dr. **Bénédicte Boutonnat-Faucher**, Dr. **Laure Joseph** et Dr**. Sandra Manceau**, ainsi que le personnel de l'hôpital de la Timone et de la Conception, **Dr. Pascale Poullin**, **Dr. Frederick Sanderson** et **Dr. Imane Agouti**. Sans eux, ce travail n'aurait pas été possible.

A tous mes amis parisiens que j'ai trop peu vu durant cette période de thèse, **Malda**, **Shin Yeng**, **Chaïma** et **Julie** merci pour votre soutien et votre patience, j'ai hâte de vous montrer Marseille.

A tous mes amis docteurs (ou presque), merci d'avoir été présent toutes ces années, dans les bons moments comme dans moins bons. **Ariane** et **Quentin**, merci d'être toujours partant pour aller prendre des verres à Cours Ju. **Alice** et **Manon,** notre coloc' à New York semble si lointaine maintenant. Je regrette de ne pas vous avoir vues plus souvent ces dernières années pour partager des brunchs végans et des soirées pyjama. Je pense toujours à vous à chaque fois que j'entends du Céline Dion. **Alice**, je viendrai te rendre visite très bientôt en Bretagne ! **Manon**, je ne sais pas encore où tu vas atterrir, mais où que ce soit je passerai t'y voir aussi ! **Julie**, on a bien changé depuis la première année de licence. Avec toi je ne me suis jamais ennuyée. Tu as toujours eu un plan, que ce soit pour aller acheter des

plantes à 8h du matin, marcher pendant des heures dans Paris où profiter de chaque occasion pour aller au Chupitos. Merci pour tous les moments inoubliables que nous avons partagés ensemble. **Hugo**, Tu étais mon partenaire originelle de l'INTS avant même que cette thèse ne commence, et tu as été un grand soutien dans les moments difficiles. Grâce à toi, je garde un très bon souvenir de l'été 2019, quand nous avons bu beaucoup, *beaucoup* de bières bon marché (même si je n'aime pas la bière à la base). Je suis fière de pouvoir t'appeler mon ami. A de nombreuses autres bières à venir, Dr. Sugier.

Marion, ça me brise le cœur que nous n'ayons pas pu passer notre thèse ensemble. Merci pour ton soutien constant. Tout au long de ces quatre années, je savais que je pouvais compter sur toi pour comprendre chaque fois que je venais me plaindre du travail, car je savais que tu vivais les mêmes frustrations à Paris. Merci pour ton soutien pendant la période du confinement, quand nous avons essayé de nous motiver pour nous lever et travailler ensemble via Zoom, et où nous avons systématiquement échoué. Merci d'être venue me voir à Marseille malgré toutes les mésaventures que tu as eu en durant tes voyages. Merci pour toutes les vacances que nous avons passées ensemble ; ce sont toujours mes moments préférés de l'année. Je suis sûre que malgré la distance, tu as eu un grand impact sur cette thèse au cours de ces quatre années. J'ai hâte de te voir défendre ta thèse à Paris et de célébrer avec toi !

A toute ma famille, merci de votre soutien et de votre patience pendant ces quatre années. **Isabelle**, **Dominique** et **grand-mère**, merci pour tous les repas que vous organisez qui nous permettent de nous rassembler tous ensemble. **Mélanie**, je te remercie, ainsi que **Moufle** de tout le soutien que vous avez pu m'apporter. Maintenant que ma thèse se termine, on peut recommencer les 'buddy reads' ! Merci à **Emeline** et **Coralie**, nous nous sommes trop peu vues ces dernières années, il faut que l'on se retrouve entre Grenoble, Paris, Marseille et Nantes ! Merci à mon grand-père, **Robert Godard**, pour toujours avoir fait l'effort de se rappeler de mon sujet de thèse, même si c'était dans le but d'en faire des jeux de mots. A ma mamie, **Michelle Faucher**, je n'ai pas fait de physique mais je suis sûre que tu aurais été ravie que j'aie moi aussi décidé de faire une thèse. **Papa**, malgré la distance, tu as toujours été très communicatif sur le fait que tu es fier de tes filles. Je te remercie pour l'enthousiasme dont tu as toujours fait preuve concernant ma thèse. **Maman**, si j'en suis arrivée là, c'est essentiellement grâce à toi. Merci de m'avoir apporté tout ton soutien, même si tu es un peu perdue quand je commence à utiliser des mots comme « drépanocytose » ou « érythropoïèse ».

Last but not least, thank you **Robert**. Zu guter Letzt, Robert. Ich fühle mich sehr glücklich, dich während meines PhDs kennengelernt zu haben. Danke für deine ständige Unterstützung im Labor und darüber hinaus. Ich hätte es nicht ohne dich geschafft. Ich freue mich darauf, zu sehen, was die Zukunft für uns bereithält.

TABLE OF CONTENTS

ABSTRACT

Sickle cell disease (SCD) is a genetic recessive disorder, characterized by painful episodes of vaso-occlusion, chronic hemolytic anemia, and progressive organ failure. It is one of the most common and severe monogenic diseases worldwide. SCD is caused by a point mutation in the β-globin gene, leading to the expression of an abnormal hemoglobin (HbS) that polymerizes under hypoxic conditions, driving red blood cells (RBC) sickling. Peripheral RBCs are extensively studied in SCD, as hemolysis is the major contributor to anemia, but little is known about erythroid differentiation in this pathology. We recently demonstrated the occurrence of ineffective erythropoiesis in the bone marrow (BM) of SCD patients, characterized by the death of a significant proportion of erythroblasts between the polychromatic and the orthochromatic stages.

The objectives of this project are to 1) Characterize the molecular mechanism underlying ineffective erythropoiesis in SCD, 2) evaluate and determine the *ex vivo* protocol best suited to investigate terminal differentiation and 3) Study the impact of erythroblast apoptosis on the erythroid niche in SCD.

In the first part of this thesis, we showed that ineffective erythropoiesis is tightly linked to the partial hypoxic environment of the bone marrow which leads to HbS polymerization and the cytoplasmic sequestration of heat shock protein 70 (HSP70). This sequestration prevents the translocation of HSP70 to the nucleus, which in turn hinders its protective effect on GATA-1 and ultimately results in the death of terminally differentiating erythroblasts. Furthermore, we used flow cytometry to study the erythropoiesis of patients with high levels of circulating nucleated erythroblasts, which has been described as an indicator of bone marrow stress. Through our analysis, we discovered a significant variability in the stages of differentiation exhibited by circulating nucleated erythroblasts among these patients. Moreover, these patients' cells differentiated *ex vivo* exhibited an accelerated erythroid differentiation compared to other patients. This variability highlights the complexity of erythroid differentiation in the context of SCD and emphasizes the need for further exploration to better comprehend the different underlying mechanisms of ineffective erythropoiesis in SCD. In the second part of this thesis, we compared two of the most used protocols of erythropoiesis, a 2-phase (2P-LC), and a 4-phase liquid culture system (4P-LC). We observed that both protocols could recapitulate the different steps of erythropoiesis. However, the 4-Phase culture system had a higher rate of reticulocytes and erythrocyte differentiation, making it better suited for the study of terminal differentiation. In the last part of the thesis, we showed that the increased apoptosis of terminally differentiating erythroblasts could negatively impact the central macrophages of the erythroblastic islands, as increased phagocytosis of hemoglobin-rich apoptotic erythroblasts can induce ferroptosis in resident macrophages. Furthermore, the surviving macrophages exhibited a shift of polarization from an anti-inflammatory to a pro-inflammatory profile, potentially contributing to the oxidative environment of the bone marrow in SCD.

In conclusion this work highlights a mechanism contributing to ineffective erythropoiesis in SCD, while showing that there is a high variability between patients suggesting other mechanisms may come into play as well. Importantly, our work also highlights the fact that Ineffective erythropoiesis could also impact the erythroid niche by leading to the death of central macrophages and their shift to pro-inflammatory cells which could further impede erythropoiesis.

Keywords: Sickle Cell Disease, Red Blood Cells, Fetal Hemoglobin, Ineffective Erythropoiesis, Ferroptosis, Erythroblastic Island, Iron, Bone Marrow

RÉSUMÉ

Etude de la dysérythropoïèse dans la drépanocytose et de son impact sur la niche érythroïde

La drépanocytose est une maladie génétique récessive caractérisée par des crises douloureuses de vaso-occlusion, une anémie hémolytique chronique, et une défaillance progressive des organes. Cette pathologie est causée par une mutation dans le gène de la β-globine aboutissant à la production d'hémoglobine anormale (HbS), qui polymérise en condition d'hypoxie, entraînant la falciformation des globules rouges (GR). Le GR est très étudié dans la drépanocytose, puisque sa destruction est un contributeur majeur à l'anémie. Cependant on en sait peu sur la différenciation érythroïde dans cette pathologie. Nous avons récemment démontré l'existence d'une dysérythropoïèse chez les patients drépanocytaires, caractérisée par la mort d'une proportion importante d'érythroblastes lors de la différenciation terminale.

Les objectifs de ce projet sont : 1) Explorer le mécanisme moléculaire sous-jacent à cette érythropoïèse inefficace. 2) Sélectionner le protocole de culture *ex vivo* le plus adapté pour étudier la différenciation érythroïde terminale. 3) Etudier l'impact de l'apoptose des érythroblastes sur la niche érythroïde.

Dans la première partie, nous avons démontré que l'érythropoïèse inefficace était étroitement liée à l'environnement partiellement hypoxique de la moelle osseuse, qui conduit à la polymérisation de l'HbS et la séquestration cytoplasmique de la protéine chaperonne HSP70. Cette séquestration empêche la translocation de HSP70 dans le noyau, réduisant son effet protecteur sur GATA-1, et conduisant à la mort des érythroblastes lors de la différenciation terminale. De plus, par cytométrie en flux, nous avons étudié l'érythropoïèse chez des patients présentant des niveaux élevés d'érythroblastes circulants, considérés comme des indicateurs de stress médullaire. Nos observations ont révélé que ces érythroblastes se trouvaient à différents stades de différenciation, avec beaucoup de variations entre les patients. De plus, les cellules de ces patients différenciées *ex vivo* présentaient une maturation accélérée comparée aux cellules des autres patients drépanocytaires. Cette variabilité met en évidence la complexité de la différenciation érythroïde dans la drépanocytose. Dans la deuxième partie, nous avons comparé deux protocoles d'érythropoïèse *ex vivo* couramment utilisés : un système de culture liquide à 2 phases (2P-LC) et un système de culture liquide à 4 phases (4P-LC). Nous avons constaté que les deux protocoles pouvaient reproduire les différentes étapes de l'érythropoïèse. Cependant le système 4P-LC permettait une meilleure différentiation érythroïde avec un taux plus élevé de réticulocytes, le rendant plus adapté pour l'étude de la différenciation terminale. Dans la dernière partie, nous avons démontré que l'augmentation de l'apoptose des érythroblastes en différenciation terminale avait un impact négatif sur les macrophages centraux des îlots érythroblastiques. En effet, nous avons démontré que la phagocytose accrue d'un très grand nombre d'érythroblastes riches en hémoglobine pouvait entrainer la mort de ces macrophages par ferroptose. De plus, les macrophages survivants présentaient un changement de polarisation, passant d'un profil anti-inflammatoire, à un profil pro-inflammatoire, ce qui pourrait contribuer à l'environnement oxydatif de la moelle osseuse dans la drépanocytose.

En conclusion, cette étude met en évidence un mécanisme contribuant à l'érythropoïèse inefficace dans la drépanocytose, tout en soulignant la grande variabilité existante entre les patients, suggérant l'implication d'autres facteurs. De plus, notre recherche met en évidence les répercussions que pourrait avoir l'érythropoïèse inefficace sur la niche érythroïde. Notamment, elle pourrait entraîner la mort des macrophages des îlots érythroblastiques et les pousser à adopter un profil pro-inflammatoire, ce qui pourrait davantage entraver l'érythropoïèse et contribuer à l'anémie dans cette pathologie.

Mots-clés : Drépanocytose, Globules Rouges, Hémoglobine Fœtale, Erythropoïèse Inefficace, Ferroptose, Îlot Erythroblastique, Fer, Moelle Osseuse

ABBREVIATIONS

2P-LC	2 Phase Liquid Culture
4P-LC	4 Phase Liquid Culture
4-HNE	4-Hydroxynonenal
7AAD	7-Aminoactinomycin D
ACC	Acetyl-CoA Carboxylase
ACSL4	Acyl-CoA Synthetases 4
BasoE	Basophilic Erythroblast
BCAM-1/Lu	Basal Cell Adhesion Molecule-1/Lutheran
BFU-E	Burst Forming Units-Erythroid
BM	Bone Marrow
BMP4	Bone Morphogenetic Protein 4
CCL	Chemokine Ligand
CFU-E	Colony Forming Units-Erythroid
CFU-GEMM	CFU-Granulocyte, Erythrocyte, Monocyte, Megakaryocyte
CLP	Common Lymphoid Progenitors
CMP	Common Myeloid Progenitors
cRBCs	cultured RBCs
DAMP	Damage-Associated Molecular Patterns
DBA	Diamond Blackfan Anemia
Dex	Dexamethasone
EBaso	Early Basophilic Erythroblast
EBIs	Erythroblastic Islands
EFS	Etablissement Français du Sang
EKLF/KLF1	Erythroid Krüppel-Like Factor
EMA	European Medicine Agency
EMP	Erythroblast Macrophage Protein
EP	Erythroid Progenitor
EPO	Erythropoietin
EPOR	Epo Receptor

ESCs	Embryonic Stem Cells
EU	European Union
FACS	Fluorescence-Activated Cell Sorting
FAO	Fatty Acid Oxidation
FDA	Food and Drug Administration
Fer-1	Ferrostatin-1
FPN	Ferroportin
FTH1	Ferritin Heavy Chain 1
FTL	Ferritin Light Chain
FVS	Fixable Viability Stain
GBT	Global Blood Therapeutic
GC	Glucocorticoid
GCL	Glutamate Cysteine Ligase
GMP	Granulocyte-Monocyte Progenitor
GPA	Glycophorin A
GPX4	Glutathione Peroxidase 4
GSH	Glutathione
GSS	Glutathione Synthetase
GSSG	GSH Disulfide
HbA	Adult Hemoglobin
HbF	Fetal Hemoglobin
HbS	Sickled Hemoglobin
HIF	Hypoxia Inducible Factors
HMOX1	Heme Oxygenase 1
HPFH	Hereditary Persistence of Fetal Hemoglobin
HSCT	Hematopoietic Stem Cell Therapy
HSP70	Heat Shock Protein 70
HSPC	Hematopoietic Stem and Progenitor Cells
HU	Hydroxyurea
ICAM	Intercellular-Adhesion-Molecule
IFC	Imaging Flow Cytometry

IFN-γ	Interferon-γ
IGF-1	Insulin-like Growth Factor 1
IL	Interleukin
iNOS	Inducer Nitric Oxide Synthase
iPSCs	Induced Pluripotent Stem Cells
IRE	Iron-Responsive Element
IRP	Iron Regulatory Protein
ISCs	Irreversibly Sickled Cells
JAK2	Janus Kinase 2
LBaso	Late Basophilic Erythroblast
LIP	Labile Iron Pool
Lip-1	Liproxstatin-1
LOXs	Lipoxygenases
MAPK	Mitogen-Activated Protein Kinase
MDA	Malondialdehyde
MEP	Megakaryocyte-Erythroid Progenitors
MerTK	Myeloid-Epithelial-Reproductive Receptor Tyrosine Kinase
MGG	May-Grünwald Giemsa
MPP	Multipotent Progenitors
MSCs	Mesenchymal Stem Cells
MUFAs	Monounsaturated Fatty Acids
NAD	Nicotinamide Adenine Dinucleotide
NCCD	Nomenclature Committee on Cell Death
NCOA4	Nuclear Receptor Coactivator 4
NET	Neutrophil Extracellular Traps
NFE2L2/NRF2	Nuclear Factor Erythroid 2-Like 2
NO	Nitric Oxide
nRBCs	nucleated RBCs
OrthoE	Orthochromatic Erythroblast
OXPHOS	Oxidative Phosphorylation
PBMCs	Peripheral Blood Mononuclear Cells

Pi3K/Akt	PhosphoInositide-3 Kinase/Akt
PL	Phospholipid
PLA	Proximity Ligation Assay
PolyE	Polychromatic Erythroblast
POM	Pomalidomide
ProE	Proerythroblast
PS	Phosphatidyl Serine
PUFAs	Polyunsaturated Fatty Acids
RBC	Red Blood Cells
ROS	Reactive Oxygen Species
RSL	Ras-Selective Lethal
SCA	Sickle Cell Anemia
SCD	Sickle Cell Disease
SCD-HCNE	SCD Patients with High Levels of Circulating Erythroblasts
SCD-NE	SCD Patients with no Circulating Erythroblasts
SCF	Stem Cell Factor
SLC	Solute Carrier Family
Stat5	Signal Transducer and Activator of Transcription 5
TF	Transferrin
TFR1	Transferrin Receptor Protein 1
TGF-α	Transforming Growth Factor-α
TLR	Toll-Like Receptor
TNF-α	Tumor Necrosis Factor α
TO	Thiazole Orange
VCAM-1	Vascular Cell Adhesion Molecule-1
VOC	Vaso-Occlusive Crisis

INTRODUCTION

I. Sickle Cell Disease

Sickle cell disease (SCD) is an autosomal recessive hereditary disorder characterized by painful episodes of vaso-occlusion, chronic hemolytic anemia, and progressive organ failure. It is one of the most common and severe monogenic diseases worldwide (Weatherall, 2010). In SCD, a single point mutation in the β-globin gene leads to the production of an abnormal hemoglobin that polymerizes under hypoxic conditions driving red blood cell (RBC) sickling. James Herrick was the first to describe these characteristic sickle-shaped erythrocytes after the examination of a patient's blood sample, commenting as follows: "The shape of the reds was very irregular, but what especially attracted attention was the large number of thin, elongated, sickle-shaped and crescent-shaped forms" (Herrick, 2001). Later, using protein electrophoresis, Linus Pauling and his group showed that the hemoglobin in patients with SCD differed from that of healthy individuals. This led them to classify SCD as a "molecular disease", making it the first disorder in which an abnormal protein was at the origin of the pathology (Pauling et al., 1949).

A. Epidemiology

SCD affects millions worldwide, with over 500 000 newborns diagnosed with this pathology each year (Piel et al., 2013; Thomson et al., 2023) (Figure 1). Most of these births occur in tropical regions, with Nigeria, the Republic of the Congo, and India being the most impacted countries due to the protection the sickle cell trait (heterozygous individuals) provides against severe malaria (Piel et al., 2017). Estimates suggest that around 75% of the global burden of SCD occurs in Sub-Saharan Africa, where, due to the lack of early diagnosis and efficient treatment, most of the children affected by the disease die undiagnosed before reaching the age of five (Grosse et al., 2011). Although a few pilot studies were carried out to establish newborn screening programs in these regions, the lack of resources combined with the high number of cases has presented a significant challenge in implementing this practice effectively (Piel et al., 2023). In the European Union, an estimated 30 000 to 50 000 individuals are affected by SCD, with France having the highest prevalence among the member states (Leleu et al., 2021; Mañú Pereira et al., 2023). As global population movements and increasing life expectancy continue, the number of SCD cases is expected to rise further. New data from the Global Burden of Disease 2021 study indicates that 7.74 million people were living with SCD in 2021, a number that is projected to increase and to exceed 14 million by 2050 (Piel et al., 2013; Thomson et al., 2023).

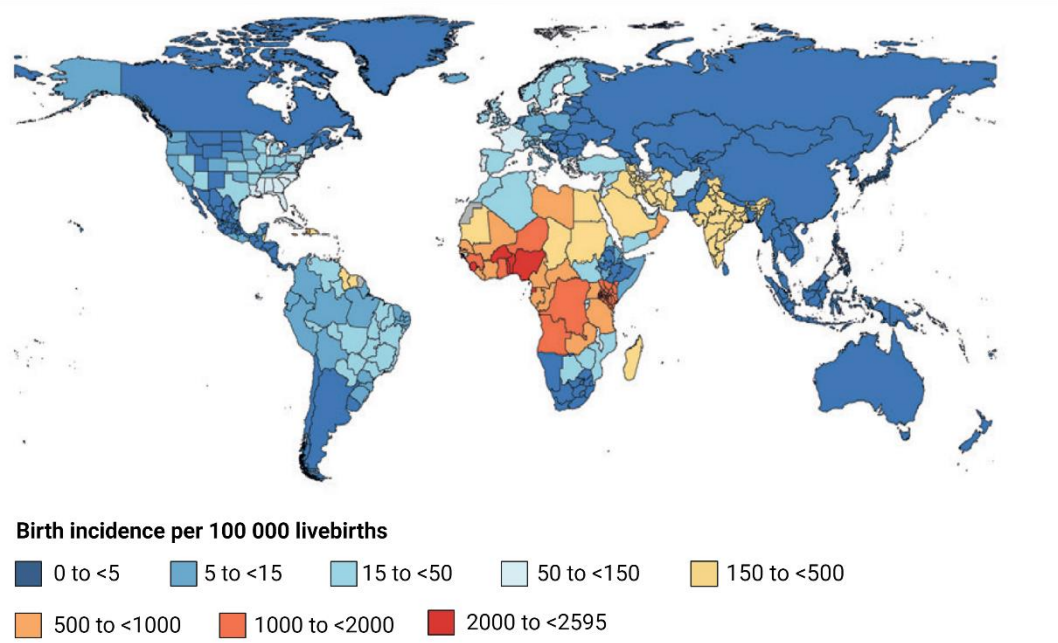

Figure 1: Global burden of SCD. A map showing the number of newborns with SCD in 2021 (Thomson et al., 2023).

B. Physiopathology

SCD is an umbrella term for all the different genotypes resulting in the same set of clinical syndromes (Rees et al., 2010). Sickle cell anemia (SCA) is the most common form of SCD, accounting for 70% of cases in patients of African ethnicity. SCA is caused by homozygous inheritance of the single point mutation β^S, which leads to the substitution of a hydrophilic glutamic acid by a hydrophobic valine at the sixth position of the β globin chain (Glu6Val) (Odièvre et al., 2011). This change results in the production of mutated hemoglobin tetramers (HbS) that can bind to each other through their hydrophobic motifs and polymerize under hypoxic conditions (Figure 2). Other forms of SCD can result from the co-inheritance of β^S with other mutations altering the stability or production of the β-globin chain, such as the β^C or a β-thalassemia mutation (Bender & Carlberg, 1993; Rees et al., 2010).

1. Hemoglobin Polymerization

The polymerization of HbS under hypoxic conditions is the primary event in the molecular pathogenesis of SCD. This process occurs during the deoxygenation following the passage of RBCs in the microcirculation. In these low oxygen conditions, β^S-globin on different HbS tetramers can bind to each other through their hydrophobic motif and initiate the formation of HbS polymers. These polymers can then grow rapidly and form long fibers that increase cell rigidity and distort the membrane leading to erythrocyte sickling, cellular stress, dehydration, impaired rheology, and premature hemolysis (Bunn, 1997; Rees et al., 2010). The rate and extent of polymerization are dependent on the degree of deoxygenation of the cell, its intracellular concentration of HbS, and the presence of fetal hemoglobin

(HbF), which can effectively reduce the concentration of HbS and interfere with its polymerization (Brittenham et al., 1985; Rees et al., 2010).

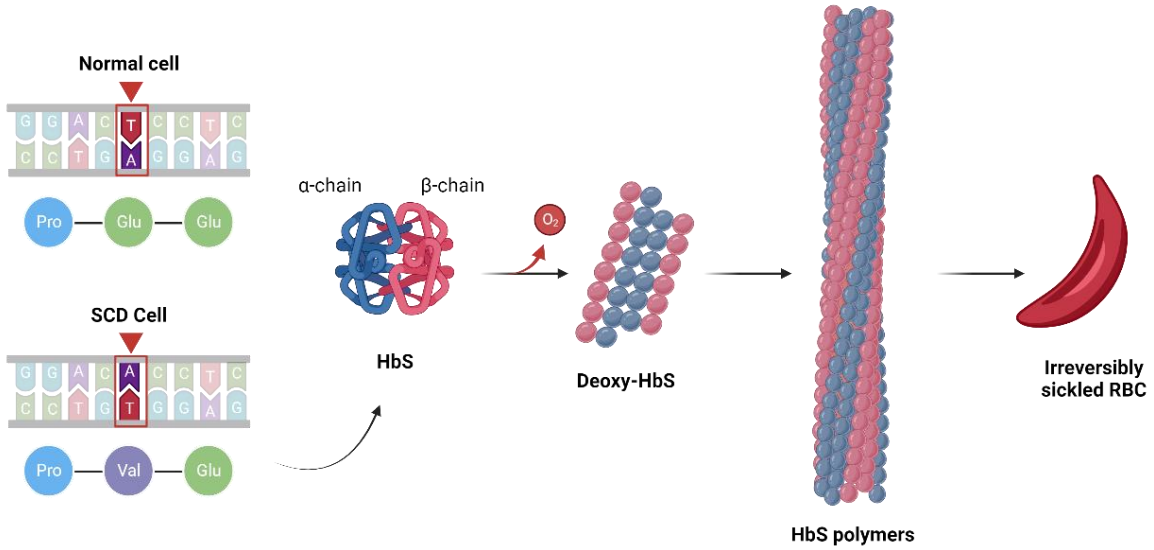

Figure 2: Polymerization of deoxy-HbS. A point mutation at the sixth position of the β-globin gene induces the substitution of a glutamic acid by a valine leading to the production of HbS. At low oxygen pressure, deoxy-HbS polymerizes and forms stiff polymer fibers that deform the RBC, leading to irreversibly sickled cell (ISCs). Figure created with biorender.com and adapted from Odièvre et al. 2011.

Furthermore, co-inheritance of genetic factors that modulate the intracellular HbS or HbF concentration can also modify SCD severity. For example, co-inheritance of α-thalassemia with SCD has been shown to diminish the severity of the disease. By decreasing HbS levels, α-thalassemia was shown to reduce the number of sickled RBCs and improve hemolysis, resulting in a reduction in the risk of stroke, pain frequency, leg ulcers, priapism, and gall stones (Piel et al., 2017; Rees et al., 2010). Additionally, hereditary persistence of fetal hemoglobin (HPFH) is a known positive modulator of disease severity in patients with SCD (Galanello et al., 2009).

2. *Vaso-occlusive Crisis*

The most common clinical manifestation of SCD is the occurrence of vaso-occlusive crises (VOCs), which often requires the intervention of emergency medical care. At their core, VOCs occur when the blood flow in the microcirculation is blocked by sickled RBCs and leukocytes to the point that tissues become deprived of oxygen (Figure 3A). However, these events occur due to the interplay between several pathological features of SCD.

a. Abnormal Membrane Properties of Sickled RBCs

Sickled RBCs are poorly deformable because of HbS polymerization and cellular dehydration. Consequently, these cells can become more easily sequestered in the microcirculation, promoting transient vaso-occlusive events (Barabino et al., 2010). Furthermore, in sickled RBCs, HbS molecules can undergo accelerated auto-oxidation, contributing to the increased intracellular production of

reactive oxygen species (ROS) (Browne et al., 1998; Hebbel & Vercellotti, 1997). This process generates iron-dependent free radicals that damage the membrane, altering the distribution and exposure of adhesion molecules and binding motifs such as basal cell adhesion molecule-1/Lutheran (BCAM-1/Lu), phosphatidyl serine (PS), integrin-associated protein (IAP), and intercellular-adhesion-molecule-4 (ICAM-4) (Barabino et al., 2010; Bunn, 1997; Kaul et al., 2009) (Figure 3B). The presence of these molecules at the surface of sickled RBCs promotes abnormal adhesion to the vascular wall, decreasing the lumen size of microvessels, slowing down the blood flow, and initiating vascular occlusion. Additionally, the increased oxidative stress in sickled RBCs leads to the production of microparticles, which contain pro-inflammatory hemoglobin products that contribute to cellular activation and the initiation of VOCs (Hebbel & Key, 2016).

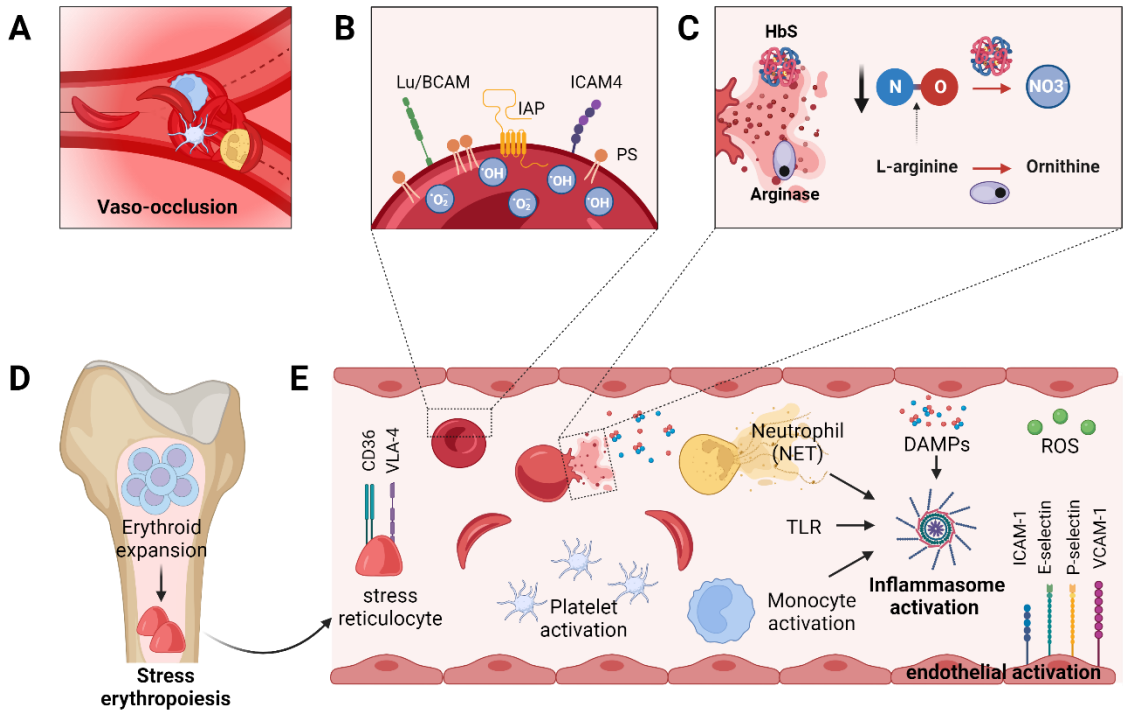

Figure 3: The molecular basis of vaso-occlusive crises (VOCs). (A) VOCs occur when the blood flow in the circulation is blocked by sickled RBCs and leukocytes. **(B)** HbS auto-oxidation leads to increased ROS at the membrane of RBCs and induces the abnormal expression or activation of adhesion molecules. **(C)** Repeated sickling episodes lead to intravascular hemolysis and to the release of free heme and arginase that induce the depletion of nitric oxide. **(D)** Chronic anemia in SCD induces stress erythropoiesis where immature reticulocytes leave the bone marrow prematurely. These reticulocytes express adhesion molecules that facilitate their interaction with other blood components. **(E)** Sickled RBCs and free heme act as damage-associated molecular patterns and activate various inflammatory pathways (NETosis, toll-like receptor signaling and immune response). ROS lead to chronic inflammation. Endothelial cells are activated and express adhesion and procoagulant molecules on their surface. Figure created with biorender.com and adapted from Shet et al., 2020. TLR = toll-like receptor, NET = neutrophil extracellular traps, DAMPs = damage-associated molecular pattern, ROS = reactive oxygen species, NO = nitric oxide.

b. Chronic Hemolysis and Endothelial Dysfunction

Sickled RBCs are subject to intravascular and extravascular hemolysis, causing chronic anemia in individuals with SCD. The free plasma hemoglobin released from the ruptured cells is a potent nitric

oxide (NO) scavenger that leads to NO depletion and to the production of superoxide and peroxide radicals. Arginase, an enzyme released from hemolyzed RBCs, also contributes to NO deficit in the circulation by depleting plasma arginine, the precursor of NO synthesis in the L-arginine pathway (Morris et al., 2005). NO is produced by the endothelium and is required for vasodilation as well as the regulation of platelet activation, inflammation, and oxidative stress. Its reduced bioavailability in SCD patients leads to impaired NO-dependent vasodilation and endothelial function, thus facilitating the occurrence of VOCs (Odièvre et al., 2011) (Figure 3C).

The chronic anemia in SCD triggers increased activity in the bone marrow (BM) as it attempts to compensate for the loss of RBCs. This compensatory response is characterized by the release of high numbers of immature erythrocytes, termed "stress reticulocytes", into the circulation (Rees et al., 2010). Stress reticulocytes express adhesion proteins such as CD36 and α4β1 integrin (VLA-4), which, under physiological conditions, allows nascent reticulocytes to remain in the BM and complete the medullar steps of their maturation process (Kaul et al., 2009). The presence of stress reticulocytes in the circulation, with their abnormal pattern of adhesion molecules, is at the origin of abnormal interactions with the other cell types of the vascular bed, including leukocytes and endothelial cells, contributing to the initiation of VOCs (Figure 3D).

c. Chronic Hemolysis and Inflammation

NO deficiency also participates in creating a prothrombotic state in SCD patients, where activated platelets readily adhere to the vascular wall participating in the creation of cellular aggregates and contributing to the release of pro-inflammatory cytokines that drive the vaso-occlusive process (Bennewitz et al., 2017; Garrido et al., 2012; Wun et al., 1998). Additionally, intravascular hemolysis, accounting for up to 30% of red cell lysis, is a major source of inflammatory molecules taking part in initiating and propagating VOCs. Indeed, the free heme and its products can be recognized as erythrocytic damage-associated molecular patterns (DAMPs) and activate multiple inflammatory pathways, such as toll-like receptor (TLR) signaling, neutrophil extracellular traps (NET) and inflammasome formation, thus promoting and propagating sterile inflammation and oxidative stress (Mendonça et al., 2016). Heme release also plays a role in activating the endothelium. As a result, endothelial cells upregulate P- and E-selectins, vascular cell adhesion molecule-1 (VCAM-1), and ICAM-1. Additionally, these cells secrete the leukocyte chemoattractant interleukin (IL)-8, and the pro-inflammatory cytokines tumor necrosis factor α (TNF-α), and IL-1β (Hebbel & Vercellotti, 1997; Solovey et al., 1997). The endothelium activation and the overall inflammatory environment created by chronic hemolysis in SCD further promote the activation of platelets, monocytes, and neutrophils, leading to their increased adhesion to each other and to endothelial cells (Figure 3E).

Finally, a major inducer of VOCs is vaso-occlusion itself. Indeed, by inducing localized hypoxia, VOCs promote further HbS polymerization and RBC sickling, fueling a new cycle of adhesion, inflammation, hemolysis, and endothelial dysfunction. Over time, repeated episodes of vaso-occlusion can lead to ischemia-reperfusion injury, oxidative damage, increased inflammatory responses, activation of adaptive and innate immune responses, and cell death (Kaul & Hebbel, 2000).

3. Clinical manifestations of SCD

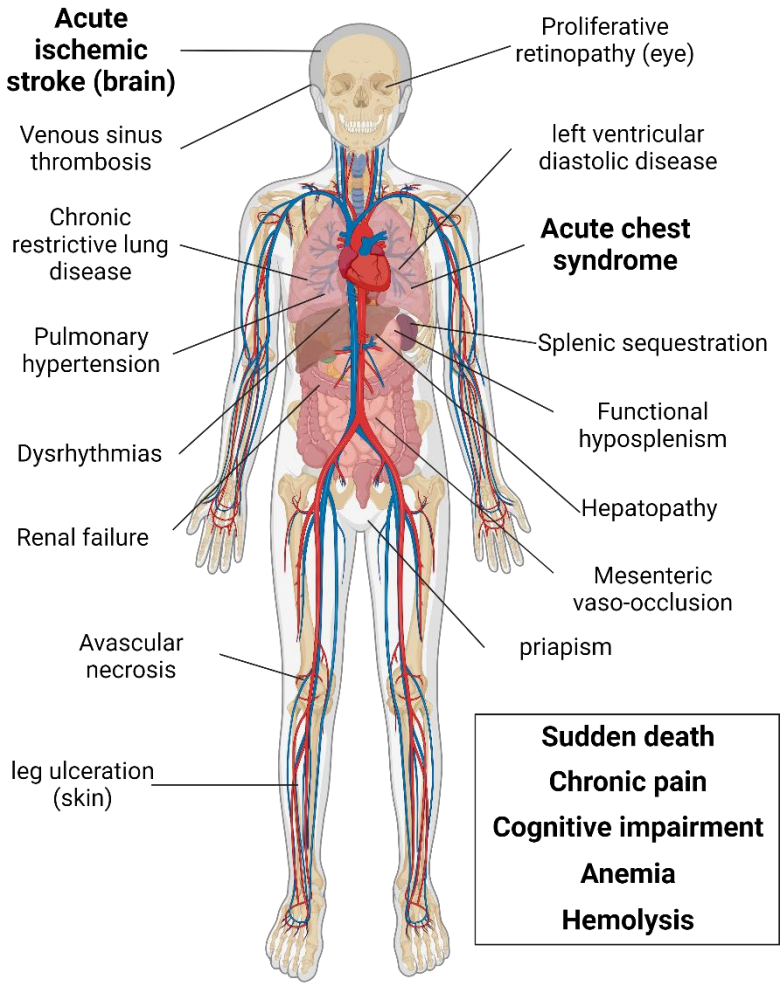

Figure 4: Common clinical manifestations of sickle cell disease. Acute complications are shown in boldface type. Figure created with biorender.com based on Piel et al., 2017.

SCD is a multisystem disease, with pain being its most prominent aspect. The major clinical manifestations are related to hemolytic anemia and vaso-occlusion, which can lead to acute and chronic pain and tissue ischemia or infarction (Piel et al., 2017). In SCD children, the first months of life are a time of low incidence of complications due to the sustained levels of protective HbF still being expressed. Clinical features do not begin until the second semester of post-natal life when HbF is being replaced by HbS (Couque et al., 2016). Dactylitis (hand-foot syndrome), caused by sickled cells getting

stuck in the blood vessels of the hands and feet, is usually the first symptom of SCD. However, other complications, such as harmful infections and splenomegaly, can occur early in life. Over their life, individuals with SCD may develop chronic complications such as strokes, priapism, leg ulcers, retinopathy, acute kidney injury, and liver (Figure 4)(Inusa et al., 2019). It is important to note that the severity of these complications varies from patient to patient, and in some cases, can lead to life-threatening consequences. Therefore, treating SCD requires a multi-disciplinary approach that addresses not only the immediate medical needs but also focuses on the long-term management of the disease and improving the patient's quality of life.

C. Treatments

Over the years, therapeutic strategies such as newborn screening, immunizations, antibiotics, and RBC transfusions with iron chelation have greatly improved the lifespan of children with SCD in high-income countries (Gardner et al., 2016). However, while life expectancy for patients continues to improve, it still falls behind that of the general population, with most patients dying prematurely in their mid-40s. Until recently, treatment options for patients with SCD were limited, with hydroxyurea (HU) being the only FDA-approved drug. The introduction of new treatment options, such as L-glutamine, crizanlizumab, and voxelotor, along with the development of gene therapy, offers hope for further improvements in the management and outcomes of SCD in the future.

1. Disease Modifying Therapies

a. Hydroxyurea

Hydroxyurea, also known as hydroxycarbamide, was the first disease-modifying drug used to reduce complications in SCD. Its use in adult patients was first approved by the Food and Drug Administration (FDA) in 1998 and later by the European Medicine Agency (EMA) in 2007 (Ware & Aygun, 2009). For decades, it remained the only drug treatment for SCD and is still considered the most effective treatment available today. Recently, the FDA extended its approval of HU to include children over 2 years old to decrease the frequency of their pain crises and reduce their need for blood transfusions. HU is a ribonucleotide reductase inhibitor initially used as a myelosuppressive agent (Elford, 1968). Its beneficial impact in SCD is attributed to its ability to increase HbF production to alleviate SCD symptoms. However, its mechanism of action remains a subject of ongoing investigation (Charache et al., 1996).

Through its inhibitor activity, HU can prevent the synthesis of daughter strands of DNA during the S-phase of the cell cycle, causing cell arrest and checkpoint activation during hematopoiesis. It is widely accepted that this process induces a "stress erythropoiesis" response, resulting in the selection of erythroid progenitors containing high HbF (Galanello et al., 1985; Stamatoyannopoulos et al., 1985).

When these cells mature, the high levels of HbF reduce the tendency of HbS to polymerize, preventing RBC from sickling and causing VOCs. Furthermore, HU also reacts with heme-containing proteins to release NO, which activates soluble guanosine monophosphate (sGC) and contributes to the induction of HbF (Cokic et al., 2003; Huang et al., 2002; Lou et al., 2009). Another mechanism of HU involving microRNAs was also shown to increase HbF through the downregulation of its repressor, *BCL11A*, *KLF1*, and *MYB* (Pule et al., 2016; Walker et al., 2011). Besides HbF induction, HU also provides other salutary therapeutic effects. It reduces the production of leukocytes, platelets, and reticulocytes, thereby reducing important players of vaso-occlusion (Bartolucci et al., 2010; Chaar et al., 2014). Finally, HU modulates vascular adhesion, inflammation, endothelial damage, hemolysis, and oxidative stress, and improves RBC hydration and rheology (Figure 5) (Gambero et al., 2007).

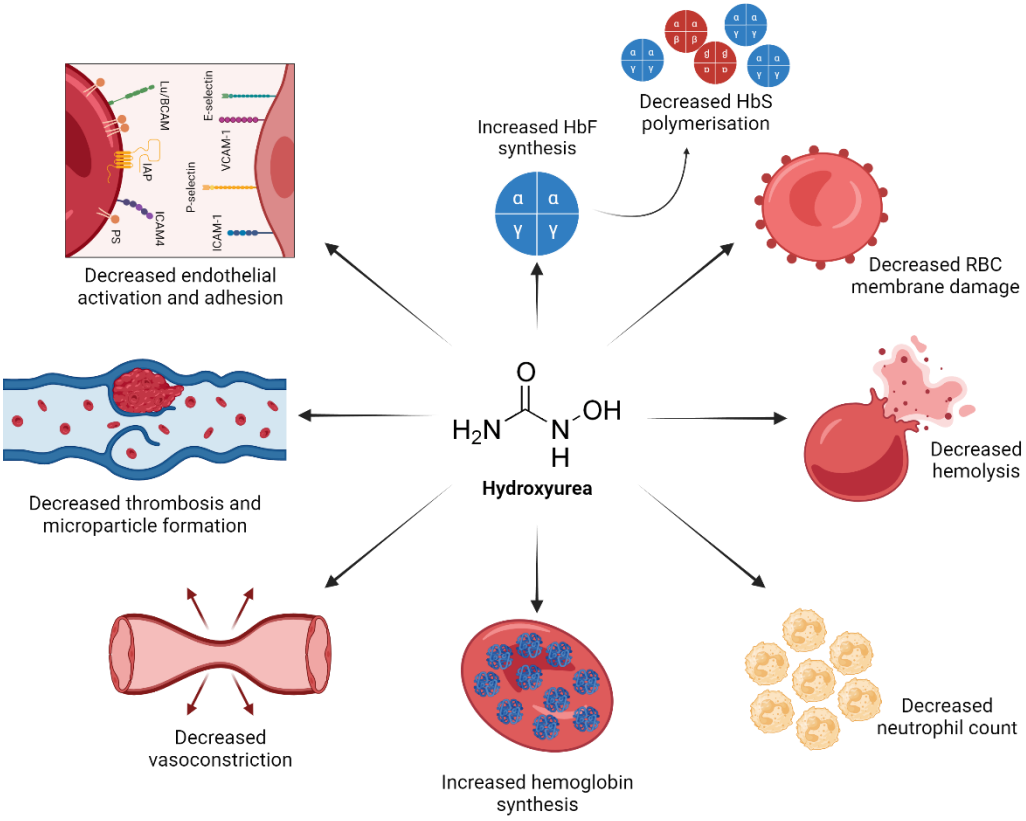

Figure 5: Multiple effects of hydroxyurea administration in sickle cell disease patients. Figure created with biorender.com and adapted from Verma et al., 2018.

After over more than 20 years of use, HU remains the best available therapeutic agent for SCD patients, with proven clinical efficacy in reducing the occurrence of various complications in both adults and children, including VOCs and acute chest syndrome events (Ware & Aygun, 2009). However, despite all the reported benefits of HU in SCD, there are challenges and limitations to its use, such as compliance with taking the medication daily, fears about potential carcinogenicity and other side effects, as well as barriers to receiving refills or accessing the medication (Bradford et al., 2022; Haywood et al., 2011).

b. L-glutamine

In 2017, L-glutamine was approved in the United States for patients aged 5 years and older, becoming the first drug to be approved for SCD treatment in almost 20 years since HU (Niihara et al., 2018). L-glutamine is an essential amino acid required in the synthesis of glutathione (GSH) and nicotinamide adenine dinucleotide (NAD), both being critical players in the maintenance of the redox balance in erythrocytes (Figure 6) (Al-Ali, 2002; Zerez et al., 1988). While the exact mechanism of action of L-glutamine is not fully characterized, its use in SCD is primarily based on its antioxidant activity. Early studies showed that oral glutamine supplementation could increase NAD synthesis and promote redox reactions resulting in improved energy levels and decreased chronic pain in SCD patients (Niihara et al., 1998). In another study, L-glutamine has been shown to decrease RBC adherence to the endothelium, suggesting a potential benefit in reducing VOCs in SCD (Niihara et al., 2005). Since then, oral administration of L-glutamine to SCD patients has been shown to reduce the frequency of acute VOCs, hospitalizations, and acute chest syndrome (Elenga et al., 2023; Niihara et al., 2018). However, while L-glutamine is well tolerated, adherence to the medication may prove challenging, as it requires to be taken twice a day. Furthermore, L-glutamine therapy comes at a significant cost, as it is 20 times more expensive than HU.

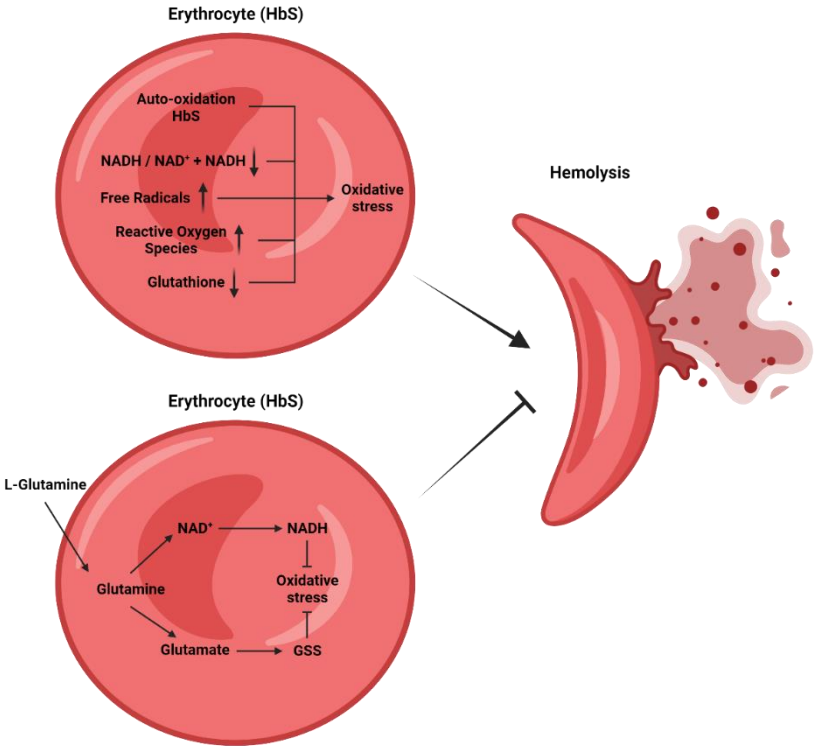

Figure 6: **Proposed mechanisms of action of L-Glutamine.** Intense oxidative stress occurs within erythrocytes carrying HbS due to a combination of auto-oxidation of HbS, increased production of free radicals and reactive oxygen species with subsequent consumption of NADH and glutathione, resulting in hemolysis of the sickle erythrocytes. L-glutamine therapy/supplement reduces the oxidative stress to ameliorate hemolysis (Jafri et al., 2022).

c. *Crizanlizumab*

Crizanlizumab is a new humanized monoclonal antibody that binds to P-selectin and blocks its interaction with its ligand, P-selectin glycoprotein ligand 1 (PSGL-1). By interacting with this molecule, crizanlizumab can block adhesive interactions among endothelial cells, platelets, leukocytes, and sickled RBCs, leading to improved microvascular blood flow (Figure 7) (Ataga et al., 2017). A clinical trial by Ataga et al. using this treatment showed that while crizanlizumab did not affect hematological parameters, it could decrease the annual rate of acute vaso-occlusive events in SCD patients regardless of SCD genotype or concomitant HU treatment (Ataga et al., 2017). Based on this successful clinical trial, FDA approved the use of crizanlizumab for SCD patients over 16 in 2019 as an add-on therapy to HU or as a monotherapy in patients for whom HU therapy proved inadequate. The EMA authorized its use in the European Union (EU) a year later. However, the medication is now being taken off the market in the EU after being rejected by the EMA following a worldwide phase 3 clinical trial (STAND) that did not confirm its clinical efficiency.

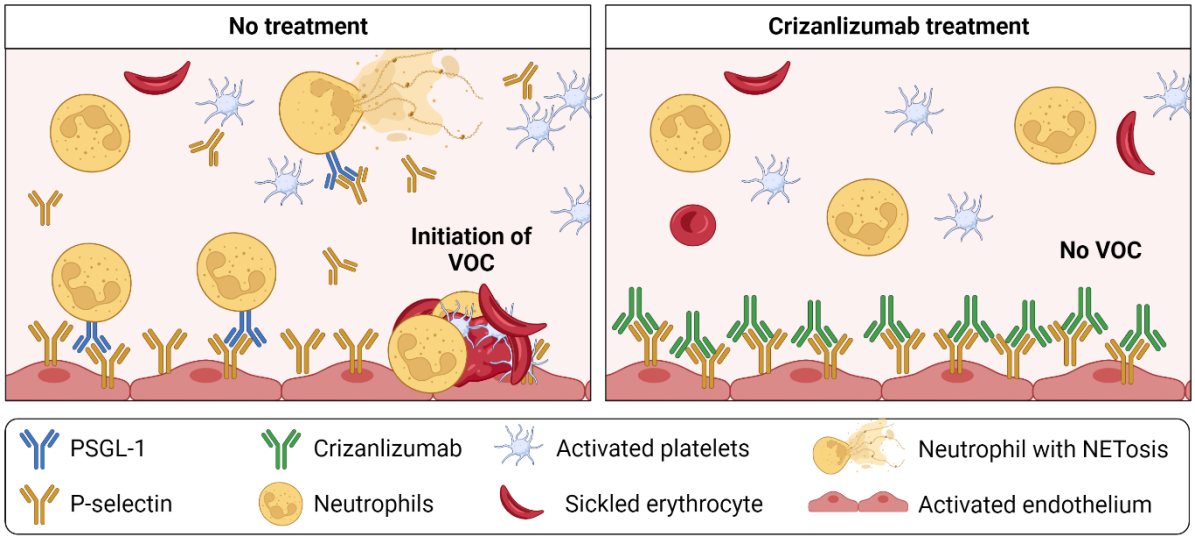

Figure 7: **Mechanisms of action of crizanlizumab**. Crizanlizumab is a humanized monoclonal antibody against P-selectin, blocking its interaction with its ligand, PSGL1. This prevents the adhesion of activated and aged neutrophils to the endothelium and reduces the formation of neutrophil extracellular traps (NETosis). As a result, vaso-occlusive crises are prevented. Figure created with biorender.com and adapted from Jafri et al, 2022. VOC = vaso-occlusive crises, NET = neutrophil extracellular traps.

d. *Voxelotor*

GBT-440, also known as voxelotor or oxbryta, is a small molecule recently developed by Global Blood Therapeutics (GBT) as an HbS polymerization inhibitor to treat SCD (Metcalf et al., 2017). Voxelotor acts by forming a reversible bond with hemoglobin to increase HbS oxygen affinity and maintain it in its oxygenated state (R-state) (Metcalf et al., 2017). This mechanism was developed to decrease polymerization and RBC sickling, the primary drivers of SCD pathophysiology (Figure 8A and 8B) (Howard et al., 2019). Clinically, voxelotor was shown to improve RBC deformability and blood viscosity,

increase hemoglobin levels and lower the percentages of sickled RBCs (Estepp et al., 2022; Howard et al., 2021; Howard et al., 2019). Importantly, the treatment had these beneficial effects regardless of HU co-treatment. However, despite improving biomarkers of hemolysis, whether voxelotor can decrease the incidence rate of VOCs is still unclear and requires further investigation (Neumayr et al., 2019). Voxelotor has been approved by the FDA in 2019, for adults and children 4 years or older, and by the EMA in 2021. So far, voxelotor has been well tolerated, but gastrointestinal side effects and the need to take pills daily may impair compliance. Additional data from ongoing clinical trials HOPE-KIDS 1 (NCT02850406) and 2 (NCT04218084) will help evaluate its use in children and assess long-term safety.

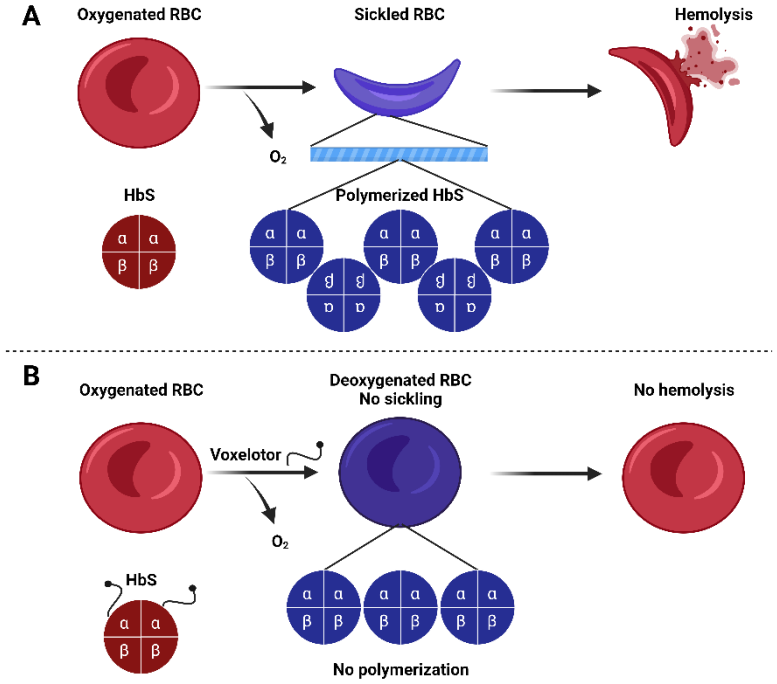

Figure 8: Mechanisms of action of voxelotor. Voxelotor binds covalently to the α-globin chain to stabilize the oxygenated HbS which prevents deoxygenation and polymerization of hemoglobin. As a result, the erythrocytes are prevented from sickling. This decreases the subsequent hemolysis and vaso-occlusive crises (Leibovitch et al., 2022).

2. *Curative Therapies*

a. *Hematopoietic Stem Cell Transplantation*

Hematopoietic stem cell transplantation (HSCT) from a healthy donor is currently the only curative option for SCD patients. Studies have shown that patients who received HSCs from HLA-matched sibling donors had a disease-free survival rate of 90-95% (Bernaudin et al., 2007; Vermylen et al., 1998; Walters et al., 2000). This treatment restored normal hematopoiesis and, if done early enough, could even restore spleen function (Vermylen et al., 1998). However, only a small fraction of patients can access this kind of treatment, as only 10-20% have HLA-matched siblings (Krishnamurti et al., 2019; Walters et al., 1996). While allogeneic-HSCT can be used as an alternative, it is associated with higher risks of complications such as graft-versus-donor disease, graft rejection, and transplantation-related

infections (Bolaños-Meade et al., 2012; Fitzhugh et al., 2017; Foell et al., 2017). Furthermore, HSCT requires the use of myelotoxic agents to clear the BM niche and make space for the engraftment of donor cells. These conditioning regimens can lead to bleeding, organ dysfunction, and the development of leukemia (Ciurea & Andersson, 2009). Finally, due to the lack of complete long-term follow-up data post-HSCT, the extent and duration of the benefits of HSCT are still unclear. For all these reasons, it can be challenging for clinicians to ascertain a risk/benefit ratio of HSCT in treating SCD patients (de Montalembert et al., 2017). Therefore, HSCT is often only considered when severe complications have occurred.

b. Gene Therapy

Gene therapy has been considered a promising alternative to HSCT since the 1990s and holds great potential as a cure for SCD. This procedure requires isolating patient HSCs, modifying them *ex vivo*, and reintroducing them into the patient's BM. Like HSCT, this process requires BM conditioning to ensure the engraftment of these therapeutic cells. However, since these cells are derived from the patient, the risk of complications such as graft-versus-host disease and transplant rejection is significantly reduced, removing the need for immunosuppression as part of the conditioning regimen. Initial approaches for HSC modification in SCD relied on the transduction of a lentiviral vector carrying either a β-globin-like gene with anti-sickling properties or a γ-globin gene to dilute HbS and prevent its polymerization in patient RBCs (Figure 9A and 9B) (Cavazzana-Calvo et al., 2010; Magrin et al., 2019). Over the past decade, this approach has been refined through iterative clinical trials and numerous technical advances, allowing better HSC collection and transduction methods (Drakopoulou et al., 2019; Masiuk et al., 2019; Uchida et al., 2019). Notably, in the largest clinical trial of gene therapy for SCD to date, this approach yielded promising results, with some patients having reduced hemolysis and complete resolution of severe VOCs (Kanter et al., 2022). Furthermore, combining lentiviral vectors with RNA interference (RNAi) technology to silence the γ-globin repressor BCL11A has also demonstrated similar encouraging results (Esrick et al., 2021).

While methods using lentiviral vectors have shown favorable results in treating SCD, other approaches involving gene editing have also shown great promise. Currently, several strategies are used to treat SCD with gene editing, using CRISPR-Cas9, TALEN, or zinc-finger nucleases (Figure 9C). For example, early clinical studies have demonstrated that suppressing BCL11A by Cas9 nuclease-mediated disruption of its erythroid enhancer can induce HbF and reduce morbidities in both SCD and β-thalassemia (Frangoul et al., 2021). Another therapeutic approach being explored to restore HbF expression is to prevent the binding of γ-globin repressors to the promoter region, mimicking HPFH. This approach was shown to modify human HSCs efficiently and is now entering clinical trials (Lux et al., 2019; Martyn et al., 2018; Traxler et al., 2016). Efforts are also being developed to directly correct

the pathogenic sickle mutation in the β-globin gene via Cas9-mediated homology-directed repair (HDR) to remove the expression of the pathologic HbS from the cells. While this approach represents a technical challenge, preclinical studies demonstrated its feasibility, and clinical trials are now underway. Newer gene editing approaches being refined currently, such as base editing and prime editing, could help optimize this approach. Indeed, prime editing was recently used to correct the SCD codon in heterologous cell lines (Anzalone et al., 2019).

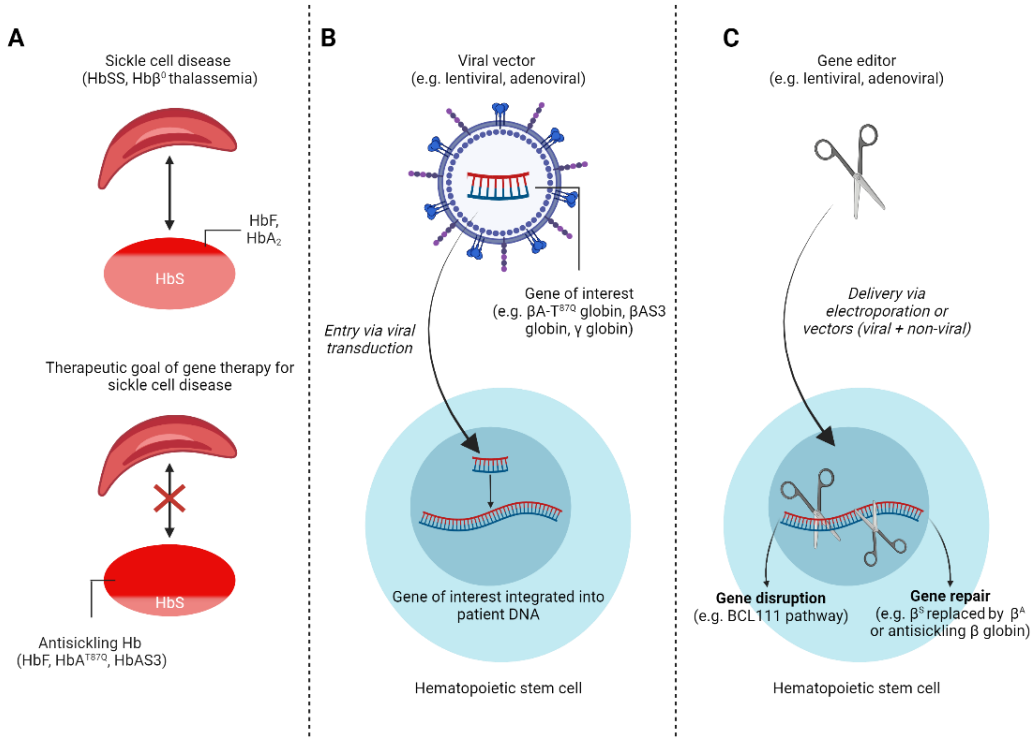

Figure 9: Gene therapy strategies for SCD. (A) Anti-sickling globin expression as a gene-therapy strategy to prevent RBC sickling. **(B)** Gene-addition strategy to deliver anti-sickling genes. **(C)** Gene-editing approaches to induce HbF by gene disruption and gene repair. Figure created with biorender.com and adapted from Abraham & Tisdale 2021.

While gene therapy offers many promising avenues for SCD treatment, it is important to keep in mind that a healthy BM environment is essential to its success. Patients with hemoglobinopathy often experience chronic inflammation and oxidative stress, which may lead to a decrease in the numbers of long-term-HSC (LT-HSC) and hinder the potential of proliferation and transduction of BM stem cells (Leonard et al., 2019). Furthermore, the aberrant vascular niche in SCD patients may reduce hematopoietic stem and progenitor cells (HSPC) homing and engraftment efficiency during HSC transplantation of SCD patients, particularly older SCD patients, where BM defects are expected to be more severe than in younger patients.

Gene therapy shows promise as a potential cure for SCD. However, it is still in its early stages of development and implementation, meaning that widespread availability will likely take a long time. In the meantime, precision medicine offers valuable possibilities to provide effective and personalized care for SCD patients (El Hoss et al., 2022).

D. Mouse Model of SCD

Over the past decades, mouse model studies have been crucial in understanding the various molecular mechanisms contributing to SCD pathophysiology. For example, mouse studies have provided insights into the events leading to VOCs (Bennewitz et al., 2017), the identification of various SCD pain receptors (Tran et al., 2019), the involvement of coagulatory components in SCD (Arumugam et al., 2015), and hemolysis driven organ injury (Ofori-Acquah et al., 2020). More recently, these models have also been valuable tools for investigating the effects of various therapeutic approaches, such as drug treatment (Oksenberg et al., 2016; Shrestha et al., 2021), lentiviral vector gene transduction (Urbinati et al., 2018) and genome-editing approaches (Newby et al., 2021).

SCD mice were developed using genome editing techniques over decades of work and multiple iterations of mice with diverse genotype/phenotype relationships (Table 1). Early models of SCD such as S Antilles (Popp et al., 1997; Rubin et al., 1991), S+S Antilles (Fabry et al., 1995), and SAD mice (Trudel et al., 1991) still expressed mouse globin chains and had varying levels of HbS expression. While these models provided important information about SCD, they only managed to mimic the sickle cell trait exhibited in human β^S heterozygous carriers. Additionally, they did not present the severe hemolytic anemia observed in homozygous SCD patients. The mild SCD phenotypes observed in these mice were eventually attributed to the presence of endogenous murine globin that could inhibit HbS sickling and attenuate its impact (Rhoda et al., 1988). As research progressed, two humanized mouse models, the Berkeley, and Townes mice, were developed and have since become the most used models for preclinical studies of SCD.

	Transgenic models expressing murine and human globin chains			Transgenic models expressing exclusively human globin chain		
Name	β^S + β^S-Antilles	SAD-1	NY1DD	Berkeley	Townes	NY1 full KO
Year	1995	1991	1992	1997	2006	2001
Human globin genes expressed	β^S, $\beta^{S\ Antilles}$, α	β^{SAD}, α	β^S, α	β^S, α, γ	β^S, α, γ	β^S, α, γ
Mouse globin genes expressed	β, α	β, α	β, α	None	None	None
Expression of sickle or sickle related genes	β^S, 42% $\beta^{S\ Antilles}$, 38%	β^{SAD}, 26%	β^S, 26%	β^S, >99 %	β^S,>99	β^S, 60% - 80%
Hemolytic anemia	Compensated	Compensated	No	Yes	Yes	Yes
Micro-occlusive disease	Moderate	Moderate	Moderate	Severe	Severe	Severe
Reference	(Fabry et al., 1995)	(Trudel et al., 1991)	(Fabry et al., 1992)	(Pászty et al., 1997)	(Wu et al., 2006)	(Fabry et al., 2001)

Table 1: Mouse models of sickle cell disease. Adapted from Nagel, 1998.

The Berkeley strain was developed by creating transgenic mice via pronuclear projection. These mice harbor disruptions of their endogenous globin genes and instead express human adult hemoglobin (HbA), HbS, and HbF (Pászty et al., 1997). In this model, HbF is expressed in very low amounts (4% - 26%) at birth, which is thought to lead to high mortality before adulthood (Pászty et al., 1997). The Townes strain was created using homologous recombination. In this model, the murine α-globin and β-globin genes were replaced with a gene cassette containing human α-, β- (β^S), and γ-globin genes along with a significant amount of upstream and downstream sequences necessary to retain temporal expression of these genes (Ryan et al., 1997; Wu et al., 2006). Importantly, Townes mice mimic the temporal switch of hemoglobin that occurs in humans after their birth. Indeed, mice of this strain are born healthy with high expression of HbF (30%-50%) but experience a dramatic HbF to HbS transition soon after birth and subsequently begin to develop characteristics of SCD at approximately 3 weeks of age.

While both mouse models present limitations in modeling some aspects of SCD pathophysiology, they do exhibit the major features of SCD, including irreversibly sickled cells (ISCs), anemia, multiorgan pathology, inflammation, oxidative stress, and endothelial activation, making them particularly useful to study this pathology (Kamimura et al., 2023; Manci et al., 2006). It is, however, important to note that due to the large size of the β-globin locus, transgenic studies have only included a subset of genes from this locus with a minimal region of the locus control region (LCR). Therefore, the transgene construction in these strains does not reflect the complex chromosomal context and extensive epigenetic regulation of the human genome. Consequently, these models cannot fully predict the biological outcomes of perturbations at the native β-globin locus (Woodard et al., 2022). While ongoing efforts aim to develop more sophisticated animal models, their implementation will still take some time and could prove too challenging in a laboratory setting (Franks et al., 2020; Kuczynski et al., 2022). Therefore, while having some limitations, SCD mice are still the best tools at our disposal to study this pathology *in vivo*.

II. Erythropoiesis

A. Human Erythropoiesis at Steady State

RBCs are generated from hematopoietic stem cells residing in the BM through a dynamic multi-step differentiation process known as erythropoiesis (Orkin, 2000). In the BM, erythroid cells differentiate within a hypoxic microenvironment, with an oxygen level between 1-7% (Mohyeldin et al., 2010; Yeo et al., 2018). The classical model for erythropoiesis posits a hierarchical process that progresses through four phases: (1) erythroid progenitor (EP) development, (2) early erythropoiesis, (3) terminal erythroid differentiation, and (4) erythrocyte maturation.

Early in hematopoiesis, HSCs form multipotent progenitors (MPPs), which can give rise to common lymphoid progenitors (CLPs) or common myeloid progenitors (CMPs). CLPs are committed to the lymphoid lineages, while CMPs are committed to myelo-erythroid lineages. CMPs give rise to two bipotent progenitors: granulocyte-monocyte progenitors (GMPs) and megakaryocyte-erythroid progenitors (MEPs), which have the potential to form erythroid or megakaryocytic progenitors (Figure 10).

This classical model of hematopoiesis, widely utilized as a reference, has significantly contributed to our understanding of HSC differentiation. However, it is likely an oversimplification of the complexity of hematopoiesis. Indeed, studies have indicated that some committed progenitors may branch off earlier in the hierarchy (Mercier & Scadden, 2015; Notta et al., 2016). Moreover, new types of HSPCs have been identified and extensively studied due to their lineage biases (Benz et al., 2012; Dykstra et al., 2007; Muller-Sieburg et al., 2004; Müller-Sieburg et al., 2002). Recent research using single-cell technology and genetic mouse models now suggests that rather than occurring through distinct steps, hematopoiesis may occur through a continuous process of differentiation. This new perspective challenges the notion of hierarchical, stepwise progression, proposing instead that individual HSCs gradually acquire lineage biases along multiple directions without the necessity of passing through hierarchically organized progenitor populations (Velten et al., 2017).

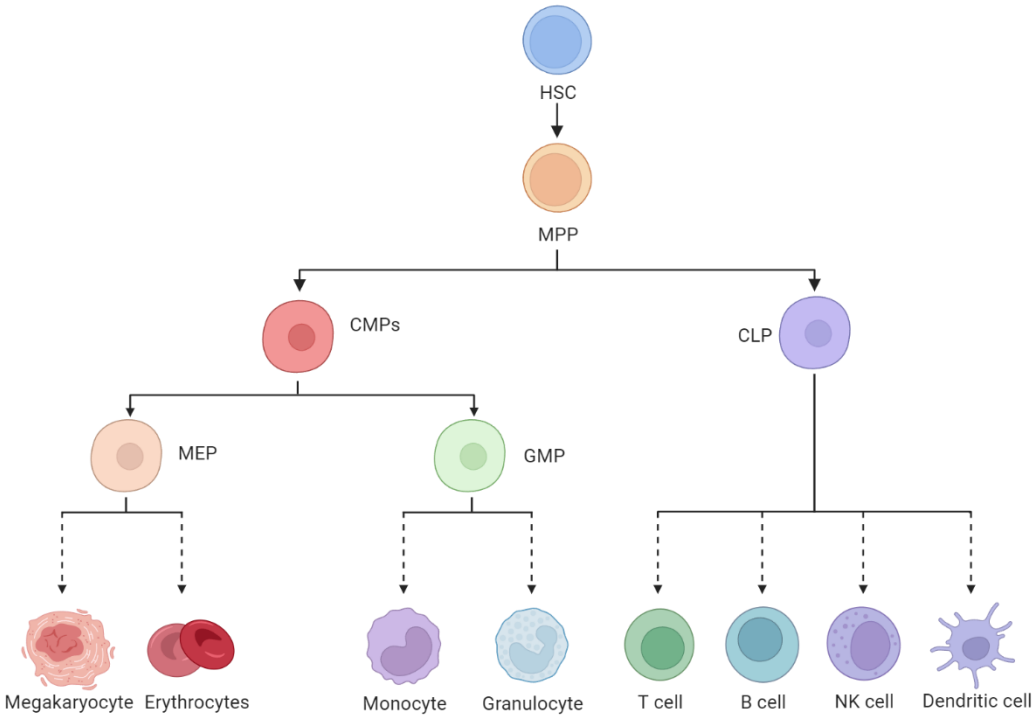

Figure 10: The classical model of human hematopoiesis. HSCs give rise to MPPs that bifurcate into CMPs and CLPs. CMPs further differentiate into GMPs and MEPs, both of which differentiate into their respective lineages; GMPs give rise to granulocytes and monocytes, whereas MEPs give rise to megakaryocytes and erythrocytes. Lymphoid lineages are derived from CLPs. Figure created with biorender.com and adapted from Schippel & Sharma, 2023. HSC = Hematopoietic stem cell;

MPP = multipotent progenitor; CLP = common lymphoid progenitor; CMP = common myeloid progenitor; GMP = granulocyte-monocyte progenitor; MEP = megakaryocyte-erythroid progenitor

During early erythropoiesis, unipotent progenitor cells arise from MEPs, named Burst Forming Units-Erythroid (BFU-E), which further differentiate into Colony Forming Units-Erythroid (CFU-E) (Schippel & Sharma, 2023). Following this step, terminal differentiation occurs with the differentiation of CFU-Es into proerythroblasts (ProEs) which then sequentially differentiate into early basophilic (EBaso), late basophilic (LBaso), polychromatic (PolyE), and orthochromatic erythroblasts (OrthoE) (Zivot et al., 2018). During this phase, hemoglobin accumulates in the cells while their size decreases, and their nucleus gets increasingly condensed before being expelled at the enucleation step (Granick & Levere, 1964).

Terminal differentiation takes place in the erythroid niche within specialized structures known as erythroblastic islands, where a central macrophage surrounded by up to 30 cells at different maturation stages drives erythroid proliferation and differentiation and phagocytes the extruded nuclei (Chasis & Mohandas, 2008). After enucleation, reticulocytes are released in the circulation, where they mature into erythrocytes and acquire their characteristic biconcave shape through membrane remodeling processes (Chasis & Schrier, 1989; Griffiths, Kupzig, Cogan, Mankelow, Betin, Trakarnsanga, Massey, Parsons, et al., 2012) (Figure 11). Red blood cells can then stay in the circulation for up to 120 days, during which they are constantly surveyed by macrophages within the reticuloendothelial system of the spleen (de Back et al., 2014).

It is important to note that while the classical model of erythropoiesis has been extensively used as a reference in many studies, it is very likely that this model represents a simplified version of adult human erythropoiesis and that there may be significant heterogeneity in cells at the stem, progenitor, and erythroblasts stages (Doulatov et al., 2012; Schippel & Sharma, 2023).

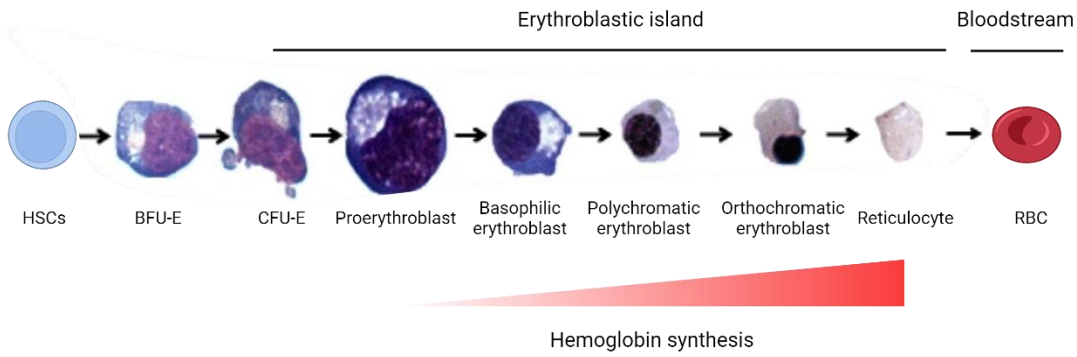

Figure 11: Human erythropoiesis. Overview of erythropoiesis, from the hematopoietic stem cell (HSC) to the red blood cell (RBC) (Zivot et al., 2018).

B. Monitoring of Erythropoiesis

The study of *ex vivo* erythroid differentiation has played an instrumental role in unraveling the mechanistic and molecular changes that occur during erythropoiesis. As cells differentiate, the expression of many membrane surface antigens changes over time, allowing differentiation to be tracked and quantified using fluorescence-activated cell sorting (FACS)-based methods (Figure 12A).

1. Hematopoietic Stem Cells

Extensive research has been conducted on the hematopoietic stem and progenitor cells (HSPC) populations preceding EPs (MPPs, CMPs, and MEPs). However, the establishment of a standardized set of markers to identify and isolate these different populations has yet to be put in place. The strategy proposed by the Weissman group, using the markers CD34, CD38, CD45RA, CD123, and CD90, has been adopted in many studies (Majeti et al., 2007). Nevertheless, other published strategies using different sets of markers are also in use (Doulatov et al., 2010). Thus, further RNA-seq, flow cytometry, and proteomic studies are needed to compare populations isolated through the alternative immunophenotyping strategies to propose a standard set of surface markers or genomic signatures for each HSPC population (Schippel & Sharma, 2023).

2. Erythroid Progenitors

Until recently, BFU-Es and CFU-Es had been characterized as $CD45^{+}GPA^{-}CD123^{-}CD34^{+}CD36^{-}CD71^{low}$ and as $CD45^{+}GPA^{-}CD123^{-}CD34^{+}CD36^{-}CD71^{high}$ cells, respectively, in cultured and BM cells (Li et al., 2014; Yan et al., 2018). However, in a recent study, Yan et al. showed that by integrating CD105 into this panel, human EP populations could be further subdivided into four subpopulations, with EP1 representing predominantly BFU-E and EP2, EP3 and EP4 representing increasingly mature CFU-E populations. All 4 populations could be differentiated based on their CD34 and CD105 expression profiles and had a reduced proliferative responsiveness to stem cell factor (SCF), indicating the presence of heterogeneity in committed progenitors (Yan et al., 2021) (Figure 12B).

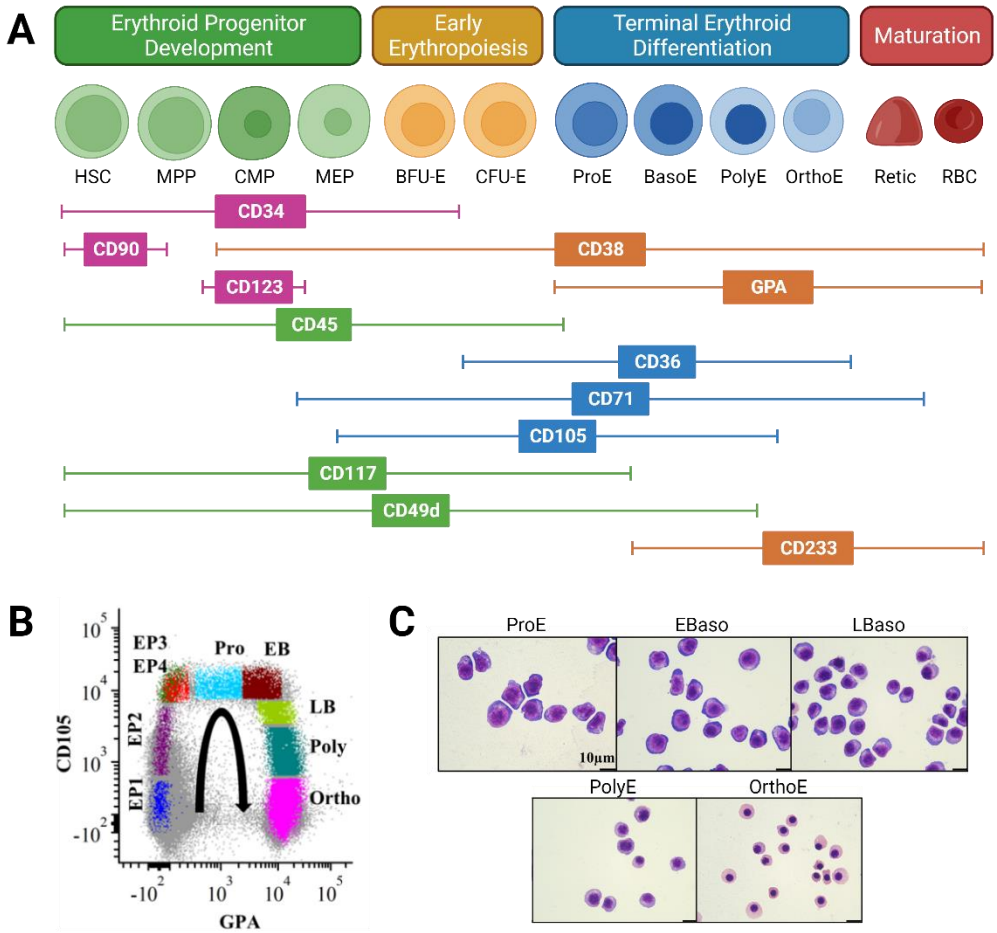

Figure 12: Flow cytometry analysis for the isolation of human erythroblasts. (A) Erythropoiesis occurs through four stages: erythroid progenitor development, early erythropoiesis, terminal erythroid differentiation, and maturation. Expression patterns for markers that are expressed only in HSPCs (pink), arise in HSPCs and extend at least into terminal differentiation (green), are transient in early erythropoiesis and terminal differentiation (blue), and are present in mature erythroid cells (orange) are depicted below. **(B)** Dot plot overlay of gated erythroid progenitor and erythroblast populations showing their expression of CD105 and GPA. The color of each population sources from the gating plot **(C)** May-Grünwald Giemsa staining of sorted erythroblasts at distinct stages from primary bone marrow. Created with biorender.com and adapted from Schippel Schara, 2021. HSC = hematopoietic stem cells, MPP = multipotent progenitor, CMP = common myeloid progenitor, MEP = megakaryocyte-erythroid progenitor, BFU-E = burst forming units-erythroid, CFU-E = colony forming units-erythroid, ProE = proerythroblasts, BasoE = Basophilic erythroblasts; EBaso = early basophilic erythroblasts, LBaso = Late basophilic erythroblasts, PolyE = polychromatic erythroblasts, OrthoE = orthochromatic erythroblasts, Retic = reticulocytes, RBC = red blood cell.

3. *Terminal Differentiation*

Hu et al. developed a strategy combining the expression of glycophorin A (GPA), Band 3, and CD49d (α4-integrin) to distinguish the erythroblast stages during terminal differentiation. They found that, within the GPA^+ cell population, the expression of CD49d was the highest in ProEs and gradually decreased over time. In contrast, the expression of Band 3 initially started at low levels at the basophilic stage and progressively increased throughout terminal differentiation (Hu et al., 2013). Using these markers, all 5 erythroblast stages could be purified, both *in vivo* and *in vitro*, and were found to exhibit expected morphological characteristics, as well as distinct proteome and transcriptome compositions (Gautier et al., 2016; Hu et al., 2013). Interestingly, Yan et al. showed that the expression kinetics of

CD105 could also be used to identify all different erythroblast stages. Indeed, their paper showed that all erythroblasts were $CD71^{+}GPA^{+}Syto16^{+}$, and the stages could be distinguished based on CD105 and GPA profiles (Yan et al., 2021) (Figure 12B).

In addition to FACS analyses, serial transplantation assays, *in vitro* colony-forming cells assays, and morphological analyses using May Grünwald Giemsa (MGG) staining (Figure 12C) are typically utilized for characterization and functional validation of HSPCs, committed EPs and erythroblasts, respectively (Hu et al., 2013; Kondo et al., 1997; Notta et al., 2011; Stephenson et al., 1971).

C. Regulation of Erythropoiesis

On average, the human body generates two million erythrocytes per second (Palis, 2014). Production at this scale requires an intricate regulation involving a complex interplay between growth factors, transcription factors, metabolic pathways, and microenvironmental signaling.

1. Cytokines

a. The HIF-EPO Pathway

A key regulator of erythropoiesis is erythropoietin (EPO), a glycoprotein synthesized in response to low tissue oxygenation whose expression is necessary to maintain the daily renewal of RBCs (Kuhrt & Wojchowski, 2015). Indeed, a negative feedback system, in which tissue oxygenation controls EPO production and EPO controls RBC production, provides homeostasis in oxygen delivery to body tissues.

Within the kidney, specialized peritubular fibroblasts are the major production sites of EPO. These cells employ the hypoxia inducible factors (HIF) pathway to regulate EPO production in response to oxygen levels (Jelkmann, 2004; Rogers et al., 2008). In normoxic conditions, the α subunit of the HIFs is hydroxylated by prolyl hydroxylase domain 2 (PHD2), an oxygen sensor enzyme. Subsequently, it binds to the von Hippel-Lindau ubiquitin ligase complex, which triggers its proteasomal degradation. Under hypoxia, this process is attenuated, and HIF-α can translocate to the nucleus, bind to its heterodimerization partner HIF-β and other co-factors, and mediates the expression of the *EPO* gene by binding to its 5' hypoxia response element (HRE) (Majmundar et al., 2010; Storti et al., 2014) (Figure 13). After being synthesized, EPO is secreted in the bloodstream and acts primarily on erythroid progenitors and early precursors by binding to the EPO receptor (EPOR) on their surface (Broxmeyer, 2013). Upon EPO binding, the EPOR signaling through Janus kinase 2 (JAK2) triggers the activation of multiple intracellular signal transduction pathways, including signal transducer and activator of transcription 5 (Stat5), phosphoinositide-3 kinase/Akt (PI3K/AKT), and p42/44 mitogen-activated protein kinase (MAPK) pathways. The activation of these pathways reduces apoptosis and promotes progenitor survival, proliferation, and differentiation (Broxmeyer, 2013).

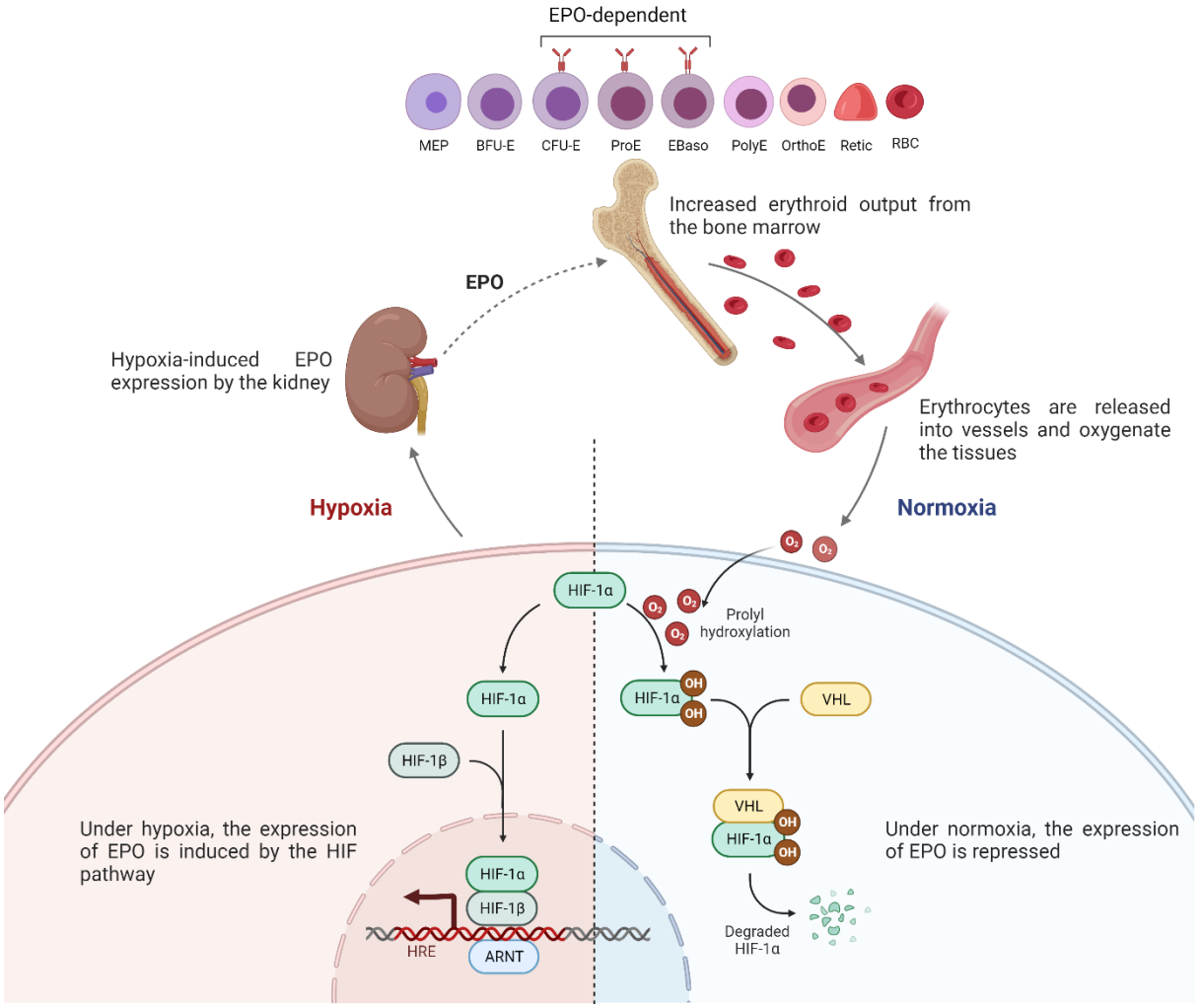

Figure 13: Stages of erythroid differentiation and oxygen-dependent feedback loop regulated by EPO. Hypoxia leads to the expression EPO by kidney cells. EPO binds to EPOR which is expressed on CFU-E, proerythroblasts and early basophilic erythroblasts, preventing these progenitor cells from apoptosis. Subsequently, increased erythrocytes in circulation lead to improvement of tissue oxygenation and therefore decreased EPO production. Figure created with biorender.com. EPO = erythropoietin, MEP = megakaryocyte-erythroid progenitor, BFU-E = burst forming unit erythroid, CFU-E = colony forming unit erythroid, ProE = proerythroblast, BasoE = basophilic erythroblast, PolyE = polychromatic erythroblast, OrthoE = orthochromatic erythroblast, RBC = red blood cell, HIF = hypoxia-inducible factor, HRE = hypoxia responsive element VHL = von Hippel lindau.

b. SCF and c-kit

Additional factors work synergistically with EPO to regulate erythropoiesis, such as SCF, thrombopoietin (TPO), Transforming Growth Factor-α (TGF-α), insulin-like growth factor 1 (IGF-1), and interleukins 1, 3, 6 and 10. Among these, only SCF was shown to be essential for *in vivo* erythropoiesis, as its deletion in mice resulted in severe anemia with varying erythroid progenitor defects (Broudy, 1997). SCF exerts its function by binding to and activating the receptor tyrosine kinase c-kit (CD117) (Lemmon & Schlessinger, 2010). Activation of c-kit leads to its autophosphorylation and the initiation of signal transduction that allows the survival and proliferation of BFU-Es and CFU-Es, as well as ProEs (Nocka et al., 1989; Sui et al., 2000). It also promotes HSC maintenance and stimulates cell cycle entry by activating the PI3K/AKT/FOXO pathway (Miyamoto et al., 2007). Furthermore, by binding to c-kit, SCF

can indirectly phosphorylate EPOR, activate EPO/EPOR signaling pathway, and thus also promote the survival, proliferation, and differentiation of early erythroid progenitors through this action (Jacobs-Helber et al., 1997).

2. *Transcriptional Regulation of Erythropoiesis*

The complex transcriptional programs that define erythropoiesis are coordinated by a set of potent transcription factors, the expression of which is capable of transdifferentiating non-erythroid cells into erythroid cells (Capellera-Garcia et al., 2016).

The GATA family of transcription factors, which comprises six members (GATA1 through GATA6), recognizes and binds to a specific DNA motif, (A/T) GATA (A/G), through two characteristic zinc-finger regions conserved among the six family members (Ko & Engel, 1993; Orkin, 1992). Of these, only GATA1 and GATA2 play crucial roles regulating erythropoiesis. Gene ablation studies in mice revealed that GATA1 is essential for the survival and differentiation of erythroid progenitors, while GATA2 regulates the maintenance and proliferation of HSPCs (Gutiérrez et al., 2008; Menendez-Gonzalez et al., 2019). Initially, GATA2 is abundantly expressed in HSPCs. However, its expression declines after the erythroid commitment of progenitors, where the increased expression of GATA1 displaces it at the multiple GATA-binding sites of the *GATA2* gene and suppresses its expression. This transcriptional change, known as GATA factor switching, is essential for survival and terminal differentiation (Kaneko et al., 2010) (Figure 14). GATA-1 is considered the master regulator of erythropoiesis as it regulates all aspects of erythroid maturation and function. Indeed, genome-wide occupancy studies (ChIP-seq) have shown that all erythroid genes are regulated by GATA1, including genes involved in heme and globin synthesis, glycophorins, anti-apoptotic genes, genes involved in cell cycle regulation, and the *EPOR* gene (Cheng et al., 2009).

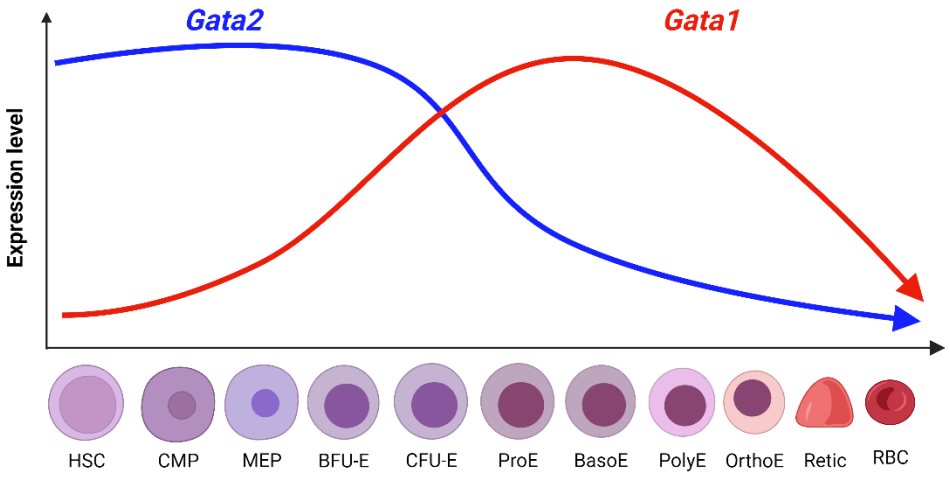

Figure 14: Reciprocal expression profiles of GATA1 and GATA2 during erythropoiesis. GATA1 expression is initiated at the CMP stage and reaches a peak at the ProE stage. From the late erythroblast stages onward, GATA1 expression levels decrease toward the maturation of RBC. GATA2 is preferentially expressed in HSC and progenitor cells, including CMP, MEP, and BFU-E.

GATA2 expression is suppressed by the increase of GATA1 activity from CFU-E stage onward. Figure created with biorender.com and adapted from Moriguchi & Yamato, 2014. HSC = hematopoietic stem cells, CMP = CMP = common myeloid progenitor, MEP = megakaryocyte-erythroid progenitor, BFU-E = burst forming unit erythroid, CFU-E = colony forming unit erythroid, ProE = proerythroblast, BasoE = basophilic erythroblast, PolyE = polychromatic erythroblast, OrthoE = orthochromatic erythroblast, RBC = red blood cell.

KLF1, also known as EKLF (erythroid Krüppel-like factor), is another critical regulator of erythropoiesis initially identified by its ability to bind the β-globin promoter (Miller & Bieker, 1993). KLF1 can suppress the megakaryocyte program and promote erythroid fate in the early stages of differentiation (Frontelo et al., 2007). It also helps orchestrate the enucleation process by triggering cell-cycle exit and chromatin condensation during terminal erythroid maturation, which is essential to this process (Borg et al., 2010; Gnanapragasam et al., 2016). Many more transcription factors form complex networks of coactivators or corepressors to modulate target gene expression. These include a major player, TAL1, which along with LMO2 and LDB1, form a coactivator complex that binds GATA1 to activate the expression of erythroid-associated genes (Hattangadi et al., 2011; Porcher et al., 2017).

3. Metabolic Regulation of Erythropoiesis

Erythropoiesis relies on a complex interplay between iron, glucose, fatty acid, and amino acid metabolism to generate the necessary output of RBCs required to sustain oxygen transport. While the intricacies of these metabolic processes are still not fully characterized, significant advances on the subject have been made over the last decade. Notably, energy metabolism was identified as a crucial regulator that shapes the balance between self-renewal potential and lineage specification. In the hypoxic niche, quiescent HSCs maintain low metabolic activity and rely upon anaerobic glycolysis for their metabolic needs (Takubo et al., 2013; Yu et al., 2013). The suppression of oxidative phosphorylation (OXPHOS) in this environment was shown to be critical for the survival of quiescent HSCs, as lower ROS levels were associated with higher stem cell potential (Chen et al., 2008; Mantel et al., 2010; Suda et al., 2011; Yu et al., 2013). Additionally, lipid metabolism, primarily fatty acid oxidation (FAO), has emerged as a critical regulator of HSC self-renewal, as inhibition of this process was shown to induce symmetric commitment of HSC daughter cells and loss of HSC quiescence (Ito et al., 2012; Yusuf & Scadden, 2012).

Furthermore, the maintenance of amino acid homeostasis was shown to play a critical role during erythropoiesis. Oburoglu et al. demonstrated that glutamine and its transporter, ACST2, are essential for the erythroid lineage commitment of $CD34^+$ HSCs (Oburoglu et al., 2016; Oburoglu et al., 2014). More specifically, they showed that HSC commitment to the erythroid lineage depends on glutamine-dependent *de novo* nucleotide biosynthesis. In the same study, they showed that nucleotides provided through the shunting of glycolytic metabolites into the pentose phosphate pathway (PPP) could enhance the magnitude and kinetics of HSC erythroid commitment, further highlighting the

importance of nucleotide in this process (Oburoglu et al., 2016; Oburoglu et al., 2014). More recently, the metabolism of arginine has also been identified as a crucial factor for erythroid differentiation (Gonzalez-Menendez et al., 2023). Indeed, spermidine, one of the catabolic products of arginine, is required for the hypusination of eukaryotic translation initiation factor 5A (eIF5A), a posttranslational modification specific to this protein. They found that hypusination of eIF5A promotes translation elongation and termination, allowing optimal protein synthesis during erythropoiesis. Importantly, under conditions where hypusination was prevented, HSPCs were not capable of undergoing erythroid differentiation and instead maintained their myeloid lineage fate (Gonzalez-Menendez et al., 2023).

As HSCs become mobilized and differentiate, their metabolism switches and relies on oxidative phosphorylation to meet the nutrient and energy demands of the cell (Ansó et al., 2017; Liu et al., 2017; Luo et al., 2017; Oburoglu et al., 2014). Gonzalez-Menendez et al. demonstrated that glutaminolysis participates in this process by generating α-ketoglutarate (αKG), which contributes to the tricarboxylic acid cycle (TCA) and directly increases oxidative phosphorylation in human erythroid precursors (Gonzalez-Menendez et al., 2021). Further studies have highlighted the importance of glutamine and its products in the regulation of erythropoiesis. For example, glutamine-derived production of succinyl-coenzyme A (succinyl-CoA) was shown to be essential to the production of heme (Burch et al., 2018). Additionally, glutamine, as well as leucine and arginine, were found to activate the mammalian target of rapamycin (mTOR) pathway, a signaling cascade regulating multiple cellular processes such as mitochondrial biogenesis, ROS production, and globin production (Chung et al., 2015; Jewell et al., 2013). Finally, Huang et al. found that phosphocholine metabolism is essential for erythroid differentiation, as it helps provide the cell with glycine and serine, two additional amino acids essential for protein synthesis (Huang et al., 2018).

During terminal differentiation, erythroid cells go through extensive alterations resulting in hemoglobin accumulation, nucleus expulsion, and the loss of all organelles, including mitochondria (Moras et al., 2017). In response to these changes, late-stage differentiated cells shift their energy metabolism from OXPHOS to anaerobic glycolysis. To adapt to these metabolic requirements, cells progressively decrease their glutamine uptake and rely on IDH1 to decrease αKG-driven OXPHOS (Gonzalez-Menendez et al., 2021). Simultaneously, glucose uptake increases during erythroblast maturation, leading to the upregulation of Glut1, the glucose transporter, at this stage (Montel-Hagen et al., 2008). Of note, human erythrocytes express a higher level of Glut1 than any other cells in the body, with over 300,000 copies of Glut1 per cell (Mueckler, 1994). Despite this metabolic switch, mitochondria activity is sustained by pyruvate until the enucleation stage, where low levels of OXPHOS are required for enucleation to occur (Liang et al., 2021).

Looking ahead, the recent emergence of novel technologies, such as the SCENITH and met-flow approaches, may help offer new insights about the heterogeneity and plasticity of metabolism during erythropoiesis at the single cell level (Ahl et al., 2020; Argüello et al., 2020).

4. *HSP70 and Caspase 3*

Healthy mature erythroblasts exhibit some features of apoptosis, such as mitochondrial depolarization and the transient activation of caspases. This activation is crucial for the proper progression of erythropoiesis. Indeed, the inhibition or depletion of caspase 3 in erythroid cells has been shown to induce maturation arrest (De Maria et al., 1999; Koury & Bondurant, 1988).

Caspase 3 also plays a significant role in the GATA1 signaling pathway (Boehm et al., 2013). It has been shown that GATA1 is protected from caspase-mediated proteolysis by interacting with the chaperon heat shock protein 70 (HSP70). For this interaction to occur, HSP70 must be translocated from the cytoplasmic to the nuclear compartment. This translocation can only occur in the presence of EPO, as EPO starvation leads to HSP70 being exported from the nucleus. HSP70 export, in turn, leaves GATA1 exposed to caspase-3 activity and results in differentiation arrest and apoptosis (Ribeil et al., 2007). This EPO-dependent mechanism ensures that no excessive erythrocyte production occurs (Figure 15).

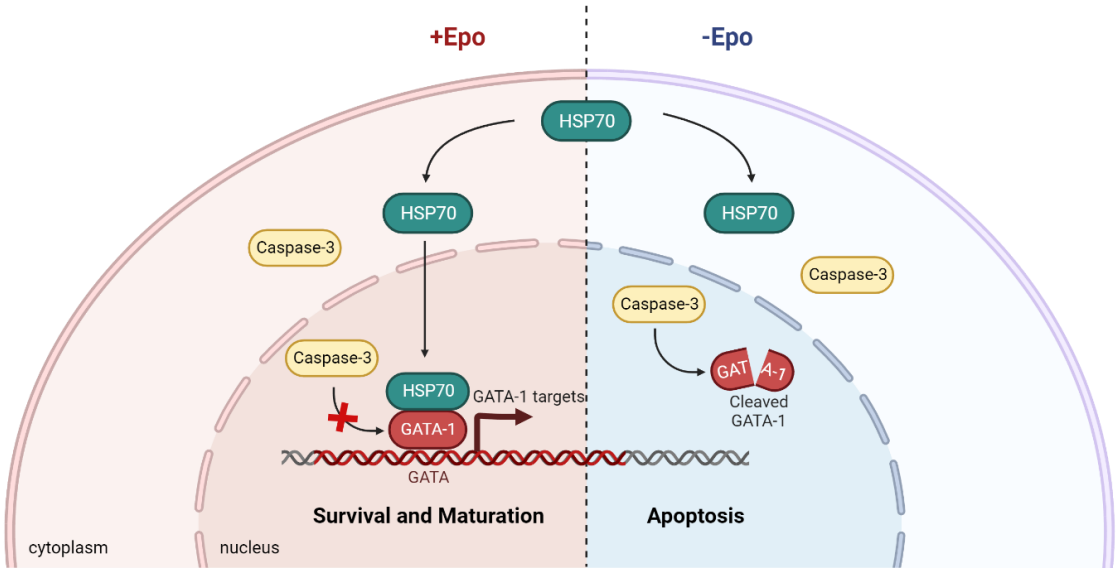

Figure 15: GATA-1 protection by HSP70 during terminal erythroid differentiation. Figure created with Biorender.com based on Ribeil et al 2007.

D. *Ex vivo* culture Systems of Erythropoiesis

Studies of human erythropoiesis have relied, for the most part, on the *in vitro* differentiation of HSPCs. Furthermore, the production of cultured RBCs holds the potential of an unlimited source of RBCs for transfusion purposes. Considering this, significant efforts have been dedicated to developing culture systems that can closely replicate the stages of human erythropoiesis and yield a substantial number of enucleated RBCs.

Fibach et al. were the first group to reportedly generate RBCs from $CD34^+$ HSPCs (Fibach et al., 1989). Since then, researchers have refined methods of primary human cell culture to obtain larger numbers of erythroid cells from relatively few HSPCs obtained either from BM (Neildez-Nguyen et al., 2002), peripheral blood (Migliaccio et al., 2002; Tirelli et al., 2011; van den Akker et al., 2010), umbilical cord blood (Baek et al., 2008; Leberbauer et al., 2005; Miharada et al., 2006), induced pluripotent stem cells (iPSCs) (Netsrithong et al., 2020), and embryonic stem cells (ESCs) (Olivier et al., 2016). These two-dimensional culture systems vary based on the number of stages involved in the culture, the presence or absence of feeder layers, as well as the various cytokines, growth factors, and steroids that may be added to the culture medium to potentiate the expansion or differentiation of cells in culture (Table 2) (Severn & Toye, 2018). Overall, all protocols follow the same steps of (1) isolating stem progenitor cells, (2) expanding the stem progenitor cells and differentiating them into the erythroid lineage, and (3) enucleating erythroid cells to give rise to mature RBCs. Although all these culture systems can produce varying amounts of enucleated erythrocytes, they all have their own challenges and limitations. Predominantly, issues such as low enucleation rates, insufficient proliferation, and persistence of fetal hemoglobin levels are the most frequently observed constraints.

Source and culture period	General protocol	Expansion	Enucleation rate	Key point	References
CB $CD34^+$ 21 days	Three stage, serum free	2 x 10^5-fold	4%	Low enucleation rate	(Neildez-Nguyen et al., 2002)
Peripheral blood MNC 13 days	HEMA culture	1 x 10^3-fold	-	-	(Migliaccio et al., 2002)
Mobilized leukapheresis $CD34^+$ 21 days	Three stages with co-culture	1.22 x 10^5-fold	98%	First co-culture with murine stromal cells	(Giarratana et al., 2005)
CB MNC, 60 days	Two stage, serum free	1x 10^9	~100%	Prolonged expansion period	(Leberbauer et al., 2005)
CB $CD34^+$ 20 days	Four stages	7 x 10^6-fold	77%	-	(Miharada et al., 2006)
CB MNC 21 days	Three stage, serum free with co-culture	8.2 x 10^3-fold	47%	Higher expansion rates when CB feeder cells used not BM feeder cells	(Baek et al., 2008)
Peripheral blood MNC	Three phases	2.3 x 10^8	>90%	First demonstration of bioreactor use	(Timmins et al., 2011)
Peripheral blood MNC 14 days	HEMA culture	2.7 x 10^9	-	CFU and flow cytometry analysis	(Tirelli et al., 2011)
Peripheral blood $CD34^+$	Three stages	6.15 x 10^4-fold	68%	2,5 ml packed reticulocytes and transfusion of in vitro cultured reticulocytes	(Giarratana et al., 2011)
Peripheral blood $CD34^+$	Three stages	>10^4 fold	55-95%	5 ml packed reticulocytes	(Griffiths, Kupzig, Cogan, Mankelow, Betin, Trakarnsanga, Massey, Lane, et al., 2012)
Peripheral blood $CD34^+$	Three stages	>10^5 fold	63%	10 ml packed reticulocytes under GMP conditions	(Kupzig et al., 2017)

Table 2: Examples of published erythroid culture systems in which expansion rates and enucleation rates were provided from Severn & Toye, 2018.

These traditional two-dimensional culture systems cannot effectively translate marrow physiology *ex vivo* as they lack the microenvironmental niches, the spatial oxygen gradients, and the dense cellularity found in the human BM (Allenby et al., 2019). New advances in the bioengineering field are now allowing researchers to move from two-dimensional cultures to more intricate three-dimensional models of the BM, with different levels of complexity. Approaches introducing active agitation in the culture, with the use of rotary culture systems or bioreactors, were shown to increase nutrient homogeneity and oxygen transfer and were able to produce high quantities of enucleated cells (S. Y. Han et al., 2021; Heshusius et al., 2019; Ratcliffe et al., 2012). Tools like hydrogels (Raic et al., 2014), solid scaffolds (Severn et al., 2019), and three-dimensional environments made of fibers can be used to mimic the intricacies of the BM micro-environment (Allenby et al., 2019; Housler et al., 2012). These more complex models have been shown to provide a better expansion of HSCs in long-term cultures and allow the generation of erythroblastic islands and enucleated erythrocytes. They could thus prove to be valuable tools for studying erythropoiesis in the future.

E. Ineffective Erythropoiesis in Hemoglobinopathies

1. Thalassemia disorders

β-thalassemia refers to a group of inherited hemolytic disorders characterized by reduced production (β-thalassemia intermedia) or complete absence (β-thalassemia major) of β-globin chains. Ineffective erythropoiesis is the core driver of β-thalassemia and the main cause of its clinical manifestations. Notably, patients with β-thalassemia major have 5- to 6-fold more erythroid precursors than healthy individuals, with a 4-fold increase in cell death (Centis et al., 2000). In this pathology, the imbalance between α and β chains triggers a cascade of events leading to the premature cell death of erythroid precursors (Figure 16). A study by Arlet et al. conducted in β-thalassemia major showed that the excess α-globin chains within the cytoplasm form molecular aggregates that interact with HSP70 and prevent its translocation to the nucleus. In this context, GATA1 is no longer protected from caspase-3 cleavage, leading to end-stage maturation arrest and apoptosis of differentiating precursors (Arlet et al., 2014). The resulting anemia causes hypoxia and increases EPO production, which, in turn, enhances erythroid differentiation and accumulation of immature precursors resulting in medullary expansion (Arlet et al., 2016).

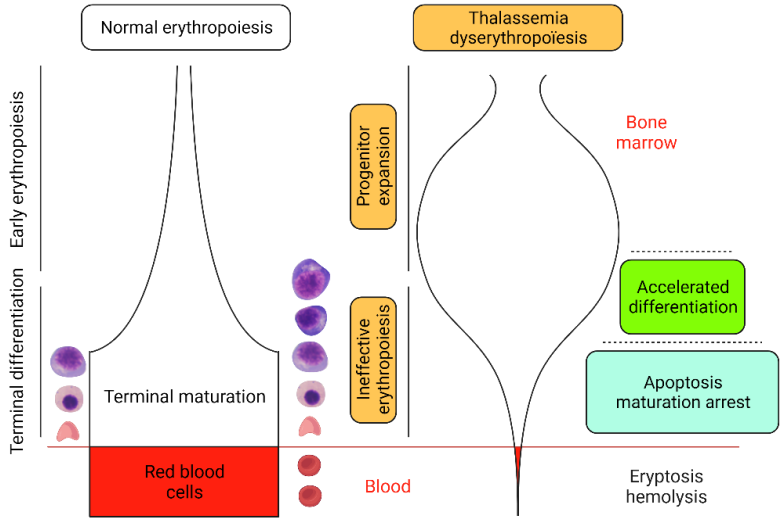

Figure 16: Difference between normal and β-thalassemia ineffective erythropoiesis (Ribeil et al., 2013).

In α-thalassemia, which arises from the underproduction or absence of α-globin synthesis, excess β-globin chains have also been described as damaging to maturing erythroid precursors. Indeed, the unpaired β-globin chains can form insoluble homotetramers leading to intracellular precipitation, acute hemolytic anemia, and ineffective erythropoiesis (Shinar et al., 1989; Yuan et al., 1995). However, the characterization of this ineffective erythropoiesis has not been as comprehensive as for β-thalassemia. Furthermore, in some patients, the free β-globin chains have been found to aggregate preferentially in older RBCs in the peripheral blood, with minimal impact on erythropoiesis, suggesting that α-thalassemia is a predominantly a hemolytic disease with minimal ineffective erythropoiesis (Amid et al., 2016)

2. *Sickle Cell Disease*

Although SCD is not primarily defined as a pathology with ineffective erythropoiesis, several studies showed abnormalities during terminal erythropoiesis in SCD, suggesting that anemia could also be impacted by defects of central origin in this pathology. For example, erythroid precursors were found to undergo sickling under deoxygenating conditions in both *in vitro* experiments and within the BM of SCD patients, with extensive marrow erythrophagocytosis (Grasso et al., 1975; Hasegawa et al., 1998). Such sickling was also reported in the SAD SCD mouse model, where late-stage erythroid precursors displayed morphologic alterations. In this context, morphological studies found high levels of hemoglobin polymers, which were associated with increased cell fragmentation occurring during the migration of reticulocytes across the endothelial layer in the BM (Blouin et al., 1999). The study of Wu and collaborators showed evidence of ineffective erythropoiesis occurring in the BM of transplanted SCD patients, where donors' healthy cells were found to have a survival advantage over SCD erythroid cells (Wu et al., 2005). Furthermore, SCD has been shown to have potentially long-term adverse effects on the BM in mice. This includes BM ischemia resulting from vaso-occlusion, pathologic angiogenesis

within the BM microenvironment, and BM hyperplasia triggered by anemia and tissue hypoxia (Park et al., 2020). These processes could contribute to the activation of osteoclasts and subsequent bone loss and could impair erythropoiesis over time. Our recent and current work has shown apoptosis between the PolyEs and OrthoEs stages, with HbF being a critical protective factor against it (El Hoss et al., 2021).

III. Macrophages

A. Tissue Macrophages and their Origins

Macrophages are highly plastic effector cells involved in both inflammation and tissue homeostasis. Based on these two properties, Mill et al. proposed a classification dividing macrophages into either classically activated (M1) or alternatively activated (M2) macrophages (Mills et al., 2000). In this model, M1 macrophages are pro-inflammatory mediators with pathogen-killing abilities, producing high levels of ROS, NO, and pro-inflammatory cytokines such as IL-1, 2, 6, 12, TNF-α, and IFN-γ. In contrast, M2 macrophages promote cell proliferation and tissue repair and secrete anti-inflammatory cytokines such as CCL-18, CCL-22, and IL-10. To refine this dual model, the M2 phenotype was later divided into M2a, M2b, M2c, and M2d subtypes based on the inducing agent and the resulting transcriptional changes (Mantovani et al., 2004; Roszer, 2015) (Figure 17A). While the M1/M2 nomenclature remains in use today, as it represents a simple model to distinguish between two opposing macrophage activities, it cannot be used to fully recapitulate the heterogeneity of tissue macrophages *in vivo* (Martinez & Gordon, 2014; Nahrendorf & Swirski, 2016).

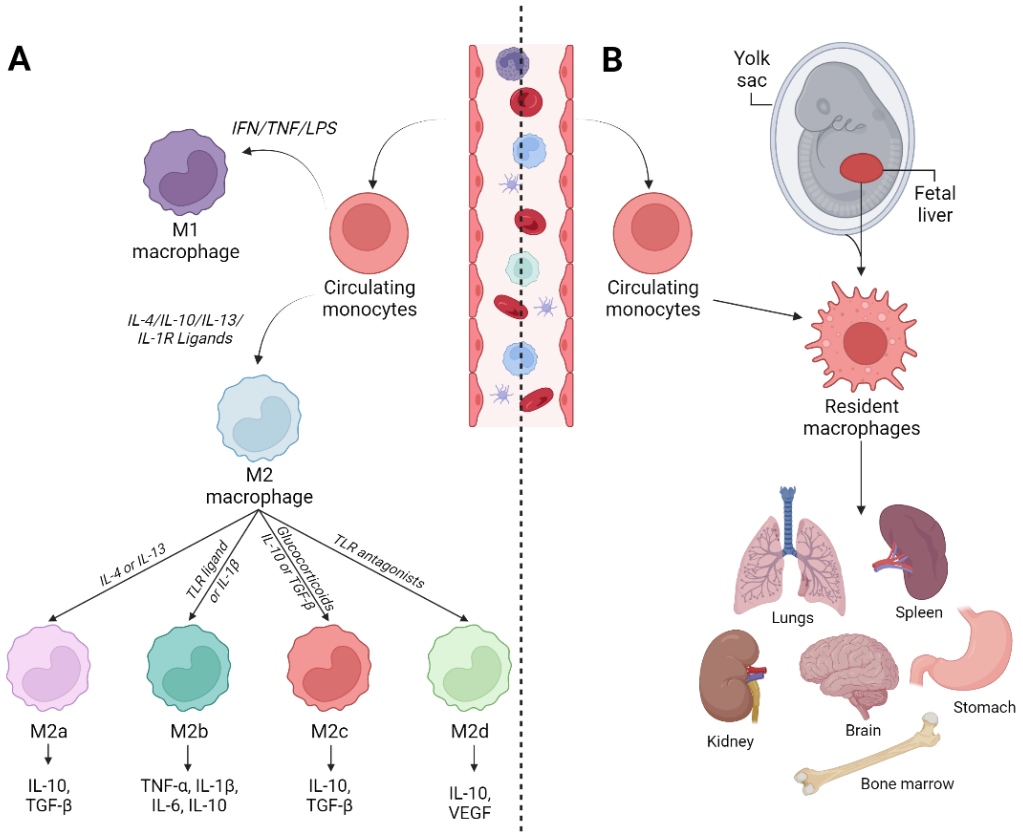

Figure 17: Origin and classification of macrophages. (A) Circulating macrophages are classified into M1 and M2 types according to their activators and functions. M2-type can be further subdivided into M2a, M2c, and M2d by different signal activation, cell surface markers, and their functions. **(B)** Based on the origin, tissue-resident macrophages can be divided into two subsets. One derives from the yolk sac and another population originates from hematopoietic progenitors and circulating monocytes. Figure created with biorender.com based on Chen et al., 2020.

Tissue-resident macrophages are present in virtually all tissues in mammals and are a highly diverse population due to complex and dynamic tissue-specific processes. For a long time they were believed to solely derive from circulating monocytes (van Furth & Cohn, 1968). However, in the past decade, parabiosis and fate-mapping experiments in mice have shown that most macrophages that reside in healthy adult tissues are established prenatally (Hashimoto et al., 2013; Yona et al., 2013). More specifically, primitive macrophages can arise without monocytic intermediates from yolk-sac macrophages and seed the whole embryo when blood circulation is established (Schulz et al., 2012). Once the fetal liver becomes the predominant embryonic site of hematopoiesis, resident macrophages can also arise from fetal liver monocytes (Gomez Perdiguero et al., 2015) (Figure 17B). The macrophages derived from both progenitors can self-maintain locally within their tissue of residence throughout life. As a result, most tissues in adult mice still harbor a significant fraction of macrophages of embryonic origin, with varying input from BM-derived monocytes. (Ginhoux & Guilliams, 2016). Overall, resident macrophages in most tissues do not require an ongoing input from circulating monocytes at steady state. However, during the depletion of the resident macrophage populations, either by experimental means or by inflammation, circulating monocytes have been shown to readily integrate into these macrophage pools and become self-renewing cells (Scott et al., 2016).

Although macrophage origins differ between organs, it does not impact their lifespan or function within their respective tissue. Instead, it was recently suggested that the properties of macrophages are determined not by their sources of origin but predominantly by their niche (Guilliams & Scott, 2017). This hypothesis was drawn from a study showing that yolk sac macrophages, fetal liver, and adult monocytes could efficiently colonize an empty alveolar niche in the mouse model *Cfsr2b* $^{-/-}$ regardless of their origin (van de Laar et al., 2016). Macrophage niches are thought to provide physical support as well as the specific signals necessary for the establishment, the self-maintenance capacities, and the tissue specification of their macrophages. Indeed, many functional studies and gene-expression analyses have shown that the local tissue environment of macrophages can modulate their transcriptional and epigenetic profile (Gautier et al., 2012; Lavin et al., 2014).

As a way to explain the differences in macrophage origin between tissues, Guilliams and Scott proposed a model of “niche competition” in which the highly plastic macrophage precursors compete for a restricted number of niches (Guilliams & Scott, 2017; Guilliams et al., 2020). In this model, the tight regulation of the niche could ensure that monocytes patrolling the tissues do not differentiate into

macrophages when the niche is full. However, when the niche is made available, during development or because of inflammation, monocytes can integrate the resident macrophage pool. Besides niche availability, another factor dictating tissue macrophage origin is thought to be niche accessibility, *i.e.*, whether macrophage precursors can access the organ via the circulation (Guilliams & Scott, 2017). Many ontology studies have been done in the past few years to identify the specific origin of resident macrophages in various organs. However, few studies have attempted to map the bone marrow macrophage origin.

B. Bone Marrow Macrophages

The BM is a complex organ encased within the bone structure, which can be divided into various compartments that are dependent on the presence of different cellular populations. Among these cells, different subsets of macrophages contribute to the regulation of erythropoiesis and hematopoietic stem cell niches, as well as bone homeostasis and repair. Three subsets of tissue resident macrophages are thought to reside in the bone: osteal macrophages, HSC niche macrophages, and macrophages from erythroblastic islands (Figure 18) (Kaur et al., 2018).

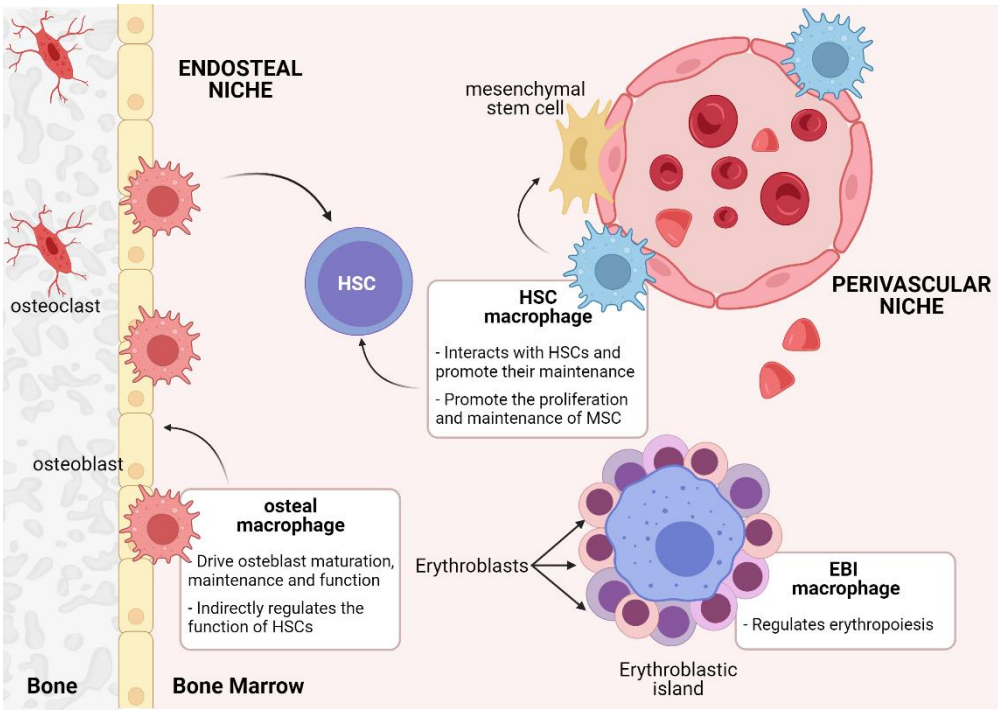

Figure 18: Different resident macrophage subsets within bone and bone marrow. EBI = erythroblastic island, HSC = hematopoietic stem cell, MSC = mesenchymal stem cells. Created with biorender.com and adapted from Kaur et al., 2017.

1. Osteal macrophages

A key population of BM macrophages is the osteal macrophages or "osteomacs". These cells can be found interspersed with other bone-lining cells at the endosteum and play a key role in bone formation and repair by driving osteoblast maturation, maintenance, and function (Chang et al., 2008; Winkler et al., 2010). Osteomacs can interact with diverse components of the hematopoietic microenvironment,

including osteoblasts and megakaryocytes, to regulate the function of HSPCs (Heideveld & van den Akker, 2017; Mohamad et al., 2017). They also have the potential to differentiate into osteoclasts, a specialized bone-resorbing multinucleated cell population. Furthermore, because of their localization, it was suggested that they might also serve as a phagocytic barrier between the bone and the BM to prevent disturbances between both tissues (Kaur et al., 2017). Osteomacs share similar phenotypical markers of BM-derived macrophages: they express, at different levels CD45, F4/80, CD68, CD11b, Ly-6G and CD169 and can be distinguished from inflammatory macrophages or osteoclasts by their lack of Mac2 and TRAP expression (Alexander et al., 2011; Alexander et al., 2017; Batoon et al., 2019; Chow et al., 2013a; Winkler et al., 2010). Even though most studies were conducted in mice, osteomacs were suggested to have a counterpart in human osteal tissues, as $CD68^+$ cells were observed both adjacent to the bone and within the bone microenvironment (Chang et al., 2008).

2. HSC niche macrophages

Besides osteomacs, other populations of resident macrophages are thought to be involved in the maintenance of HSC niches (Winkler et al., 2010). Within these specific microenvironments, these macrophages, also called "HSC macrophages", are thought to be in direct contact with both HSCs and other cells and exert their specialized functions to maintain niche homeostasis. In several studies, the function of these macrophages was assessed *in vivo* by depleting the monocyte/macrophage population from mouse BM, by using clonodrate-loaded liposomes, transgenic animals such as the MAFIA (macrophage Fas-induced apoptosis) or the CD169-diphtheria toxin receptor mice (Chow et al., 2011; Winkler et al., 2010). In these studies, the loss of BM macrophages led to the mobilization of HSCs out of the BM and into the peripheral blood and extramedullary lymphoid organs. This was associated with a decreased expression of retention factors by niche cells, such as CXCL12, suggesting that these macrophages crosstalk with niche components to retain HSC in the BM. For example, HSC macrophages were shown to promote the proliferation and maintenance of $nestin^+$ mesenchymal stem cells (MSCs), which in turn express a variety of HSC retention factors (Chow et al., 2011; Ehninger & Trumpp, 2011). Additional studies have suggested that macrophages also play a role in HSC dormancy through direct mechanisms. Indeed, Hur et al. demonstrated that HSC macrophages could interact with HSCs residing in the endosteal niches through CD234 to promote their quiescence (Hur et al., 2016). Finally, more recently, HSC macrophages were found to modulate HSC engraftment after transplantation (Kaur et al., 2018).

Although the specific identity of HSC macrophages is still ambiguous, they are currently described as being $CD11b^+F4/80^+Ly6G^{neg}CD169^+VCAM\text{-}1^+CD234^+$ in mice (Kaur et al., 2017). However, whether these cells correspond to a functionally and phenotypically homogenous population or represent different subsets of macrophages is still unclear (Heideveld & van den Akker, 2017; Kaur et al., 2018). Indeed,

significant overlaps remain in macrophage identification and depletion methods, making it difficult to determine the distinct contribution of each of these macrophage populations to hematopoietic processes. Consequently, the number of discrete BM macrophage populations and their potential plasticity remains to be investigated (McCabe & MacNamara, 2016). The final subset of BM macrophages described in the literature is the central macrophage of the erythroblastic island, which will be described in the next section.

C. Macrophages in Erythroblastic Islands

Erythroblastic islands (EBIs) are specialized microenvironments distributed uniformly across the BM, constituted by one or two central macrophages surrounded by rings of developing erythroblasts at various stages of maturation (Lee et al., 1988; Mohandas & Prenant, 1978). Since their first description in 1958, EBIs have been demonstrated *in vivo* at all sites of mammalian definitive erythropoiesis, namely the fetal liver, bone marrow, and splenic red pulp (Allen & Dexter, 1982). Morphologically, central macrophages are often large with many cytoplasmic protrusions, facilitating their interaction with up to 30 erythroblasts in human BM (Lee et al., 1988) (Figure 19).

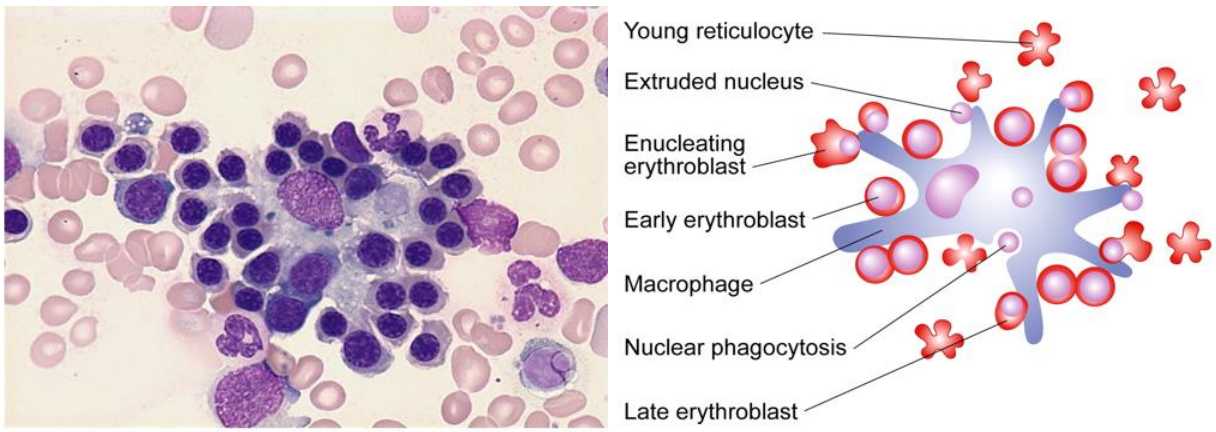

Figure 19: The erythroblastic island. May Grunwald Giemsa staining of an erythroblastic island (Author: Peter Maslak, Copyright © 2019 American Society of Hematology) associated with an illustration of the erythroblastic island with a star shaped central macrophage and early erythroblasts, late erythroblast, and enucleated reticulocyte (Chasis & Mohandas, 2008)

1. Diverse Contribution of Macrophages to Erythropoiesis

Within EBIs, central macrophages serve as anchors for erythroblasts providing the cellular interactions necessary for regulating erythroid proliferation and differentiation. They also help generate functional enucleated reticulocytes by engulfing and degrading the pyrenocytes after enucleation. Furthermore, central macrophages can regulate the rate of erythropoiesis through a balance of positive and negative feedback mechanisms (Figure 20). For example, macrophages have been shown to secrete IGF-1 to stimulate proliferation during the early stages of erythropoiesis (W. Li et al., 2019; Sawada et al., 1989). Under conditions of stress erythropoiesis, they have also been found to secrete bone morphogenetic protein 4 (BMP4) to promote proliferation of stress erythroid progenitors (Millot et al., 2010). Other

secreted factors were found to negatively regulate erythropoiesis, such as IL-6, TNF-α and INF-γ which downregulate erythroid differentiation, or TGF-β which is known to block erythroblast proliferation and survival (Bohmer, 2004; Dai et al., 2003; De Maria et al., 1999; Zermati et al., 2000). In addition, INF-γ induce the secretion of TNF related apoptosis inducing ligand (TRAIL) by both macrophage and erythroblasts, which was also shown to inhibit erythroid differentiation (Zamai et al., 2000). Of note, erythroblasts also contribute to the EBI integrity by secreting vascular endothelial growth factor A (VEGF-A), placental growth factor (PGF) and growth-arrest specific 6 (Gas-6) that are thought to aid macrophage proliferation (Angelillo-Scherrer et al., 2008; Tordjman et al., 2001). Recently, in a model of EBI-like macrophages generated from iPSCs, Lopez Yrigoyen et al. identified three other cytokines (ANGPTL7, IL33, and SERPINB2), that might also contribute to the regulation of erythropoiesis by macrophages. Indeed, these secreted factors were able to significantly enhance the production of mature enucleated red blood cells *in vitro*, suggesting that they could potentially play a role in EBIs *in vivo* (M. Lopez-Yrigoyen et al., 2019). Finally, EBI macrophages also contribute to heme synthesis by transferring iron directly to attached erythroblasts (Bessis & Breton-Gorius, 1962; Leimberg et al., 2008).

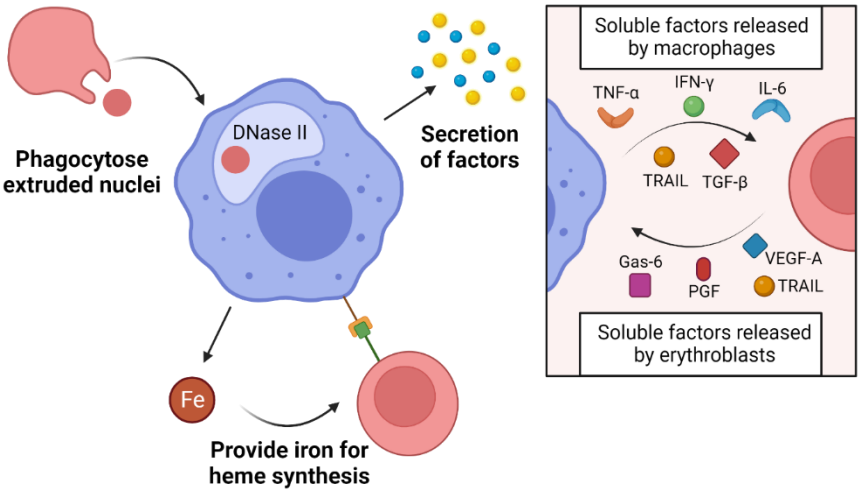

Figure 20: Role of EBI macrophages in erythropoiesis. In healthy steady-state erythropoiesis, EBI macrophages support and promote erythropoiesis via membrane–protein interactions, by secreting soluble factors and by providing iron for heme synthesis. During terminal differentiation, EBI macrophages phagocytose nuclei extruded from differentiating erythroid cells with DNase II associated with its degradation. Created with biorender.com and adapted from May & Forrester, 2020.

2. *Adhesive Interactions Within the Islands*

Central macrophages are known to express a variety of adhesion proteins that mediate macrophage/erythroblast interactions and are necessary for the formation of stable EBIs (Figure 21). Historically, the first adhesion molecule described to be important for EBI integrity was the erythroblast macrophage protein (EMP), which is expressed on both the central macrophages and the erythroblasts (Hanspal & Hanspal, 1994). The direct association between macrophages and erythroblasts through EMP was shown to be crucial for efficient erythropoiesis, as the absence of EMPs resulted in impaired

proliferation and terminal differentiation as well as increased apoptosis in EBI cultures (Hanspal et al., 1998; Soni et al., 2008). In a recent study, Wei et al demonstrated that EMP expressed by macrophages but not by erythroblasts is important for the EBI formation, challenging the preconceived notion that EMP drives EBI formation solely through homophilic interactions (Wei et al., 2019).

Besides EMPs, several other adhesion molecules were found to be important for the stability of EBIs. These include VCAM-1 and αV-integrins on macrophages which bind to ICAM-4 and α4β1, respectively, on erythroid precursors (McGrath et al., 2008; Sadahira et al., 1995). Of note, ICAM-4 also mediates binding between erythroid cells. Furthermore Spring et al. suggested that the tetraspanins CD81 and CD82, expressed on human erythroblasts, could interact with α4β1, and facilitate its binding to VCAM-1 on macrophages (Spring et al., 2013). The hemoglobin/haptoglobin receptor CD163 was also found to interact directly with erythroid precursors up to the pro-erythroblast stage (Fabriek et al., 2007). However, its counter receptor on erythroblasts has yet to be identified. Similarly, although EBI macrophages have been shown to promote erythroid maturation by interacting with erythroblasts via the CD169 receptor, its counter receptor was unknown for a long time (Chow et al., 2013a). However, a recent study revealed that CD169 may interacts with CD43 on early erythroblasts (Bai et al., 2023). Finally, a recent *ex vivo* study on human BM macrophages demonstrated that the ephrin receptor B4 (EPHB4) expressed at the surface of erythroblasts between the ProE and OrthoE stages, also contribute to the formation of stable EBIs by interacting with EPHB2 on macrophages (Hampton-O'Neil et al., 2020).

3. Pyrenocytes and Organelle Clearance

During terminal maturation, proteins associated with cellular adhesion, such as EMP, integrins, and ICAM, are sorted toward the plasma membrane of pyrenocytes. This facilitates their interaction with the central macrophage and their subsequent phagocytosis, while enucleated reticulocytes are released into the circulation (Bell et al., 2013; Lee et al., 2004). Clearance of these pyrenocytes by the central macrophage was shown to occur via MerTK, a member of the TAM family of receptor. This protein can recognize and bind phosphatidylserines exposed on pyrenocytes in a protein S-dependent manner, resulting in their internalization (Toda et al., 2014). However, although *MerTK*-deficiency blocked the uptake of pyrenocytes by the central macrophages *in vitro*, *MerTK*-deficient mice did not present any defects in pyrenocytes clearance, suggesting that a compensatory system operates *in vivo* (Toda et al., 2014). Because of this, it was suggested that the other TAM-receptor family members, AXL and TYRO3, may also play a role in the enucleation process (Heideveld et al., 2018; W. Li et al., 2019; Toda et al., 2014). TIM4, another PS receptor, was also found to be expressed by central macrophages and could thus contribute to the enucleation process as well (Figure 21) (W. Li et al., 2019; Miyanishi et al., 2007). After pyrenocyte engulfment, central macrophages rely on DNAse II to degrade the

nuclear DNA. Indeed, in DNAse II-deficient mice, the macrophages were unable to remove the phagocytosed nuclei which resulted in severe anemia (Kawane et al., 2001). In addition to facilitating the enucleation process, EBI macrophages are also implicated in the process of organelle clearance. Indeed, a recent study in mice demonstrated that early erythroblasts could transfer mitochondria to the EBI macrophages through a network of tunneling nanotubes. When EBI macrophages were depleted, the proper elimination of mitochondria was compromised, resulting in reduced mature RBCs (Yang et al., 2021).

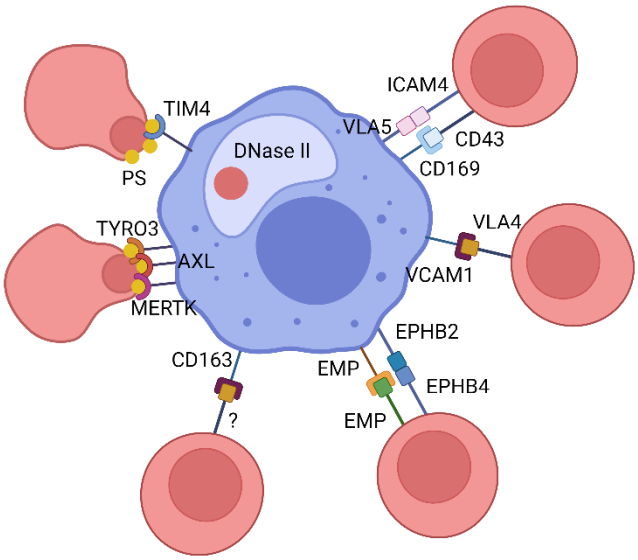

Figure 21: Adhesive Interactions within the EBI. Macrophages interact with erythroblasts through various adhesion molecules such as VCAM1, αV-integrins (VLA5), EPHB4, EMP, CD169 and CD163. Moreover, phosphatidylserine (PS)-exposed pyrenocytes are recognized and phagocytosed by PS-receptors such as members of the TAM family (TYRO3, AXL, MERTK) or TIM4. The pyrenocytes are then engulfed and degraded in a DNase II-dependent manner. Created with biorender.com and adapted from Ovchynnikova et al., 2018.

4. Phenotype and Heterogeneity of the EBI Macrophages

Quantitative light and electron microscopy on rat BM showed a difference in the composition of EBIs based on their proximity to the sinusoids (Yokoyama et al., 2003). EBIs distant from sinusoids were mainly in close contact with ProEs, while those adjacent to sinusoids were enriched in OrthoEs. These observations led to the hypothesis that EBIs might be motile and potentially migrate towards the sinusoids as their erythroblasts become more differentiated. Interestingly, the quantities of EBaso and PolyE were found to be equivalent in both types of islands. In a more recent study, Yeo et al. were also able to isolate 2 different classes of EBI from mouse BM, termed “flat EBI” and “domed EBIs” (Yeo et al., 2019; Yeo et al., 2016). Besides having distinct morphologies, these islands differed in the type and the frequency of erythroblasts attached to their central macrophage and could, therefore, correspond to the distinct niches previously described in rat BM. These studies imply that there may exist at least two distinct types of EBIs, wherein macrophages might serve different roles. In an “immature EBI”, macrophages might secrete growth factors that promote the proliferation and differentiation of early-

stage erythroblasts. Conversely, macrophages within “mature EBIs” may promote the maturation and enucleation of late-stage erythroblasts.

Human EBI macrophages seem to express a set of M2 resident macrophages markers such as CD163, CD169 and CD206 (Crocker et al., 1990; Fabriek et al., 2007; Takahashi et al., 1998) and have also been described as being $CD4^+$, $CD11a^+$, $CD11c^+$, $CD13^+$, $CD14^+$, $CD16^+$, $CD18^+$, $CD31^+$, $CD32^+$, $FcRI^+$, HLA-DR^+, and $CD35^-$, $CD11b^{dim}$ in an early study (Lee et al., 1988). However, few *in vivo* studies have been conducted to characterize EBI macrophages in humans, as their localization in the BM makes them challenging to study. Consequently, most of the research is done in mice where central macrophages are studied using a combination of typical myeloid macrophage markers including F4/80, CD169 and VCAM1 (Jacobsen et al., 2014). However, these markers lack the specificity or sensitivity required to identify only or all EBI macrophages.

Recently, multispectral imaging flow cytometry (IFC) has proven to be an effective tool for high throughput study and characterization of the EBI structure. By utilizing established markers for central macrophage and erythroid cells, this tool allows the analyses of the structural and morphological details of the central macrophages and its associated cells (Figure 22) (Seu et al., 2017; Tay et al., 2020). Using this innovative method, Seu et al. were the first to show that F4/80, CD169, and VCAM1 had a heterogenous expression on EBI macrophages (Seu et al., 2017). Subsequent investigations showed that only a small subset of EBI macrophages expressed CD163 and Ly6C, while Ly6G, previously reported as an EBI macrophage marker, was not expressed on the EBI macrophages in mouse BM, fetal liver, and spleen (W. Li et al., 2019). In addition, CD11b (Mac-1) which was previously thought to be expressed on EBI macrophages, was found to be expressed by other non-erythroid cells associated with the islands. These cells were identified as CD11b+ granulocytic precursors, and were found in about 75% of the EBIs at steady state in mice BM, suggesting that EBIs are common niche for terminal erythropoiesis and granulopoiesis (Romano et al., 2023; Romano et al., 2022).

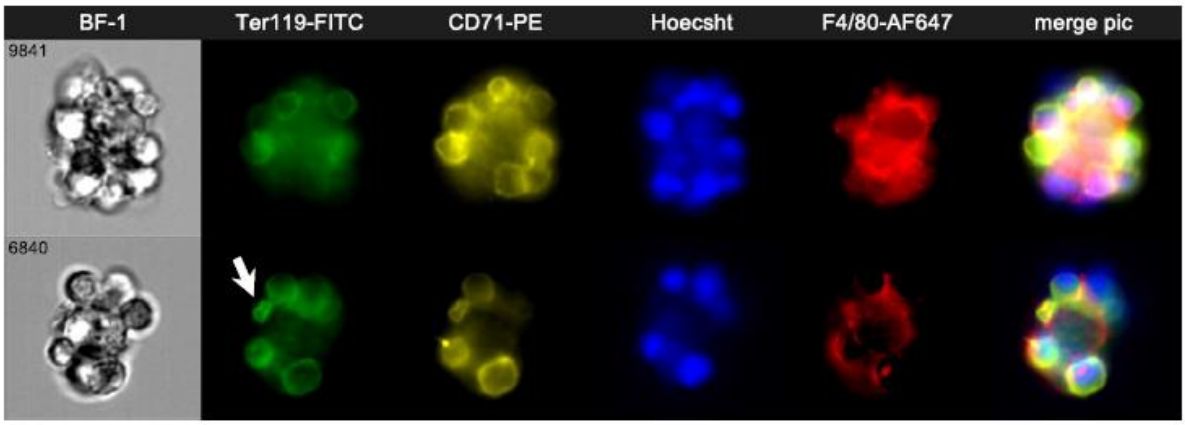

Figure 22: Erythroblastic islands (EBIs) analyzed by imaging flow cytometry (IFC). Example characterized by a central F4/80+ macrophage surrounded by CD71+ and/or Ter119+ erythroblasts. An enucleated reticulocyte (arrow) is occasionally seen, still in contact with the macrophage. (Seu et al., 2017)

Furthermore, A recent study by Li et al. found that more than 90% of EBI macrophages express EPOR in murine BM, spleen, and fetal liver as well as human BM and fetal liver (W. Li et al., 2019). This Highlights a possible marker to identify EBI macrophages from the rest of BM macrophages. The RNA-seq analysis done on these EPOR$^+$ macrophages showed that this population expresses many of the genes expected to be expressed in EBI macrophages. Interestingly, even within this population, significant heterogeneity was observed with regards to the expression of other EBI macrophage associated surface markers (W. Li et al., 2019). Additionally, EPOR$^+$ macrophages were shown to be highly enriched for KLF1 (W. Li et al., 2019). In a separate study, the activation of KLF1 in macrophages derived from iPSCs was shown to induce a shift towards an EBI-like phenotype (M. Lopez-Yrigoyen et al., 2019). Building on these studies, the Bieker group explored the importance of KLF1 in EBI development by working on F4/80$^+$ macrophages from developing mouse fetal liver. Utilizing a single-cell analysis approach, this investigation showed that F4/80$^+$ macrophages in the fetal liver are also a heterogeneous population of cells. Furthermore, they demonstrated that KLF1$^+$ macrophages represent a transient population of macrophages that are required for proper establishment of EBIs in the developing embryo (Mukherjee et al., 2021). Of note, a recent single cell analysis of human fetal liver hematopoiesis showed that KLF1 and many of its target genes are also expressed in VCAM$^+$ EBI macrophages in human fetal liver (Popescu et al., 2019). Overall, these studies reveal that EBI macrophages are inherently composed of heterogenous subpopulations, each potentially having distinct functional roles and contributing to various aspects of erythropoiesis regulation.

5. Ex vivo Models of human EBIs

As previously mentioned, the study of EBIs is extremely challenging as the human EBI niche is inaccessible and BM samples are very limited. Therefore, there has been a growing interest in the development of a reliable *in vitro* model system to mimic the human erythroblastic island. This would allow the study of functional interactions between macrophages and erythroid cells and help understand not only the normal processes involved in erythropoiesis but also the pathological processes involved in erythropoietic disorders in which support cells play an important but ill-defined role. Further down the line, new models to study interactions between erythroid cells and macrophage could help optimize current *in vitro* erythropoiesis protocols and help produce transfusion ready red cells.

The first human co-culture studies showed that monocyte-derived macrophages could promote erythroblast proliferation and survival *in vitro* (Leimberg et al., 2008; Ramos et al., 2013). However, the role and phenotype of these macrophages were not fully characterized, and these cells might not

recapitulate all the functions of a central macrophage. More recently, Heideveld et al., showed that using glucocorticoid (GC) on $CD14^+$ cells promoted their differentiation into macrophages with an EBI-like phenotype (Heideveld et al., 2018). Indeed, these macrophages, termed "GC-macrophages", were shown to support erythropoiesis by increasing HSPC survival, interacting with erythroid cells of all stages and phagocytosing the extruded pyrenocytes. Furthermore, they also shared phenotypic characteristics with resident macrophages from both human BM and fetal liver, such as high expression of CD169, CD163, and CD206 as well as a variety of adhesion molecules. In an erythroid stress model, Falchi et al. reported that $CD34^+$ cells cultured with glucocorticoid could also give rise to small populations of macrophages that could interact with erythroid cells (Falchi et al., 2015). Interestingly, in addition to a $CD169^+$ population that could form multiple "loose" interactions with erythroblasts and promote their proliferation, they also identified a $CD169^-$ population of macrophages that established "tight" interactions with erythroid cells and seemed to be able to phagocyte them.

In a recent study, Lopez-Yrigoyen et al. suggested that primary monocyte-derived macrophages might not accurately reflect the EBI niche, as tissue-resident macrophages are thought to have an embryonic origin. Instead, they developed an *in vitro* system to model the human EBI niche using macrophages derived from iPSCs genetically programmed to an EBI-like phenotype by inducible activation of the transcription factor KLF1 (Figure 23) (M. Lopez-Yrigoyen et al., 2019). In addition to increasing the production of functional enucleated erythroblasts, these EBI-like macrophages were able to secrete factors that could positively regulate erythroid maturation.

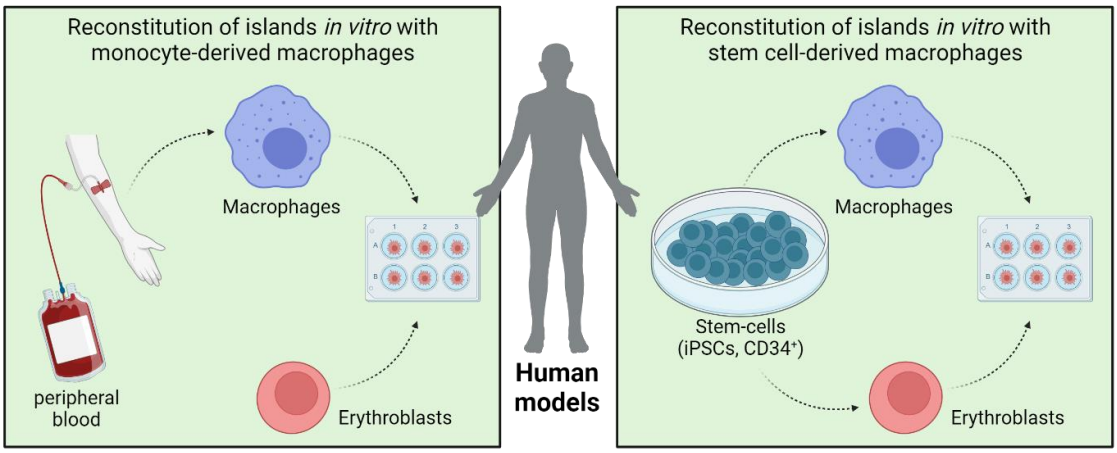

Figure 23: Modeling erythroblastic islands *in vitro*. Created with biorender.com, adapted from May & Forrester, 2020.

6. *Central Macrophages and Stress Erythropoiesis*

Depletion of macrophages through clonodrate poisoning or $CD169^+$ deletion was shown to markedly reduce the number of erythroblasts in the BM but only resulted in mild anemia at steady-state, suggesting that central macrophages have a limited role in regulating erythroid homeostasis (Chow et al., 2013a). This is further supported by the fact that erythroblasts can complete definitive

erythropoiesis without macrophages when cultured *in vitro*. However, under conditions of erythroid stress, such as induced anemia, the loss of macrophages resulted in a severe delayed recovery indicating that BM macrophages play a key role in the fast recovery responses to stress-induced erythropoiesis (Chow et al., 2013a; Ramos et al., 2013). These studies suggest that although the contribution of central macrophages to erythropoiesis might be limited at steady state, they appear to have a crucial role at times of severely increased erythroid output, for example during stress erythropoiesis (Heideveld & van den Akker, 2017).

Stress erythropoiesis is best understood in mice, where it occurs extramedullary in the adult spleen and liver. This process utilizes a specialized population of stress erythroid progenitors which are different from the erythroid progenitors at steady state. Recently, stress erythropoiesis has been studied in a mouse model of inflammation. Indeed, patients with chronic inflammation often have an inflammation-induced anemia where pro-inflammatory cytokines, such as TNF-α and IFN-γ, inhibit steady-state erythropoiesis (Nemeth & Ganz, 2014). A recent study demonstrated that this inhibition can be compensated by an increase in stress erythropoiesis. Indeed, signaling through TLRs paradoxically stimulated the phagocytosis of erythrocytes by splenic macrophages, facilitating heme-dependent expression of the transcription factor SPI-C, which, in turn, promoted the expression of both GDF15 and BMP4, which act to increase the proliferation of stress erythroid progenitors (Figure 24A) (Bennett et al., 2019).

Several additional studies, both *in vivo* and *in vitro*, have shown that the interaction between progenitor cells and central macrophages in the stress erythropoiesis niche was crucial to this process (Chow et al., 2013a; Chow et al., 2011; Ramos et al., 2013; Xiang et al., 2015). Since macrophages play an important role in maintaining erythropoiesis in conditions of acute stress, it is not unexpected that they might also play a role in erythropoietic disorders. Indeed, macrophages were found to play a significant part in the pathophysiology of polycythemia vera and β-thalassemia, which are both considered disorders of chronic enhanced erythropoiesis. In the murine models for both of these pathologies, the disease outcome was improved when central macrophages were depleted, suggesting that these macrophages could also have a function in disease progression (Figure 24B) (Chow et al., 2013a; Ramos et al., 2013). However, very little is known about how these macrophages exert their function in these pathologies.

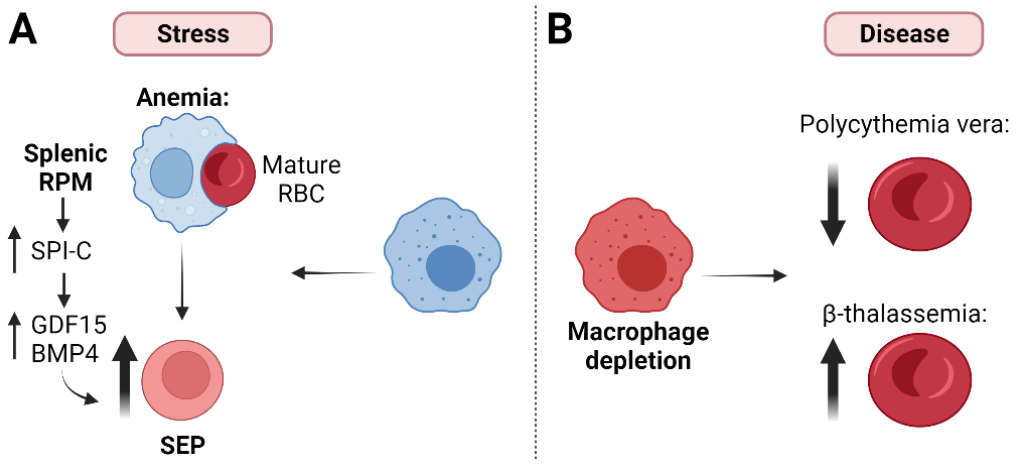

Figure 24: Macrophages during stress erythropoiesis. In models of stress erythropoiesis, anemia led to the phagocytosis of mature RBCs by splenic red pulp macrophages, which increased expression of SPI-C, Gdf15, and Bmp4, resulting in an increase in the proliferation of stress erythroid progenitors. Macrophage depletion led to the normalization of RBC numbers in disease models of polycythemia vera and β-thalassemia by decreasing and increasing red blood cells, respectively. Created with biorender.com and adapted from May & Forrester, 2020

Stress erythropoiesis occurs in the spleen and liver in mice instead of the BM. Therefore, it is very challenging to draw conclusions on what happens in humans. More work involving human macrophages and erythroid cells is necessary to corroborate the significance of recent findings for human physiology and pathology.

IV. Ferroptosis, a New Form of Cell Death

A. The Emergence of the Concept of Ferroptosis

1. *Classification of Cell Death*:

Cell death has been a subject of inquiry for a long time, and its understanding has evolved significantly over the years. The earliest observation of cell death occurred in 1842 by the German scientist Carl Vogt while studying toads' development (Vogt, 1842). Several other scientists continued investigating cell death throughout the 19th century and into the early 20th, contributing to the development of fundamental concepts related to this process (Cohnheim, 1889; Flemming, 1885; Goldschmidt, 1914; Pérez, 1910). However, the concept of "programmed" cell death only began emerging in the 1960s with the development of electron microscopy (Bellairs, 1961). Ten years later, John Kerr used the term "apoptosis" for the first time to describe this process after observing its ultrastructural features in rat liver hepatocytes (Kerr, 1965; Kerr et al., 1972). In this study, Kerr et al. defined apoptosis as a form of programmed cell death with morphological changes distinct from necrosis.

Following this work, an attempt was made to classify the different types of cell death based on the morphological and structural details of individual tissues and cells (Schweichel & Merker, 1973). The classification included three distinct modes of cell death: apoptosis (type I), autophagic-dependent cell death (type II), and necrosis (type III). This morphological classification was used for many years and is

still extensively employed. However, with the discovery of new cell death modalities, it became clear that cell deaths displaying a similar morphology can have significant functional, biochemical, and immunological differences (Galluzzi et al., 2012). For example, while necrosis was first believed to be a completely uncontrolled form of cell death, a study in the 1980s showed that death with a necrotic morphology could be molecularly modulated in some cases, leading to the emergence of the term "necroptosis" (Laster et al., 1988). Furthermore, many instances were found in which cell death displayed mixed features, with signs of both apoptosis and necrosis for example. This showed that there are no clear-cut distinctions between different forms of cell death based only on morphological criteria (Berry & Baehrecke, 2007; Nicotera & Melino, 2004).

To address the need for more precise classification, the editors of Cell Death and Differentiation created the Nomenclature Committee on Cell Death (NCCD) in 2005 (Kroemer et al., 2005). It led to the publication of several papers formulating guidelines to define cell death from morphological, biochemical, and functional perspectives (Galluzzi et al., 2015; Galluzzi et al., 2012; Kroemer et al., 2009). Currently, cell death can be fundamentally divided into accidental cell death, where unexpected attacks and injuries overwhelm any possible control mechanisms, and regulated cell death, which involves precise signaling cascades and dedicated molecular machinery and can thus be modulated. As it stands, the notion of regulated cell death is now being subdivided based on the molecular mechanisms involved in the cell death process. By doing so, the NCCD identified twelve major regulated cell death routines that, while all being distinct, exhibit a considerable degree of interconnectivity (Figure 25) (Bedoui et al., 2020; Galluzzi et al., 2018). However, the pathophysiological relevance of some of them is still being questioned as they have only been observed *in vitro* as a response to specific toxins.

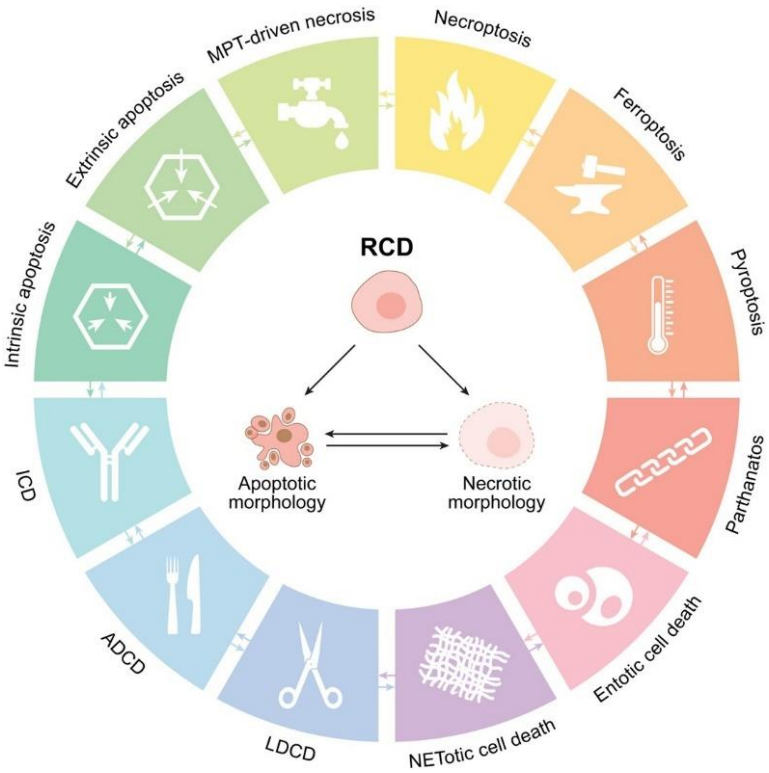

Figure 25: Major cell death subroutines. ADCD = autophagy-dependent cell death, ICD = immunogenic cell death, LDCD = lysosome-dependent cell death, MPT = mitochondrial permeability transition, RCD = regulated cell death (Galluzzi et al., 2018).

2. Early Observations of Ferroptosis:

One of the most recent forms of cell death identified is ferroptosis, an iron-dependent form of cell death induced by the accumulation of lipid peroxides in the cell membrane. However, while the term ferroptosis was coined for the first time in 2012 (Dixon et al., 2012), ferroptosis-like cell death had been observed long before, for instance, as a type of oxidative-stress-induced cell death termed “oxytosis” (Hirschhorn & Stockwell, 2019; Tan et al., 2001).

During the 1950s and the 1960s, the work of Harry Eagle and his team on amino acid and lipid metabolism provided the foundation for ferroptosis. Indeed, they demonstrated the crucial role of cellular cystine deprivation and glutathione depletion in inducing cell death (Eagle, 1955a, 1955b, 1959; Eagle et al., 1961). In the following years, several studies confirmed these findings, linked this type of cell death with lipid peroxidation, and revealed that iron chelators and lipophilic antioxidants could prevent such death (Figure 26) (Bannai et al., 1977; Mitchell et al., 1973). Moreover, ROS were found to drive this death process in many types of mammalian cells, including human embryonic fibroblasts (De Brabander et al., 1979), hybridomas and myelomas (Mercille & Massie, 1994), cortical neurons (Ratan et al., 1996; Schubert et al., 1992), oligodendroglia, oligodendrocytes (Rosin et al., 2004; Wang et al., 2004), and hair cells (Sunami et al., 1998). All these characteristics are now considered to be fundamental features of ferroptosis.

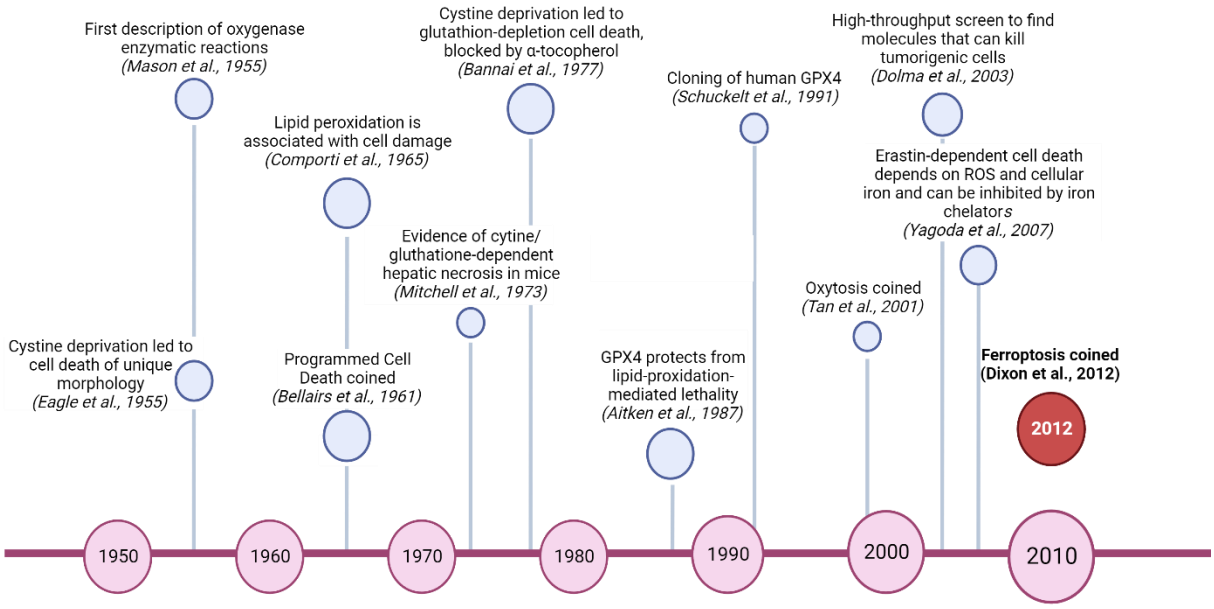

Figure 26: The development of the concept of ferroptosis. Schematic timeline highlights key discoveries that contributed to the emergence of the concept of ferroptosis. Created with biorender.com and adapted from Hirschhorn & Stockwell, 2019.

3. *The Discovery of Ferroptosis*

The discovery of ferroptosis began in 2001-2003, when the Stockwell Lab conducted a high-throughput screen to find small molecules that could selectively kill engineered tumorigenic cells – cells expressing oncogenic mutant HRAS as well as the T oncoprotein – while sparing their isogenic normal cell counterparts (Dolma et al., 2003). This screen led to the discovery of RAS-selective lethal compounds (RSL). One compound emerged from the screening as the most selectively lethal: a novel compound with no known activity that the team called “erastin” due to its ability to Eradicate RAS and Small T transformed cells. While most other compounds from the screen induced apoptosis, erastin-induced cell death did not present its classical features, such as mitochondrial cytochrome c release, caspase activation, and chromatin segmentation. Instead, this cell death depended on the accumulation of oxidative stress and cellular iron that could be inhibited by iron chelators and lipophilic antioxidants (Yagoda et al., 2007). RSL-3 was later identified in an additional screen as a molecule that could similarly induce nonapoptotic iron-dependent oxidative cell death, confirming that erastin was not unique in its ability to activate this type of cell death (Yang & Stockwell, 2008). Following these discoveries, the term ferroptosis was coined in 2012 to describe this iron-dependent, nonapoptotic form of cell death induced by erastin and RSL3.

Mechanistic investigations found that erastin induced ferroptosis by blocking cystine uptake through the x_c^- system, resulting in the depletion of cysteine and glutathione and leading to deregulated redox homeostasis (Dixon et al., 2014). The molecular target of RSL3 was identified soon after as the selenoproteins glutathione peroxidase 4 (GPX4), an enzyme downstream of the system x_c^- involved in the repair of oxidative damage to lipids (Yang et al., 2014). These studies helped determine that not all

ROS function equally in ferroptosis and that lipid peroxidation is the primary driver of ferroptotic death (Yang & Stockwell, 2016).

B. Core Metabolic Pathways in Ferroptosis

Cells that undergo ferroptosis are morphologically, biochemically, and genetically distinct from those that undergo apoptosis, classic necrosis, and other forms of nonapoptotic cell death. Typical morphological changes of ferroptosis were revealed by transmission electron microscope, which mainly showed a reduction in the size of the mitochondria, diminished or vanished mitochondria cristae, followed by the rupturing of the outer mitochondrial membrane (Dixon et al., 2012; Friedmann Angeli et al., 2014; Yagoda et al., 2007). Some instances of ferroptosis also display a "ballooning" phenotype, characterized by an enlarged empty cytoplasm resulting from cytoskeleton rearrangement (Agmon et al., 2018; Dodson et al., 2019). Recent years have witnessed rapid progress in our understanding of the mechanisms governing ferroptosis. Importantly, all these studies converge on cellular metabolism and have revealed an intimate relationship between ferroptosis and metabolic pathways, including iron, lipid, and glutathione metabolisms.

1. Glutathione Metabolism

As discussed previously, ferroptosis was initially characterized based on the effect of RSL3 and erastin, two molecules tightly linked to glutathione metabolism. GSH is the most abundant low-molecular-weight thiol in mammalian cells and is an essential antioxidant, free radical scavenger, and detoxifying agent (Wu et al., 2004). GSH comprises three amino acids: cysteine, glutamic acid, and glycine. Among these three, cysteine is the most limiting enzyme for GSH synthesis. It can be produced by *de novo* synthesis through the transsulfuration pathway or by protein catabolism (McBean, 2012). However, the primary source of intracellular cysteine comes from the x_c^- system, which exchanges intracellular glutamate for extracellular cystine. This system has two subunits: the solute carrier family 7A member 11 (SLC7A11, also known as cystine-glutamate transporter) and the SLC3A2 (Koppula et al., 2021). Imported cystine is then reduced via cystine reductase and used by two enzymes, glutamate cysteine ligase (GCL) and glutathione synthetase (GSS), to generate GSH. Finally, GSH can be used by GPX4 to reduce lipid peroxides to their benign alcohol form, an essential step in preventing ferroptosis (Brigelius-Flohé & Maiorino, 2013). This process oxidizes GSH to the form of GSH disulfide (GSSG). The recovery of GSH from GSSG can then be mediated by the NADH-consuming enzyme glutathione-disulfide reductase (GSR/GR) (Figure 27).

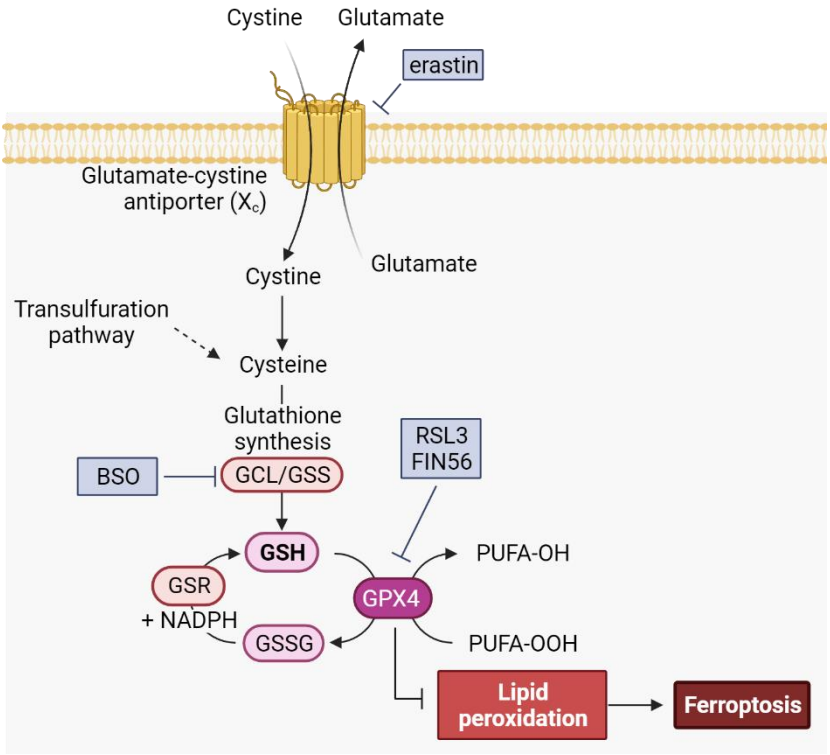

Figure 27: Glutathione metabolism and ferroptosis. The canonical ferroptosis-suppressing pathway involves the uptake of cystine via the cystine–glutamate antiporter (system x_c^-), which results in glutathione (GSH) biosynthesis. Using GSH as a cofactor, the glutathione peroxidase 4 (GPX4) reduces phospholipid hydroperoxides to their corresponding alcohols. In blue are examples of ferroptosis inducers targeting the glutathione metabolism. BSO = buthionine sulfoximine, Glu = glutamate, GSR = glutathione disulfide reductase, GSSG = glutathione disulfide, PUFA = polyunsaturated fatty acid. Created with biorender.com and adapted from Fang et al., 2023.

GPX4's protective role against the detrimental effects of lipid peroxidation places it at the center of ferroptosis regulation. Even before ferroptosis was discovered, studies showed that GPX4 had a unique role in physiology. Systemic deletion of GPX4 in mice was shown to cause embryonic lethality, which was not observed when other GPX genes were deleted (Imai et al., 2003; Yant et al., 2003). Moreover, *gpx4*-related conditional knockout mice also displayed selective developmental defects, increased cell death or disease susceptibility (Friedmann Angeli et al., 2014; Imai et al., 2009; Liang et al., 2009; Sengupta et al., 2013). These *in vivo* studies helped provide a clearer picture of how ferroptosis is relevant in living organisms. Interestingly, while GPX4 is now often associated with ferroptosis, a ferroptosis-independent role of GPX4 was recently described during terminal erythroid differentiation, where its role in lipid metabolism was shown to mediate enucleation (Ouled-Haddou et al., 2020)

GPX4 activity can be lowered by direct enzyme inhibition (loss of activity or enzyme protein degradation) or by inhibiting proteins involved in GSH biosynthesis. As discussed, RSL3 can bind directly to GPX4 to inhibit its activity (Yang & Stockwell, 2008). The small molecules caspase-independent lethal compound 56 (CIL56) and its analog ferroptosis-inducer 56 (FIN56) identified by the Stockwell team were also found to induce the degradation of GPX4 and contribute to the execution of ferroptosis. Furthermore, the inhibition of system x_c^- (using erastin and its analogs, as well as sorafenib and

sulfasalazine) or GCL (using buthionine sulfoximine) was shown to trigger ferroptosis in various cells (Dixon et al., 2012; Gout et al., 2001; Louandre et al., 2013; Mãrtensson & Meister, 1991). Depleting GSH through other mechanisms can also sensitize cells to ferroptosis. Indeed, the multidrug resistance gene 1 (MDR1) drives increased sensitivity to ferroptosis by causing an efflux of GSH (Cao et al., 2019), and the cys catabolic enzyme cys dioxygenase 1 (CDO1) drives sensitivity to ferroptosis by depleting cysteine and in turn GSH (Hao et al., 2017).

Because ferroptosis was first discovered through the lens of glutathione metabolism via the direct or indirect inhibition of GPX4, GPX4-dependent ferroptosis has been termed “canonical ferroptosis”. However, numerous studies have revealed that the mechanisms by which ferroptosis can be induced and suppressed are more diverse than initially supposed, extending beyond the glutathione-GPX4 axis. This led to the emergence of the term “non-canonical” ferroptosis (Wen et al., 2022).

2. Lipid Metabolism

In ferroptosis, the specific effectors responsible for mediating the cell death cascade downstream of lipid peroxidation remain unclear. This places lipid metabolism and the accumulation of oxidized lipids as the key mechanisms responsible for the occurrence of ferroptosis. A current hypothesis is that during ferroptosis, lipid peroxides accumulate and disrupt the thickness, permeability, and structure of the membrane. This process could then drive increased accessibility to oxidants and pore formation, eventually resulting in membrane destruction (Agmon et al., 2018). Lipid peroxide breakdown products can also arise from this reaction, such as 4-hydroxynonenal (4-HNE) and malondialdehyde (MDA) which can form adducts with proteins and DNA and damage cellular processes (Dalleau et al., 2013; Niedernhofer et al., 2003).

Phospholipids (PLs) containing polyunsaturated fatty acid tails (PUFAs) are the primary substrates of lipid peroxidation due to their intrinsic susceptibility to peroxidation chemistry (Porter et al., 1979; Rouzer & Marnett, 2003). Indeed, their multiple double bonds are arranged so that hydrogen molecules can be more readily extracted from the acyl chain than from the saturated or monounsaturated fatty acid groups (MUFAs). (Wagner et al., 1994). Because of this, many studies have found that the composition of plasma membrane PLs determines ferroptosis sensitivity. The presence of PL-PUFAs in the membrane depends on the action of lipid remodeling enzymes that catalyze the insertion of fatty acids into membrane PLs. PUFAs can be scavenged from the environment and dietary sources or can be synthesized from acetyl-CoA through the action of Acetyl-CoA Carboxylase (ACC). These PUFAs are then converted into acyl-CoA forms by acyl-CoA synthetases 4 (ACSL4). Finally, they are incorporated into the membrane via lysophosphatidylcholine acyltransferase enzymes 3 (LCAT3) (Figure 28). By virtue of their role in facilitating the incorporation of PUFAs into membrane lipids, this group of

enzymes was among the first pro-ferroptotic proteins to be identified. For example, in an insertional mutagenesis screen, the inactivation of ACSL4 and LPCAT3 prevented ferroptosis induced by the GPX4 inhibitors RSL3 and ML162 (Dixon et al., 2015). In contrast, ACSL3, which favors MUFAs activation rather than PUFAs, was shown to promote ferroptosis resistance (Magtanong et al., 2019). A recent study also showed that ACC phosphorylation following energy stress could inhibit fatty acid synthesis and thus increase ferroptosis resistance in cells under glucose starvation (Lee et al., 2020).

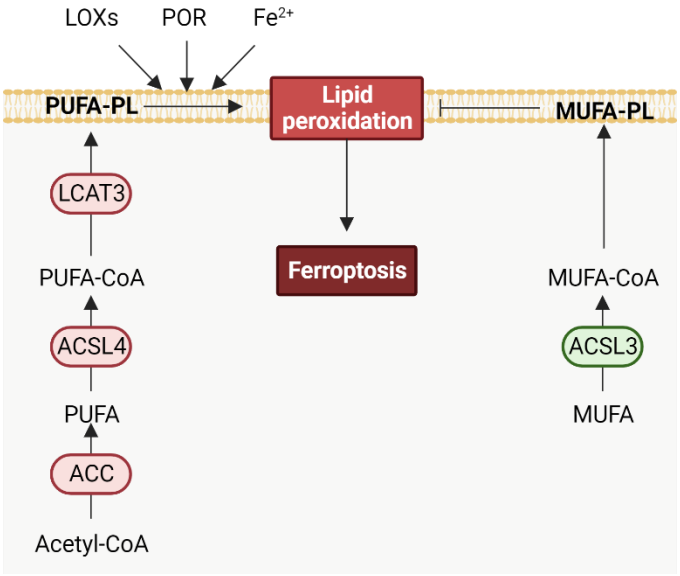

Figure 28: Lipid metabolism and ferroptosis. The activation of acetyl-CoA carboxylase (ACC), acyl-CoA synthetases 4 (ACSL4), and lysophosphatidylcholine acyltransferase enzymes 3 (LCAT3) in the lipid metabolic pathway promotes lipid peroxidation and ferroptosis. LOX = lipoxygenase, MUFA = monounsaturated fatty acid, POR = cytochrome P450 oxidoreductase PUFA = polyunsaturated fatty acid. Created with biorender.com and adapted from Fang et al., 2023.

Interestingly, while ACSL4 is generally considered to be a universal ferroptosis regulator whose expression is necessary for ferroptosis to occur (Jiang et al., 2021), several studies showed that ferroptosis can be executed in its absence (Chu et al., 2019; Shui et al., 2021). In a recent study, Leslie Magtanong et al. established that ACSL4 is more important for the execution of ferroptosis following direct GPX4 inactivation than in cystine deprivation (Magtanong et al., 2022), highlighting the fact that ferroptosis regulation is highly context specific.

3. *Iron Metabolism*

Ferroptosis, as its name suggests, relies on the existence of high levels of intracellular iron for its execution. Initially, the importance of iron to ferroptosis was demonstrated by the fact that iron chelators could suppress ferroptotic death both *in vitro* and *in vivo* (Dixon et al., 2012; Yang & Stockwell, 2008). Furthermore, the addition of iron into cell cultures was found to accelerate erastin-induced ferroptosis (Dixon et al., 2012), and both heme and non-heme iron sources were also shown to induce ferroptosis (Li et al., 2017). It is now widely accepted that iron promotes ferroptosis through two distinct mechanisms. First, the presence of free ferrous iron within cells significantly impacts their redox

status and induces oxidative stress. Indeed, this iron can react with cellular oxidants to generate harmful hydroxyl radicals through the Fenton reaction, thus promoting ferroptosis (Cheng & Li, 2007). Second, several enzymes involved in phospholipid peroxidation and the generation of ROS, including heme and non-heme lipoxygenases (LOXs) and cytochrome P450 oxidoreductase (POR), rely on iron to perform their function (Cheng & Li, 2007). Consequently, iron metabolism aspects such as absorption, storage, and utilization play vital roles in ferroptosis.

In plasma, iron readily binds with transferrin (TF), forming transferrin-bound iron. This complex can then interact with its receptor, transferrin receptor protein 1 (TFR1), on the cell surface (Frazer & Anderson, 2014). Following this interaction, the TFR-TFR1 complex is internalized by receptor-mediated endocytosis. Within the highly acidified endosome, iron is released from TF following its reduction by the STEAP3. Subsequently, ferrous iron is transported to the cytoplasm solute carrier family 11 member 2 (SLC11A2/DMT1), while TFR1 and TF are recycled to the cell surface to be reused by the cell. In the cytoplasm, the regulation of the labile iron pool (LIP) is managed by ferritin, a cytosolic storage protein comprised of two subunits, ferritin heavy chain 1 (FTH1) and Ferritin Light Chain (FTL). These proteins can oxidize ferrous iron to its ferric state and store this less reactive form within a 24-subunit complex. The resulting ferritin-bound iron can be stored for later uses or degraded to be used in enzymatic reactions. Iron-saturated ferritin is degraded by nuclear receptor coactivator 4 (NCOA4)-mediated autophagy, a process known as ferritinophagy, which allows the release of its iron content back into the LIP. Upon mobilization, iron can be exported from the cell by ferroportin (FPN/SLC40A1), a process regulated by circulating hepcidin levels (Figure 29).

Given that excess free reactive iron can initiate iron-dependent lipid peroxidation, proteins facilitating an increase in the labile iron pool have been identified as promoters of ferroptosis. Conversely, proteins associated with the export or storage of iron act as negative regulators, helping to decrease the levels of intracellular ferrous iron and the ensuing lipid peroxidation leading to ferroptosis (X. Chen et al., 2020). Consequently, TF and its receptor have been identified as crucial positive regulators of ferroptotic cell death. Notably, the absence of TF in the serum prevented amino-acid starvation-induced ferroptosis (Gao et al., 2015). Likewise, the expression of TFR1 in cancer cells was found to be positively correlated with the ferroptotic response induced by erastin (Song et al., 2016; Wu et al., 2019). Therefore, TFR1 expression levels are now utilized as a biomarker for ferroptosis sensitivity, as the more it is expressed, the more likely cells will be sensitive to iron-induced ferroptosis. Another positive regulator of ferroptosis is NCOA4. Its knockdown blocks ferritin degradation and suppresses erastin-induced ferroptosis in fibroblasts and pancreatic cancer cells, whereas its overexpression promotes ferroptosis by degrading ferritin (Hou et al., 2016). Ferritin, essential for safe iron storage within cells, protects against ferroptosis. Their overexpression could inhibit erastin-induced ferroptosis

(Wang et al., 2016). Moreover, ferroportin also acts as a negative regulator of ferroptosis, as it aids in decreasing excess cellular iron (Li et al., 2018).

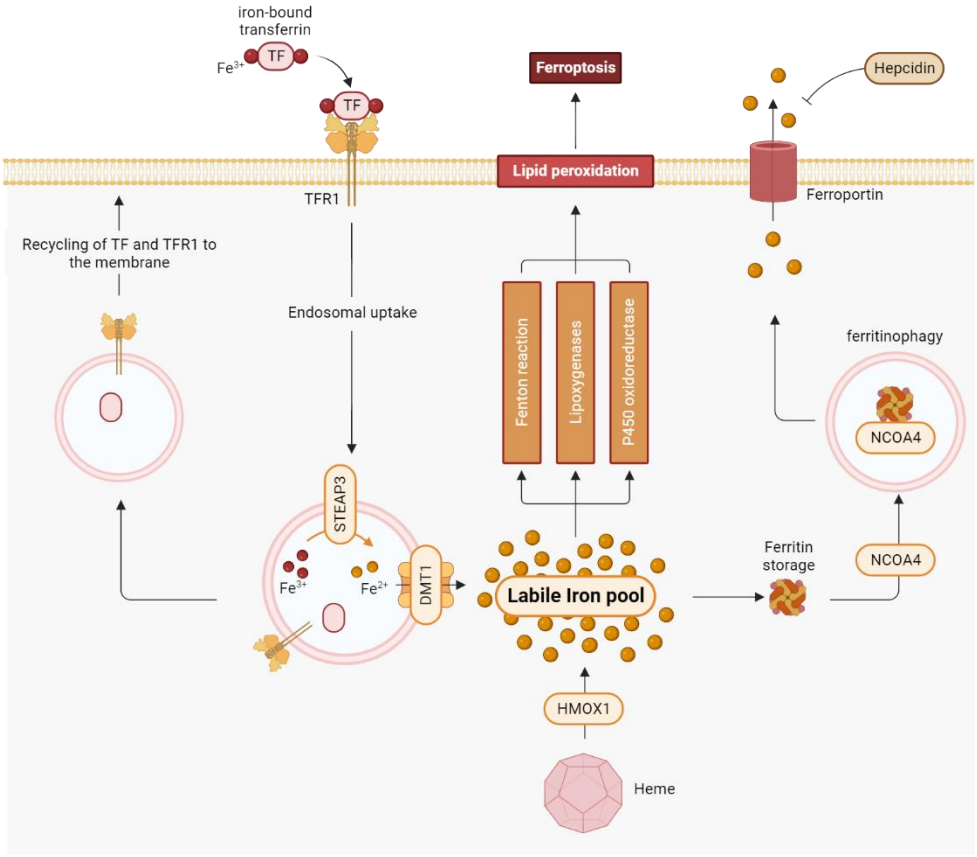

Figure 29: Iron metabolism and ferroptosis. At the cellular level, ferroptosis is driven primarily by iron-dependent lipid peroxidation. Many aspects of iron metabolism such as the absorption, storage and utilization of iron have important roles in regulating ferroptosis. At the cellular level, non-heme iron is transported into cells by either transferrin receptor protein 1 (TFR1)-mediated, transferrin (TF)-bound iron uptake or metal transporter solute carrier family 39 member 14 (SLC39A14; also known as metal cation symporter ZIP14)-mediated, non-TF-bound iron uptake. In addition, heme degradation and nuclear receptor coactivator 4 (NCOA4)-mediated Ferritinophagy can increase the labile iron pool (LIP), thereby sensitizing cells to ferroptosis via the Fenton reaction. FPN = ferroportin, HMOX1 = heme oxygenase 1, STEAP3 = metalloreductase STEAP3. Created with biorender.com and adapted from Fang et al., 2023.

The LIP can also be enhanced through erythrophagocytosis, a process wherein iron is released from heme and catabolized by heme-oxygenase 1 (HMOX1). HMOX1 degrades heme into three products: carbon monoxide, biliverdin, and free iron. While HMOX1 is recognized for its cytoprotective effects against various stress-related conditions, it has also been identified as a critical mediator in ferroptosis induction, whose activity elevates the LIP and increases ferroptosis. Therefore, HMOX1 appears to play a dual role in the ferroptotic process. On one hand, erastin has been demonstrated to upregulate HMOX1 expression. Inhibition of HMOX1 prevents erastin-induced ferroptosis, while the inducer of HMOX1, hemin, accelerates erastin-induced ferroptosis (Kwon et al., 2015). On the other hand, HMOX1 can also exert inhibitory effects on ferroptosis in some instances. For example, in renal proximal tubular cells, the knockout of HMOX1 increases erastin or RSL3-induced cell death, suggesting that the role of HMOX1 in ferroptosis may be dependent on the cellular context (Adedoyin et al., 2018).

Multiple transcription factors regulate ferroptosis by modulating the expression of genes involved in iron metabolism. One pivotal example is nuclear factor erythroid 2-like 2 (NFE2L2/NRF2), a transcription factor central to the regulation of cytoprotective responses against ferroptotic damage. Among its anti-ferroptotic mechanisms, it upregulates several genes involved in iron metabolism, such as FTH1, SLC40A1, and HMOX1 (Fang et al., 2019; Shin et al., 2018; Sun et al., 2016). In addition, HIF factors also play a complex role in ferroptosis. Both HIF1 and HIF2 regulate numerous genes essential for iron homeostasis, such as TFRC, SLC11A2, SLC40A1, and HMOX1. Under hypoxia, HIF1α has been shown to inhibit ferroptosis by upregulating the expression of cytoprotective proteins such as SLC7A11 and HMOX1 (Feng et al., 2021). In contrast, HIF2α increased the expression of PLIN2 and HILPDA, elevating lipid accumulation and oxidative stress and, finally, enhancing ferroptosis (Singhal et al., 2021). Finally, iron homeostasis is regulated at the posttranscriptional levels by iron regulatory proteins (IRP) that can bind iron-responsive elements (IRE) on mRNAs. The binding of IRPs to 5' IREs inhibits mRNA translation, whereas the binding of IRPs to 3' IREs inhibits the mRNA degradation and promotes its translation. Therefore, the regulation of the IRP-IRE system can also modulate ferroptosis sensitivity.

C. Ferroptosis: A Flexible Death Mechanism

While iron, glutathione and lipid metabolism have been defined as the core metabolism of ferroptosis in most studies, several groups have found other pathways that could promote ferroptosis independently. As previously mentioned, the work of Magtanong et al. demonstrated that previously identified ferroptosis regulators may not always be essential for mediating ferroptosis and that their roles are highly context specific. Indeed, they showed that the disruption of ACSL4 or LPCAT3 suppresses GPX4 inhibition-induced ferroptosis but not erastin-induced ferroptosis. This observation suggests the existence of distinct mechanisms that govern the execution of ferroptosis. Similarly, further studies showed that canonical ferroptosis pathways were not involved when ferroptosis was induced by the combination of p53 expression and tert-butyl hydroperoxide or by photodynamic therapy (Chu et al., 2019; Shui et al., 2021). In a recent study, Bersurker et al. identified FSP1, a CoQ oxidoreductase, as another ferroptosis suppressor which acts parallel to the system X_c^-/GPX4 and is entirely independent of the intracellular expression levels of GSH, GPX4, and ACSL4 (Bersuker et al., 2019).

Many studies regarding ferroptosis have been conducted *in vitro*, encompassing a wide variety of cell types with a predominant focus on cancer cells. It is important to recognize that some of the molecular mechanisms identified and initially thought to be universally applicable might instead depend upon the unique characteristics of individual cell types. Consequently, although numerous ferroptosis markers have been identified, establishing a definitive and singular mechanism has proven challenging. In fact, the only consistent way to identify ferroptosis cell death is to observe high levels of lipid peroxide

accumulation coupled with an increase in cell death that can be prevented by specific ferroptosis inhibitors (Wiernicki et al., 2020).

A recent review by Dixon and Pratt suggests that there is no single universal ferroptosis pathway. Instead, they propose that many different metabolites and proteins can individually initiate, promote, and regulate ferroptosis, with none being necessary. According to this model, the central mechanism revolves around lipid peroxidation, encircled by distinct biochemical defense mechanisms within cells that can be modulated by many regulatory inputs. Therefore, the likelihood of ferroptosis depends on the balance between the total defense capacity of the cell and its susceptibility to lipid peroxidation, both of which can change over time or in response to external stimuli (Figure 30) (Dixon & Pratt, 2023).

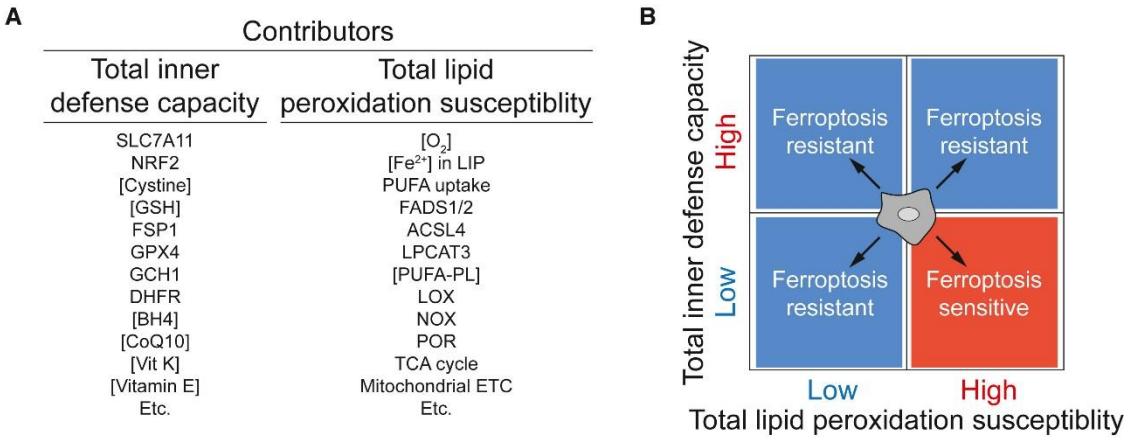

Figure 30: Visualizing the contribution of different molecules to ferroptosis. (A) The total inner defense capacity and total lipid peroxidation susceptibility of the cell can be influenced by many metabolites and proteins, some of which are listed here. The relative contribution of each molecule to ferroptosis sensitivity will vary between contexts. **(B)** Quadrant diagram summarizing four different possible states in which a cell may exist. Cells with low total inner defense capacity and high total lipid peroxidation susceptibility will be most sensitive to ferroptosis. The boundaries between these states are likely to be fluid. (Dixon & Pratt, 2023)

D. Ferroptosis and Macrophages

Due to their integral role in the body's iron recycling process, macrophages frequently accumulate high intracellular iron levels. Additionally, they can be found within pro-oxidant environments, where they contribute to inflammation by releasing pro-inflammatory cytokines or by generating ROS, to help eliminate foreign entities like bacteria and microorganisms. Despite exposure to these various signals that promote ferroptosis, macrophages exhibit heightened resistance to this process. Notably, erastin treatment and SLC7A11 expression deletion in mice did not independently induce macrophage ferroptosis; instead, elevated iron levels were required for its initiation (Fang et al., 2020; Wang et al., 2017).

However, recent studies have shown some instances where ferroptosis can occur, particularly in the context of excessive erythrophagocytosis. Experiments have shown that augmented erythrophagocytosis, driven by IgG-coated erythrocytes, increases lipid peroxidation and cell death in a mouse model of transfusion. This process was countered by the ferroptosis inhibitor Ferrostatin-1 (Fer-1) (Catala et al., 2020; Youssef et al., 2018) (Figure 31). Similarly, erythrophagocytosis of mutant JAK2^{V617F} or normal erythrocytes led to ferroptosis, which was abrogated by the ferroptosis inhibitor liproxstatin-1 (Lip-1) (Liu, Ostberg, et al., 2022). Furthermore, in an atherosclerosis mouse model, erythrophagocytosis of RBCs could also induce cell death (Puylaert et al., 2023).

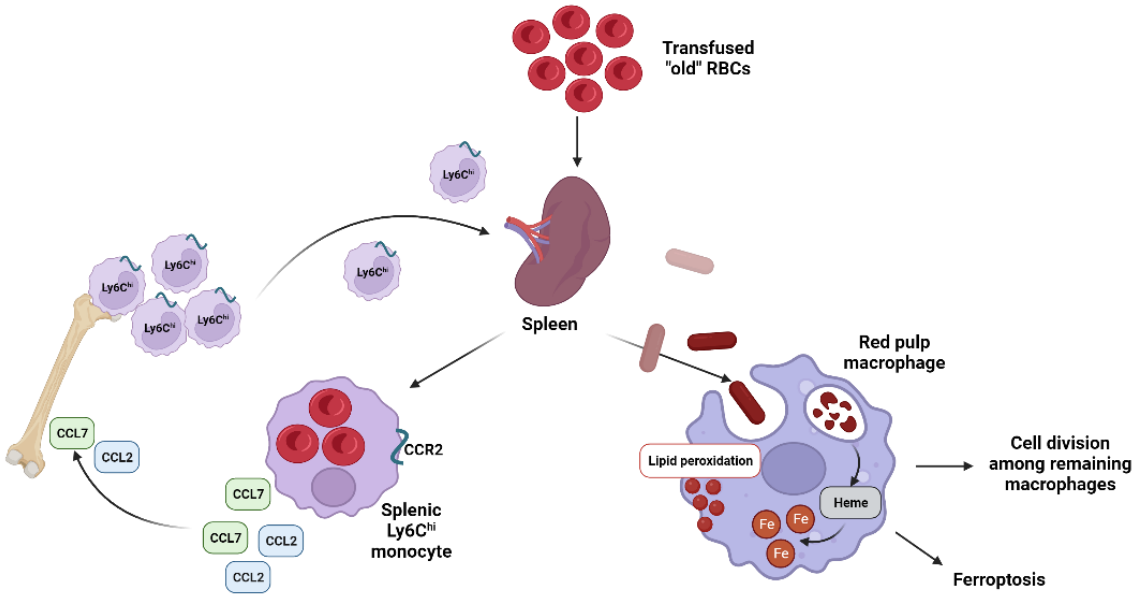

Figure 31: Increased erythrophagocytosis can lead to ferroptosis (Youssef et al., 2018).

Interestingly, in M1 macrophages, the absence of GPX4 did not impact their viability or inflammatory properties. On the contrary, ferroptosis was induced when GPX4 was deleted in M2 macrophages, suggesting that ferroptosis may depend on macrophage polarization (Piattini et al., 2021). This polarization-dependent resistance can be attributed, in part, to the distinct characteristics of M1 and M2 macrophages. M1 macrophages possess higher concentrations of inducer NO synthase (iNOS), resulting in an elevated production of NO free radicals. These increased iNOS levels provide superior protection against lipid peroxidation, setting them apart from M2 macrophages characterized by their anti-inflammatory function and lower iNOS concentration (Kapralov et al., 2020).

Further studies propose that iron overload contributes to M1 polarization by increasing M1 markers, such as IL-6, TNF-α, and IL-β, while decreasing M2 markers (Handa et al., 2019). Elevated ROS production and p53 acetylation induced by iron overload significantly contribute to M1 polarization as well (Zhou et al., 2018). This shift in polarization sometimes escalates the release of inflammatory factors, intensifying inflammation and fostering an environment conducive to the potential occurrence

of ferroptosis. Notably, pro-inflammatory markers such as IL-6 not only promote lipid peroxidation but also disrupt iron homeostasis in bronchial epithelial cells, ultimately culminating in ferroptosis (F. Han et al., 2021). Similarly, TNF-α, another pro-inflammatory cytokine, upregulates ACSL3, facilitating lipid accumulation in cells, thus promoting the potential occurrence of ferroptosis (Jung et al., 2020). Interestingly, there are instances where ferroptosis byproducts can induce an M2-like phenotype instead. For example, chronic iron overload prompts THP-1 monocyte-derived macrophages to exhibit M2 characteristics while downregulating M1 markers (Kao et al., 2020).

E. Ferroptosis in Sickle Cell Disease

Since 2012, ferroptosis has been detected in various biological systems and in the pathological progression of diseases such as ischemia-reperfusion injury, stroke, inflammatory bowel disease, organ failure, and tumor progression. More recently, it has also been linked to erythroid disorders such as Diamond Blackfan anemia (DBA). Indeed, the delayed globin chain synthesis in DBA leads to an abnormal accumulation of heme within erythroblasts during erythropoiesis. This excess heme has been shown to ultimately trigger cell death through the mechanism of ferroptosis (Doty et al., 2022; Yang et al., 2016).

Iron overload is a common complication in patients requiring frequent transfusions, such as thalassemic patients and SCD patients, and can lead to damaging effects on organs and tissues. Consequently, ferroptosis might also play a role in the pathogenesis of these diseases. The excess iron can saturate the transferrin iron transport system, giving rise to non-transferrin-bound iron and labile plasma iron. These forms of iron circulate in the plasma and can eventually accumulate within susceptible cells (Hershko, 2010; Leecharoenkiat et al., 2016). Prolonged uptake and accumulation of these molecules can exceed the cell's capacity, potentially triggering ferroptosis (Cabantchik, 2014). In a recent study using the Townes model, researchers demonstrated that this process occurs in the heart of SCD mice. They found that excess circulating free heme can upregulate cardiac HMOX1, leading to nonheme iron accumulation and lipid peroxidation in cardiomyocytes, ultimately causing ferroptosis and impaired cardiac function (Menon et al., 2022). Further evidence of ferroptosis in SCD was demonstrated in a study by Liu et al., which revealed that patrolling monocytes that phagocytose RBCs in the circulation also exhibited increased expression of HMOX1, resulting in their death (Liu et al., 2019).

OBJECTIVES

Ineffective erythropoiesis is a well-described phenomenon in β-thalassemia, but it has received less attention in SCD, where anemia is generally attributed to hemolysis. While some elements in the literature have hinted at potential alterations during erythroid differentiation in SCD (Blouin et al., 1999; Finch et al., 1982; Hasegawa et al., 1998; Park et al., 2020; Wu et al., 2005), questions remain pending regarding the existence and degree of such ineffective erythropoiesis, in relation with SCD pathophysiology.

My thesis aimed at investigating erythropoiesis and the erythroid niche in SCD. This was achieved by addressing the following objectives:

1. To investigate ineffective erythropoiesis in SCD by:
    a. Exploring the molecular and cellular mechanisms of ineffective erythropoiesis and the protective role of HbF during this process.
    b. Assessing the extent of ineffective erythropoiesis in patients with high levels of circulating erythroblasts.
2. To set up an *ex vivo* protocol adapted for the study of terminal erythropoiesis in SCD.
3. To assess the impact of erythroid cell death during terminal erythropoiesis on the central macrophage of the erythroblastic island.

CHAPTER 1:
Ineffective Erythropoiesis in Sickle Cell Disease: Hypoxia, HbF and Nucleated Red Blood Cells

I. RESULTS

While the pathophysiology of circulating mature red blood cells (RBCs) has been extensively studied in sickle cell disease (SCD), the process through which these cells are generated, known as erythropoiesis, remains poorly documented in this pathology. Unlike thalassemia, where ineffective erythropoiesis is a well-known contributor to anemia, its role in SCD has not yet been critically explored, despite a limited number of reports describing cellular alterations during erythroid differentiation. For instance, studies have shown that erythroblasts, whether differentiated *in vitro* or isolated from the bone marrow (BM) of SCD patients, tend to sickle under hypoxic conditions (Hasegawa et al., 1998). Additionally, Wu and collaborators showed evidence of ineffective erythropoiesis occurring in the BM of transplanted SCD patients with an imbalance favoring the survival of the donor erythroid progenitor cells (Wu et al., 2005).

In this chapter, we explored the extent of ineffective erythropoiesis in SCD patients by utilizing both *in vitro* and *in vivo* derived human erythroblasts. Our primary focus centered on the terminal phase of erythroid differentiation. Specifically, we examined the influence of BM hypoxia on the polymerization of HbS and the subsequent cell death of differentiating erythroblasts, in relation with HbF expression. This portion of my thesis represents a collaborative work with a former PhD student from our research group who completed her thesis in 2019. Furthermore, the findings from this work were published in 2021 in Haematologica (Appendix on page 176; DOI: 10.3324/haematol.2020.265462) and discussed in a review published in 2021 in Current Opinion in Hematology (Appendix on page 190; DOI: 10.1097/MOH.0000000000000642).

After completing our initial research on SCD patients, we decided to work on patients with high levels of circulating erythroblasts, as the presence of these cells in the periphery may reflect BM damage or severe erythropoiesis defects. Our aim was to further investigate the role of ineffective erythropoiesis in this specific patient population.

A. Cell Death during the Terminal Stages of Erythroid Differentiation of SCD Erythroblasts *in vitro*

The BM environment has been well documented to be hypoxic (0.1 to 6% O2) (Mantel et al., 2015; Mohyeldin et al., 2010; Yeo et al., 2018). As hypoxia induces HbS polymerization, we hypothesized that cell death may occur *in vivo* because of HbS polymer formation in the late stages of differentiation characterized by high intracellular hemoglobin concentration. To test our hypothesis, we performed *in vitro* erythroid differentiation using $CD34^+$ cells isolated from SCD patients and from healthy donors. A 2-phase erythroid differentiation protocol was used, and cultures were performed at two different oxygen conditions, i.e., normoxia and partial hypoxia (5% O2), starting at day 3 (D3) of the second phase, at which time hemoglobin synthesis begins to increase markedly (Figure 1).

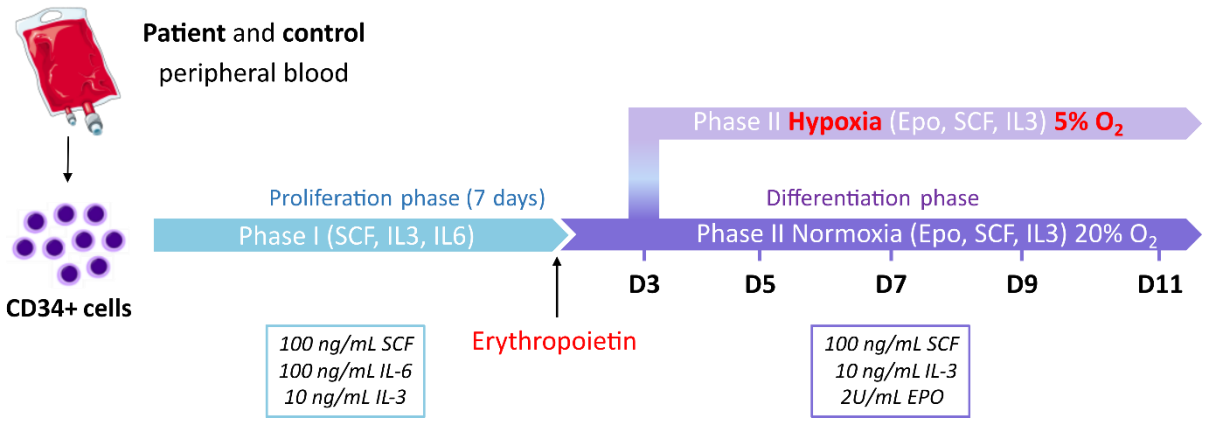

Figure 1: ***in vitro*** **model of erythropoiesis.** A scheme representing the *in vitro* erythropoiesis protocol. Cells were put under normoxia or partial hypoxia (5% O2) starting from day 3 (D3) of phase II of culture.

The choice of 5% O_2 was made since it falls at the high end of the reported oxygen tension range of the hematopoietic niche (0.1-6% O_2), and because it drives HbS polymerization and cell sickling, as we previously reported (Lizarralde Iragorri et al., 2018). Differentiation of control erythroblasts showed no difference in the general waterfall pattern between normoxia and hypoxia (Figure 2A and 2B), although hypoxia translated into a consistently higher but not statistically significant increase in total cell count (Figure 2C). Under normoxia, SCD differentiation showed a mild deceleration till D9 as compared to control (Figure 2A and 2B), with a proliferation that was negatively impacted by hypoxia (Figure 2C). Under both oxygen conditions, cell proliferation was significantly higher in the control than in the SCD cultures, starting from D7 (Figure 2C). In addition, higher proportions of enucleated cells were found in control cells at D9 (Figure 2B) and D11 (Figure 2D). Enucleation was improved under hypoxia for control erythroblasts while it was significantly diminished for SCD cells (Figure 2D), indicating a negative impact of hypoxia at this critical maturation step in the context of SCD. To assess if the decrease in proliferation in SCD was due to cell death, we measured the percentage of apoptotic cells in the cultures by staining the GPA-positive cells with annexin V. The percentage of annexin V^+ cells was higher in SCD than in control cultures under both oxygen conditions at D7 and D9, with a greater variability among SCD than in control cells (Figure 2E). Furthermore, the extent of apoptosis of SCD cells was higher under hypoxia than under normoxia at both time points while no difference was noted for control cells (Figure 2E). Altogether, these findings imply that even under a conservative choice of 5% O_2 to mimic BM hypoxia there is increased cell death during the terminal differentiation stages in SCD cells only.

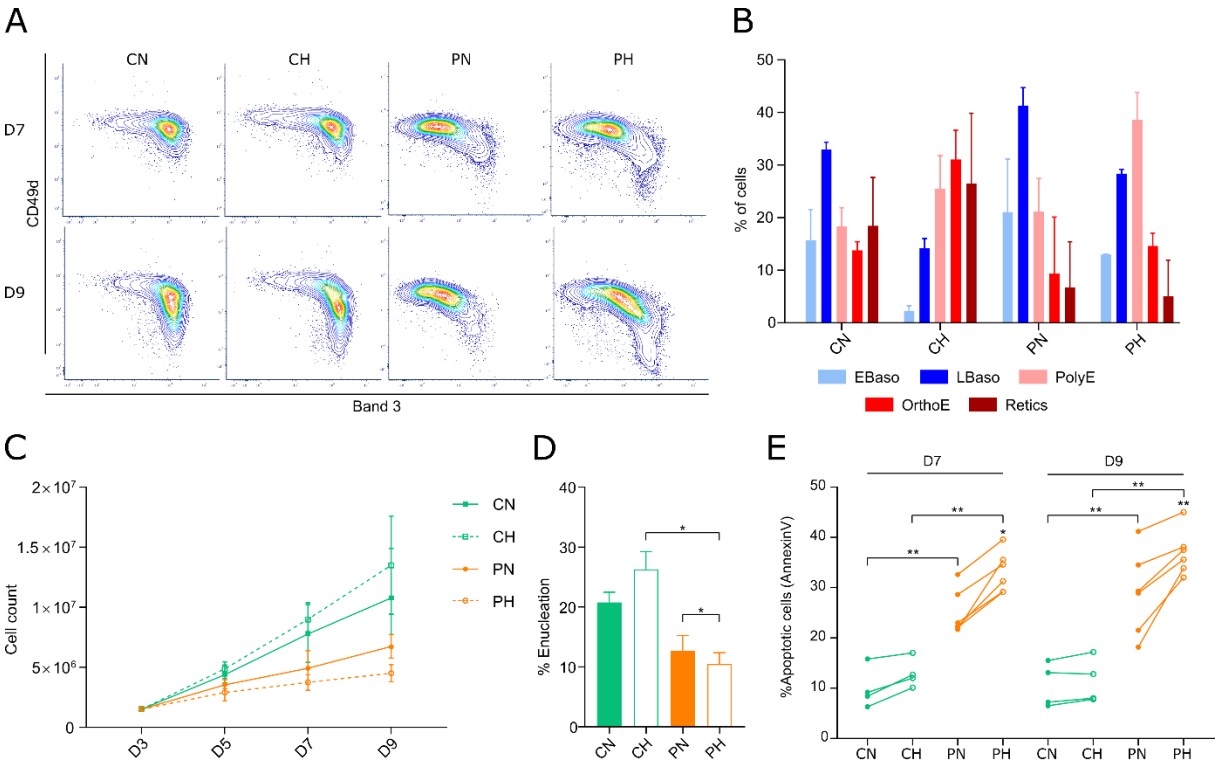

Figure 2: Cell proliferation and apoptosis during terminal erythroid differentiation *in vitro* under normoxia and partial hypoxia. (A) A contour plot representing the distribution of GPA-positive cells with respect to the expression of Band 3 (x-axis) and CD49d (y-axis) at D7 and D9 of phase II of culture in control erythroid precursors under normoxia (CN) or hypoxia (CH), and in patient erythroid precursors under normoxia (PN) or hypoxia (PH). **(B)** graph representing the cellular distribution as means ± SEM of early basophilic (EBaso), late basophilic (LBaso), polychromatic (PolyE), orthochromatic (OrthoE) and reticulocytes (Retics) at D9 of culture of CN, CH, PN and PH **(C)** Cell count of erythroid precursors at D3, 5, 7 and 9 in control (n = 4) and patient (n = 6) under normoxia and hypoxia (means ± SEM). **(D)** Percentage of enucleation measured at D11 for CN, CH, PN and PH erythroblasts (means ± SEM; CN and CH: n = 3; PN and PH: n = 6). **(E)** Percentage of apoptotic cells in control (n = 4) and patients (n = 6) under normoxia and hypoxia at D7 and D9 of phase II of culture. *p<0.05, **p < 0.01; Wilcoxon paired test and Mann-Whitney test (D and E).

B. HbS-HSP70 Protein Complexes in SCD Cells Under Hypoxia Lead to HSP70 Cytoplasmic Sequestration

As cytoplasmic sequestration of the chaperone protein HSP70 by α-globin aggregates is associated with cell death during erythropoiesis in β-thalassemia major, we investigated if apoptosis of SCD erythroblasts might be due to cytoplasmic trapping of HSP70 by HbS polymers (Arlet et al., 2016). We performed western-blot analyses to quantify HSP70 in the cytoplasmic and nuclear extracts of erythroblasts at D7 of phase II of culture (Figure 3A). There was less HSP70 in the nucleus and more in the cytoplasm of SCD erythroblasts under hypoxia compared to normoxia (Figure 3A), indicating mislocalization of HSP70 in SCD cells under hypoxia. Importantly, these lower amounts of nuclear HSP70 were associated with lower amounts of GATA-1 (Figure 3A), suggesting that cell death under these conditions was likely due to altered protection of GATA-1 by HSP70. To explore the molecular mechanism of cytoplasmic trapping of HSP70, we performed proximity ligation assays (PLA), that show fluorescent spots when two proteins are at a distance <40 nm (Schallmeiner et al., 2007). We detected

SCD cells with fluorescent spots (PLA+) under both normoxic and hypoxic conditions (Figure 3B) that were further quantified by imaging flow cytometry (Figure 3C). The percentage of PLA+ cells was very low in control, with values close to background levels (1-1.5%) under both normoxia and hypoxia, while SCD cells showed higher values under normoxia (4.5-18.5%) with a systematic and significant increase under hypoxia (9.5-36%) (Figure 3D), indicating proximity between HSP70 and HbS but not HSP70 and HbA. Moreover, PLA^+ SCD cells showed higher mean fluorescence intensity under hypoxia than under normoxia (Figure 3E), indicating that hypoxia induces the formation of more potent HbS-HSP70 complexes that could account for cytoplasmic retention of HSP70. To explore the potential of HbS polymers and HSP70 interacting within the same protein complex, we performed co-immunoprecipitation assays. SCD RBC suspensions were placed at normoxia, or hypoxia then lysed, and HSP70 was immunoprecipitated. Using an anti-α-globin antibody we found co-immunoprecipitation of HSP70 and α-globin under hypoxia but not under normoxia (Figure 3F) supporting the presence of HbS-HSP70 protein complex. Of note, despite using the same amounts of RBCs for both conditions, there was less immunoprecipitated HSP70 under hypoxia than normoxia likely due to decreased solubility of HbS polymer fibers under hypoxia as evidenced by the color of the lysates under both conditions and the presence of a small red colored precipitate under hypoxia (data not shown).

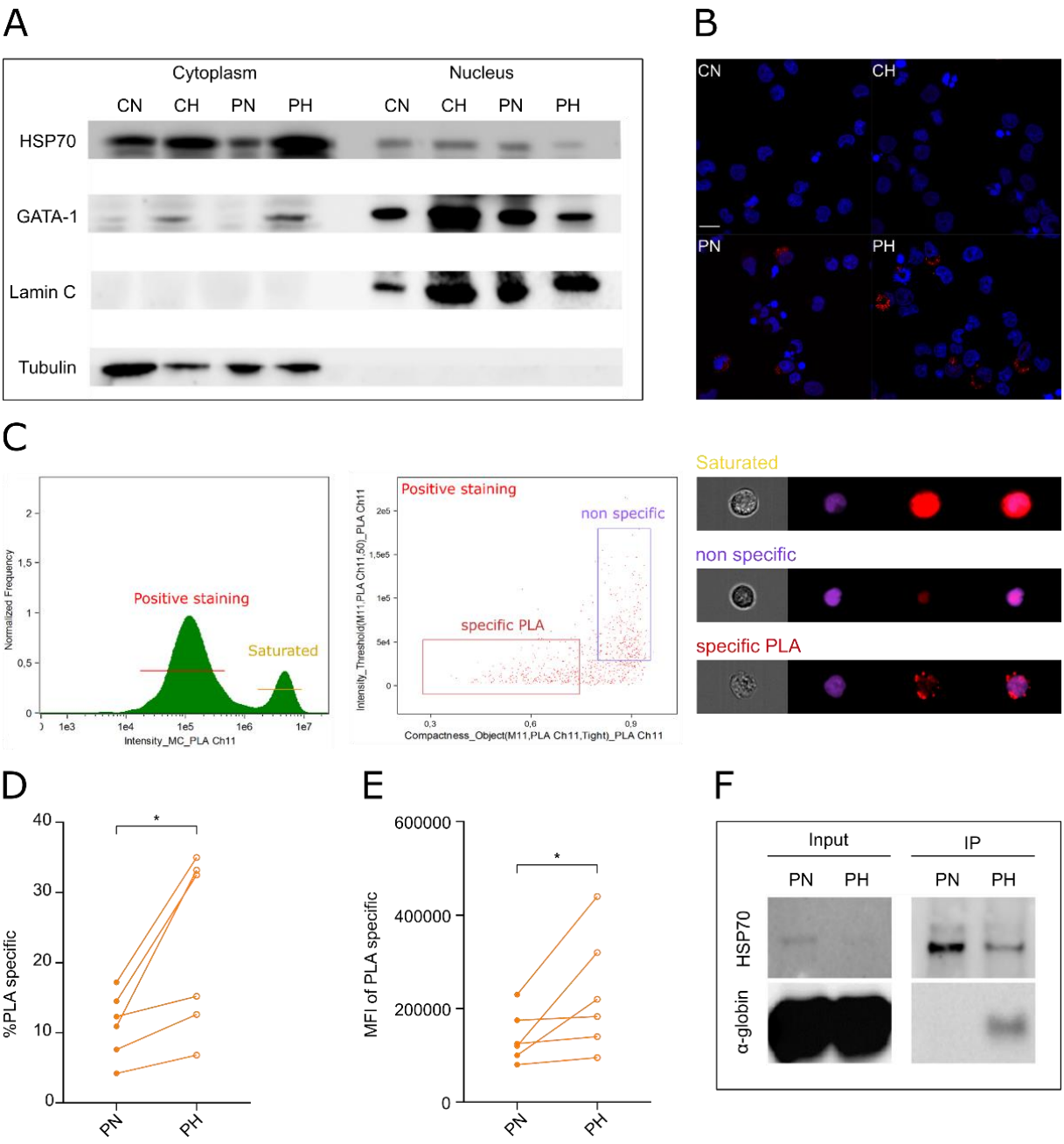

Figure 3: HSP70 and α-globin colocalization and co-immunoprecipitation. (A) Western-blot analysis of HSP70, GATA-1, Lamin C and Tubulin performed on cytoplasmic and nuclear extracts of erythroid precursors at D7 of phase II of culture from control normoxia (CN), control hypoxia (CH), patient normoxia (PN) and patient hypoxia (PH). **(B)** Proximity Ligation Assay (PLA) between HSP70 and α-globin at D7 of phase II of culture. Red spots indicate proximity (< 40 nm) between both proteins. Spots were observed in PN and PH cultures, while no spots were seen in CN and CH. A representative image of each culture is shown (n = 3); scale bar: 10µm. **(C)** (Left) A histogram representing the intensity of APC signal generated by PLA, a gating of positive staining and saturated staining is indicated. (Middle) A dot plot representing an analysis mask using the compactness feature (x-axis) and intensity feature (y-axis) to discriminate between PLA specific staining and non-specific staining. (Right) Representative images of each gate. **(D)** Percentage of cells and **(E)** mean fluorescence intensity of PLA-specific staining in erythroid precursors of PN and PH at D9 of phase II of culture (n = 6). **(F)** Co-immunoprecipitation assay of HSP70 with α-globin using circulating SCD red blood cells incubated under normoxia (PN) or hypoxia (PH) for 1 hour. HSP70 and α-globin bands are detected in the lysates (left panel) and after HSP70 immunoprecipitation (right panel). *p < 0.05, Wilcoxon paired test (D and E).

C. F-cells Are Enriched During SCD Erythroid Differentiation and the Induction of HbF Protects Against Cell Death.

Using flow cytometry, we measured the percentage of cells expressing HbF (F-cells) during *in vitro* differentiation. The percentage of F-cells (%F-cells) in control cultures fell within the reported range of 20-40%, while it was very variable for SCD cells reaching more than 70% at D9 (Figure 4A) (Antoniani et al., 2018; Y. Zhang et al., 2018). Interestingly, there was no difference of %F-cells between normoxia and hypoxia for control cells, while for SCD, %F-cells was higher under hypoxia than under normoxia for all the 6 independent primary cell samples (Figure 4A). Taken together with the apoptosis data, these findings imply that F-cells were positively selected under hypoxia in SCD. This inference was supported by flow cytometry data showing higher percentages of dead cells, based on the fixable viability stain (FVS), within the non-F-cell population as compared to the F-cell population for SCD cells (Figure 4B). In contrast, these percentages were similar between both cell populations in the control 9 (Figure 4B), confirming preferential apoptosis of the cells with low/no HbF expression in the SCD context only.

To confirm the anti-apoptotic role of HbF in SCD erythroblasts we induced its expression *in vitro* using pomalidomide (POM), an immunomodulatory drug previously shown to induce HbF expression during erythropoiesis, and determined if higher HbF levels could rescue the cells from apoptosis (Dulmovits et al., 2016; Moutouh-de Parseval et al., 2008). As we were interested in monitoring the stages during which hemoglobin is synthesized, POM was added at D1 of phase II of culture. As expected, POM-treated SCD cultures showed higher percentages of F-cells than untreated cultures (Figure 4C). HbF induction by POM was associated with significantly lower levels of apoptosis compared to untreated cultures under both hypoxia and normoxia (Figure 4E). Importantly, there was no significant difference in the apoptosis levels between normoxic and hypoxic conditions of POM-treated cells indicating that the higher F-cell levels protected SCD cells from apoptosis under hypoxia. To specifically address the role of HbF, we used a CRISPR-Cas9 approach that we have recently developed to mimic the effect of hereditary persistence of fetal hemoglobin (HPFH) by disrupting the binding site for HbF repressor LRF in the fetal γ-globin promoters (HBG1 and HBG2) (Weber et al., 2020). CD34+ cells were transfected either with a gRNA targeting the LRF binding site (-197) or a gRNA targeting an unrelated locus (AAVS1). Genome editing efficiency at the γ-globin promoter ranged between 23.2% and 73.5%, as determined by Sanger sequencing at D6 of phase I of culture. Cells were grown and differentiated under normoxia or hypoxia. As expected, the disruption of the LRF binding site resulted in HbF induction as shown by higher %F-cells compared to AAVS1 control (Figure 4D). These higher levels of F-cells resulted in decreased apoptosis, under both normoxic and hypoxic conditions (Figure 4F), clearly demonstrating the positive and selective effect of HbF on SCD cell survival.

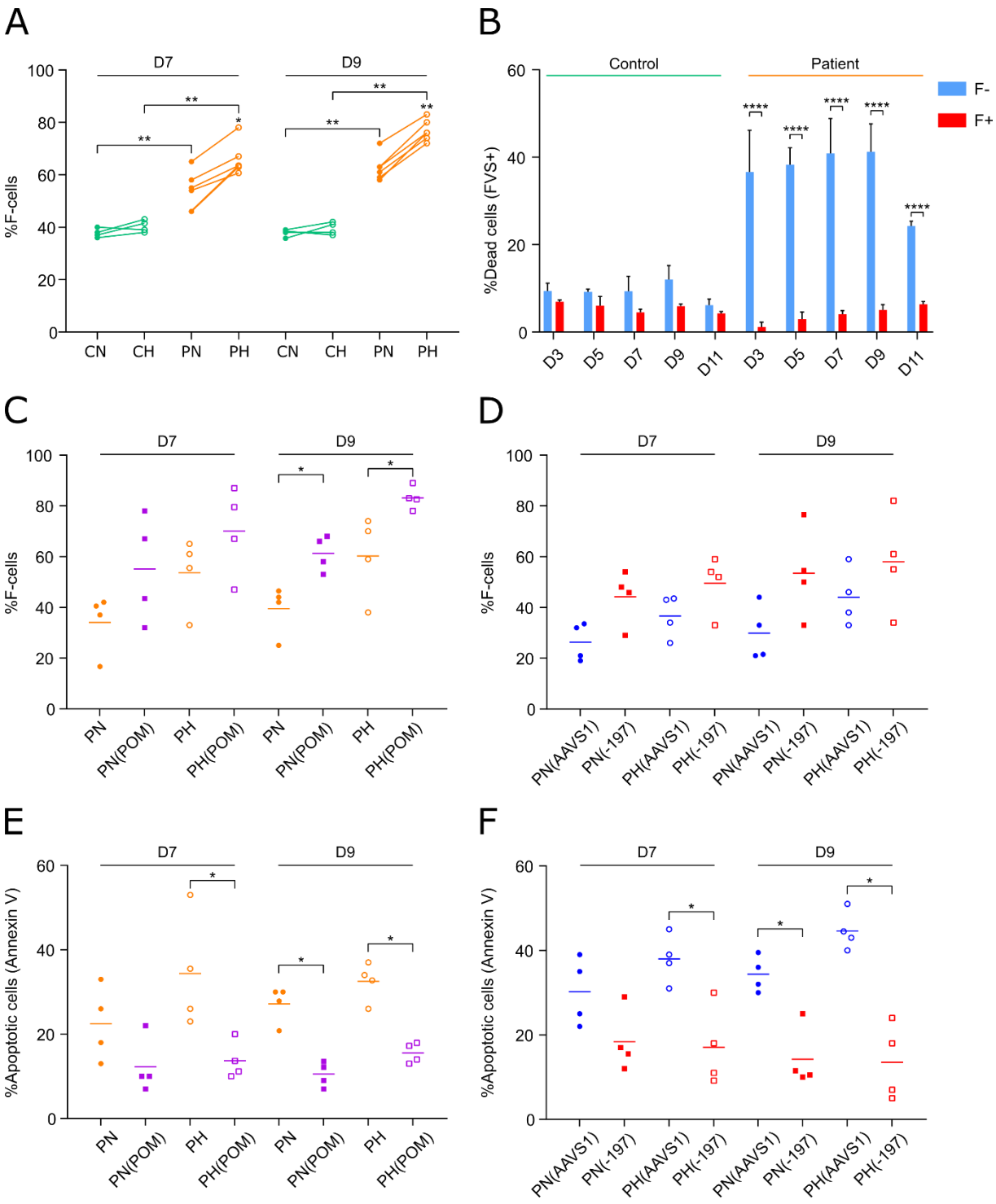

Figure 4: Distribution of erythroid precursors expressing HbF *in vitro*. (A) Percentage of F-cells measured at D7 and D9 of phase II of culture in control (n = 4) and patient cells (n = 6) under normoxia (N) and hypoxia (H). **(B)** Percentage of dead cells (means ± SEM) measured by fixable viability stain (FVS APC-Cy7), in non-F (F-) (in blue) and F-cells (F+) (in red) for control and patient cells under hypoxia. **(C)** Percentage of F-cells at D7 and D9 of phase II of culture of culture in patient erythroblasts under normoxia (PN), hypoxia (PH), normoxia with POM [PN(POM)] and hypoxia with POM [PH(POM)] (n = 4). **(D)** Percentage of apoptotic cells measured by flow cytometry in PN, PH, PN(POM) and PH(POM) at D7 and D9 of phase II of culture of culture (n = 4). **(E)** Percentage of F-cells at D7 and D9 of phase II of culture in PN and PH treated with gRNA targeting the LRF binding site (-197) or an unrelated locus as control (AAVS1) (n = 4). Genome editing efficiency was 56.1% ± 9.6% and 79.2%± 2.8 for -197 and AAVS1 samples, respectively. **(F)** Percentage of apoptotic cells at D7 and D9 of phase II of culture in PN and PH treated with gRNA targeting the LRF binding site (-197) or an unrelated locus as control (AAVS1) (n = 4). Horizontal bars represent the

mean of each group; *p < 0.05, **p < 0.01, ****p < 0.0001; Wilcoxon paired test (A) and Mann-Whitney test (A, B, C, E and F).

D. Cell Death During the Terminal Stages of Erythroid Differentiation in the Bone Marrow of SCD Patients

To validate direct relevance of the *in vitro* findings to *in vivo* conditions, we analyzed terminal erythroid differentiation using unmanipulated marrow samples from SCD patients. BM aspirates were obtained from 5 SCD patients and cells were stained for surface markers GPA, CD49d and Band 3 and analyzed by flow cytometry. Differentiating erythroblasts were determined using the CD49d and Band 3 staining pattern within the GPA^+ population (Figure 5A), as previously described (Hu et al., 2013). Imaging flow cytometry was used to confirm gating of all nucleated cells and cell homogeneity within each of the 4 gated populations by cellular features of size, morphology and nuclear size and polarization (Figure 5B). We quantified the cells at the early basophilic (EBaso), late basophilic (LBaso), polychromatic (PolyE) and orthochromatic (OrthoE) stages. Considering the GPA positive population as 100%, the mean percentages of EB, LB, polychromatic and orthochromatic cells were 5.1%, 10.2%, 20.4% and 25.2% (Figure 5A), indicating loss of the expected cell doubling between the polychromatic and orthochromatic stages (1.24 +/- 0.1, $p < 0.01$; Figure 5C), implying that cell death occurs between these two stages in a significant proportion of erythroblasts, which is in accordance with our *in vitro* data. Similar analysis was performed with BM aspirates of 5 controls that confirmed the expected doubling of cells with successive cell divisions without cell loss between development stages during normal erythropoiesis (Figure 5C). Next, we stained the cells with an anti-HbF antibody to measure the percentage of F-cells at the different stages. There was a significant increase in %F-cells between the PolyE (16.4% ± 4) and OrthoE stages (32.4% ± 4.79) (Figure 5D and 5E), concomitant with the cell loss observed between these stages (Figure 5C), indicating preferential survival of F-cells during late stages of erythroblast maturation *in vivo* and supporting our hypothesis for an anti-apoptotic role of HbF during *in vivo* erythropoiesis in SCD.

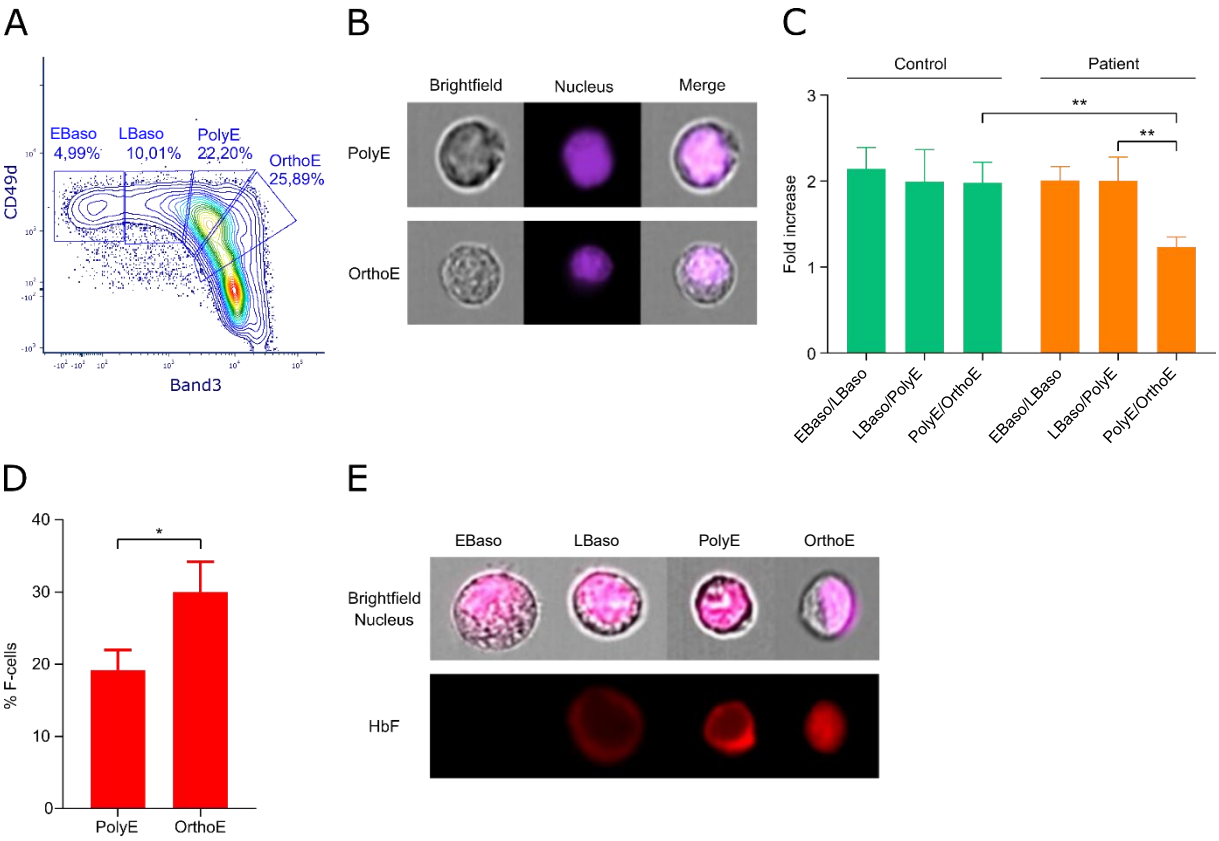

Figure 5: Analysis of human terminal erythroid differentiation *in vivo*. (A) A contour plot representing the distribution of GPA-positive cells with respect to Band 3 (x-axis) and CD49d (y-axis) from a bone marrow sample of a SCD patient. **(B)** Images obtained using imaging flow cytometry from the gating of polychromatic (PolyE) and orthochromatic (OrthoE) erythroblasts. Nucleus was stained with Hoechst. **(C)** The fold increase of cells between the early basophilic (EBaso) and late basophilic (LBaso) (EBaso/LBaso), LBaso and PolyE (Poly/LBaso), PolyE and OrthoE (OrthoE/PolyE) stages in 5 controls and 5 SCD patients (means ± SEM). **(D)** Percentage of F-cells *in vivo* in the PolyE and OrthoE subpopulations of the patient bone marrow samples (n = 5) (means ± SEM). **(E)** Imaging flow cytometry images of EBaso, LBaso, PolyE and OrthoE precursors. Upper images are a merge of brightfield and nucleus, lower images are for HbF staining (red). *p < 0.05, **p < 0.01; Mann-Whitney test (C and D).

E. Characterization of Circulating Erythroblasts in SCD Patients and their Link with Ineffective Erythropoiesis

After demonstrating the occurrence of ineffective erythropoiesis in SCD patients, we decided to work on patients with high levels of circulating erythroblasts, sometimes also referred to as nucleated RBCs (nRBCs). To better understand the interplay between circulating nRBCs and ineffective erythropoiesis in SCD, we characterized these cells in transfusion dependent SCD patients with an nRBC count >3%. Additionally, we investigated terminal erythroid differentiation in these patients using our 2-phase erythroid differentiation protocol.

To characterize the type of erythroblasts present in the peripheral blood of patients with high levels of circulating erythroblasts (SCD-HCNE) (from 16- to 52-year-old, median: 30 years-old), we isolated their peripheral blood mononuclear cells (PBMCs) and stained them for the surface markers CD71, CD105, and GPA, as previously described (Yan et al., 2021). As expected, SCD-HCNE patients exhibited a higher

percentage of $CD71^{+}GPA^{+}$ nucleated cells (3.99% ± 3.19) than patients without circulating erythroblasts (SCD-NE) (from 15- to 51-year-old, median: 25 years-old) and control individuals (Figure 6A). The analysis of the differentiation stages, using the combination of the 3 markers, showed that all the terminal differentiation stages were present in the circulation of SCD-HCNE patients, although at varying proportions. In most patients, high levels of LBaso (20.66% ± 10.67), PolyE (25.99% ± 7.99), and OrthoE (41.51% ± 21.56) could be found, with significantly lower levels of Ebaso compared to the other stages (6.4%± 5.47) (Figure 6B). The distribution of these differentiation stages varied between patients, with some individuals having predominantly EBaso or PolyE stages, while others had a majority of OrthoE in their circulation (Figure 6C), indicating some heterogeneity within this subset of patients. Notably, despite this inter-patient diversity, the percentages of these differentiation stages in the peripheral blood of SCD-HCNE patients resembled those typically observed in the BM.

Using flow cytometry, we measured the percentage of F-cells in the circulation of control individuals, SCD-NE patients and SCD-HCNE patients. As expected, %F-cells were significantly higher in SCD-NE patients (17.62% ± 8.637) compared to control individual (0.6% ± 0.21). However, while SCD-HCNE patients also had significantly increased %F-cells compared to control individuals (7.286% ± 7.022), these levels were significantly lower than those of SCD-NE patients (Figure 6D), suggesting a possible link between the presence of circulating RBCs and the low percentages of F-cells in these patients.

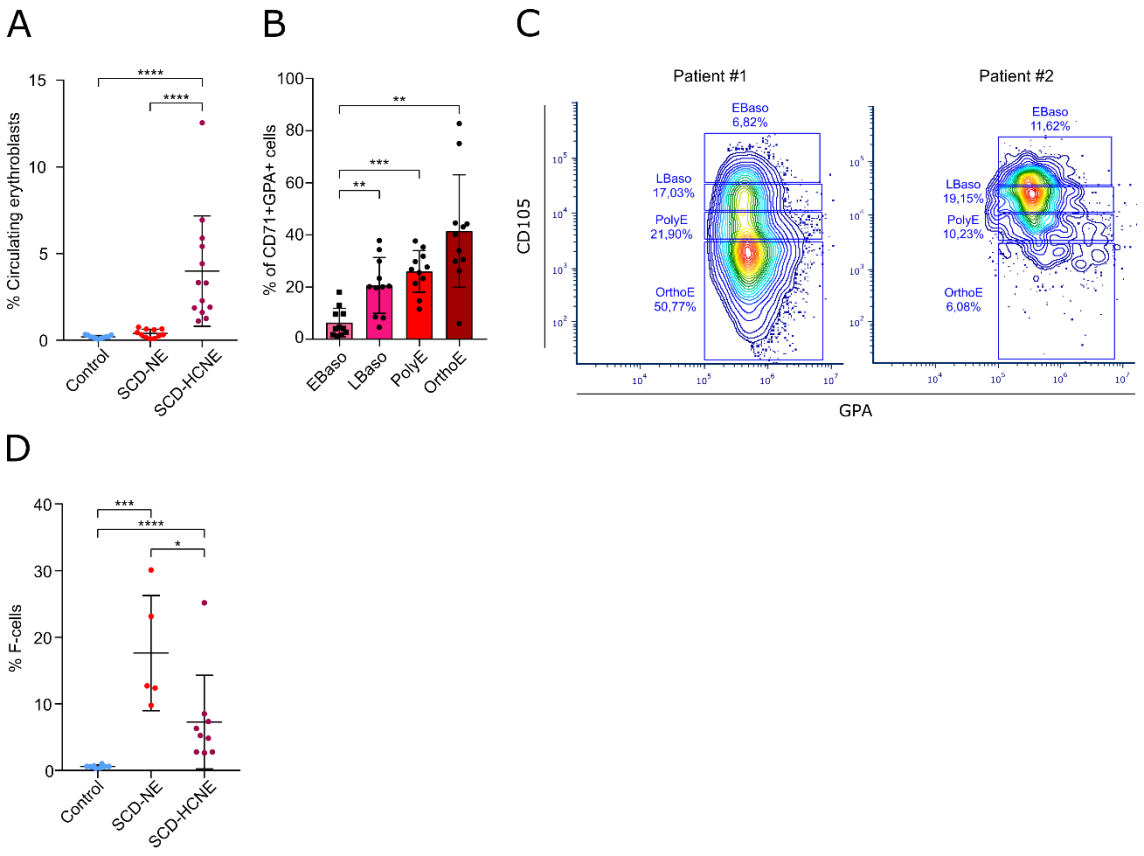

Figure 6: Characterizing circulating erythroblasts in a subset of SCD patients with circulating erythroblasts. (A) Percentage of nucleated GPA+ cells in peripheral blood mononuclear cells (PBMCs) in control (n=11), SCD-NE (n=11) and SCD-HCNE

(n=12). **(B)** Graph depicting the cellular distribution of early basophilic (EBaso), late basophilic (LBaso), polychromatic (PolyE), and orthochromatic erythroblasts (OrthoE) within $CD71^+GPA^+$ cells from PBMCs from SCD-HCNE patients (n=12). **(C)** Contour plots representing the distribution of $CD71^+GPA^+$ cells with respect to GPA (x-axis) and CD105 (y-axis) from the PBMCs of two SCD-HCNE patients. **(D)** Percentage of F-cells measured in the peripheral blood of control (n=8), patients with non-detectable levels of circulating erythroblasts (SCD-NE) (n=5) and patients with high levels of circulating erythroblasts (SCD-HCNE) (n=9). (means ± SD) *p < 0.0332, **p < 0.0021, ***p < 0.0002, ****p < 0.0001; Mann-Whitney test (B, C and D).

To further investigate terminal differentiation in this subset of patients, we conducted *in vitro* erythroid differentiation under normoxic conditions using $CD34^+$ cells obtained from both SCD-HCNE patients and age-matched SCD-NE patients, following the two-phase differentiation protocol described previously. While the acquisition of GPA showed no significant difference between the two patient subsets (Figure 7A), the differentiation process in SCD-HCNE patients appeared to progress faster compared to SCD-NE patients. This acceleration was particularly evident at D9 of culture, where a significant decrease of EBaso and a significant increase of PolyE and OrthoE could be observed in the SCD-HCNE culture (Figure 7B, 7C, 7D, 7E and 7F). This acceleration was systematically observed for all SCD-HCNE patients when compared to their age-matched SCD-NE counterparts (Figure 7G). Despite this difference in differentiation speed, there were no significant variations in terms of proliferation, viability, and enucleation between SCD-NE and SCD-HCNE cells (Figure 8A, 8B, and 8C). However, we observed a notable decrease in the %F-cells in the cultures of SCD-HCNE patients compared to SCD-NE patients, reflecting what we had observed in the peripheral blood of these patients (Figure 8D).

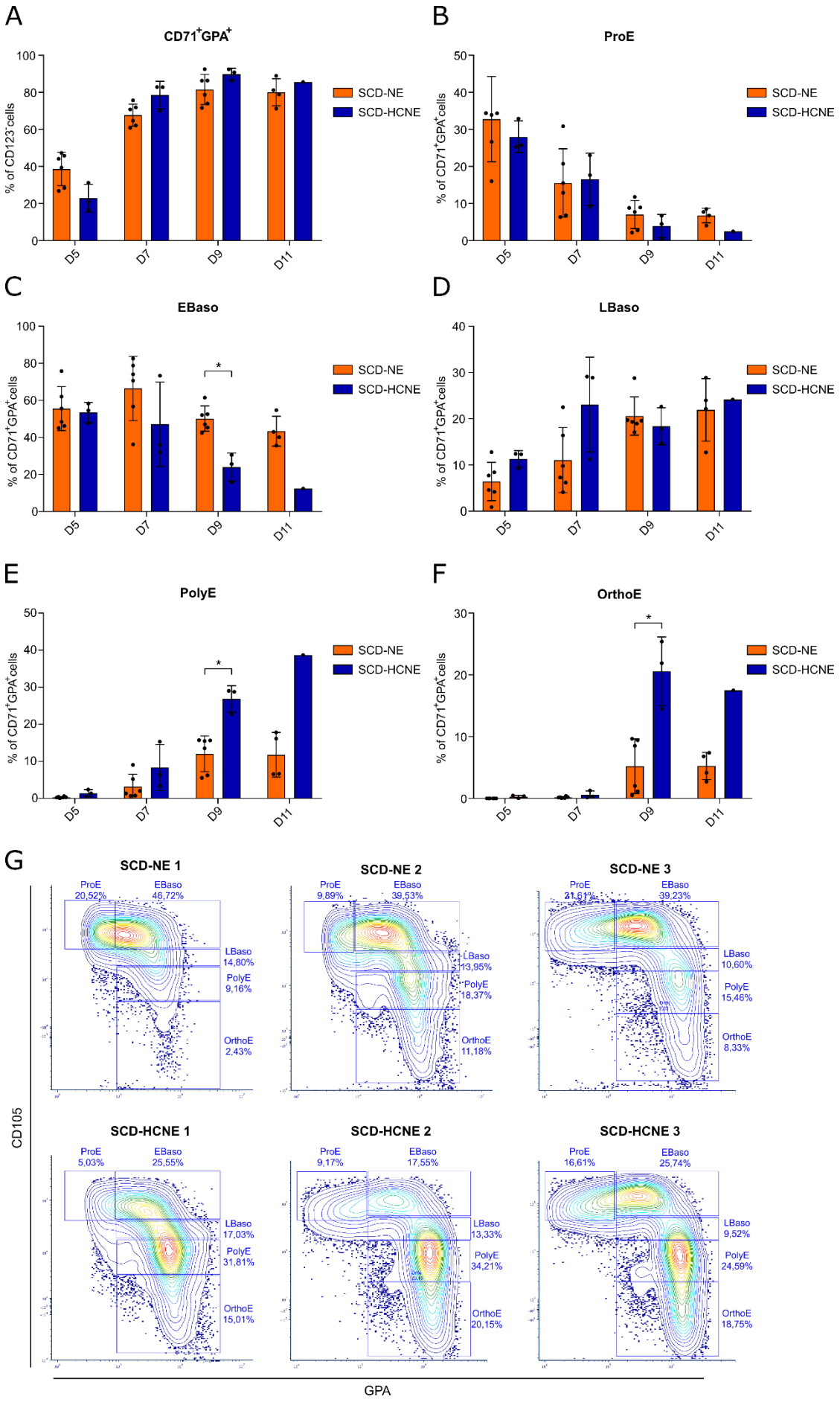
A
CD71+GPA+
% of CD123- cells
SCD-NE
SCD-HCNE
D5
D7
D9
D11
B
ProE
% of CD71+GPA+ cells
C
EBaso
D
LBaso
E
PolyE
F
OrthoE
G
SCD-NE 1
ProE 20,52%
EBaso 46,72%
LBaso 14,80%
PolyE 9,16%
OrthoE 2,43%
SCD-NE 2
ProE 9,89%
EBaso 39,53%
LBaso 13,95%
PolyE 18,37%
OrthoE 11,18%
SCD-NE 3
EBaso 39,23%
LBaso 10,60%
PolyE 15,46%
OrthoE 8,33%
SCD-HCNE 1
ProE 5,03%
EBaso 25,55%
LBaso 17,03%
PolyE 31,81%
OrthoE 15,01%
SCD-HCNE 2
ProE 9,17%
EBaso 17,55%
LBaso 13,33%
PolyE 34,21%
OrthoE 20,15%
SCD-HCNE 3
ProE 16,61%
EBaso 25,74%
LBaso 9,52%
PolyE 24,59%
OrthoE 18,75%
CD105
GPA

Figure 7: SCD-HCNE CD34+ cells exhibit accelerated differentiation compared to SCD-NE patients under normoxia. (A) Frequency of $CD71^+/GPA^+$ cells within the CD123- compartment and **(B-F)** Frequency of early basophilic (EBaso), late basophilic (LBaso), polychromatic (PolyE), and orthochromatic erythroblasts (OrthoE)within the $CD71^+/GPA^+$ compartment from day 5 (D5) to day 11 (D11) of the second phase of culture in patients with non-detectable levels of circulating erythroblasts (SCD-NE) (n=6) and patients with high levels of circulating erythroblasts (SCD-HCNE) (n=3). **(G)** Contour plots representing the distribution of $CD71^+GPA^+$ cells with respect to GPA (x-axis) and CD105 (y-axis) from SCD-HCNE and their age-matched SCD-NE patients at day 9 of phase II of culture (means ± SD). *p < 0.0332, Mann-Whitney test (C, E and F)

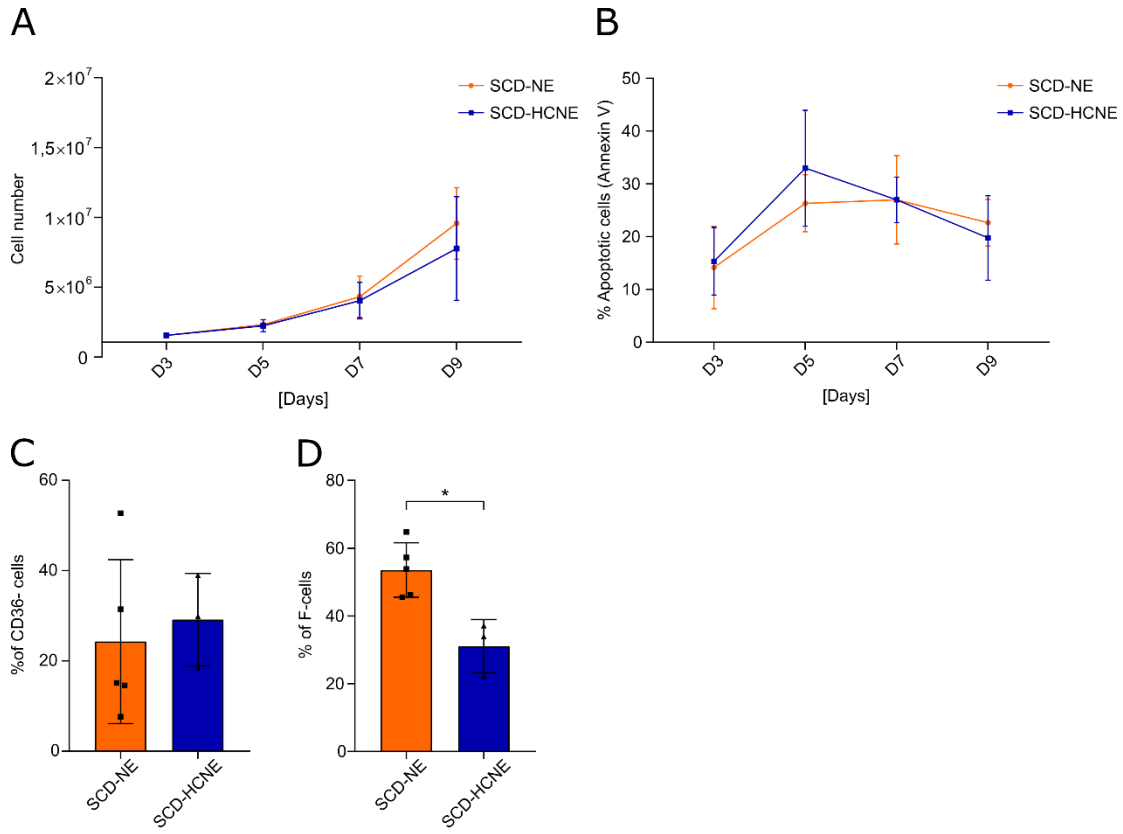

Figure 8: Analysis of terminal differentiation in SCD-HCNE patients. (A) Cell count of erythroid precursors at D3, 5, 7 and 9 in SCD-NE (n = 6) and SCD-HCNE patients (n = 3) under normoxia (means ± SD). **(B)** Percentage of apoptotic cells in SCD-NE (n = 5) and SCD-HCNE (n = 3) under normoxia D3, D5, D7 and D9 of phase II of culture. **(C)** Percentage of enucleation measured at D9 of phase II of culture for SCD-NE (n = 5) and SCD-HCNE (n = 3) under normoxia (mean ± SD). **(D)** Percentage of F-cells measured at D9 for SCD-NE (n = 5) and SCD-HCNE (n = 3) under normoxia (mean ± SD). *p<0.0332, Mann-Whitney test (Figure D).

II. DISCUSSION

Ineffective Erythropoiesis and the Role of HbF in SCD

Ineffective erythropoiesis has been previously suggested to be a feature of SCD (Blouin et al., 1999; Finch et al., 1982; Hasegawa et al., 1998; Wu et al., 2005) but it has not been critically evaluated and documented. Our present findings provide direct evidence for ineffective erythropoiesis in SCD patients, with significant cell death occurring at the late stages of terminal erythroid differentiation *in vivo*.

Among previous reports, the study by Wu and collaborators has highlighted abnormalities during erythropoiesis in the BM of transplanted SCD patients by showing progressive intramedullary loss of SCD erythroblasts and relative enrichment of donor erythroid precursors at the onset of hemoglobinization in a small cohort of patients (Wu et al., 2005). Our results further demonstrate significant cell death between the PolyE and the OrthoE stages, when cellular HbS concentration reaches sufficiently high levels to promote polymer formation under partial hypoxia. Our *in vivo* data unequivocally document the occurrence of ineffective erythropoiesis in non-transplanted SCD patients, in the absence of confounding factors like conditioning drugs and exogenous donor-related factors that can impact the hematopoietic niche and interfere with the survival of patient's erythroblasts.

Our study also reveals a new role for HbF in SCD by showing that it protects a subpopulation of differentiating erythroblasts from apoptosis, both *in vivo* and *in vitro*. HbF is a known modulator of disease severity in SCD as it inhibits HbS polymerization at the molecular level, preventing or attenuating RBC sickling and alleviating disease complications (Powars et al., 1984; Sewchand et al., 1983). In healthy adults, HbF accounts for less than 1% of total hemoglobin (Boyer et al., 1977) and is restricted to a small subset of RBC (2%) called F-cells (Boyer, Belding, Margolet, et al., 1975; Boyer, Belding, Margolte, et al., 1975; Wood et al., 1975). In SCD, the expression of HbF is higher than in healthy individuals and varies considerably among patients. Although the mechanisms underlying increased expression of HbF are not completely elucidated, stress erythropoiesis and preferential survival of F-cells in the circulation are suggested contributing factors (Dover et al., 1978; Franco et al., 1998; Franco et al., 2006; Maier-Redelsperger et al., 1994; Stamatoyannopoulos et al., 1985). Our study shows that HbF has a dual beneficial effect in SCD by conferring a preferential survival of F-cells in the circulation and by decreasing ineffective erythropoiesis. These findings thus bring new insights into the role of HbF in modulating clinical severity of anemia in SCD by both regulating red cell production and red cell destruction.

Our findings show that *in vitro* induction of HbF by pomalidomide rescues SCD erythroblasts from cell death and improves their differentiation, in accordance with improved efficiency of erythropoiesis *in vivo* in treated SCD mice (Meiler et al., 2011). Furthermore, results using genetically modified

$CD34^+$ cells strongly imply that overexpression of HbF and concomitant down-regulation of HbS (Weber et al., 2020) in a specific and selective manner corrects the apoptosis observed during erythroid differentiation, which is therefore presumably a feature of HbS.

HSP70 is a chaperone protein that plays an important role during erythropoiesis by protecting GATA-1 from cleavage by caspase-3 in the presence of Epo (Ribeil et al., 2007), thus promoting normal terminal differentiation. From a mechanistic perspective, sequestration of HSP70 in the cytoplasm through interaction with HbS polymers is therefore a possible mechanism for ineffective erythropoiesis in SCD. Co-immunoprecipitation of HSP70 and HbS under hypoxia is indeed highly suggestive of such interactions between these proteins. Furthermore, specific HSP70 sequestration in the pool of SCD dead cells under hypoxia could account for the lower HSP70 nuclear content of these cells and the subsequent lower GATA-1 nuclear levels. As the molecular event that initiates HSP70 trapping in SCD, namely HbS polymerization, occurs in cells with high cellular concentration of HbS, required for polymer formation, our results show the absence of cell death in the early stages of differentiation where the intracellular concentration of HbS is likely insufficient to induce sickling. Likewise, low levels of HbF are less protective against cell death, since a minimal threshold of intracellular HbF is needed for a protective polymer-inhibiting effect (Noguchi et al., 1989). At physiological levels of hypoxia, there is however not an exclusive selection of F-cells, as significant amounts of cells with no/low HbF were found to complete erythroid differentiation. Further studies are needed to fully address the biological mechanisms underlying this observation and the commitment of erythroid progenitors to the F lineage in SCD.

Furthermore, this study sheds light on the importance of applying partial hypoxia during erythroid differentiation *in vitro* to mimic *in vivo* conditions in SCD. In our view, this together with cell proliferation and apoptosis are important parameters to consider in assessing the beneficial impact of therapeutic approaches in SCD such as HbF induction (Antoniani et al., 2018; McArthur et al., 2020; Paikari & Sheehan, 2018), anti-sickling molecules such as voxelotor (Howard et al., 2019; Vichinsky et al., 2019), or gene therapy aiming at expressing a therapeutic β-globin (Ribeil et al., 2017). In addition, specific targeting of ineffective erythropoiesis should presumably have a major beneficial clinical impact.

Exploring Circulating Erythroblasts in SCD: Insights, Mechanisms, and Future Directions

Circulating erythroblasts can occasionally be detected in SCD patients during routine blood tests, especially in those experiencing episodes of severe hemolysis (Ballantine et al., 2019; Juwah et al., 2004). The presence of these cells in the peripheral blood of adults is generally believed to reflect BM disease and has been linked to excessive erythropoietic activity or activated extramedullary

hematopoiesis in other hematological disorders (Danise et al., 2011; Karakukcu et al., 2015). Case reports have shown that the development of BM necrosis in patients with SCD is associated with very high numbers of circulating nRBCs (Ataga & Orringer, 2000). Furthermore, in SCD, the presence of these cells in the periphery is also thought to result from various factors, including chronic hemolysis, splenic dysfunction, inflammation, and tissue hypoxia (Dulay et al., 2008; Kuert et al., 2011; Porter et al., 2017). It is worth noting that these factors can manifest differently in individual patients. Therefore, circulating erythroblasts might arise through multiple mechanisms in SCD (Bain, 2021; Constantino & Cogionis, 2000). While some evidence suggests a link between nRBCs and disease severity, it has not yet been identified as a consistent marker, as SCD patients with high levels of nRBCs can exhibit varying symptoms and disease manifestations (Ballantine et al., 2019). For example, a recent retrospective study on patients hospitalized for uncomplicated vaso-occlusive episodes revealed that while an increase of nRBC counts during hospitalization could be associated with developing acute chest syndrome or the requirement for RBC transfusion, the initial nRBC count in these patients was not linked to disease severity (Ballantine et al., 2019).

Our results reveal a reduced enucleation rate in SCD precursor cells compared to control cells, further exacerbated by hypoxia. This suggests that alterations during the final stages of differentiation could impact organelle and protein sorting, as well as terminal maturation. These defects under hypoxia may be attributed to the accumulation of HbS fibers in the cytoplasm, potentially disrupting the enucleation process. Moreover, when we analyzed the differentiation stages of circulating erythroblasts in SCD-HCNE patients, we noted that these cells were predominantly orthochromatic erythroblasts. This observation is consistent with the existence of an enucleation defect. Our *in vitro* preliminary data showed no significant difference in enucleation between $CD36^-$ cells from SCD-HCNE patients and SCD-NE patients. It is noteworthy that we have not yet cultured SCD-HCNE erythroid cells under hypoxic conditions; such experiments would be important to perform to get closer to physiological conditions and explore whether cells from these patients exhibit a more severe phenotype compared to other SCD patients.

Circulating erythroblasts may also result from defects in macrophage–erythroblast interactions within the erythroblastic island (EBI), which might explain the presence of earlier differentiation stages (PolyE, EBaso, and LBaso) in SCD-HCNE patients (Sesti-Costa et al., 2023). This hypothesis is further explored in the third chapter of this thesis.

Another interesting observation is that most SCD-HCNE patients exhibited low levels of F-cell. Low F-cells are typically linked to more severe SCD cases (Akinsheye et al., 2011; Platt et al., 1994; Powars et al., 1984). Considering that high levels of nRBCs have been suggested as an additional marker of disease

severity, it may be interesting to investigate whether this association is merely a correlation or if there is a link between the two parameters. Notably, HCNE CD34$^+$ cells cultured *in vitro* produced significantly fewer F-cells than SCD-NE patients without any discernable impact on their viability. In this study, we focused primarily on patients who were not treated with hydroxyurea (HU). However, it would be interesting to know if similar findings could be found in patients treated with HU, as this treatment promotes HbF expression (Galanello et al., 1985; Stamatoyannopoulos et al., 1985). Interestingly, HU-treated patients have been found to have more nRBCs than non-HU treated patients (Ballantine et al., 2019). SCD HCNE patients present a valuable opportunity for comprehensive research into the mechanisms governing F-cell regulation and its implications for SCD. Investigating the genetic, molecular, and environmental factors influencing F-cell levels in these patients can provide crucial insights into the pathophysiology of the disease.

Although our study primarily concentrated on terminal differentiation, exploring the earlier stages of erythropoiesis could also prove interesting (Minniti et al., 2020; Tolu et al., 2020). Characterizing the phenotype and gene expression signatures of patrolling HSPCs in SCD patients, whether they have circulating erythroblasts or not, could offer valuable insights into the mechanisms underlying the appearance of nRBCs in peripheral blood. In our *in vitro* experiments, we observed an accelerated maturation of CD34$^+$ cells from the peripheral blood of SCD-HCNE patients, in contrast to those from patients without detectable nRBCs. This indicates a potential intrinsic difference in patrolling HSPCs between these patient populations. While this accelerated maturation was not accompanied by a significant difference in proliferation during terminal differentiation, considering the overall proliferation throughout the entire culture period may offer a more comprehensive perspective. Therefore, the study of erythroid progenitors in our *in vitro* experiment could also offer valuable insights into the properties of SCD-HCNE HSPCs.

In certain pathological circumstances, mainly as a compensatory mechanism for the destruction of the proper function of the BM, the genesis of blood cells can move to other organs, mostly the ones involved in fetal hematopoiesis, such as the liver and the spleen (Cenariu et al., 2021; Hu & Shilatifard, 2016). This process is called extramedullary hematopoiesis and has been linked with the appearance of circulating erythroblasts in many pathologies (Cenariu et al., 2021). Given the ineffective erythropoiesis observed in SCD, we hypothesize that a similar process might occur in SCD patients. Transcriptomic studies have already indicated the possibility of distinguishing differences in extramedullary gene expression profiles in patrolling HSPCs between healthy donors and patients with conditions like lupus (Kokkinopoulos et al., 2021). Therefore, conducting such studies on HSPCs from SCD patients with varying phenotypes and comparing these results to patients with other pathologies characterized by circulating erythroblasts, such as β-thalassemia, lupus, or atherosclerosis, could

provide valuable insights. Furthermore, exploring the homing capacities of HSPCs from SCD-HCNE patients through engraftment experiments in mice could also help determine whether these circulating HSPCs exhibit altered properties (Bonig et al., 2006). Such findings would open the door to investigating whether BM HSCs from the same patients exhibit altered characteristics, which could impact their regenerative and BM reconstitution abilities. These factors are critical considerations, particularly in gene therapy research (Leonard et al., 2019; Weidt et al., 2007).

The accelerated erythroid maturation observed in SCD-HCNE patients might also be reminiscent of myeloproliferative neoplastic disorders, such as polycythemia vera. These pathologies are known to have high levels of circulating erythroblasts due to deteriorated BM function (Danise et al., 2011). Notably, myeloid neoplasms have occasionally been observed in patients with SCD, although the underlying connection between the two conditions remains unclear (Brunson et al., 2017; Y. Li et al., 2019; Seminog et al., 2016). To explore this connection, it would be interesting to perform next-generation sequencing on $CD34^+$ cells from SCD-HCNE patients to identify mutations associated with a higher risk of developing myeloproliferative neoplastic disorders.

While the presence of circulating erythroblasts in SCD patients opens numerous avenues for research, it is crucial to acknowledge that while SCD has a 'simple' genetic cause, its complications and treatments are far from straightforward, influenced by a multitude of factors, some of which are not easily discernible (Brousse et al., 2014; El Hoss et al., 2022). Consequently, each patient presenting HCNE may have a distinct pathophysiologic basis for elevated nRBCs, making it challenging to pool patients together and pinpoint a single cause for this clinical manifestation. Furthermore, circulating erythroblasts levels may also change over time, adding a layer of complexity to the study of this phenomenon. Overcoming this challenge might involve conducting longitudinal studies on SCD-HCNE patients.

III. MATERIAL AND METHODS

A. Biological Samples

The study was conducted according to the declaration of Helsinki with approval from the Medical Ethics Committee (GR-Ex/CPP-DC2016-2618/CNILMR01). All SCD patients were of SS genotype. Blood bags from SCD patients enrolled in an exchange transfusion program were obtained from Necker-Enfants Malades Hospital (Paris, France), and the Conception Hospital (Marseille, France). BM aspirates from five SCD patients undergoing surgery and BM tissues from five non-anemic donors undergoing hip/sternum surgery, were obtained after informed consent, from Necker-Enfants Malades Hospital (Paris, France), and the North Shore-LIJ Health System (New York, USA) under Institutional Review Board (IRB) approval. Control blood bags from healthy donors were obtained from the Etablissement Français du Sang (EFS).

B. Antibodies and Fluorescent dies

BV421-conjugated anti-GPA, APC-conjugated anti-CD49d, PE-conjugated anti-HbF, APC-conjugated anti-CD71, and APC-conjugated anti-CD36 mouse monoclonal antibodies were obtained from BD Biosciences. The APC-A750-conjugated anti-GPA, BV786-conjugated anti-CD71, BV660-conjugated anti-CD123 and BV450-conjugated anti-CD105 mouse monoclonal antibodies and the DRAQ7 stain were obtained from Biolegend. The PE-conjugated anti-Band 3 mouse monoclonal antibody (PE-BRIC6) was obtained from Bristol Institute for Transfusion Sciences. Anti-Lamin A/C and anti-α hemoglobin mouse monoclonal antibodies were obtained from Santa Cruz Biotechnology. Hoechst33342 was obtained from Life Technologies; Hoechst34580, Fixable viability stain (FVS) 780, 7-Aminoactinomycin D (7AAD), Retic-Count™, and PE-conjugated Annexin V were obtained from BD Biosciences. Rabbit anti-HSP70/HSP72 polyclonal antibody was obtained from Enzo Lifesciences. Mouse HRP anti-actin monoclonal antibody was obtained from Santa Cruz Biotechnology. Anti-rabbit and anti-mouse IgG, HRP-linked secondary antibodies were purchased from Cell Signaling. Goat anti-rabbit Alexa 633 and Alexa 488 secondary antibodies were obtained from Invitrogen. DAPI Fluoromount – G mounting media was obtained from Southern Biotech.

C. *In vitro* Differentiation of Human Erythroid Progenitors

Peripheral blood mononuclear cells were isolated from blood samples after Pancoll fractionation (PAN Biotech). $CD34^+$ cells were then isolated by a magnetic sorting system (Miltenyi Biotec CD34 Progenitor cell isolation kit) following the supplier protocol. $CD34^+$ cells were placed in an *in vitro* two-phase liquid culture system, as previously described (Freyssinier et al., 1999). During the first phase, cells were expanded for 7 days in a medium containing 100 ng/ml of human recombinant (hr) interleukin (IL)-6 (Miltenyi Biotec), 10 ng/ml of hr IL3 (Miltenyi Biotec) and 100 ng/ml hr stem cell factor (SCF) (Miltenyi Biotec) in Iscove's Modified Dulbecco's Medium (IMDM) (Gibco) supplemented with 15% BIT 9500 (Stem Cell Technologies), 100 U/ml Penicillin Streptomycin (Gibco) and 2 mM L-Glutamine (Gibco). On

day 7, cells were harvested and cultured for 11 days with the second phase medium [10 ng/ml hr IL-3, 100 ng/ml hr SCF, and 2 U/ml of EPO]. At day 3 of phase II, 2 cell suspensions were split into 2 and one half was cultured under partial hypoxia (5% O2) until day 11 while the other was cultured at normoxia. Cells were diluted at $0.5x10^6$ cells/ml at day 3, 5, 7, 9 and 11 of phase II.

For cultures treated with pomalidomide, cells were incubated with 1 mM pomalidomide (Sigma) as previously described (Dulmovits et al., 2016), starting from day 1 of phase II of culture. For γ-globin derepression experiments using CRISPR/Cas9, patient $CD34^+$ cells were immunoselected and cultured for 48 hours and then electroporated with ribonucleoprotein (RNP) complexes containing Cas9-GFP protein (4.5 mM) and the -197 guide RNA (gRNA) targeting both *HBG1* and *HBG2* γ-globin promoters (5' ATTGAGATAGTGTGGGGAAGGGG 3') or a gRNA targeting the Adeno-associated virus integration site 1 (AAVS1; 5' GGGGCCACTAGGGACAGGATTGG 3') (Weber et al., 2020). Cleavage efficiency was evaluated in cells harvested 6 days after electroporation by Sanger sequencing followed by tracking of indels by decomposition (TIDE) analysis (Brinkman et al., 2014).

D. Imaging Flow Cytometry of Human Bone Marrow Samples

BM samples were processed as previously described (Hu et al., 2013). For BM samples from SCD patients, mononuclear cells were fixed with PBS 1% formaldehyde (Sigma), 0.025% glutaraldehyde (Sigma) for 15 min, washed twice with PBS, permeabilized with 0.1 M Octyl β-D-Glucopyranoside (Sigma) for 15 min and saturated in PBS, 1% BSA, 2% goat serum for 30 min. Cells were then stained for GPA, CD49d, Band 3 and HbF for 30 min in the dark. Cells stained with the isotype control antibodies were used as a negative control. Compensation was performed using BD Biosciences compensation beads following the supplier instructions. Samples were then analyzed using the Imagestream ISX MkII flow cytometer (Amnis Corp, EMD Millipore) and the INSPIRE software version 99.4.437.0. Acquired data was analyzed using IDEAS software version 6.2 (Amnis Corp, EMD Millipore).

E. Flow Cytometry

Cells were analyzed using a BD FACScanto II flow cytometer, BD LSR Fortessa SORP flow cytometer (BD Biosciences) and Cytoflex S flow cytometer (Beckman Coulter) and acquired using the Diva software version 8 (BD Biosciences) and the Cytexpert software (Beckman Coulter). Data was analyzed using FCS Express 6 software (DeNovo Software) or the Cytexpert Software (Beckman Coulter).

1. Surface marker staining

In vitro cultured cells were stained for surface expression of GPA, Band 3 and CD49d on days 3, 5, 7, 9 and 11. Briefly, 10^5 cells were suspended in 20 µl of PBS supplemented with 0.5% of bovine serum albumin (BSA), incubated with fluorescence-conjugated antibodies for 30 min in the dark, washed twice with PBS, 0.5% BSA before incubation with 7AAD for 5 min prior to analysis.

Cells in culture were also analyzed for surface expression of GPA, CD71, CD105 and CD123 on days 3, 5, 7, 9 and 11, as well as cells from PBMCs. For this $2.5.10^5$ cells were washed twice with phosphate-buffered saline (PBS) supplemented with 2% fetal bovine serum (FBS) and 1 mM EDTA. After blocking with 0.4% human AB serum for 20 min on ice, cells were stained with fluorochrome-conjugated antibodies for 30 min on ice. Cells were washed twice with PBS 2% FBS 1 mM EDTA and stained with 300 nM of DRAQ7 for 15 min at RT before analysis.

2. Enucleation analysis

Cells (10^5) were washed once with PBS, stained with 1 µg/ml Hoechst34580 for 45 min at 37°C, washed twice with PBS, 0.5% BSA and incubated with anti-CD36 antibody for 30 min in the dark. Cells were then washed twice with PBS, 0.5% BSA and analyzed.

3. Apoptotic cells

Cells were stained with PE-conjugated Annexin V to measure the percentage of apoptotic cells. Briefly, 10^5 cells were washed once with Annexin buffer, resuspended in 25 µl of the same buffer and stained with 2.5 µl of PE-conjugated Annexin V for 20 min in the dark. Samples were then diluted with 200 µl of Annexin buffer prior to analysis.

4. HbF staining on cultured erythroblasts and bone marrow samples

Cells were stained with FVS at a dilution of 1/1000 for 20 min in the dark, washed twice with PBS then fixed with 1% formaldehyde, 0.025% glutaraldehyde in PBS for 15 min. Cells were then washed twice with PBS, permeabilized in 0.1 M Octyl βD-Glucopyranoside for 15 min and saturated in PBS, 1% BSA, 2% goat serum for 30 min. Cells were then stained with anti-HbF and anti-GPA antibodies for 30 min in the dark, washed twice and analyzed. Hoechst33342 nucleus dye was added before analyzing the cells with imaging flow cytometry.

5. HbF staining on peripheral blood

Three µl of RBCs were fixed in with 1% formaldehyde, 0.025% glutaraldehyde, PBS 1x for 15 min. After 2 washes with PBS, RBCs were permeabilized in 0.1 M Octyl β-D-Glucopyranoside for 15 min and saturated in PBS, 1% BSA, 0.2% goat serum for 30 min. The RBC pellet was suspended in 60 µl of saturation solution and 10 µl of this suspension were incubated with 5 µl of PE-conjugated HbF antibody (Life Technologies) and with 5 µl of APC-conjugated CD71 antibody (Invitrogen), for 20 min. RBCs were washed and suspended in 200 µl of BD Retic-Count™ (thiazole orange) reagent. After 30 min of incubation, cells were analyzed.

F. Cytospin

Cytospin was performed using 100,000 cells. Cells were washed twice with PBS and spun on slides using the Cytospin 2 centrifuge (Shandon). Slides were stained with May-Grunwald Giemsa (MGG) following manufacturer's instructions (Sigma). Slides were then washed with deionized water and left to dry. Slides were covered by a coverslip using the EUKITT classic (O. Kindler ORSA Tech). Cells were imaged using an inverted microscope (Leica DM6000 B) with a 20x/0.4 HCX PL FLUOTAR, equipped with a DFC300 FX color camera. Analysis was performed using the Fiji software (Schindelin et al., 2012).

G. Proximity Ligation Assay

Proximity ligation assays (PLA) were performed with cells from D7 of phase II of culture. Acquisition was made on LSM700 Zeiss confocal microscope using Zen software. Analysis was performed using Fiji. Cells (10^5) from day 7 of phase II were washed and fixed with 1% formaldehyde, 0.025% glutaraldehyde for 15 min, treated with 50 mM NH4Cl (Sigma) for 10 min and washed twice with PBS. Cells were then permeabilized with 1% β-D-glucopyranoside (Sigma) for 15 min, incubated with a saturation solution (1% BSA and 2% goat serum) overnight then with rabbit anti-Hsp70/72 and mouse anti-α hemoglobin (sc-514378 Santa Cruz Biotechnology) for 1 hour at room temperature. After 3 washes with PBS, proximity ligation assay was performed using the Duolink flow PLA Detection Kit – FarRed (Sigma). Cells were incubated with oligonucleotide-conjugated secondary antibodies (PLA probe PLUS anti-mouse and PLA probe MINUS anti-rabbit) for 1 hour at room temperature and spun onto slides. Ligation and amplification steps were performed according to the manufacturer's guidelines. For imaging flow cytometry, all incubations were performed with cells in Eppendorf tubes, and Hoechst33342 nucleus dye was added before analyzing the cells.

H. Cell fractionation and Western Blot

Cytoplasmic and nuclear protein fractions were extracted from erythroblasts at D7 of phase II of culture using the NE-PER nuclear and cytoplasmic kit (Pierce-Thermo Scientific). Ten µg of nuclear and cytoplasmic proteins were analyzed by SDS-PAGE, using 10% polyacrylamide gels, followed by immunoblotting. The antibodies used were rabbit anti-HSP70, mouse anti-actin and mouse anti-lamin A/C as a control for the nuclear extract. Proteins were revealed using electrochemiluminescence (ECL) clarity (Biorad) and the Chemidoc MP imaging system (Biorad). Analysis was performed using Image Lab (Biorad).

I. Co-immunoprecipitation Assays

Co-immunoprecipitation of HSP70 and hemoglobin was performed with lysates of 10 million RBC from SCD patients that were either exposed to hypoxia or not for one hour. HSP70 was immunoprecipitated by incubating the lysates with mouse anti- HSP70 antibody (Enzo Lifesciences) overnight at 4°C followed

by a 45-minute incubation with protein-G sepharose beads (Cytiva-GE-Healthcare) at 4°C. Eluted proteins were analyzed by SDS-PAGE using a 4-12% polyacrylamide gel, followed by immunoblotting with mouse anti-α-globin (Santa Cruz Biotechnology) or rabbit anti-HSP70 (Santa-Cruz) antibodies. Proteins were revealed using ECL clarity and the Chemidoc MP imaging system.

J. Statistical Analysis

Statistical analyses were performed with GraphPad Prism (version 7). The data was analyzed using Mann-Whitney unpaired test and Wilcoxon paired test, as indicated in the figure legends.

CHAPTER 2:
A Comparative Study of Two Routinely Used Protocols for *ex vivo* Erythroid Differentiation

I. RESULTS

In this study, we undertook a comparative analysis of the erythroid differentiation potential of peripheral blood CD34$^+$ cells using two of the most frequently used and cost-effective xeno- and feeder-free culture systems (Freyssinier et al., 1999; Yan et al., 2018). We assessed erythroid differentiation kinetics in details using molecular and cellular markers at the gene and protein expression levels. We present data supporting the use of one protocol or another to investigate normal and pathological human erythropoiesis depending on the differentiation stage of interest and the objective of a given study.

A. Higher Cell Proliferation and Viability in the 4P-LC Compared to the 2P-LC

Human CD34$^+$ cells isolated from peripheral blood were cultured in the 2 phase (2P) and the 4 phase (4P) liquid culture (LC) systems as summarized in Figure 1. Cell proliferation, viability and apoptosis were assessed in the two culture systems and compared. Cell proliferation was calculated as the relative expansion of the cells seeded on D0 (Starting value = 1). Cells in the 4P-LC proliferated at a higher rate compared to the 2P-LC (p=0.0047), reaching a ~25,000-fold expansion (24 947 ± 8790) at D15 compared to ~2,000-fold (2 117 ± 1182) in the 2P-LC (Figure 2A). This was particularly noticeable during the exponential growth phase, with a shorter doubling time in the 4P-LC (27h ± 11.11) than in the 2P-LC (35.6h ± 14.45) (Figure 2B and 2C). As expected, cell growth plateaued in both systems by the end of the culture, indicating decreased cell division with terminal erythroid differentiation. However, while the cell expansion fold in the 4P-LC decreased by half between D15 and D20 (13 211 ± 4988), cells in the 2P-LC continued proliferating until the end, albeit at a lower rate (5 954 ± 3725) (Figure 2A). Overall, cell proliferation parameters were more enhanced in the 4P-LC than in the 2P-LC.

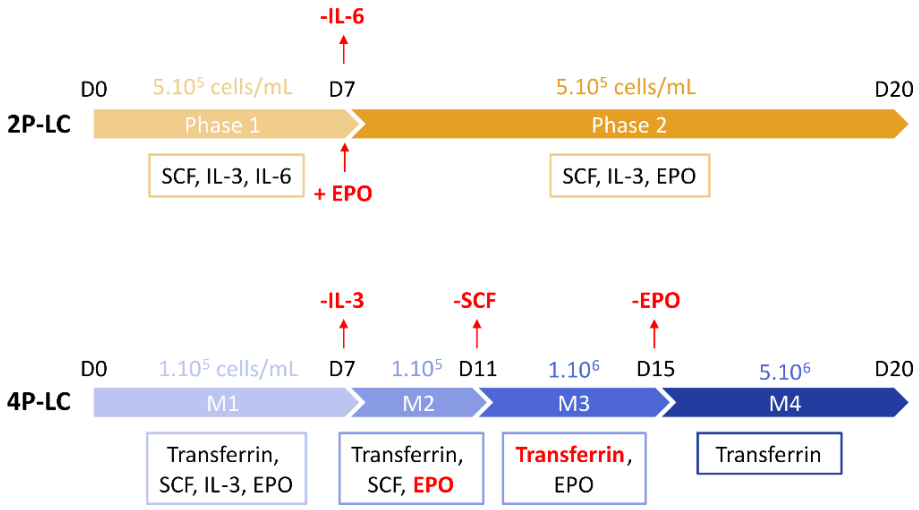

Figure 1: Schematic representation of the two erythroid differentiation culture systems used in the study: the 2-phase (2P-LC) and 4-phase (4P-LC) liquid culture systems.

In the first 7 days of culture, there was no difference in cell viability (> 86%) or apoptosis (< 13%) between the two protocols (Figure 2D and 2E). From D8 onward, cell viability decreased significantly in the 2P-LC reaching 28% ± 6.12 at D20 compared to 77.33% ± 1.70 in the 4P-LC (Figure 2D). As expected, this was associated with a concomitant increase of apoptosis (AV^+DRAQ7^- cells), that was at 63.93% and 17.28% at D20 in the 2P-LC and the 4P-LC, respectively (Figure 2E). A higher amount of debris was observed in the 2P-LC culture from D8 (Figure 2F).

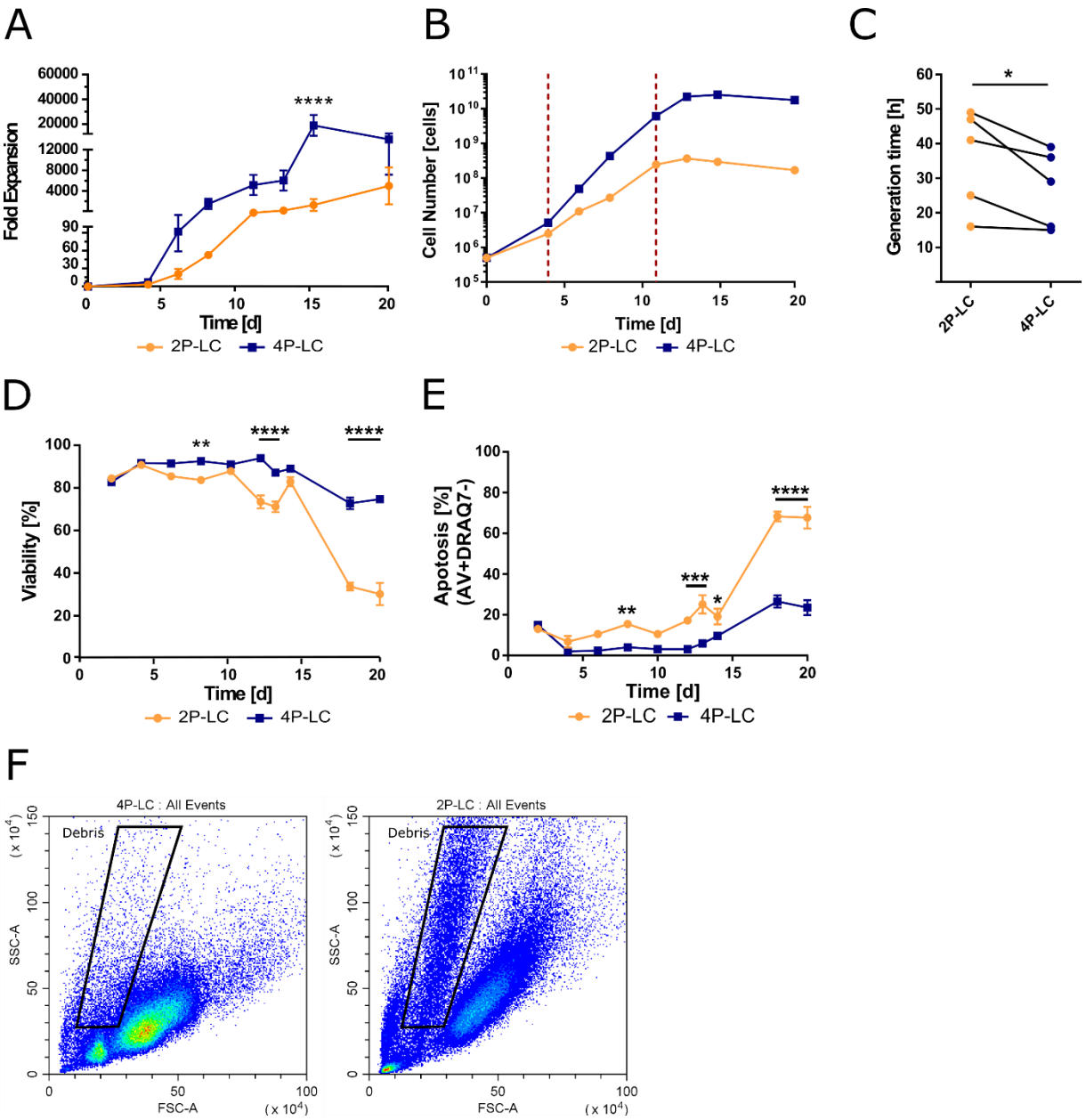

Figure 2: Cell proliferation, viability and apoptosis in the 2P-LC and the 4P-LC. (A) Fold expansion of cells in the 2P-LC and the 4P-LC from D0 to D20 (mean ± SEM, n = 4); ****p<0.0001 Two-way ANOVA. Percentage of **(B)** Representative growth curves of cells in the 2P-LC and the 4P-LC (n=1), the exponential growth of both culture systems is delimited by the red dotted lines. **(C)** Generation time (in hours) of cells undergoing exponential growth in the 2P-LC and the 4P-LC (n = 5; *P<0.0332, paired t test). **(D)** viable cells or **(E)** apoptotic cells (AV^+DRAQ7^- cells) in the 2P-LC and the 4P-LC from D2 until the end of the culture (mean ± SD, n = 3) **(F)** Forward scatter (FSC) versus side scatter (SSC) plots of flow cytometric analysis on D12 of culture in the 4P-LC (left panel) and the 2P-LC (right panel). *p<0.0332, **p<0.0021, ***p<0.0002, ****p<0.0001 Two-way ANOVA.

B. Faster Differentiation Kinetics in the 4P-LC

Erythroid differentiation of $CD34^+$ cells was monitored by flow cytometry using the surface expression of CD34, GPA, CD71 and CD36. As expected, CD34 expression decreased with a concomitant increase of GPA expression in both protocols over time, although by following different kinetics. In the 2P-LC, $CD34^+$ cells were present in the culture until D9 while in the 4P-LC they decreased rapidly as early as D4 and were almost undetectable by D7 (Figure 3A). This was associated with a faster acquisition of GPA in the 4P-LC where 13.75± 9.80% of the cells were GPA^+ at D4, a percentage reached only at D6 in the 2P-LC (11.70%± 7) (Figure 3B). The slower acquisition of GPA in the 2P-LC was indicative of a delayed terminal erythroid differentiation, as documented by lower levels of $CD71^+$ and $CD36^+$ cells between D4 and D10 (Figure 3C and 3D). At D18, the expected drop in the percentage of $CD71^+$ and $CD36^+$ cells occurred only in the 4P-LC, with 3.16 ± 0.06% of $CD36^+$ and 16.62 ± 16.03% of $CD71^+$ cells as compared to 59.05 ± 23.73% and 75.34 ± 24.39 in the 2P-LC, respectively (Figure 3C and 3D). These data indicated slower kinetics of erythroid differentiation in the 2P-LC.

We performed a detailed analysis of erythroid differentiation using a recently published method of immuno-phenotyping that allows the characterization of all the stages of human erythroid differentiation, from erythroid progenitor 1 (EP1) to orthochromatic erythroblast (OrthoE) (Yan et al., 2021). We first assessed the erythroid progenitor compartment ($CD123^-GPA^-CD71^+$), that could be sub-divided into four subpopulations of progressively mature progenitor cells, based on the expression levels of CD34 and CD105: $CD34^+CD105^-$ as EP1, $CD34^+CD105^{low}$ as EP2, $CD34^{+/low}CD105^{high}$ as EP3 and $CD34^-CD105^{high}$ as EP4 (Yan et al., 2021). The four EP populations were present in both culture systems but followed different differentiation kinetics, with a marked delay in the 2P-LC as compared to the 4P-LC (Figure 3E). At D8, most of the cells in the 4P-LC were at the terminal differentiation stage, with few EPs represented by a small proportion of EP4, while the majority of the cells in the 2P-LC were composed of EPs (Figure 3E and 3G). These data indicated a shorter phase of the early differentiation stage in the 4P-LC.

We further investigated the EP results by performing a functional colony-formation assay. Cells from 2P-LC and 4P-LC were seeded in a semisolid culture medium and incubated for 14 days. The number of colonies formed was counted and served as an indicator of the presence of EPs in the seeded cells. The number of colonies formed from D4-seeded cells from 2P-LC and 4P-LC was not different whereas a higher number of colonies was formed from D6-seeded cells from 2P-LC compared to D6-seeded cells from 4P-LC (Figure 3H). At D8, only sporadic colonies were observed for both conditions (data not shown). The different types of CFUs (myeloid CFU, CFU-GEMM, BFU-E and CFU-E) were identified using an inverted microscope. No significant difference in colony distribution was observed with D4-seeded

and D6-seeded cells from 2P-LC and 4P-LC, both conditions showed a similar proportion of myeloid and erythroid colonies (Figure 3I). Our results show that the 2P-LC maintain a prolonged colony formation activity compared to the 4P-LC.

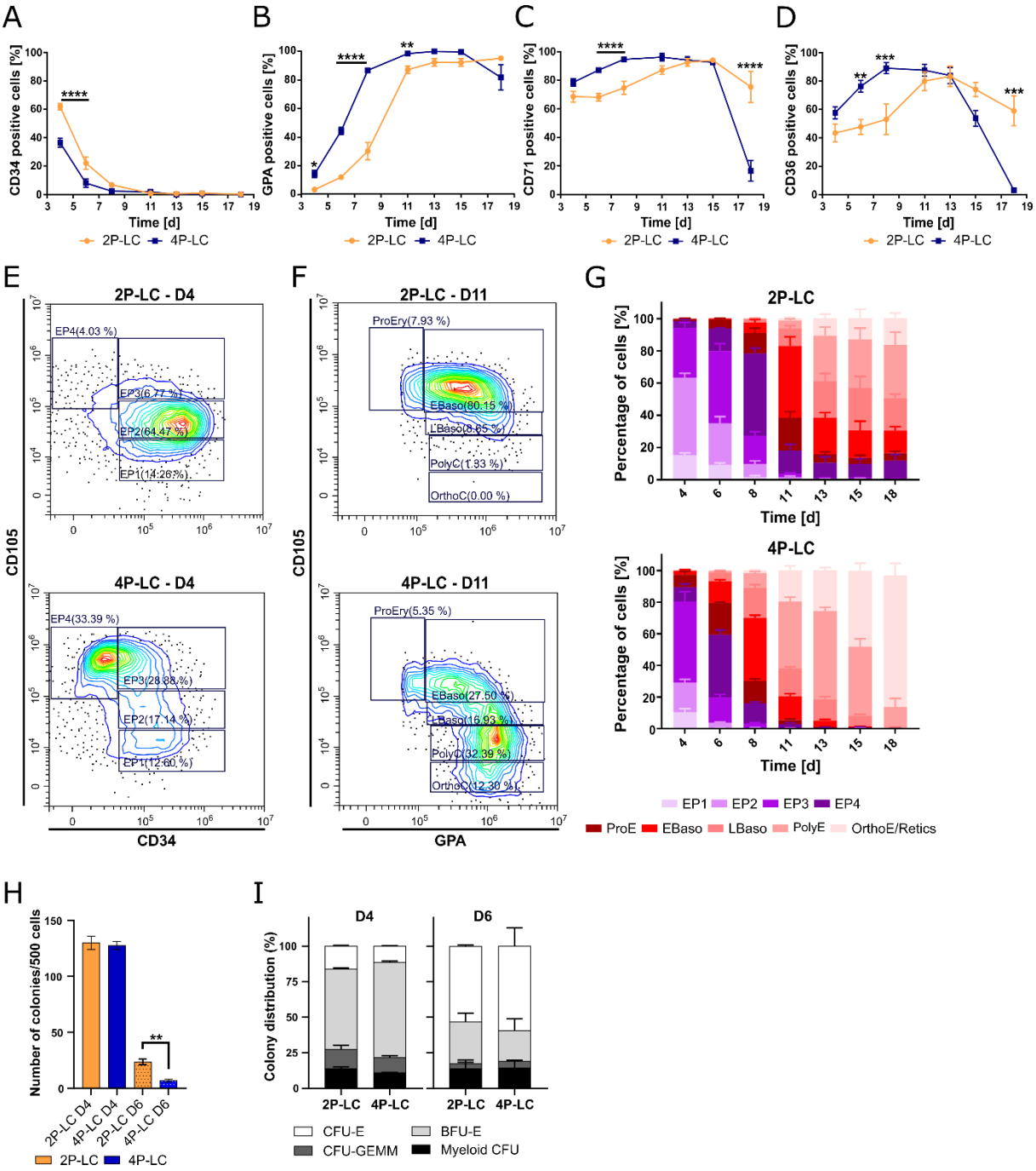

Figure 3: Erythroid maturation kinetics in the 2P-LC and the 4P-LC. Quantification of **(A)** CD34, **(B)** GPA, **(C)** CD71 and **(D)** CD36 expression, monitored by flow cytometry, on the indicated days of culture in the 2P-LC and the 4P-LC (mean ± SD, n = 5) *p<0.0332, **p<0.0021, ***p<0.0002, ****p<0.0001 Two-way ANOVA. **(E)** Early erythroid differentiation was monitored and representative plots of CD105 *versus* CD34 within the $CD123^{-}GPA^{-}CD71^{+}$ subset are shown in the 2P-LC (upper panel) and in the 4P-LC (lower panel) on D4. **(F)** Terminal erythroid differentiation was monitored and representative plots of CD105 versus GPA within the $CD123^{-}GPA^{+}CD71^{+}$ subset are shown in the 2P-LC (upper panel) or in the 4P-LC (lower panel) on D11. **(G)** Quantitative analysis of the percentages of erythroid progenitors (EP1, EP2, EP3 and EP4) and erythroblasts (ProE, EBaso, Lbaso, PolyE and OrthoE+Retics) are shown in the 2P-LC (upper panel) or in the 4P-LC (lower panel) on the indicated days of culture (mean ± SD, n = 3). **(H)** Total number of CFU derived from 500 cells taken at D4 and D6 from the 2P-LC and the 4P-LC

(mean ± SEM, n = 6) **p=0.0022 Mann-Whitney test. **(I)** Distribution of colony types at D4 and D6 of the 2P-LC and the 4P-LC. Colony types were classified according to morphological criteria in Myeloid CFU, CFU-GEMM, BFU-E, and CFU-E.

We then monitored the expression levels of CD105 and GPA on $CD71^{+}GPA^{+}$ cells to assess the terminal differentiation stages. Specifically, we identified the following stages: $GPA^{int}CD105^{high}$ as proerythroblasts (ProE), $GPA^{high}CD105^{high}$ as early basophilic erythroblasts (EBaso), $GPA^{high}CD105^{int}$ as late basophilic erythroblasts (LBaso), $GPA^{high}CD105^{low}$ as polychromatic erythroblasts (PolyE), and $GPA^{high}CD105^{-}$ as orthochromatic erythroblasts and reticulocytes (OrthoE+Retics). As expected, cells in the 4P-LC differentiated at a faster rate than those in the 2P-LC (Figure 3F). Although cells in the 2P-LC initiated terminal differentiation later than those in the 4P-LC, cells in both culture systems were able to reconstitute all distinct stages of terminal erythropoiesis and to reach the OrthoE/Retic stage, albeit in different proportions (Figure 3G). By D18 of culture, while most cells reached the OrthoE/Retic stage in the 4P-LC (83.06 ± 17.11), the proportion was only of 16.67 ± 7.13% in the 2P-LC, with cells from the earliest differentiation stages still present in the culture, such as EBaso (13.94 ± 5.61%) and LBaso (20.32 ± 5.17%) (Figure 3G). This delay in terminal differentiation in the 2P-LC was further confirmed by MGG staining. On D15, in the 4P-LC, there was a higher proportion of cells at terminal stages (PolyE and OrthoE) and already reticulocytes, whereas the 2P-LC still contained cells ProE and BasoE cells. On D20 basophilic erythroblasts were still detected in 2P-LC whereas the 4P-LC showed almost exclusively reticulocytes (Figure 4). Overall, cells were able to differentiate further and in a more synchronous manner in the 4P-LC than in the 2P-LC. Interestingly, cells in the 2P-LC culture did not appear to have the capacity to further differentiate beyond a certain point, as most cells were apoptotic by D20, suggesting that by that time, cells in the 2P-LC had reached their proliferation potential and were no longer able to differentiate.

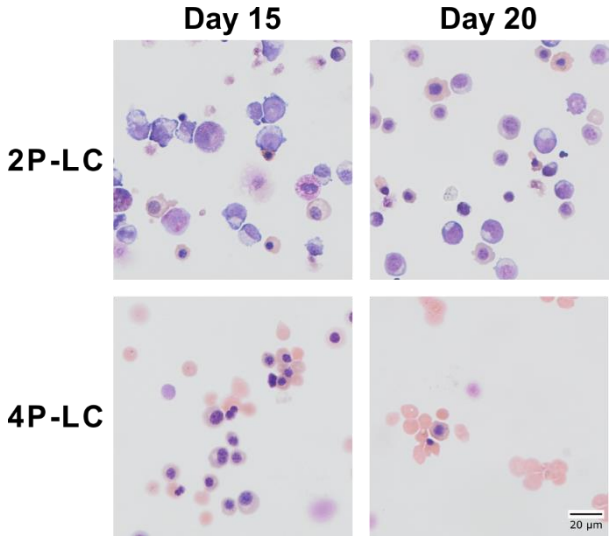

Figure 4*:* Representative cytospin images of differentiated erythroblasts derived from the 2P-LC and the 4P-LC on the indicated days of culture; scale bar=20µm.

C. Higher Enucleation Rate in the 4P-LC than in the 2P-LC

At the end of the cultures, the enucleation rate was much higher in the 4P-LC (80.27± 2.17) than in the 2P-LC (28.87± 5,38) (Figure 5A and 5B), consistent with the faster differentiation kinetics and better synchronicity of the 4P-LC. Of note, the presence of enucleated cells was detected as early as D14 of culture in the 4P-LC, albeit at low levels (2.91±0.45%) (Figure 5B). We refined the enucleation analysis by gating on CD36$^-$ cells to restrict the quantification to the cell populations having reached the same differentiation stage. Only 50.8 ± 6.47% of CD36$^-$ cells were enucleated in the 2P-LC compared to 81.84 ± 9.2 % in the 4P-LC (Figure 5C). This different enucleation potential between the 2 systems of phenotypically similar cell populations suggests intrinsic differences between the cells generated by the two culture methods. This was supported by further analyses showing that most enucleated cells in the 2P-LC were still reticulocytes (TO$^+$), while those in the 4P-LC were mostly of the cultured RBC phenotype (cRBCs) (TO$^-$) (Figure 5D and 5E).

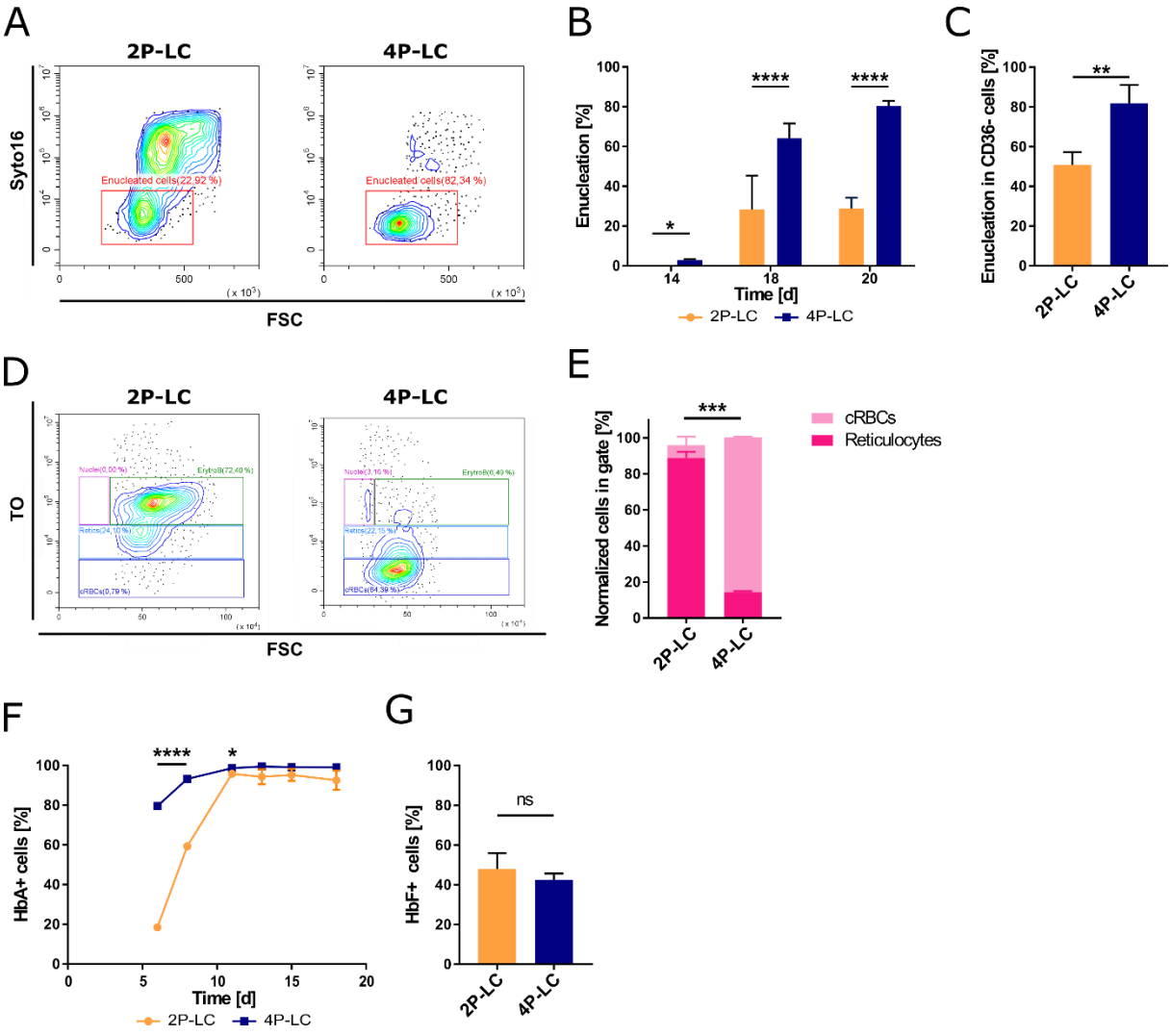

Figure 5: Terminal differentiation: enucleation, reticulocyte maturation and hemoglobin expression in the 2P-LC and the 4P-LC. (A) Representative plots of nucleated erythroblasts (SYTO16$^+$) and enucleated cells (Retics + cRBCs) from the 2P-LC

(left) and the 4P-LC (right) on D20. **(B)** Percentage of enucleation on D14, D18 and D20 in the 2P-LC and the 4P-LC (mean ± SD, n = 4) *p<0.0332, ****p<0.0001 Two-way ANOVA. **(C)** Percentage of enucleation in the $CD36^-$ cells on D20 in the 2P-LC and the 4P-LC (mean ± SD, n = 4). *p<0.05; unpaired t-test. **(D)** Representative plots of erythroblasts (TO^{high}), reticulocytes (TO^+) and cRBCs (TO^-) from the 2P-LC (left) and the 4P-LC (right) on D20. **(E)** Quantification of the percentages of reticulocytes and cRBCs in the 2P-LC and the 4P-LC on D20. ***p<0.0002 unpaired t-test. **(F)** Quantification of adult hemoglobin (HbA) expression, monitored by flow cytometry, on the indicated days of culture in the 2P-LC and the 4P-LC (mean ± SD, n = 3) *p<0.0332, ***p<0.001, ****p<0.0001 Two-Way ANOVA. **(G)** Percentage of fetal Hemoglobin (HbF) positive cells in the 2P-LC and the 4P-LC detected by flow cytometry at D18 (mean ± SD, n = 3).

We measured the hemoglobin content and expression kinetics in differentiating cells by flow cytometry. Cells expressing adult hemoglobin (HbA) were detected as early as D6 in both protocols, with higher proportions in the 4P-LC than in the 2P-LC (79.57% ± 1.75 and 18.49 ± 1.70, respectively), reaching > 99.5% of the cells at D18 in both systems (Figure 5F). Expression of fetal hemoglobin (HbF) was also assessed and found in high proportions of differentiating cells, with no significant difference between the two systems (41.30% 2P-LC *vs* 35.61% 4P-LC at D18) (Figure 5G).

D. Cells in the 4P-LC Express Higher Levels of Erythroid Transcription Factors than Cells in the 2P-LC

To monitor terminal erythroid differentiation at the molecular level, we assessed the mRNA expression of several genes critical for erythropoiesis and its regulation: the transcription factors GATA1, KLF1, and TAL1, and the MYB gene, known to be involved in the globin switching.

In line with our flow cytometry data, genes involved in erythroid lineage commitment were upregulated during erythroid differentiation in both culture systems, with some differences in their expression level and kinetics. As expected, *GATA1*, *KLF1*, and *TAL1* mRNA expression levels were markedly higher in cells from the 4P-LC, as for instance the 5-fold higher expression level of *GATA1* at D15. Similarly, the expression of *KLF1* and *TAL1* was also increased at D15 by 4 and 5 folds, respectively (Figure 6A, 6B and 6C). These data confirmed the faster kinetics of the 4P-LC cells, achieving terminal differentiation by D15, with higher numbers of OrthoE in which a peak of *GATA1*, *KLF1*, and *TAL1* is known to occur (Novershtern et al., 2011; Yan et al., 2018).

Conversely, the expression of *MYB*, known to be high in erythroid progenitors and decreasing during differentiation (Yan et al., 2018), was higher in the 2P-LC than in the 4P-LC (Figure 6D). In the 2P-LC, *MYB* expression was higher than in the 4P-LC at all time points and remained stable from D4 till D15 before initiating a decrease. The sustained high expression of *MYB* at D18 reflected the inability of the 2P-LC cells to achieve a complete differentiation. In the 4P-LC, the highest expression of *MYB* was detected at D4, after which it decreased progressively to reach a low-level plateau between D11 and 18 (Figure 6D).

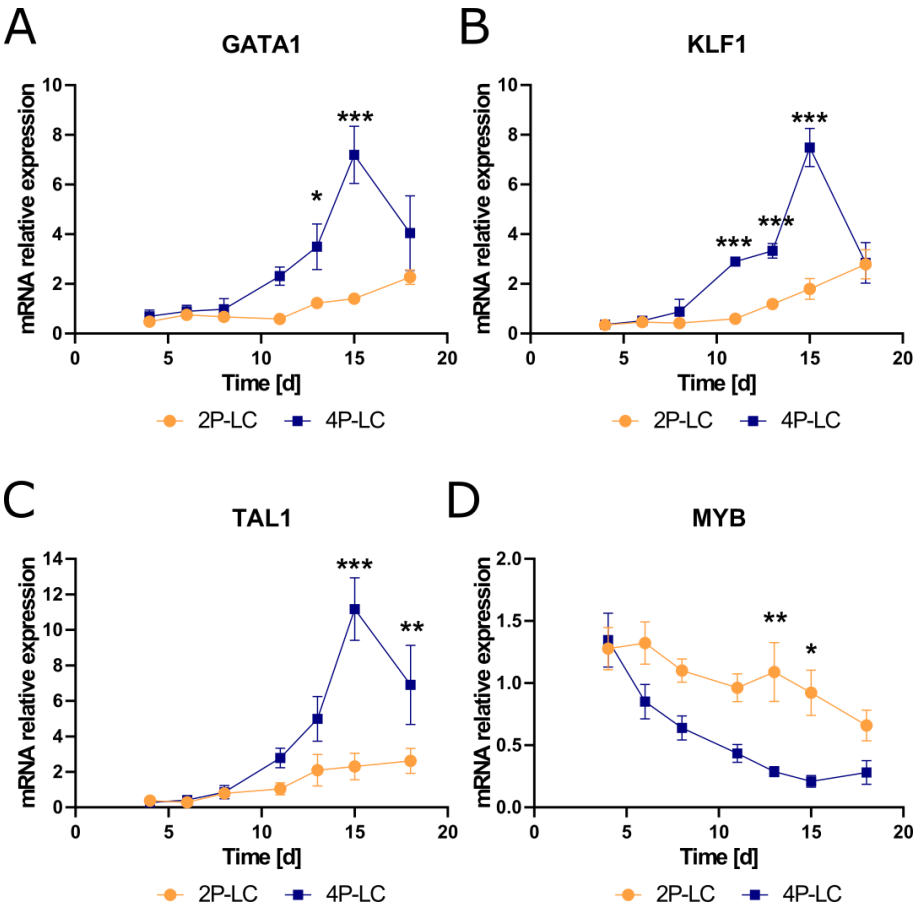

Figure 6: Expression of erythroid master regulators in the 2P-LC and the 4P-LC. qPCR analysis of **(A)** GATA1, **(B)** KLF1, **(C)** TAL1 and **(D)** MYB expression in RNA purified from cells in the 2P-LC and the 4P-LC at the indicated time. Data was normalized to the expression of HPRT1 and GAPDH (mean ± SD, n = 4). *p<0.0332, **p<0.0021, ***p<0.0002 Two-way ANOVA.

II. DISCUSSION

In this study, the two most commonly used erythroid differentiation protocols were compared using molecular and cellular tools. Erythropoiesis was induced and investigated by both protocols in parallel using the same pool of human $CD34^+$ cells, isolated from peripheral blood of healthy donors, to avoid donor-derived variability.

The 4P-LC exhibited higher overall proliferation and better viability, which seem to result from the presence of EPO, that was added as early as the first day of culture. In addition to its proerythroid role, EPO was identified as a hematopoietic hormone harboring a broad range of actions protecting from oxidation, apoptosis and inflammation (Koury & Bondurant, 1990). EPO also promotes cell proliferation by bringing dormant erythroid progenitors to enter the cell cycle (Spivak et al., 1991). In contrast, the 2P-LC system had an initial EPO-independent phase, with a cytokine mix restricted to SCF, IL-3 and IL-6. These cytokines are assumed to support the proliferation of early non-lineage committed hematopoietic cells, favoring the proliferation of all myeloid-biased progenitors. This is in agreement with our results from semisolid cultures, that showed a prolonged colony formation potential in the 2P-LC system. However, our data did not show the supposed better culture efficiency when adult $CD34^+$ cells are expanded by applying an EPO-independent priming phase. Our study shows that adding EPO from the beginning of the culture has a dual positive effect, improving proliferation and protecting cells from apoptosis, in agreement with the fact that EPO maintains cell viability by upregulating Bcl-xL, an anti-apoptotic gene of the Bcl-2 family (Silva et al., 1996). The increased cell death in the 2P-LC system following the addition of EPO may be associated with the Hayflick limit (Shay & Wright, 2000), with a premature shortening of telomeres in the progenitors during the initial EPO-free phase, preventing them from reaching a full differentiation potential during the subsequent phase of the culture. Of note, the increased cell death in the 2P-LC system resulted in the accumulation of debris. These debris can have detrimental effects by exacerbating the level of cell death and by introducing a bias in the data generated by RT-qPCR and Western Blot.

In the 4P-LC, there was a preferential induction of erythroid precursors driven by the early stimulation with EPO, SCF, and IL-3. ProEs were present in the culture at D4, and OrthoEs were detected as early as D8. During the early differentiation stages, up to D4, cells expressed high levels of the transferrin receptor CD71 and the early erythroid antigen CD36. However, after D15, CD36 and CD71 expression gradually decreased, in line with developing differentiation. GPA expression was detected at D4, and by D8 it was expressed on almost all cells. Furthermore, most GPA^+ cells became $CD71^-$ and $CD36^-$, which is known to be a sign of cell cycle arrest and terminal maturation into erythrocytes (Wangen et al., 2014). In the 2P-LC system, the first ProEs and OrthoEs were present at D6 and D13, respectively. These erythroid cells expressed lower levels of CD36 and CD71 compared to cells from the 4P-LC that remained stable till the end of the culture, suggesting the inability of the cells to achieve complete

maturation. This was reflected by higher rates of reticulocytes and erythrocytes in the 4P-LC, highlighting its suitability to investigate the molecular mechanisms involved in enucleation and reticulocyte maturation as opposed to the 2P-LC system. In addition to better erythroid maturation, the 4P-LC conditions showed improved synchronization of cell divisions, with cells progressing through subsequent maturation stages in a homogeneous manner as compared to 2P-LC cells. As a matter of fact, at D18, cells from the 4P-LC were almost exclusively OrthoEs and Retics/cRBCs, whereas 7 different subpopulations were concomitantly present in the 2P-LC (EP4, ProEs, EBasos, LBasos, PolyEs, OrthoEs and Retics/RBCs).

Many experimental models have been used to study erythropoiesis over the past years. As there is substantial evidence indicating that the bone marrow (BM) microenvironment impacts erythroid differentiation and enucleation, stromal cell and/or macrophage-based co-culture methods were developed (Giarratana et al., 2005; Martha Lopez-Yrigoyen et al., 2019). These models provide optimal approaches for studying the interaction between erythroid cells and the complex environment of the BM niche. Recently, 3D cultures using scaffolds that mimic the BM architecture have been also developed (Severn et al., 2019). Culture cells in 3D enhance the value of such cell-based assays and the generation of more accurate and physiologically relevant results. According to several studies, including ours, a 3D architecture in combination with media perfusion/circulation creates a dynamic system that advances cell-based models towards the recreation of a more "*in vivo*-like" conditions.

In the current study, we chose to focus on 2D culture systems that are easily accessible and that do not require specific material to set. The 2P-LC and 4P-LC systems are standardized protocols that are frequently used in hematology research laboratories to investigate cell autonomous mechanisms in normal and pathological erythropoiesis.

Despite the differences between the 2P-LC and the 4P-LC systems that were revealed by our study, they both are powerful tools for fundamental and translational research in the field of human erythropoiesis. They provide accessible means to investigate the kinetics of surface protein expression, including blood group antigens (Koehl et al., 2023), and the defects of erythropoiesis in hematological diseases such as in thalassemia (Arlet et al., 2014) and in sickle cell disease (El Hoss et al., 2021).

III. MATERIAL AND METHODS

A. Blood Samples and Isolation of $CD34^+$ Cells

Peripheral Blood Mononuclear Cells (PBMCs) of healthy blood donors were isolated from platelet leukoreduction filters obtained from the Etablissement Français du Sang (EFS), after informed consent. The study is performed in accordance with the French blood donation regulations and ethics and with the French Public Health Code (article L.1221-1). First, dextran sedimentation was performed by mixing blood with 2% dextran solution (Sigma), after 30 min sedimentation, the RBC-depleted upper layer was collected and PBMCs were isolated on a Ficoll gradient (Eurobio), the remaining RBCs were lysed using RBC lysis buffer (Thermofisher). $CD34^+$ cells were purified by a magnetic sorting system (Stemcell technologies) according to the manufacturer's protocol. The purity of the isolated $CD34^+$ cells, checked by flow cytometry, was always 90-96%.

B. Cell Culture

Cells were cultured for 20 days simultaneously in a 2-Phase Liquid Culture (2P-LC) and in a 4-Phase Liquid Culture (4P-LC).

1. 2 Phases Liquid Culture (2P-LC)

Cells were cultured at a density of 5.10^5 cells/ml and media was diluted every two days. Composition of the base medium was Iscove's Modified Dulbecco's Medium (IMDM) (Life technologies) supplemented with 15% BIT 9500 (Stemcell Technologies), 100 U/ml Penicillin Streptomycin (Life technologies) and 2 mM L-Glutamine (Life technologies). In the first phase (D0-6), cells were expanded in the presence of 100 ng/ml human recombinant (hr) stem cell factor (SCF) (Miltenyi Biotec), 10 ng/ml of hr interleukin (IL)-3 (Miltenyi Biotec) and 100 ng/ml of hr IL-6 (Miltenyi Biotec). In the second phase (D7-20), IL-6 was replaced with 2 U/ml of erythropoietin (EPO) (Stemcell Technologies).

2. 4 Phases Liquid Culture (4P-LC)

Composition of the base culture medium was IMDM, 2% human peripheral plasma, 3% human AB serum, 3IU/ml heparin (Stemcell technologies), 10 µg/ml insulin (Sigma) and 100 U/ml Penicillin Streptomycin (Life technologies). In the first phase (D0-6), cells were cultured at a concentration of 1.10^5 cells/mL in the presence of 200 µg/ml Holo-human transferrin (Sigma), 10 ng/ml SCF, 1 ng/ml IL-3 and 3 IU/ml EPO. In the second phase (D7-10), IL-3 was removed from the media, and the concentration of EPO was reduced to 1 IU/ml. In the third phase (D11-14), the cell concentration was increased to 1.10^6 cells/mL, SCF was removed from the media and the concentration of transferrin was increased to 1mg/ml. Finally, in the fourth phase (D15-20), the cell concentration was increased to 5.10^6 cells/mL, and EPO was removed from the media.

C. Analysis of Proliferation and Differentiation by Flow Cytometry

Cell viability and cell proliferation were determined by trypan blue staining (Sigma) and microscopic evaluation. Cells were sampled from the cultures every two days to assess apoptosis. Briefly, $2.5.10^5$ cells were washed once with Annexin buffer and stained with PE-conjugated Annexin V and 300 nM of DRAQ7 for 15 min at room temperature (RT). Samples were then diluted with 200 µl of Annexin buffer before analysis. To monitor differentiation, cells were analyzed for surface expression of glycophorin A (GPA), CD34, CD36, CD71, CD105, CD123 (Biolegend). For this $2.5.10^5$ cells were washed twice with phosphate-buffered saline (PBS) supplemented with 2% fetal bovine serum (FBS) and 1 mM EDTA. After blocking with 0.4% human AB serum for 20 min on ice, cells were stained with fluorochrome-conjugated antibodies for 30 min on ice. Cells were washed twice with PBS 2% FBS 1 mM EDTA and stained with 300 nM of DRAQ7 (Biolegend) for 15 min at RT before analysis. To study enucleation, cells were first incubated with anti-CD36 antibodies for 30 min on ice. Cells were then stained with 100 nM of Syto16 dye (Thermofisher) for 15 min at RT and washed once before analysis.

Cells are also analyzed for adult hemoglobin (HbA) and fetal hemoglobin (HbF) expression. For this, 5.10^5 cells were fixed, permeabilized and saturated as previously described (El Hoss et al., 2021). Cells were stained with anti-GPA, anti-HbA and anti-HbF antibodies for 30 min on ice and washed twice with PBS 2% FBS 1 mM EDTA before analysis.

Cells were analyzed on Cytoflex S flow cytometer (Beckman Coulter) and acquired using the CytExpert software (Beckman Coulter). Data was analyzed using the same software.

D. Cytospin Preparation

For analysis of cell morphology, 2.10^5 cell in 100 µL PBS were used to prepare cytospin preparations on non-coated slides, using the Cytospin 4 Shandon centrifuge (Thermofisher). The slides were stained with May-Grunwald-Giemsa (MGG) following manufacturer's instructions (Sigma). The slides were imaged using an Olympus BX41 (Zeiss) inverted microscope.

E. Colony Forming Assay

Colony forming assays were performed on days 4, 6 and 8. At any given day, 500 cells were plated in triplicate in 6-well culture plates containing methylcellulose-based medium (Methocult H4434, StemCell). Cells were incubated for 14 days at 37°C and 5% CO_2. BFU-E, CFU-E, CFU-GEMM and myeloid colonies were enumerated by microscopy according to the standard previously described criteria (Eaves & Lambie, 1995).

F. qPCR Analysis

Total RNA was isolated using the RNeasy kit (Qiagen). cDNA was reverse transcribed using M-MLV RT (Promega ref M1701), random hexamer (Life ref N8080127), dNTP (fisher ref 100833232) and real-time PCR analyses were performed using Power Sybr Green PCR Master Mix (Life ref 4367659). The primers shown in Table 1 were used to target GAPDH, HPRT1, GATA1, KLF1, TAL1, MYB. Each experiment was carried out in triplicate, and average Ct was calculated with StepOne 2.1 software (Invitrogen). The results are normalized using the two housekeeping genes GAPDH and HPRT1.

Table 1: Primers pairs used in qPCR.

Gene	Forward primer	Reverse primer
GAPDH	GTCTCCTCTGACTTCAACAGCG	ACCACCCTGTTGCTGTAGCCAA
HPRT1	CATTATGCTGAGGATTTGGAAAGG	CTTGAGCACACAGAGGGCTACA
GATA1	CACGACACTGTGGCGGAGAAAT	TTCCAGATGCCTTGCGGTTTCG
KLF1	TTGCGGCAAGAGCTACACCAAG	GTAGTGGCGGGTCAGCTCGTC
TAL1	CCACCAACAATCGAGTGAAGAGG	GTTCACATTCTGCTGCCGCCAT
MYB	GGGAACAGATGGGCAGAAATCG	GCTGGCTTTTGAAGACTCCTGC

G. Statistical Analysis

Statistical analyses were performed with GraphPad Prism (version 7). The data was analyzed using unpaired and paired t test, Mann-Whitney test or two-way ANOVA and $p<0.05$ was considered to indicate statistical significance.

CHAPTER 3:
Novel Insights into the Impact of Ineffective Erythropoiesis on the Erythroblastic Island in Sickle Cell Disease

I. RESULTS

In the context of SCD, we expect that the central macrophage of the erythroblastic island (EBI), being the cell with phagocytic capacities in direct interaction with differentiating erythroblasts, would engulf high numbers of apoptotic erythroblasts that arise during terminal differentiation. Previous ultrastructural studies of bone marrow (BM) aspirates support a role for BM macrophages in clearing away defective erythroid cells during ineffective erythropoiesis. Indeed, extensive marrow erythrophagocytosis was shown in SCD and beta-thalassemia patients (Angelucci et al., 2002; Grasso et al., 1975; Wickramasinghe & Hughes, 1978). This process may result in the accumulation of high amounts of hemoglobin and iron within their cytoplasm, which in turn, may induce the generation of free radicals, trigger lipid peroxidation, and ultimately induce cell death through a mechanism known as ferroptosis, an iron-dependent form of non-apoptotic cell death (Dixon et al., 2012).

In this chapter, we studied erythrophagocytosis-induced ferroptosis *in vitro*, using a model of EBI-like macrophages differentiated in the presence of dexamethasone (Dex) (Hampton-O'Neil et al., 2020; Heideveld et al., 2018). We exposed these macrophages to RBCs and apoptotic erythroblasts obtained from healthy donors (HD) and SCD patients. Our findings revealed that high levels of erythrophagocytosis induced ferroptosis in EBI-like macrophages, regardless of their origin, and was associated with increases in reactive oxygen species (ROS) and lipid peroxidation, which were reduced by ferroptosis inhibitors ferrostatin-1 (Fer-1) and liproxstatin-1 (Lip-1). Additionally, surviving macrophages shifted their phenotype towards an inflammatory profile. Furthermore, we explored ferroptosis markers and gene regulation pathways in the SCD Townes mouse model, specifically in EBI macrophages isolated from the bone marrow and the spleen of SS (sickle cell), AS (sickle cell trait), and AA (control) mice. Interestingly, we observed a ferroptosis signature in the EBI macrophages from SS mice, whereas AS and AA mice did not exhibit such characteristics.

We propose that ineffective erythropoiesis in SCD can affect the EBI by either inducing ferroptosis in the central macrophages or shifting its phenotype to an inflammatory profile. Overall, this could compromise the ability of these macrophages to effectively support the proliferation and differentiation of erythroid cells while also promoting a chronic inflammatory state within the bone marrow.

A. Dexamethasone-treated monocytes from healthy donors and SCD patients generate “EBI-like” macrophages.

To model EBI macrophages *in vitro*, we used the culture system of Heideveld et al. in which macrophages are derived from $CD14^+$ monocytes and differentiated with Dex. The differentiated cells were reported to exhibit phenotypic characteristics similar to resident macrophages found in the human BM and fetal liver, displaying an M2 tissue-resident profile based on the surface markers CD14

(lipopolysaccharide [LPS]-receptor), CD16 (FcγRIII), CD163, CD169, CD206 (mannose receptor), and TAM-receptor family members, such as Mer tyrosine kinase (MerTK). Moreover, they were shown to successfully replicate the functional characteristics of EBI macrophages, such as the ability to interact with erythroid cells at all stages, to phagocytose extruded nuclei, and to support erythroid expansion (Hampton-O'Neil et al., 2020; Heideveld et al., 2018).

Monocytes isolated from peripheral blood of healthy donors and SCD patients were differentiated in the presence of M-CSF and Dex. As expected, cells collected on the seventh day of culture expressed all the previously described markers (CD14, CD16, CD163, CD169, CD206, and MerTK) (Figure 1A). Consistent with previous studies, these EBI-like macrophages displayed a homogenous rounded shape, unlike the elongated fibroblast-like morphology typically observed in M2 macrophages *in vitro* (Figure 1B). This was associated with high motility, as observed with real time live microscopy (data not shown) and the ability to interact with a high number of erythroid cells, as shown in our cytospin analysis (Figure 1C).

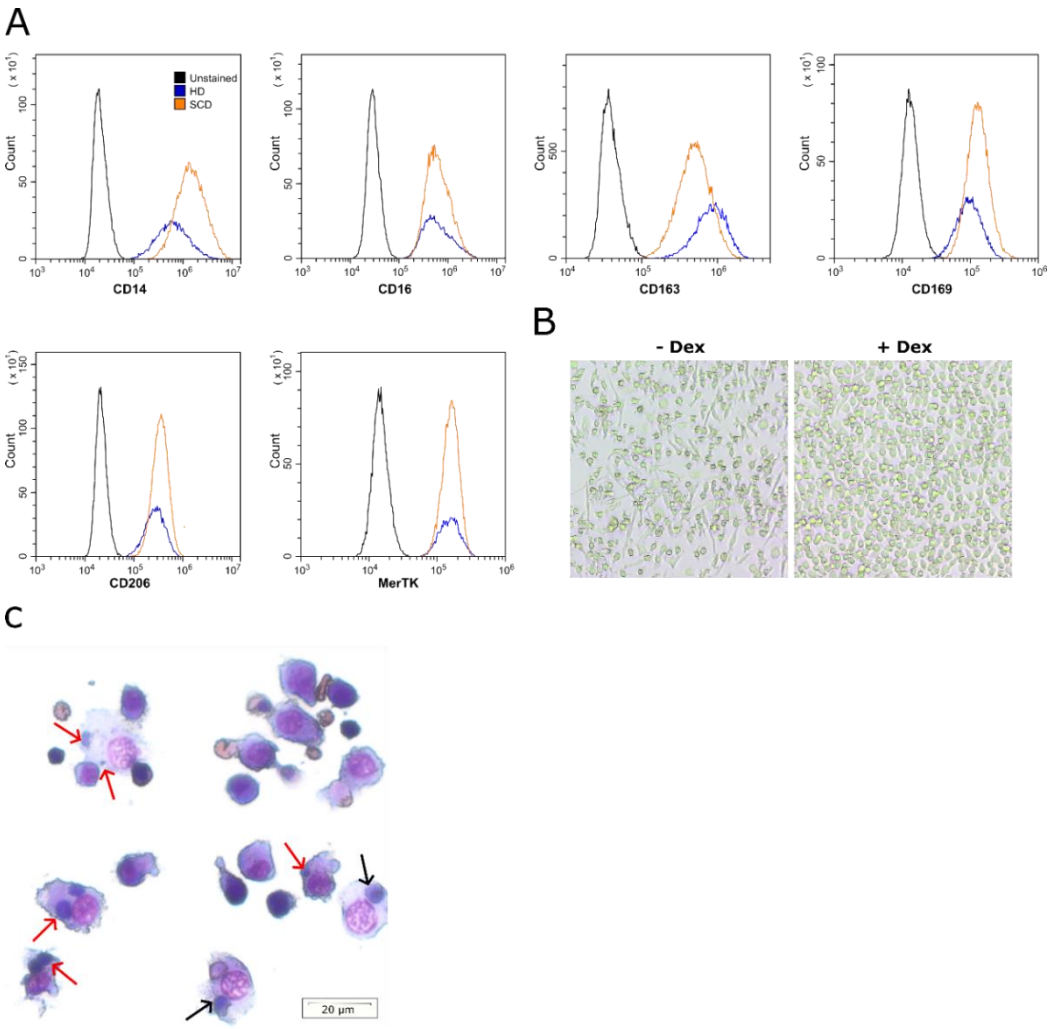

Figure 1: Characterization of EBI-like macrophages. (A) Flow cytometry plots showing the expression of CD14, CD16, CD163, CD169, CD206 and MerTK on macrophages from a healthy donor (HD) and a sickle cell patient (SCD) differentiated in the

presence of M-CSF and dexamethasone **(B)** Microscopic images of macrophages differentiated with M-CSF and with (+ Dex) or without dexamethasone (- Dex) for 7 days, as observed under a light microscope at total magnification of 100X. **(C)** May Grünwald-Giemsa staining (scale bar 20µm). Macrophages were co-incubated 24h with erythroblasts at D13 of culture. EBI-like macrophages can bind nucleated and enucleated cells and can phagocyte pyrenocytes (red arrows) and some erythroid cells (black arrows).

B. Phagocytosis of Red Blood Cells Induces ROS Production, Lipid Peroxidation, and Cell Death in EBI-like Macrophages.

To investigate whether increased internalization of hemoglobin-rich cells could induce ferroptosis in EBI-like macrophages, we first conducted phagocytosis experiments using CellTrace-labeled red blood cells (RBCs). As previously described, the RBCs used in this assay were preheated at 50°C (H50) to alter their biomechanical properties and induce their phagocytosis (Dupuis et al., 2022). We chose to work with a macrophage-to-RBC ratio of 1:30 to conform with the ratio described in the human BM (Lee et al., 1988). To measure the phagocytic activity of our macrophages, we calculated the phagocytosis index by assessing the average amount of internalized RBCs per phagocytic macrophage. This was done by quantifying the Mean Fluorescence intensity (MFI) of CellTrace$^+$ macrophages and normalizing it with the RBC staining intensity. Incubating the EBI-like macrophages with H50 RBCs for 3 hours led to important phagocytosis as measured by the percentage of CellTrace$^+$ macrophages and the phagocytosis index, that were both higher compared to the condition where macrophages were incubated with non-heated (NH) RBCs (Figure 2, Figure 3A and 3B). This was confirmed by imaging flow cytometry, showing the presence of CellTrace$^+$ fluorescent spots within the cytosol of nearly all macrophages in the H50 condition (Figure 3C). Increased erythrophagocytosis led to elevated reactive oxygen species levels (Figure 3D), lipid peroxidation (Figure 3E) and cell death (Figure 3F) suggesting the occurrence of ferroptosis, as lipid peroxidation is a hallmark of this process. This was further confirmed using 2 specific ferroptosis inhibitors, Fer-1 and liproxstatin-1 Lip-1 that did not alter phagocytosis (Figure 3G and 3H) while they significantly decreased ROS production (Figure 3I), lipid peroxidation (Figure 3J), and cell death (Figure 3K).

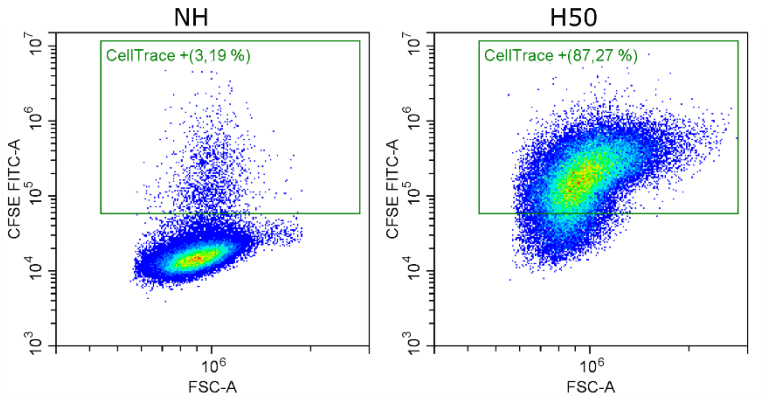

Figure 2: Measuring erythrophagocytosis in EBI-like macrophages. After co-incubating EBI-like macrophages with CFSE or CTV-stained RBCs for 3h, cells were collected, and RBCs were washed away and lysed. Flow cytometry plot representing the percentage of CFSE-positive macrophages in the NH (left panel) and H50 (right panel) conditions.

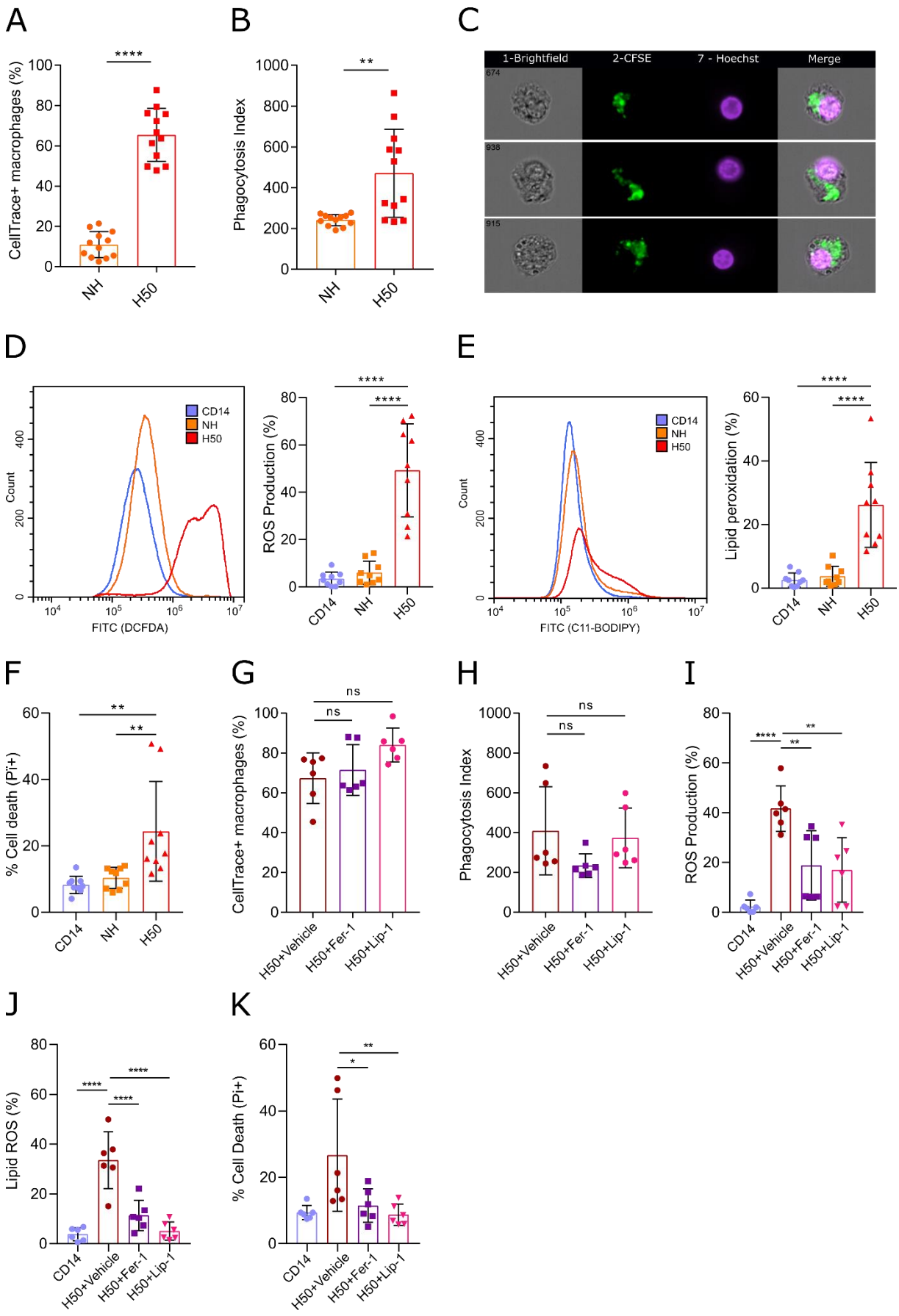

Figure 3: Erythrophagocytosis induces ROS production, lipid peroxidation and cell death in EBI-like macrophages. EBI-like macrophages from control individuals were either incubated alone (CD14), with non-heated RBCs (NH), or with heated RBCs

(H50). To monitor their phagocytosis, RBCs were first stained with CFSE or CellTrace Violet (CTV) fluorescent dye. After 3h of co-incubation, non-internalized RBCs were washed away and lysed, and EBI-like macrophages were analyzed using flow cytometry **(A)** Phagocytosis of RBCs was quantified by measuring CTV or CFSE positivity in EBI-like macrophages **(B)** and by measuring the phagocytosis index (mean ± SD, n = 12). ** p<0.0021; **** p< 0.0001; paired t-test. **(C)** Phagocytosis was further confirmed by imaging flow cytometry. **(D)** Reactive oxygen species (ROS) production was measured using DCFDA (mean ± SD, n = 9). **(E)** Lipid peroxidation was measured using C11-BODIPY 581/591. (mean ± SD, n = 9**). (F)** Cell death was measured using propidium iodide (PI) labeling. (mean ± SD, n = 9). EBI-like macrophages were incubated with heated RBCs combined with vehicle, 10 µM Ferrostatin-1 (Fer-1) or 1 µM Liproxstatin-1 (Lip-1). **(G)** Phagocytosis of RBCs was quantified by measuring CTV or CFSE positivity (H) and by measuring the phagocytosis index (mean ± SD, n = 6). **(I)** ROS production, **(J)** lipid peroxidation and **(K)** cell death was measured by flow cytometry (mean ± SD, n = 6). *p<0.0332, **p < 0.0021, ***p < 0.0002, ****<0,0001; One-Way ANOVA followed by Tukey's multiple comparison test.

To further explore the ferroptosis-like phenomenon that was triggered by RBC phagocytosis, we monitored the expression of genes related to iron, oxidative stress, glutathione, and polyunsaturated fatty acid metabolism (Figures 4). As expected, we observed a significant increase in the expression of *HMOX1* following increased erythrophagocytosis, both at the mRNA (Figure 4A) and protein levels (Figure 4H), that was abrogated by Lip-1 (Figure 4A), consistent with the reported upregulation of *HMOX1* in response to the oxidative stress associated with rapid heme metabolism and detoxification following phagocytosis of RBCs (Kwon et al., 2015).

We also observed a significant downregulation of *TFRC* in cells having phagocytosed many RBCs, likely due to the increased iron concentration in these cells. Interestingly, this was also prevented by the presence of Lip-1 in the media, showing that Lip-1 can help maintain TFRC expression regardless of iron levels in EBI-like macrophages (Figure 4B). In contrast, the expression of GPX4, an antioxidant enzyme that plays a pivotal role in ferroptosis, was not altered (Figure 4C). This is consistent with previous studies that showed that GPX4 expression is unchanged in iron-induced ferroptosis (Menon et al., 2022; Yu et al., 2020). There was no significant change in the expression of *NRF2* in the H50 condition (Figure 4D). However, we observed a significant upregulation of *NQO1,* an oxidative stress response gene, which was reverted when inhibiting ferroptosis with Lip-1 (Wang et al., 2023) (Figure 4E). Similarly, the expression of *SLC7A11,* a gene responsible for maintaining cellular levels of glutathione and involved in ferroptosis suppression*,* was also increased, while the expression of ACSL4, a protein that indirectly promotes ferroptosis, was significantly decreased (Dixon et al., 2012; Doll et al., 2017; Jiang et al., 2015; W. Zhang et al., 2018) (Figure 4F, 4G and 4H). Interestingly, in addition to preventing the upregulation of *HMOX1* and *NQO1*, Lip-1 could significantly upregulate *NRF2* and *GPX4* expression, surpassing all other conditions. This observation suggests that while Lip-1 is primarily recognized as a ferroptosis inhibitor due to its ROS scavenging activity, it can also induce response against oxidative stress (Figure 4C and 4D).

These results indicate that increased erythrophagocytosis can induce ferroptosis in EBI-like macrophages, and that surviving macrophages can actively modulate their gene expression pattern to promote an anti-ferroptosis response.

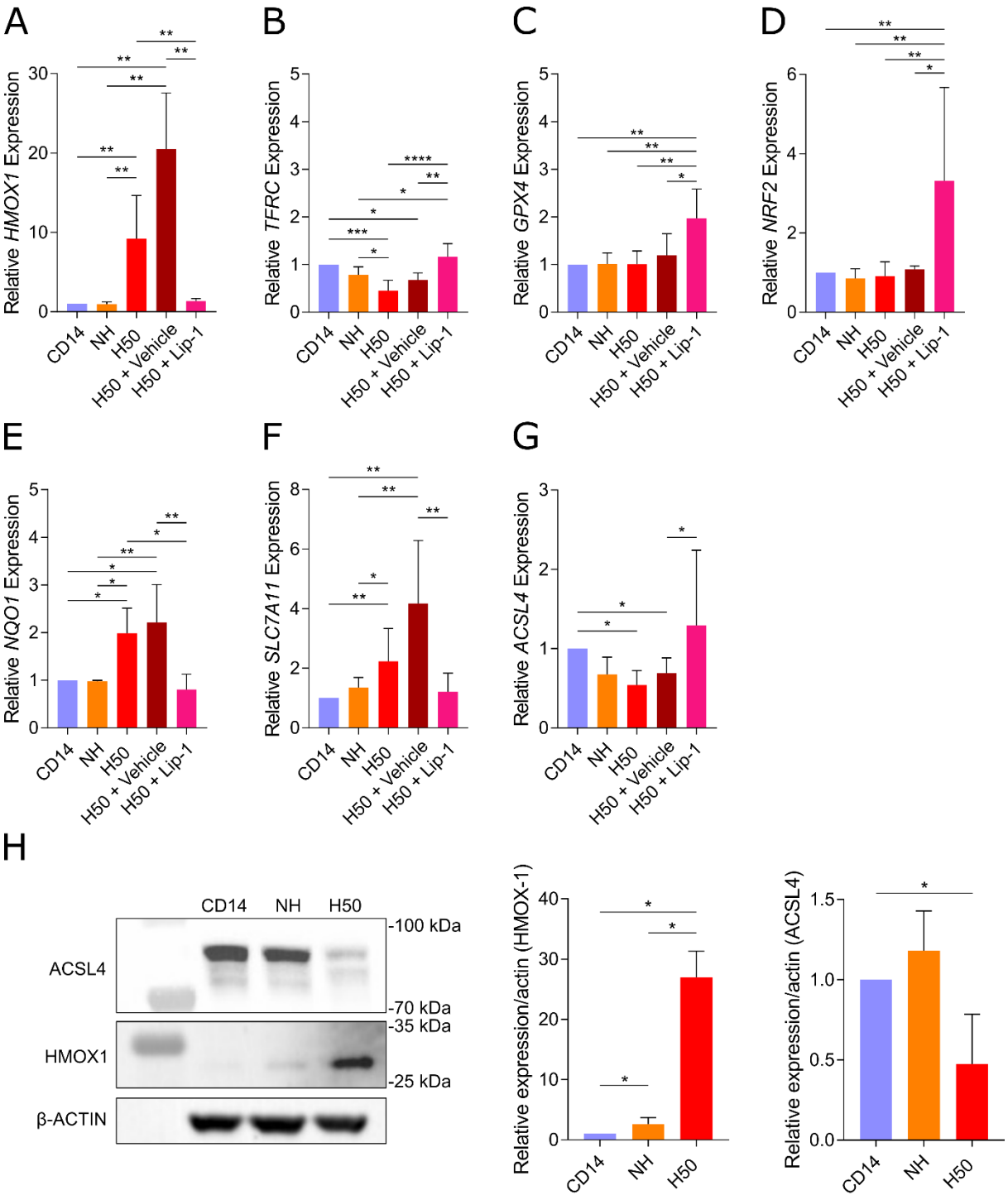

Figure 4: Increased Erythrophagocytosis modulates gene expression in EBI-like macrophages. EBI-like macrophages from control individuals were incubated alone (CD14), with non-heated RBCS (NH) or with heated RBCs (H50), combined with vehicle or Lip-1. After 3h, RBCs were washed away and lysed. Real-Time quantitative PCR analysis of **(A)** *HMOX1*, **(B)** *TFRC*, **(C)** *GPX4*, **(D)** *NRF2*, **(E)** *NQO1*, **(F)** *SLC7A11*, and **(G)** *ACSL4* was performed on the remaining EBI-like macrophages (mean ± SD, n = 6). **(H)** Western Blot analysis of HMOX1 and ACSL4 was performed on cell lysates from the same experiments for the CD14, NH and H50 conditions (mean ± SD, n = 4). *p<0.0332, **p < 0.0021, ***p < 0.0002, ****<0,0001; One-Way ANOVA followed by Tukey's multiple comparison test.

C. Erythrophagocytosis Leads "EBI-like Macrophages" to Shift from an Anti- to a Pro-inflammatory Profile.

To further determine the effect of increased RBC phagocytosis on the phenotype of surviving macrophages, we conducted ELISA assays and gene expression profiling to quantify the levels of pro-inflammatory and anti-inflammatory cytokines at the protein and gene expression levels.

When co-incubated with H50 RBCs, macrophages showed significantly decreased expression of anti-inflammatory M2 marker TGF-β (Figure 5A), with a concomitant increase of pro-inflammatory M1 marker TNF-α (Figure 5B). Notably, this shift in expression was effectively mitigated when inhibiting ferroptosis with Lip-1 (Figure 5A and 5B). It is noteworthy that, although not statistically significant at this timepoint, there were similar variations in the expression of other markers, such as CD206, CD80 and CD86 (Figure 5A and 5B). These results collectively suggest that the ferroptosis induction in macrophages induces a shift of polarization, transitioning from an anti-inflammatory to a pro-inflammatory phenotype, which can be prevented by treatment with Lip-1.

We performed the same experiment after 6h and 24h of co-incubation to investigate whether this polarization shift would persist over time. After 6h, we observed the same shift of polarization, with decreased expression of anti-inflammatory markers CD206 and CD163 and increased expression of CD80 and IL-6, all of which were reversed when cells were treated with Lip-1 (Figure 5C and 5D). Similarly, at 24h, we observed an increase in the expression of CD86 and CD80, demonstrating that macrophages could maintain their M1 polarization at this time point (Figure 5F). This observation was corroborated by ELISA assays, which revealed the accumulation of pro-inflammatory cytokines IL-6 and TNF-α in the supernatant of cells co-incubated with heated RBCs, alongside a reduction of anti-inflammatory cytokine TGF-β under the same conditions (Figure 5G). However, we did not observe any significant decrease in anti-inflammatory cytokines at this time point and even noted an increased expression of CD163, which was absent in the presence of Lip-1 (Figure 5E). This suggests that macrophages exhibit pro-inflammatory properties at this stage but might also retain their ability to revert to an anti-inflammatory phenotype.

Our results demonstrate a transition from an M2 to an M1 macrophage phenotype in response to elevated intracellular iron levels and oxidative stress. Interestingly, prolonged co-incubation of these macrophages with H50 RBCs suggests they could revert to an M2 phenotype, as indicated by the increased expression of CD163. However, further assays would be necessary to confirm this hypothesis.

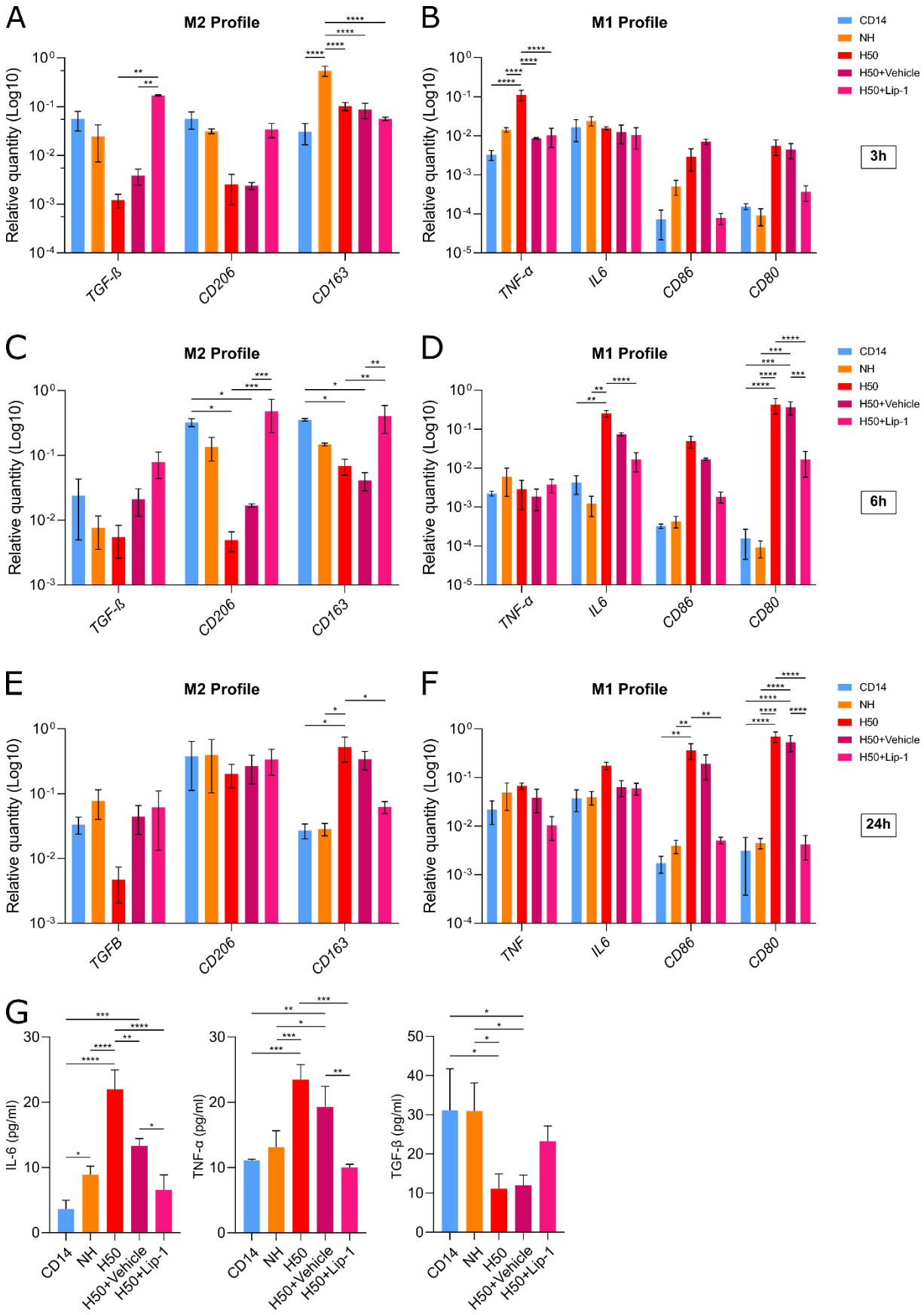

Figure 5: Increased Erythrophagocytosis induces a shift to an M1 phenotype in EBI-like macrophages. EBI-like macrophages from control individuals were incubated alone (CD14), with non-heated RBCS (NH) or with heated RBCs (H50), combined with vehicle or Lip-1. After 3h, 6h, and 24h, RBCs were washed away and lysed. Real-Time quantitative PCR analysis of M2 macrophage associated genes (*IDO1*, *TGF-β*, *IL-10*, *CD206*, *CD163*) at **(A)** 3h, **(C)** 6h and **(E)** 24h, and M1 macrophage associated

genes (*IL-6*, *TNF-α*, *NOS2*, *CD86*, *CD80*) at **(B)** 3h **(D)** 6h and **(F)** 24h (mean ± SEM, n=3). **(G)** At 24h, the supernatant of each condition was collected and IL-6, IL-10, TNF-α, and TGF-β production was measured by ELISA assay (mean ± SD, n=3). *p<0.0332, **p < 0.0021, ***p < 0.0002, ****<0,0001; One-Way ANOVA followed by Tukey's multiple comparison test.

D. Phagocytosis of Mature but not Immature Erythroblasts leads to Ferroptosis.

To get closer to the physiological conditions of the bone marrow, we performed phagocytosis experiments replacing RBCs by differentiating erythroblasts. CD34⁺ cells isolated from healthy donors' peripheral blood were cultured and differentiated in media containing SCF, EPO, IL-3, and transferrin, following a 4-Phase protocol of *in vitro* erythropoiesis (Yan et al., 2018). Regular monitoring of the differentiation kinetics by flow cytometry and MGG staining identified day 13 (D13) of culture as the timepoint at which >83% (± 6,71%) of the cells were at the polychromatic or the orthochromatic stage, with <25 % of enucleation (Figure 6A, 6B, and 6C). D13 differentiating erythroblasts were exposed to UV light to trigger apoptosis, put in culture for 24h then incubated with EBI-like macrophages. Exposure to UV induced high levels of Annexin V⁺ apoptotic cells (Figure 6D), that were efficiently phagocytosed by macrophages as compared to the non-irradiated cells (Figures 7A and 7B).

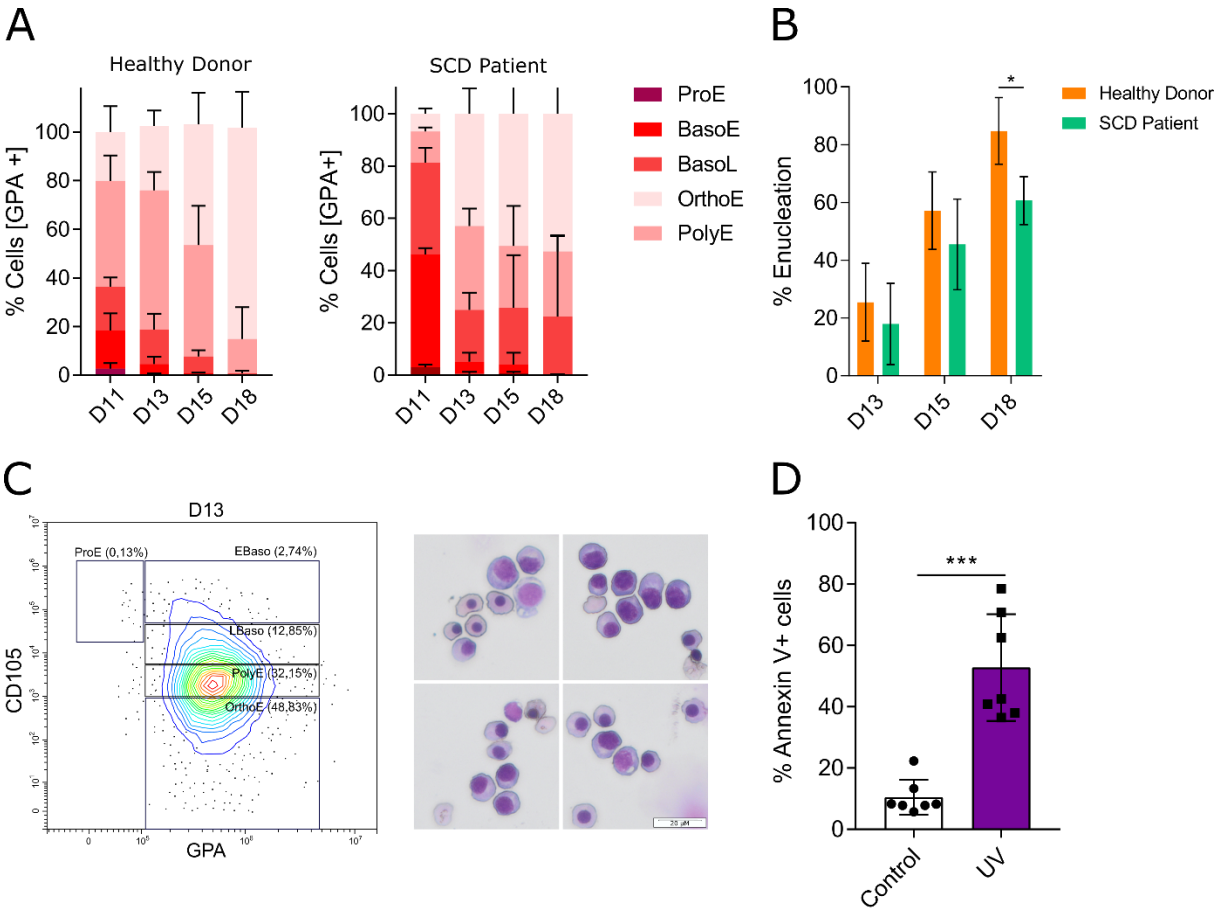

Figure 6: Erythropoiesis of control and SCD patients following a 4 phases liquid culture protocol. CD34⁺ cells were isolated from healthy donors or SCD patients' peripheral blood and cultured following an *ex vivo* erythropoiesis protocol with 4 phases under normoxic conditions **(A)** Stacked histogram representing the percentages of the different maturation stages: proerythroblast (ProE), early and late basophilic erythroblasts (EBaso and LBaso), polychromatic erythroblast (PolyE) and orthochromatic erythroblast (OrthoE) on days 11, 13, 15 and 18 of the culture of healthy donor cells (left panel) or SCD patient's cells (right panel). (mean ± SD, n = 5 for healthy donor and n=3 for SCD patient). **(B)** Percentage of enucleation on

days 13, 15 and 18 during the culture of healthy donors and SCD patients' cells (mean ± SD, n = 5). *p<0.0332 One-Way ANOVA followed by Tukey's multiple comparison test. **(C)** Erythroblast differentiation was followed by flow cytometry using a combination of the two surface markers: GPA and CD105. Differentiation stages were further characterized by doing May Grünwald-Giemsa (MGG) staining (scale bar 20µm). **(D)** On day 13 of culture, erythroblasts were irradiated with UV to induce their apoptosis and co-incubated with macrophages under normoxia or under hypoxia (mean ± SD, n = 7) ***p<0.001; paired t-test.

We assessed the impact of phagocytosis on the macrophages by gating on $CD163^{+}GPA^{-}$ cells to exclude residual erythroblasts in the cell suspension (Figure 7C), as, unlike RBCs, erythroblasts cannot be removed through osmotic shock following co-incubation with macrophages. After 3 hours of incubation with apoptotic erythroblasts, we observed elevated ROS levels (Figure 7D), lipid peroxidation (Figure 7E) and cell death (Figure 7F) in EBI-like macrophages. There was a further increase of ROS levels (Figure 7D) and lipid peroxidation (Figure 7E) after 18 hours of co-incubation, as well as increased cell death reflected by fewer attached cells at this timepoint with increased percentages of PI^{+} cells in the macrophages that were still attached to the culture dish (Figure 7F and 7G). Imaging flow cytometry experiments confirmed that lipid peroxidation was occurring in the macrophage compartment as the C11-BODIPY staining did not colocalize with internalized erythroblasts (Figure 7H).

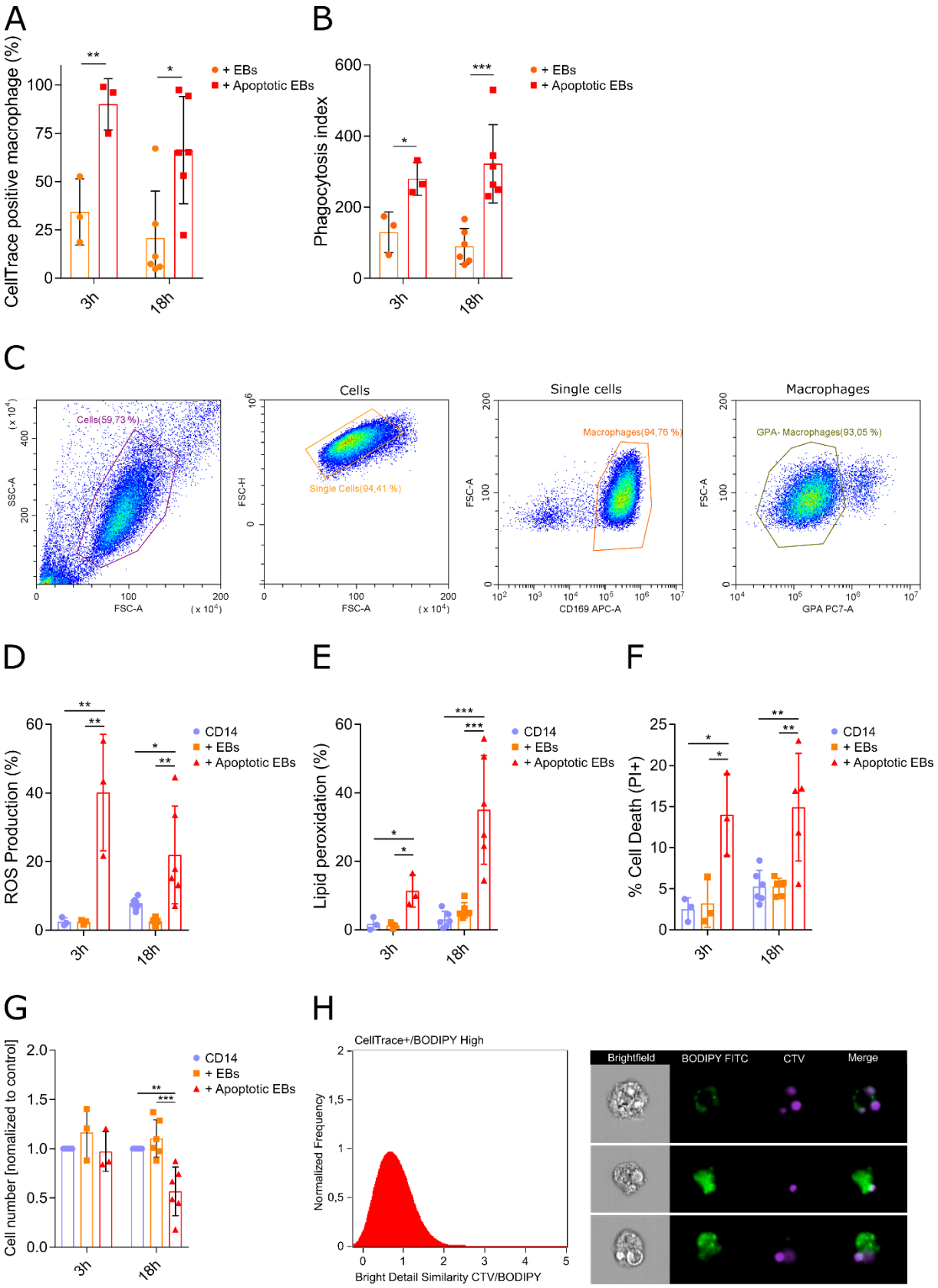

Figure 7: Increased Phagocytosis of terminally differentiating erythroblasts induces ferroptosis in EBI-like macrophages from Control and SCD Patients. CD34⁺ cells from control individuals were cultured for 13 days under normoxic conditions following a 4-Phase protocol of *ex vivo* erythropoiesis. On day 13 part of these erythroblasts were irradiated with UV to induce their apoptosis. EBI-like macrophages from control individuals were incubated alone (CD14) or co-incubated with either the remaining healthy erythroblasts (+ EBs) from that culture, or the apoptotic erythroblasts (+ Apoptotic EBs). Cells were co-

incubated together under normoxia for 3h and 18h **(A)** Phagocytosis of erythroblasts was quantified by measuring CTV or CFSE positivity in EBI-like macrophages and by **(B)** measuring the phagocytosis index (mean ± SD, n = 3 for 3h and n=6 for 18h). **(C)** Macrophages were determined by the forward (FSC) and side scatter (SSC). From this gate, single cells were gated on, and macrophages without erythroblast on their surface were analyzed based on the expression of CD169 and GPA. **(D)** ROS production was measured using DCFDA **(E)** Lipid peroxidation was measured using C11-BODIPY 581/591. **(F)** Cell death was measured using propidium iodide (PI) labelling. (mean ± SD, n = 3 for 3h and n=5 for 18h). **(G)** Number of EBI-like macrophages obtained after co-incubation alone, with control erythroblasts, and UV-exposed erythroblasts. (mean ± SD, n = 3 for 3h and n=5 for 18h). **(H)** The colocalization of CTV and BODIPY^{high} staining was measured using the Similarity Bright Detail Feature in IDEAS.

Further experiments were conducted where apoptotic GPA$^-$ progenitors, i.e., before the hemoglobin expression stage, were co-incubated with macrophages and were efficiently phagocytosed (Figure 8A). While we observed the expected increase in ROS levels following the phagocytosis of these cells (Figure 8B), this was not associated with increased lipid peroxidation or cell death (Figure 8C and 8D), supporting the occurrence of ferroptosis in EBI macrophages only upon phagocytosis of hemoglobinized erythroblasts. We also showed that ferroptosis was not triggered by soluble factors during the co-incubation step as there was no change in ROS, lipid peroxidation or cell death when macrophages were co-cultured with apoptotic D11 GPA$^+$ erythroblasts in a transwell system that prevents cell-cell contact (Figure 8B, 8C and 8D).

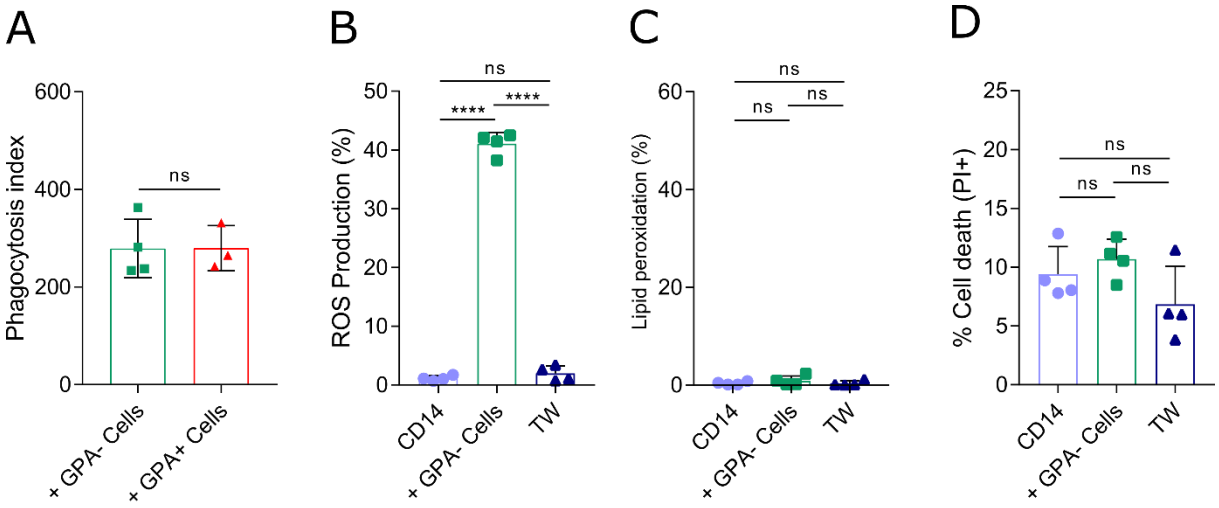

Figure 8: Increased Phagocytosis of GPA- cells does not induce ferroptosis in EBI-like macrophages. CD34$^+$ cells from control individuals were cultured under normoxic conditions for 7 days following a 2-Phase protocol of *ex vivo* erythropoiesis to generate GPA$^-$ erythroid progenitors (GPA$^-$ cells), or for 13 days following a 4-Phase protocol of *ex vivo* erythropoiesis to generate terminally differentiating erythroblasts (GPA$^+$ cells). On these respective days, cells from both cultures were exposed to UV to induce their apoptosis. EBI-like macrophages from control individuals were either incubated alone (CD14) or co-incubated in direct contact with GPA$^-$ or GPA$^+$ cells for 3h under normoxic conditions. The same macrophages were also incubated in indirect contact with GPA$^+$ cells for 3h using a transwell system (TW). After the erythrophagocytosis experiment **(A)** The Phagocytosis Index was measured (mean ± SD, n = 4) **(B)** and ROS production, **(C)** lipid peroxidation and **(D)** cell death was analyzed by flow cytometry (mean ± SD, n = 4).

We performed similar experiments using cells from SCD patients. As expected, ROS levels, lipid peroxidation and cell death were all increased upon phagocytosis of apoptotic hemoglobin-rich SCD erythroblasts by EBI-like SCD macrophages (Figure 9A, 9B, 9C, and 9D). While there was a significant reduction of the ROS production and lipid peroxidation in the presence of ferroptosis inhibitors Lip-1,

this was not sufficient to prevent the increased cell death observed in this experiment (Figure 9B, 9C, and 9D).

Additionally, we performed experiments at 5% O_2 to mimic the bone marrow environment. EBI-like macrophages were cultured for 7 days under partial hypoxic conditions, at 5% O_2. The co-incubation of apoptotic erythroblasts and EBI-like macrophages in these conditions did not significantly impact the phagocytosis index (Figure 9A). Furthermore, we observed similar levels of ROS, lipid peroxidation and cell death as compared to those observed under normoxic conditions (Figure 9B, 9C, and 9D). These results suggest that hypoxia does not prevent the occurrence of cell death following increased phagocytosis of apoptotic erythroblasts.

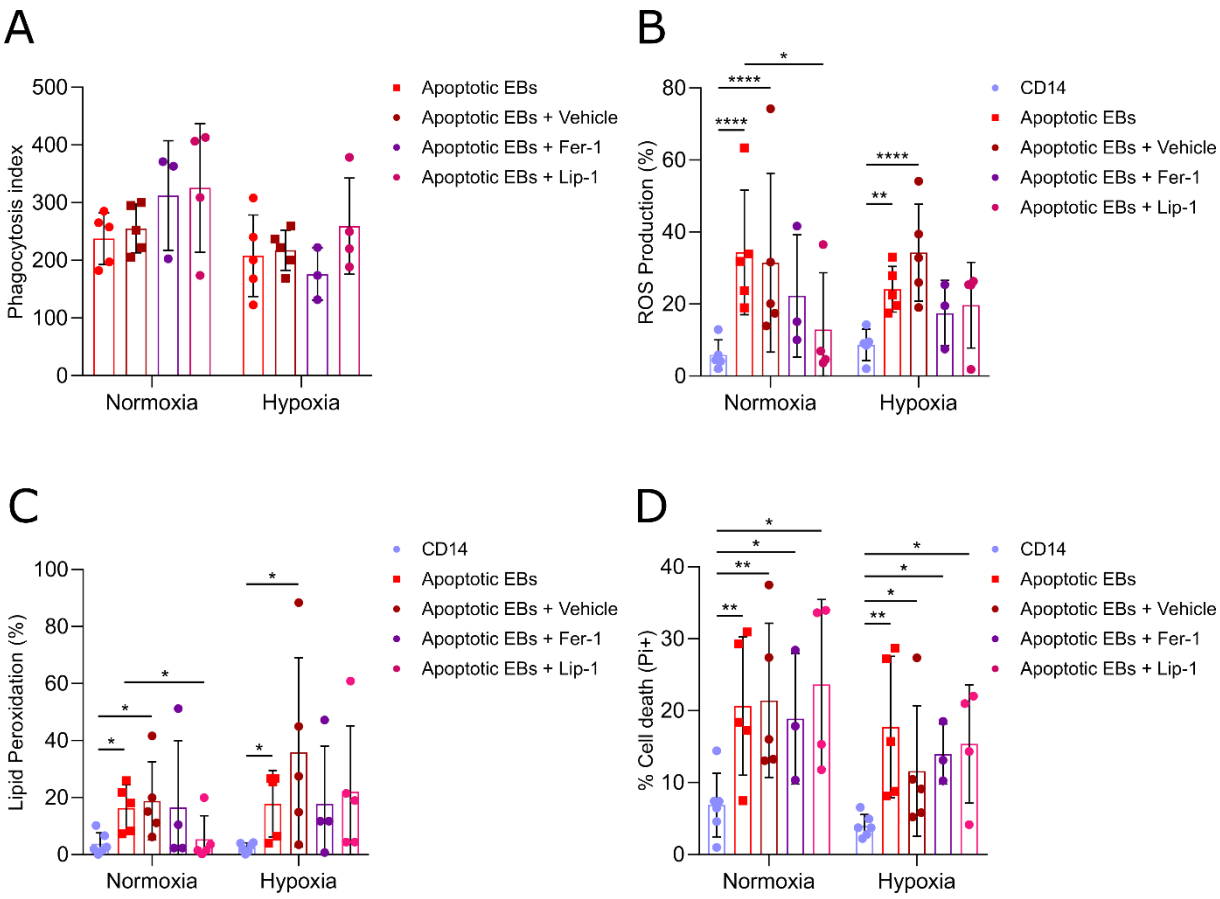

Figure 9: Evaluation of ferroptosis in SCD macrophages: CD34⁺ cells from SCD patients were cultured for 13 days under normoxic conditions following a 4-Phase protocol of *ex vivo* erythropoiesis. On day 13 of culture, SCD erythroblasts were irradiated with UV to induce their apoptosis (Apoptotic EBs). EBI-macrophages, cultured under normoxic or hypoxic conditions, were incubated alone (CD14) or co-incubated with these apoptotic erythroblasts with or without vehicle, Fer-1 and Lip-1 for 3h. After **(A)** the phagocytosis index, **(B)** ROS production, **(C)** lipid peroxidation and **(D)** cell death was analyzed by flow cytometry (mean ± SD, n = 5). *p<0.0332, **p < 0.0021, ***p < 0.0002, ****<0,0001; One-Way ANOVA followed by Tukey's multiple comparison test.

E. Higher Levels of Lipid Peroxidation Observed in Sickle Mice

To investigate whether ferroptosis occurs in the macrophages of the BM in SCD, we employed an *in vivo* approach using the Townes mouse model. While various research groups have identified a

multitude of molecules expressed by EBI macrophages, including EMP, αV-integrin, KLF1, and Dnase2α (Chow et al., 2013b; Kawane et al., 2001; Mankelow et al., 2004; Porcu et al., 2011; Sadahira et al., 1995; Soni et al., 2006), the most reliable combination of surface markers to identify these cells remains F4/80, CD169 and VCAM1 (W. Li et al., 2019; Seu et al., 2017). Consequently, to quantify the numbers of F4/80$^+$VCAM$^+$CD169$^+$ macrophages, we stained the BM with these markers along with Ly6G, to gate out granulocytes, and Ter119, to exclude erythroid cells (Figure 10). Calculation of the cell number revealed that the overall population of F4/80$^+$ macrophages in the BM showed no significant differences between SS Townes mice and their AA and AS counterparts (Figure 11A). However, while there were ~ 0.44x10^6 F4/80$^+$VCAM$^+$CD169$^+$ cells (±0.15x10^6) in BM cells from 2 femurs and 2 tibias in AA mice, and ~ 0.31x10^6 cells (±0.14x10^6) in AS mice, this number was significantly decreased in the BM of SS mice with ~ 0.11x10^6 cells (±0.04x10^6) (Figure 11B).

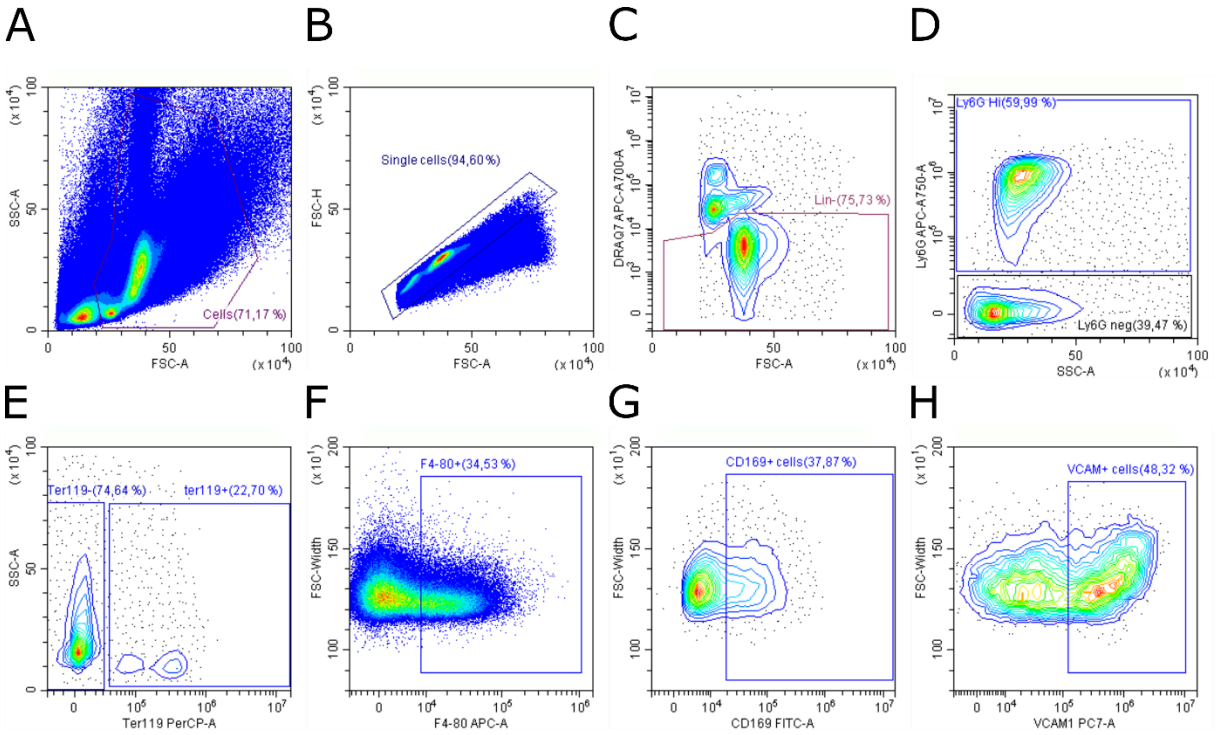

Figure 10: Representative gating strategy for F4/80$^+$VCAM1$^+$CD169$^+$ macrophages in mouse BM. 3-month-old mice were sacrificed and bone marrow and spleen cells were isolated. **(A)** Plot of FSC-A and SSC-A of all events, **(B)** plot of FSC-A and FSC-H of gated population in (A). From the single cells gate **(C)** Lineage negative (Lin-) and live cells were analyzed **(D)** Ly6G$^-$ were analysed **(E)** Ter119$^-$ cells were analyzed **(F)** F4/80$^+$ cells **(G)** CD169$^+$ and **(H)** VCAM1$^+$ cells were analyzed. FSC-A: forward scatter area; SSC-A: side scatter area; FCS-H: forward scatter height.

In mice, stress erythropoiesis is extramedullary and occurs in the spleen. Therefore, we also isolated cells from the spleen and quantified the number of F4/80$^+$ and F4/80$^+$CD169$^+$VCAM1$^+$ cells in this organ. SS mice developed a marked splenomegaly, with a significant increase in spleen weight compared to HbA and HbAS mice (Figure 11C). Consequently, HbS mice had an increased total cell count, which was reflected by the elevated numbers of F4/80$^+$ and F4/80$^+$CD169$^+$VCAM1$^+$ macrophages, both of which were significantly higher in SS mice in comparison to AS and AA mice (Figure 11D and 11E).

Interestingly, despite this increased total cell count, we noted a significant decrease in the percentages of $F4/80^+$ and $F4/80^+CD169^+VCAM1^+$ cells within the $Ly6G^-Ter119^-$ cell population in SS mice, in comparison to AS and AA individuals (Figure 11F and 11G). These results suggest a shift in the composition of the macrophage subpopulations in the BM and the spleen of SS mice.

We also investigated whether macrophages of SS mice had increased lipid peroxidation by staining BM cells with C11-BODIPY and an anti-F4/80 antibody. C11-BODIPY fluorescence was higher in the $F4/80^+$ cells of SS mice as compared to AA and AS mice (Figure 11H), which is indicative of lipid peroxidation, a hallmark of ferroptosis. This was specific to $F4/80^+$ cells and was not a general feature of BM cells, as there was no difference in C11-BODIPY fluorescence of the rest of the BM cells (F4/80-) among the mice of the 3 genotypes (Figure 11I), although we cannot exclude that other specific sub-populations of cells may also be impacted. We also measured lipid peroxidation levels in the splenocytes of the same mice. Interestingly, we did not observe a significant difference of C11-BODIPY fluorescence between SS, AS and AA individuals. This was the case for the macrophages of the spleen as well as the rest of the splenocytes (F4/80-) (figure 11J and 11K). These results suggest that ferroptosis is likely occurring in the macrophages of the BM of SCD mice, as demonstrated by the increased lipid peroxidation levels observed in these cells, but not in the macrophages of the spleen.

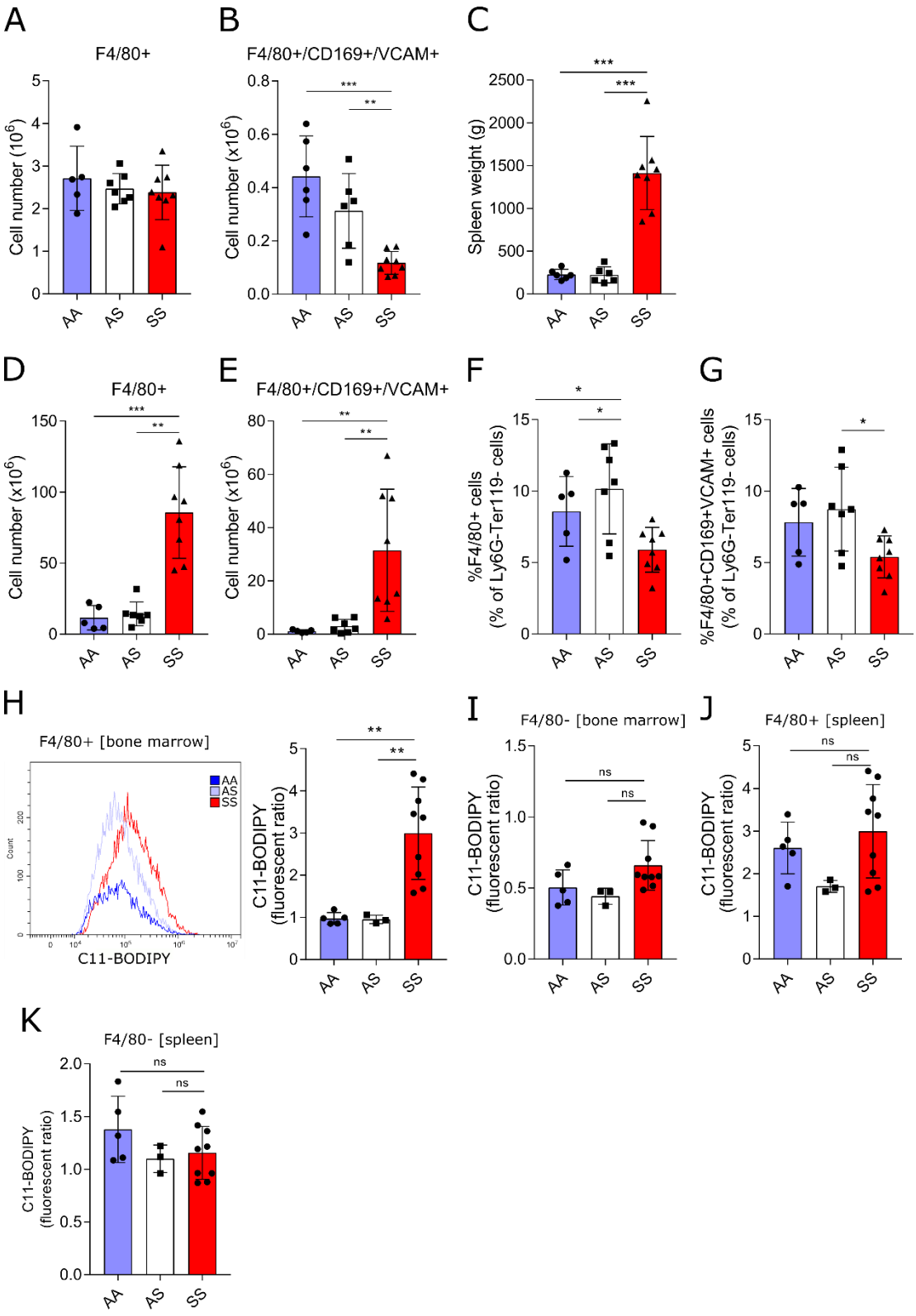

Figure 11: Characterizing F4/80+ macrophages of BM and spleen mice using flow cytometry. 3-month-old mice were sacrificed, and bone marrow and spleen cells were isolated. Total numbers of **(A)** F4/80$^+$ and **(B)** F4/80$^+$CD169$^+$VCAM1$^+$ cells in AA, AS, and SS mice BM. Total numbers of **(C)** F4/80$^+$ and **(D)** F4/80$^+$CD169$^+$VCAM1$^+$ cells in AA, AS, and SS mice spleen. (mean ± SD, n=5 AA, n=7 AS, n=8 SS). **(E)** Spleen weight in grams of AA, AS and SS mice. **(F)** Percentages of F4/80$^+$ and **(G)** F4/80$^+$CD169$^+$VCAM1$^+$ cells in Lin$^-$Ly6G$^-$Ter119$^-$ cells AA, AS, and SS mice spleen. **(H)** Lipid peroxidation was measured by flow cytometry with the C11-BODIPY 581/591 staining, in macrophages (F4/80$^+$), **(I)** or the rest of the cells (F4/80$^-$) of the BM and **(J)** in macrophages **(K)** or the rest of the cells of the spleen (mean ± SD, n=5 AA, n=4 AS, n=9 SS), **p < 0.0021, ***p < 0.0002, Mann Whitney test.

II. DISCUSSION

Our first study provided evidence for ineffective erythropoiesis in individuals with SCD. Specifically, we observed a loss of cell doubling between the polychromatic and orthochromatic stages in the BM, with a mean fold increase of only 1.24, suggesting the loss of around 40% of maturing erythroblasts (El Hoss et al., 2021). In the current study we provide evidence that phagocytosis of such high amounts of apoptotic cells may induce cell death of SCD EBI macrophages through the process of ferroptosis.

Erythrophagocytosis-Induced Ferroptosis in EBI-like Macrophages

After enhanced erythrophagocytosis, EBI-like macrophages showed increased cell death, accompanied by elevated levels of ROS and lipid peroxidation, a hallmark of ferroptosis. This phenomenon occurred when macrophages ingested substantial numbers of RBCs or terminally differentiating erythroblasts. However, while increased phagocytosis of early erythroid progenitors resulted in elevated ROS levels, it did not show a concurrent increase in lipid peroxidation or cell death. These distinct responses suggest that heme and its catabolized product, iron, are critical for this erythrophagocytosis-induced cell death, aligning with the characteristics of ferroptosis. It is worth noting that the increased ROS production observed in these experiments might result from an oxidative burst occurring in macrophages after the uptake of any apoptotic cells and is thus not specific to ferroptosis (Lam et al., 2010; Panday et al., 2015).

Co-treatment with ferroptosis inhibitors Fer-1 and Lip-1 effectively reduced ROS production, lipid peroxidation, and cell death associated with H50 RBC phagocytosis. This aligns with their function as radical-trapping antioxidants and further demonstrates the occurrence of ferroptosis following erythrophagocytosis. These results are consistent with previous studies demonstrating that excessive engulfment of damaged RBCs could induce ferroptosis in splenic red pulp macrophages of mice (Youssef et al., 2018). Likewise, erythrophagocytosis-induced ferroptosis was also shown to be a feature of atherosclerosis (Liu, Östberg, et al., 2022; Puylaert et al., 2023). Interestingly, after phagocytosis of apoptotic erythroblasts, these inhibitors did not protect EBI-like macrophages from cell death. We hypothesize that the large numbers of apoptotic erythroblasts used in this experiment may have consumed Lip-1 resulting in its faster depletion in the culture media, particularly under hypoxic conditions, where higher basal levels of ROS are expected. This hypothesis will be challenged by increasing the concentration of Fer-1 and Lip-1 in future experiments.

Erythrophagocytosis-induced Transcriptional Changes in EBI-like Macrophages:

Our RT-qPCR analyses revealed an increase in HMOX1 expression following erythrophagocytosis, which could also be observed at the protein level. This rise in HMOX1 levels can be partially attributed to the increased phagocytosis of RBCs, a process demanding rapid heme metabolism and detoxification

(Kovtunovych et al., 2010; Poss & Tonegawa, 1997; Yachie et al., 1999). However, excessive HMOX1 activity has been associated with ferroptosis induction as it increases labile Fer (II) concentration, even when ferritin levels are insufficient to store it effectively (Kwon et al., 2015; Suttner & Dennery, 1999). This process is commonly called 'non-canonical ferroptosis' (Hassannia et al., 2018). In our experiments, we observed a substantial increase in HMOX1 expression following erythrophagocytosis, with up to 30-fold increase in some cases. This excessive HMOX1 expression may cause ferroptosis in EBI-like macrophages. Furthermore, we did not observe changes in the expression of GPX4 after erythrophagocytosis, suggesting that the observed ferroptosis may not be initiated through a canonical GPX4-mediated pathway, consistent with previous reports (Puylaert et al., 2023).

We also observed increased expression of SLC7A11 and NQO1, both known to enhance antioxidant defense and to reduce ferroptosis susceptibility (Dixon et al., 2012; Ross & Siegel, 2017). Their upregulation following erythrophagocytosis suggests an adaptive response from surviving EBI-like macrophages, protecting them from ferroptosis by enhancing their antioxidant defense. Despite these results, we did not observe any modulation of *NRF2* mRNA expression, although examining its protein expression may be needed to gain further insights into its activity in our model. As a major antioxidative system, NRF2 has been shown to prevent the toxic accumulation of ROS and to suppress ferroptosis through transcriptional regulation of genes such as *SLC7A11*, *HMOX1*, *GPX4*, and *NQO1* (Chen et al., 2017; Kang et al., 2021; Wang et al., 2022). However, the observed anti-ferroptotic response observed in our experiments may be coordinated by NRF2-independent pathways, as described in previous studies (Greaney et al., 2016; Kim et al., 2023; Lim et al., 2019; Y. Zhang et al., 2021). For instance, Kang et al. demonstrated that HMOX1 levels substantially increased in muscle atrophy, with its expression depending on FoxO1, not NRF2 (Kang et al., 2014). Similarly, in peritoneal macrophages, hemin induced HMOX1 expression occurred independently from NRF2 activation (A. Zhang et al., 2021).

Interestingly, the expression of NRF2 was upregulated when cells were co-treated with the ferroptosis inhibitor Lip-1, indicating that Lip-1 may possess an antioxidant function that relies on NRF2 expression. This effect is reflected by the concurrent increase in GPX4 expression, one of NRF2 targets also known for its protective role against ferroptosis. While Lip-1 is a commonly used agent in ferroptosis studies, its role as an inhibitor has yet to be comprehensively characterized. It is often considered primarily as a radical-trapping antioxidant, and its detailed mechanism remains to be fully elucidated.

Macrophage Phenotype Shift in Response to Erythrophagocytosis:

Our results demonstrate a shift in the phenotype of EBI-like macrophages following increased phagocytosis, transitioning from an anti-inflammatory state to a pro-inflammatory one. This shift is

marked by the increased expression of M1 markers such as CD80, CD86, and TNF-α, along with a decrease in M2 markers like CD163 and CD206.

Prior studies have demonstrated that iron overload can promote the polarization of macrophages toward the M1 phenotype via ROS/acetyl-p53 pathway (Handa et al., 2019; Zhou et al., 2018). Additionally, heme was also identified as a stimulus capable of inducing a similar phenotype shift, leading to the emergence of 'heme-activated macrophages', that closely resemble classically activated M1 cells (Murray, 2017). This shift was found to be mediated through Toll-like receptor 4 (TLR4)/ROS signaling and serves to initiate an inflammatory response designed to restore homeostasis (Bozza & Jeney, 2020; Dutra & Bozza, 2014; Figueiredo et al., 2007; Pradhan et al., 2020).

In the context of SCD, where chronic hemolysis leads to elevated levels of free heme, multiple studies have reported similar findings. For instance, excess heme has been demonstrated to induce an M1 phenotype shift in hepatic macrophages, which in turn promotes sterile inflammation and exacerbates hepatic fibrosis and organ damage commonly associated with SCD (Belcher et al., 2014; Gladwin & Ofori-Acquah, 2014; Vinchi et al., 2016). Moreover, heme has been shown to strongly impair the functional response of macrophages to the presence of apoptotic cells, aligning with previous research demonstrating that M1 macrophages exhibit lower phagocytic capacity compared to M2 macrophages (Denney et al., 2012; Tierney et al., 2009). Therefore, this phenotypic shift prevents the efficient phagocytosis and clearance of apoptotic cells, ultimately inhibiting the resolution of inflammation and the process of tissue repair (Sharma et al., 2023).

It has been suggested that iNOS expression in inflammatory macrophages negatively regulates the onset of ferroptosis, rendering them resistant to this type of cell death (Kapralov et al., 2020; Piattini et al., 2021). Our results indicate that while some EBI-like macrophages may die through ferroptosis following increased erythrophagocytosis, the remaining ones shift to a pro-inflammatory phenotype, helping them better withstand ferroptosis-induced stress. However, this M2-to-M1 phenotype shift may have a negative impact as it could lead to the accumulation of apoptotic cells in the BM, further damaging the tissue and leading to sustained inflammation. In our experiments, macrophages co-incubated with H50 RBCs exhibited increased expression of CD163 after 24h, suggesting a potential reversion to an M2 phenotype. However, while these observations indicate a potential resolution of inflammation after 24h *ex vivo*, the constant production of apoptotic cells in an *in vivo* setting may hinder this resolution.

EBI Macrophage Populations in SCD Townes Mice

Markers historically suggested for the identification of EBI macrophages in mice are F4/80, CD169, and VCAM1 (Chow et al., 2013b; Jacobsen et al., 2014; Ramos et al., 2013). Analysis of the BM erythropoietic niche in Townes mice revealed a decrease in the number of F4/80$^+$/CD169$^+$/VCAM$^+$ macrophages in HbS mice compared to HbAS and HbAA mice. In contrast, the total number of F4/80$^+$ macrophages in the BM remained relatively constant across all genotypes. Additionally, we observed an increased C11-BODIPY fluorescent signal in F4/80$^+$ cells of HbS but not HbAA or HbAS mice, indicative of lipid peroxidation in these cells in the context of SCD.

These results suggest that SS mice may have fewer EBIs in their BM, as indicated by the reduced number of F4/80$^+$CD169$^+$VCAM$^+$ macrophages. This decline in EBI macrophages could result from increased cell death of these cells, possibly though ferroptosis, as increased lipid peroxidation was observed in SS mice BM macrophages. However, EBI macrophages may have undergone a phenotypic shift as an adaptive response to the SCD BM environment, as seen in our *ex vivo* experiments with human cells. This hypothesis is supported by the fact that the total number of macrophages remained uniform between HbAA, HbAS, and HbSS mice. Notably, previous studies have shown a similar phenotypic shift in mice treated with GM-CSF, where a reduction in the number of EBI macrophages was accompanied by a shift of BM macrophages from an anti-inflammatory to a pro-inflammatory phenotype, leading to decreased clearance of pyrenocytes and apoptotic erythrocytes (Cao et al., 2022; Tay et al., 2020). Additionally, in a mouse model of systemic lupus erythematosus, loss of EBI macrophages was also observed, with a shift to a pro-inflammatory phenotype and a down-regulation of genes required for adhesion and provision of nutrients to erythroid precursors (Maria et al., 2023).

Townes mice have a marked increase in the size of the spleen attributed to severe congestion and increased stress erythropoiesis (Gallivan et al., 2022; Nyffenegger et al., 2022; Ryan et al., 1997; Trucas et al., 2023). In the spleen of SS mice, we observed a substantial increase in the number of F4/80$^+$ and F4/80$^+$CD169$^+$VCAM1$^+$ cells, reflecting the splenomegaly. Interestingly, despite this increased total cell count, we noted a significant decrease in the percentages of F4/80$^+$ and F4/80$^+$CD169$^+$VCAM1$^+$ cells within the Ly6G$^-$Ter119$^-$ cell population in SS mice in comparison to AS and AA individuals. This indicates a shift in the composition of the splenic microenvironment in SS mice, possibly in response to the increased stress erythropoiesis, and suggests that the number of macrophages may be insufficient to adequately support the heightened demands of erythropoiesis in the spleen of these mice. However, it is essential to note that monocytes have also been described as participating in stress erythroid niches, as they are recruited from the circulation and mature alongside stress erythroid progenitors (Liao et al., 2018). Therefore, a more comprehensive characterization of the monocyte population, in

addition to the macrophages, is needed to uncover possible discrepancies between the spleen of SS, AS, and AA mice.

Contrary to the BM results, F4/80^{+} cells in HbS mice spleen did not present an increased C11-BODIPY fluorescent signal, denoting no difference in the peroxidation levels of these cells compared to the splenocytes of HbAS and HbAA mice. This suggest the absence of ferroptosis in the EBIs of the spleen, probably because the spleen environment is less hypoxic compared to the BM, resulting in a more efficient erythropoiesis, with less or no cell death during terminal erythroid differentiation. However, we cannot exclude that such events might occur gradually and reach significant levels in older mice, as iron accumulation is a common occurrence in the spleen of SCD Townes mice (Alvarez-Argote et al., 2023). In mice, stress erythropoiesis is extramedullary (Bennett et al., 2018). Thus, the reduced count of EBI macrophages may also be indicative of an elevated stress erythropoiesis, necessitating the shift of erythropoiesis from the BM to the spleen.

Our results demonstrate that the increased erythrophagocytosis of RBCs and mature erythroblasts leads to ferroptosis in EBI-like macrophages. Our preliminary *in vivo* results support these observations. However, a more comprehensive characterization of the distinct EBI macrophage subpopulations within the BM and spleen of Townes mice using -omic approaches is necessary to draw definitive conclusions. Moreover, the structural study of EBIs might help decipher which of these cell populations is involved in the formation of these islands in the Townes mouse model. We are currently conducting an in-depth characterization of Townes mice erythropoiesis to gain a more complete understanding of the BM and spleen landscape in this model.

III. MATERIAL AND METHODS

A. Ethical Approval

The study was conducted according to the declaration of Helsinki with approval from the Medical Ethics Committee (GR-Ex/CPP-DC2016-2618/CNILMR01), and followed the French blood donation regulations and ethics, as well as the French Public Health Code (article L.1221-1). Platelet leukoreduction (LR) filters from healthy donors were obtained from the Etablissements Français du Sang (EFS). Blood bags from adult SCD patients enrolled in an automated red blood cell exchange (erythrapheresis) transfusion program were obtained after informed consent. All SCD patients were of SS genotype.

B. Isolation of CD34+ cells and CD14+ Cells

Dextran sedimentation was performed by mixing blood with 2% dextran solution (Sigma). After 30 minutes sedimentation, the RBC-depleted upper layer was collected and PBMCs were isolated on a Ficoll gradient (Eurobio), the remaining RBCs were lysed using RBC lysis buffer (Thermofisher). CD34+ cells were purified by a magnetic sorting system (Stemcell technologies) according to manufacturer's protocol. From the CD34- cells, CD14+ cells were then isolated by a magnetic sorting system (Miltenyi Biotec) following the supplier protocol. The purity of the isolated CD34+ and CD14+ cells, checked by flow cytometry, was always between 90-96%.

C. *in vitro* Differentiation of Erythroid Progenitors and Erythroblasts

1. 2 Phases Liquid Culture (2P-LC)

Cells were cultured at a density of 5.10^5 cells/ml and media was diluted every two days. Composition of the base medium was Iscove's Modified Dulbecco's Medium (IMDM) (Life technologies) supplemented with 15% BIT 9500 (Stemcell Technologies), 100 U/ml Penicillin Streptomycin (Life technologies) and 2 mM L-Glutamine (Life technologies). In the first phase (D0-6), cells were expanded in the presence of 100 ng/ml human recombinant (hr) stem cell factor (SCF) (Miltenyi Biotec), 10 ng/ml of hr interleukin (IL)-3 (Miltenyi Biotec) and 100 ng/ml of hr IL-6 (Miltenyi Biotec). In the second phase (D7-20), IL-6 was replaced with 2 U/ml of erythropoietin (EPO) (Stemcell Technologies). To perform the erythrophagocytosis experiments, cells on day 7 of the first phase were used.

2. 4 Phases Liquid Culture (4P-LC)

Composition of the base culture medium was Iscove's Modified Dulbecco's Medium (IMDM) (Life Technologies), 2% human peripheral plasma, 3% human AB serum, 3IU/ml heparin (Stemcell technologies), 10 µg/ml insulin (Sigma) and 100 U/ml Penicillin Streptomycin (Pen/Strep) (Life technologies). In the first phase (day 1-7), cells were cultured at a concentration of 1.10^5 cells/mL in the presence of 200µg/ml Holo-human transferrin (Sigma), 10 ng/ml stem cell factor (SCF) (Miltenyi), 1 ng/ml human recombinant (hr) interleukin (IL)-3 (Miltenyi Biotec) and 3IU/ml erythropoietin (EPO) (Stemcell Technologies). In the second phase (day 8-11), IL-3 was removed from the media, and the

concentration of EPO was reduced to 1IU/ml. In the third phase (day 13-15), the cell concentration was increased to 1.10^6 cells/mL, SCF was removed from the media and the concentration of transferrin was increased to 1mg/ml. Finally, in the fourth phase (day 16-20), the cell concentration was increased to 5.10^6 cells/mL, and EPO was removed from the media. To perform the erythrophagocytosis experiments, cells on day 13 were used.

D. Macrophage culture

CD14+ cells isolated as detailed above were seeded at a density of $1x10^6$cells/mL in Roswell Park memorial institute (RPMI) medium (Life Technologies), supplemented with 100 U/ml Penicillin Streptomycin, 10% Fetal Bovine Serum (FBS) (Life Technologies), 25 ng/mL M-CSF (Stemcell Technologies) and 1µM dexamethasone (Dex). The media was changed on Day 1 and Day 4 of culture, and macrophages were considered mature at Day 7.

E. *In vitro* Erythrophagocytosis Experiment

In vitro phagocytosis experiments were conducted using two different types of cells: RBCs and erythroblasts.

For the RBC phagocytosis experiment, RBCs obtained from EFS were washed twice with phosphate buffered saline (PBS) (Corning) and resuspended at a concentration of $10x10^6$cells/mL. The cells were then stained with 10µM of CellTrace Violet (Invitrogen) for 20 minutes at 37°C and 300 rpm. After the staining, the reaction was stopped with FBS, and the cells were washed twice with RPMI supplemented with 10% FBS. The efficacy of the CellTrace staining was confirmed by flow cytometry. To induce phagocytosis, the RBCs were incubated for 30 minutes at 50°C and washed again with RPMI. Both heated and non-heated RBCs were incubated with macrophages in RPMI supplemented with 100 U/ml Penicillin Streptomycin and 10% Fetal Bovine Serum at a ratio of RBCs/macrophage: 30/1. Following 3h of incubation at 37°C, the macrophages were washed twice with PBS to remove free RBCs. The macrophages were then detached using 0.25% trypsin-EDTA (Life Technologies) and counted using the CASY® (OLS OMNI life Science). To eliminate any remaining non-internalized RBCs, the cells were incubated for 15 minutes in an RBC lysis buffer (Santa Cruz technology). Finally, the cells were analyzed by flow cytometry.

For the erythroblast phagocytosis experiment, erythroblasts at specific differentiation stages (D13 of the 4P-LC and D7 of the 2P-LC) were induced to undergo apoptosis by exposing to UV-light in a UV chamber (Uvitec). After washing with PBS and resuspending at a concentration of $1x10^6$ cells/mL, the cells were stained with 1µM CellTrace Violet for 20 minutes at 37°C. Following the staining, the reaction was stopped with FBS, and the cells were washed with RPMI supplemented with 10% FBS. Similar to the RBC experiment, erythroblasts were incubated with macrophages in RPMI (100 U/mL Penicillin-

Streptomycin, 10% FBS) at a ratio of erythroblasts/macrophage: 30/1. After 3 hours of incubation at 37°C, macrophages were washed with PBS to remove free erythroid cells. Cell detachment was performed using 0.25% trypsin-EDTA, and cell counting was carried out using the CASY® system. Finally, the cells were analyzed by flow cytometry.

In these experiments CellTrace$^+$ macrophages were considered as cells having phagocytized at least one cell. The phagocytosis index was calculated as followed: geometrical mean fluorescence intensity (GeoMFI) of CellTrace$^+$ macrophages divided by the GeoMFI of CellTrace-stained RBCs * 100. Similar erythrophagocytosis experiments were conducted in the presence of 100µM Ferrostatin-1 (Fer-1) (Sigma), and 1 µM Liproxstatin-1 (Lip-1) (Sigma).

F. Flow Cytometry

All experiments were performed on a Cytoflex S flow cytometer (Beckman Coulter) and acquired using the CytExpert software (Beckman Coulter). The data was analyzed using the same software. Imaging flow cytometry experiments were analyzed with the Imagestream ISX MkII flow cytometer (Amnis Corp, EMD Millipore) and the INSPIRE software version 99.4.437.0. Acquired data was analyzed using IDEAS software version 6.2 (Amnis Corp, EMD Millipore). Unless otherwise specified, all antibodies were purchased from Biolegend.

1. Stainings to monitor erythropoiesis.

Cells were taken from the cultures every two days to assess differentiation, apoptosis, enucleation, and hemoglobin expression.

a. Apoptosis

To measure cell death, erythroblasts were washed once and stained with PE-conjugated Annexin V for 15 minutes at room temperature. Samples were then diluted with 200 µl of Annexin buffer (Biolegend) and analyzed by FACS.

b. Erythroid differentiation

To monitor erythroid differentiation cells were analyzed for surface expression of glycophorin A (GPA), CD34, CD36, CD71, CD105, CD117, CD123. For this, cells were blocked with 0,4% human AB serum for 20 minutes at 4°C, and then incubated with fluorochrome-conjugated antibodies for 30 minutes at 4°C. Cells were washed twice with FACS buffer and stained with 300 nM of DRAQ7 (Biolegend) for 15 minutes at room temperature before analysis.

c. Enucleation

To study enucleation, cells were first incubated with anti-GPA-PE-Cy7 and anti-CD36-APC antibodies for 30 minutes on ice. Cells were then stained with 100 nM of Syto16 dye (Thermofisher) for 15 minutes at RT and washed once before analysis.

d. Hemoglobin

Cells were also analyzed for adult hemoglobin (HbA) and Fetal Hemoglobin (HbF) expression. For this, cells were fixed, permeabilized and saturated as previously described (El Hoss et al., 2021). Cells were stained with anti-GPA-BV421, anti-HbA-PE (Santa Cruz) and anti-HbF-APC (Miltenyi) antibodies for 30 minutes on ice and washed twice with FACS buffer before analysis.

2. Stainings on macrophages

a. Macrophage phenotype

Detached macrophages were first incubated with human FcR blocking reagent (Miltenyi) diluted 1/10 in FACS buffer (PBS with 2% of FBS and 1mM of EDTA) for 20 minutes at 4°C, to block nonspecific binding sites. After washing twice with FACS Buffer, macrophages were then stained with anti-CD14-PE (Invitrogen), anti-CD16-APC-Cy7 (BD Biosciences), anti-CD163-FITC (BD Biosciences), anti-CD169-APC (Invitrogen) and anti-CD206-BV421 (BD Biosciences), or anti-MerTK-APC and anti-CD106-PE-Cy7 (Invitrogen) for 30 minutes at 4°C. Cells were washed twice and immediately analyzed by flow cytometry.

b. Cell death

Detached macrophages were first stained with anti-GPA-FITC as described previously. To measure cell death, macrophages were washed once and stained with APC-conjugated Annexin V for 15 minutes at room temperature. Samples were then diluted with 200 µl of Annexin buffer. Propidium iodide was added to the samples just before measuring.

c. ROS production

To measure ROS production macrophages were incubated with 10µM of 2',7'-Dichlorofluorescin diacetate (DCFDA) (Sigma) for 30 minutes at 37°C. Cells were washed twice with PBS and then either stained with anti-GPA-PE-Cy7 and anti-CD169-APC or immediately analyzed by flow cytometry.

d. Lipid peroxidation

To measure lipid peroxidation macrophages were incubated with 2µM of C11-BODIPY 581/591 (C11-ODIPY) (Invitrogen) for 30 minutes at 37°C. Cells were washed twice with PBS and immediately analyzed by flow cytometry or by imaging flow cytometry.

G. Quantitative Reverse Transcriptase PCR

Total RNA was isolated using the RNeasy kit (Qiagen). cDNA was reverse transcribed using Moloney murine leukemia virus reverse transcriptase (MMLV-RT) (Promega), random hexamer (Invitrogen), dNTP (Invitrogen) and real-time PCR analyses were performed using Power Sybr Green PCR Master Mix (Invitrogen). The expression of all genes was evaluated by real-time quantitative PCR using specific primers (Table 1). Each experiment was carried out in triplicate, and average Ct was calculated with StepOne 2.1 software (Invitrogen). The results are normalized using the two housekeeping genes GAPDH and β-ACTIN.

Table 1: primer pairs used in qPCR.

Gene	Forward primer	Reverse primer
ACSL4	CCGACCTAAGGGAGTGATGA	CCTGCAGCCATAGGTAAAGC
β-ACTIN	CACCATTGGCAATGAGCGGTTC	CACCATTGGCAATGAGCGGTTC
BACH1	CACCGAAGGAGACAGTGAATCC	GCTGTTCTGGAGTAAGCTTGTGC
CD80	CTCTTGGTGCTGGCTGGTCTTT	GCCAGTAGATGCGAGTTTGTGC
CD86	CCATCAGCTTGTCTGTTTCATTCC	GCTGTAATCCAAGGAATGTGGTC
CD163	CCAGAAGGAACTTGTAGCCACAG	CAGGCACCAAGCGTTTTGAGCT
CD206	AGCCAACACCAGCTCCTCAAGA	CAAAACGCTCGCGCATTGTCCA
FTH1	TCCTACGTTTACCTGTCCATGT	GTTTGTGCAGTTCCAGTAGTGA
FTL	TACGAGCGTCTCCTGAAGATGC	GGTTCAGCTTTTTCTCCAGGGC
GAPDH	GTCTCCTCTGACTTCAACAGCG	ACCACCCTGTTGCTGTAGCCAA
GPX4	AGAGATCAAAGAGTTCGCCGC	TCTTCATCCACTTCCACAGCG
GSTM1	TGATGTCCTTGACCTCCACCGT	GCTGGACTTCATGTAGGCAGAG
HMOX1	CCAGGCAGAGAATGCTGAGTTC	AAGACTGGGCTCTCCTTGTTGC
IDO1	GCCTGATCCATAGAGTCTGGC	TGCATCCCAGAACTAGACGTGC
IL-6	CCAGGAGAAGATTCCAAAGATG	GGAAGGTTCAGGTTTGTTTTCT
IL-10	GGGGGTTGAGGTATCAGAGGTAA	GCTCCAAGAGAAAGGCATCTACA
NOS2	GACTTTCCAAGACACACTTCACC	TATCTCCTTTGTTACCGCTTCC
NQO1	TAGGGATTCACGGCATTGGT	GAATGACCGGTGCAAGGATC
NRF2	CAAAAGGAGCAAGAGAAAGCC	TCTGATTTGGGAATGTGGGC
PTGS2	CCCTTGGGTGTCAAAGGTAA	GCCCTCGCTTATGATCTGTC
SLC7A11	GCTGTGATATCCCTGGCATT	GGCGTCTTTAAAGTTCTGCG
TFR1	ACTTCTTCCGTGCTACTTCCAG	ACTCCACTCTCATGACACGATC
TGF-β	GACATCAAAAGATAACCACTC	TCTAGACAAGTTCAAGCAGA

TNF-α	AGGAGAAGAGGCTGAGGAACAAG	GAGGGAGAGAAGCAACTACAGACC

H. Western Blot

Macrophages were lysed in RIPA buffer containing protease inhibitor on the ice for 40 minutes and then centrifuged at 14,000*g* for 10 minutes to generate protein lysates. The protein concentration was determined using the BCA protein assay kit (Pierce Biotechnology). Proteins were mixed with Laemmli buffer 5X, and denaturated at 98°C for 5 minutes. These samples were separated using 10% SDS polyacrylamide gel and transferred onto nitrocellulose membranes. The membranes were then blocked with 5% of non-fat milk in TBS-T and immunostained with primary antibodies anti-GPx4 (Cell Signaling Technology, 52455, 1:1000), anti-NRF2 (Cell Signaling Technology, 12721, 1:1000), anti-FTH1 (Cell Signaling Technology, 4393, 1:1000), anti-ACSL4 (Santa Cruz, sc-271800, 1:1000), and anti-HMOX1 (Enzo Life Sciences, ADI-SPA-896, 1:1000) at 4°C overnight and detected using HRP-conjugated secondary antibodies.

I. ELISA Assay

Levels of interleukin IL-6, IL-10, TNF-α and TGF-β were measured in cell supernatants using an enzyme-linked immunosorbent assay technique (R&D systems) according to manufacturer's instructions.

J. Cytospin Preparation

For analysis of cell morphology, 2.10^5 cell in 100µL PBS were used to prepare cytospin preparations on non-coated slides, using the Cytospin 4 Shandon centrifuge (Thermofisher). The slides were stained with May-Grunwald-Giemsa (MGG) following manufacturer's instructions (Sigma). The slides were imaged using an Olympus BX41 (Zeiss) inverted microscope.

K. Mice and Procedures

All animal experiments were performed in compliance with the local ethics committee. We worked on male and female Townes-AA (HbAA), Townes-AS (HbAS) and Townes-SS (HbSS) mice on a 129/B6 mixed genetic background, obtained from the Jackson laboratory (strain #013071). Mouse genotypes were confirmed by PCR, using protocols established by the Jackson Laboratories. All mice were between 12 and 16 weeks-old at the time of the experiments.

Mouse BM cells were isolated from the femur and tibia using a method described previously (Grenier et al., 2021). The bone marrow suspensions were filtered through a 70µM-pore-size cell strainer and centrifuged for 400g for 8 minutes. Cells from the spleen were isolated by passing spleen tissue through 70µm filters. The isolated splenocytes were incubated in 5mL of RBC cell lysis buffer for 5 min at room temperature and washed twice with PBS. To measure lipid peroxidation, the samples were incubated with 2µM of C11-BODIPY (Invitrogen) for 30 minutes at 37°C. Cells were washed twice with PBS and

were then incubated with mouse FcR blocking reagent (Miltenyi) diluted 1/10 in FACS buffer for 20 minutes at 4°C, to block nonspecific binding sites. After washing twice with FACS Buffer, samples were stained using anti-F4/80 BV421 for 30 minutes at 4°C. Cells were washed twice and immediately analyzed by flow cytometry.

L. Statistical Analysis

Statistical analyses were performed using GraphPad PRISM 7 (Graphpad Software Inc.,San Diega, California, USA). Values on graphs are depicted as mean ± standard deviation (SD). Differences between groups were assessed with Mann-Whitney test, unpaired Student t test, or one-way analysis of variance (ANOVA) with post hoc test, as indicated in the legend of the figures. Statistical significance threshold was set at a P value of 0.05.

CONCLUSION AND PERSPECTIVES

Our work demonstrated the occurrence of ineffective erythropoiesis in SCD and revealed a molecular mechanism involving HSP70 cytoplasmic sequestration, triggered by its interaction with HbS polymers. An important finding of our study is the protective role of HbF during terminal erythroid differentiation, extending its well-known protective role in the circulation to the very early stages of the RBC production process. Thus, we may expect that therapies that induce HbF expression may also improve ineffective erythropoiesis by rescuing differentiating erythroblasts from cell death. Future studies should investigate the impact of such treatments on terminal erythropoiesis in SCD by focusing on the apoptosis and proliferation rates of erythroblasts as primary readouts. Such studies can be conducted *in vivo* using the Townes mouse model and *in vitro* with the condition of applying partial hypoxia during the terminal differentiation phase to mimic the BM environment. Furthermore, we may also expect that therapies targeting HbS polymerization, to inhibit sickling and increase the lifespan of RBCs in the circulation, may also have a beneficial effect during erythropoiesis. For instance, we think that the significant hemoglobin increase induced by Voxelotor (GBT440), a molecule that increases hemoglobin affinity for oxygen, in the phase 3 clinical trial (Vichinsky et al, NEJM 2019) may be partly attributable to improved erythropoiesis and a better yield of RBC production. Mitapivat (AG348) is a pyruvate kinase activator that increases hemoglobin affinity to oxygen by increasing ATP levels and decreasing those of 2,3-diphosphoglycerate (2,3 DPG). Like Voxelotor, Mitapivat was shown to rise hemoglobin levels in SCD patients (Xu et el, Blood 2022) and we may also expect a positive effect on terminal erythropoiesis. Studies focusing on the effect of these molecules during erythroid differentiation are being designed in our laboratory.

Our research on patients with high levels of circulating erythroblasts reveals a distinct profile in this patient population, characterized by accelerated terminal maturation *in vitro*, low HbF levels, and the presence of all stages of terminal maturation in the circulation. Further investigations are necessary to decipher the functional and biological relevance of these results, including whether these properties are transient or specific to some patients. Such investigations will include a whole genome sequencing approach to have a comprehensive overview of the genetic landscape of these patients, which may reveal contributing factors involved in HbF gene expression. This work underscores the heterogeneity in erythropoiesis among SCD patients and may help understand the clinical significance of circulating erythroblasts in this pathology.

In the second part of this thesis, we compared two *ex vivo* erythropoiesis protocols and highlighted their distinctions. Although the defects we have revealed take place in the terminal stage of differentiation, one would expect the earlier stage of differentiation to be impacted by the inflammatory environment of the bone marrow in SCD. On the other hand, we observed enucleation defects in SCD patients compared to control individuals. Our comparative study gives valuable

information on which protocol to use to address specific dysfunctions during the differentiation process.

In the final part of this thesis, we demonstrated that EBI macrophages undergo ferroptosis following increased phagocytosis of erythroblasts, with a shift to a pro-inflammatory phenotype of the surviving macrophages, potentially impacting their function as a support for erythroid maturation; this may in turn worsen ineffective erythropoiesis and contribute to inflammation of the bone marrow environment. While the scope of this research focused on the central macrophage of the erythroblastic island, as it is the closest cell to the erythroblasts, other cell populations may also be affected by ineffective erythropoiesis in SCD. Therefore, a comprehensive examination of if and how ineffective erythropoiesis affects additional components of the bone marrow microenvironment, including osteoblasts and endothelial cells, would be of interest to gain a deeper understanding of SCD pathophysiology. Furthermore, while our work focused on terminal erythroid differentiation, it is worth noting that ongoing research in our laboratory aims to elucidate the potential impact of SCD on HSCs and erythroid progenitors.

In summary, our study demonstrates the occurrence of ineffective erythropoiesis in SCD, offering insights into its underlying mechanism and potential therapeutic avenues. Furthermore, it shows evidence of cellular abnormalities within the erythroblastic island associated with a perturbed inflammatory status of resident macrophages, paving the way to future studies focusing on the bone marrow environment and hematopoiesis in this pathology.

BIBIOGRAPHY

REFERENCES

Abraham, A. A., & Tisdale, J. F. (2021). Gene therapy for sickle cell disease: moving from the bench to the bedside. *Blood*, *138*(11), 932-941. https://doi.org/10.1182/blood.2019003776

Adedoyin, O., Boddu, R., Traylor, A., Lever, J. M., Bolisetty, S., George, J. F., & Agarwal, A. (2018). Heme oxygenase-1 mitigates ferroptosis in renal proximal tubule cells. *Am J Physiol Renal Physiol*, *314*(5), F702-f714. https://doi.org/10.1152/ajprenal.00044.2017

Agmon, E., Solon, J., Bassereau, P., & Stockwell, B. R. (2018). Modeling the effects of lipid peroxidation during ferroptosis on membrane properties. *Sci Rep*, *8*(1), 5155. https://doi.org/10.1038/s41598-018-23408-0

Ahl, P. J., Hopkins, R. A., Xiang, W. W., Au, B., Kaliaperumal, N., Fairhurst, A.-M., & Connolly, J. E. (2020). Met-Flow, a strategy for single-cell metabolic analysis highlights dynamic changes in immune subpopulations. *Communications Biology*, *3*(1), 305. https://doi.org/10.1038/s42003-020-1027-9

Akinsheye, I., Alsultan, A., Solovieff, N., Ngo, D., Baldwin, C. T., Sebastiani, P., Chui, D. H., & Steinberg, M. H. (2011). Fetal hemoglobin in sickle cell anemia. *Blood*, *118*(1), 19-27. https://doi.org/10.1182/blood-2011-03-325258

Al-Ali, A. K. (2002). Pyridine nucleotide redox potential in erythrocytes of saudi subjects with sickle cell disease. *Acta Haematol*, *108*(1), 19-22. https://doi.org/10.1159/000063062

Alexander, K. A., Chang, M. K., Maylin, E. R., Kohler, T., Muller, R., Wu, A. C., Van Rooijen, N., Sweet, M. J., Hume, D. A., Raggatt, L. J., & Pettit, A. R. (2011). Osteal macrophages promote in vivo intramembranous bone healing in a mouse tibial injury model. *J Bone Miner Res*, *26*(7), 1517-1532. https://doi.org/10.1002/jbmr.354

Alexander, K. A., Raggatt, L. J., Millard, S., Batoon, L., Chiu-Ku Wu, A., Chang, M. K., Hume, D. A., & Pettit, A. R. (2017). Resting and injury-induced inflamed periosteum contain multiple macrophage subsets that are located at sites of bone growth and regeneration. *Immunol Cell Biol*, *95*(1), 7-16. https://doi.org/10.1038/icb.2016.74

Allen, T. D., & Dexter, T. M. (1982). Ultrastructural aspects of erythropoietic differentiation in long-term bone marrow culture. *Differentiation*, *21*(2), 86-94. https://doi.org/10.1111/j.1432-0436.1982.tb01201.x

Allenby, M. C., Panoskaltsis, N., Tahlawi, A., Dos Santos, S. B., & Mantalaris, A. (2019). Dynamic human erythropoiesis in a three-dimensional perfusion bone marrow biomimicry. *Biomaterials*, *188*, 24-37. https://doi.org/10.1016/j.biomaterials.2018.08.020

Alvarez-Argote, J., Dlugi, T. A., Sundararajan, T., Kleynerman, A., Faber, M. L., McKillop, W. M., & Medin, J. A. (2023). Pathophysiological characterization of the Townes mouse model for sickle cell disease. *Translational Research*, *254*, 77-91. https://doi.org/https://doi.org/10.1016/j.trsl.2022.10.007

Amid, A., Chen, S., Brien, W., Kirby-Allen, M., & Odame, I. (2016). Optimizing chronic transfusion therapy for survivors of hemoglobin Barts hydrops fetalis. *Blood*, *127*(9), 1208-1211. https://doi.org/10.1182/blood-2015-10-673889

Angelillo-Scherrer, A., Burnier, L., Lambrechts, D., Fish, R. J., Tjwa, M., Plaisance, S., Sugamele, R., DeMol, M., Martinez-Soria, E., Maxwell, P. H., Lemke, G., Goff, S. P., Matsushima, G. K., Earp, H. S., Chanson, M., Collen, D., Izui, S., Schapira, M., Conway, E. M., & Carmeliet, P. (2008). Role of Gas6 in erythropoiesis and anemia in mice. *J Clin Invest*, *118*(2), 583-596. https://doi.org/10.1172/jci30375

Angelucci, E., Bai, H., Centis, F., Bafti, M. S., Lucarelli, G., Ma, L., & Schrier, S. (2002). Enhanced macrophagic attack on beta-thalassemia major erythroid precursors. *Haematologica*, *87*(6), 578-583. https://www.ncbi.nlm.nih.gov/pubmed/12031913

Ansó, E., Weinberg, S. E., Diebold, L. P., Thompson, B. J., Malinge, S., Schumacker, P. T., Liu, X., Zhang, Y., Shao, Z., Steadman, M., Marsh, K. M., Xu, J., Crispino, J. D., & Chandel, N. S. (2017). The mitochondrial respiratory chain is essential for haematopoietic stem cell function. *Nat Cell Biol*, *19*(6), 614-625. https://doi.org/10.1038/ncb3529

Antoniani, C., Meneghini, V., Lattanzi, A., Felix, T., Romano, O., Magrin, E., Weber, L., Pavani, G., El Hoss, S., Kurita, R., Nakamura, Y., Cradick, T. J., Lundberg, A. S., Porteus, M., Amendola, M., El Nemer, W., Cavazzana, M., Mavilio, F., & Miccio, A. (2018). Induction of fetal hemoglobin synthesis by CRISPR/Cas9-mediated editing of the human β-globin locus. *Blood*, *131*(17), 1960-1973. https://doi.org/10.1182/blood-2017-10-811505

Anzalone, A. V., Randolph, P. B., Davis, J. R., Sousa, A. A., Koblan, L. W., Levy, J. M., Chen, P. J., Wilson, C., Newby, G. A., Raguram, A., & Liu, D. R. (2019). Search-and-replace genome editing without double-strand breaks or donor DNA. *Nature*, *576*(7785), 149-157. https://doi.org/10.1038/s41586-019-1711-4

Argüello, R. J., Combes, A. J., Char, R., Gigan, J. P., Baaziz, A. I., Bousiquot, E., Camosseto, V., Samad, B., Tsui, J., Yan, P., Boissonneau, S., Figarella-Branger, D., Gatti, E., Tabouret, E., Krummel, M. F., & Pierre, P. (2020). SCENITH: A Flow Cytometry-Based Method to Functionally Profile Energy Metabolism with Single-Cell Resolution. *Cell Metab*, *32*(6), 1063-1075.e1067. https://doi.org/10.1016/j.cmet.2020.11.007

Arlet, J. B., Dussiot, M., Moura, I. C., Hermine, O., & Courtois, G. (2016). Novel players in β-thalassemia dyserythropoiesis and new therapeutic strategies. *Curr Opin Hematol*, *23*(3), 181-188. https://doi.org/10.1097/moh.0000000000000231

Arlet, J. B., Ribeil, J. A., Guillem, F., Negre, O., Hazoume, A., Marcion, G., Beuzard, Y., Dussiot, M., Moura, I. C., Demarest, S., de Beauchêne, I. C., Belaid-Choucair, Z., Sevin, M., Maciel, T. T., Auclair, C., Leboulch, P., Chretien, S., Tchertanov, L., Baudin-Creuza, V., . . . Courtois, G. (2014). HSP70 sequestration by free α-globin promotes ineffective erythropoiesis in β-thalassaemia. *Nature*, *514*(7521), 242-246. https://doi.org/10.1038/nature13614

Arumugam, P. I., Mullins, E. S., Shanmukhappa, S. K., Monia, B. P., Loberg, A., Shaw, M. A., Rizvi, T., Wansapura, J., Degen, J. L., & Malik, P. (2015). Genetic diminution of circulating prothrombin ameliorates multiorgan pathologies in sickle cell disease mice. *Blood*, *126*(15), 1844-1855. https://doi.org/10.1182/blood-2015-01-625707

Ataga, K. I., Kutlar, A., Kanter, J., Liles, D., Cancado, R., Friedrisch, J., Guthrie, T. H., Knight-Madden, J., Alvarez, O. A., Gordeuk, V. R., Gualandro, S., Colella, M. P., Smith, W. R., Rollins, S. A., Stocker, J. W., & Rother, R. P. (2017). Crizanlizumab for the Prevention of Pain Crises in Sickle Cell Disease. *N Engl J Med*, *376*(5), 429-439. https://doi.org/10.1056/NEJMoa1611770

Ataga, K. I., & Orringer, E. P. (2000). Bone marrow necrosis in sickle cell disease: a description of three cases and a review of the literature. *Am J Med Sci*, *320*(5), 342-347. https://doi.org/10.1097/00000441-200011000-00009

Baek, E. J., Kim, H. S., Kim, S., Jin, H., Choi, T. Y., & Kim, H. O. (2008). In vitro clinical-grade generation of red blood cells from human umbilical cord blood CD34+ cells. *Transfusion*, *48*(10), 2235-2245. https://doi.org/10.1111/j.1537-2995.2008.01828.x

Bai, J., Fan, F., Gao, C., Li, S., Li, W., Wei, T., Cheng, S., Yu, J., Zheng, C., Zhao, J., Zou, L., Feng, L., Yi, J., & Qin, H. (2023). CD169-CD43 interaction is involved in erythroblastic island formation and erythroid differentiation. *Haematologica*, *108*(8), 2205-2217. https://doi.org/10.3324/haematol.2022.282192

Bain, B. J. (2021). *Blood cells: a practical guide*. John Wiley & Sons.

Ballantine, J. D., Kwon, S., & Liem, R. I. (2019). Nucleated Red Blood Cells in Children With Sickle Cell Disease Hospitalized for Pain. *J Pediatr Hematol Oncol*, *41*(8), e487-e492. https://doi.org/10.1097/mph.0000000000001467

Bannai, S., Tsukeda, H., & Okumura, H. (1977). Effect of antioxidants on cultured human diploid fibroblasts exposed to cystine-free medium. *Biochem Biophys Res Commun*, *74*(4), 1582-1588. https://doi.org/10.1016/0006-291x(77)90623-4

Barabino, G. A., Platt, M. O., & Kaul, D. K. (2010). Sickle cell biomechanics. *Annu Rev Biomed Eng*, *12*, 345-367. https://doi.org/10.1146/annurev-bioeng-070909-105339

Bartolucci, P., Chaar, V., Picot, J., Bachir, D., Habibi, A., Fauroux, C., Galactéros, F., Colin, Y., Le Van Kim, C., & El Nemer, W. (2010). Decreased sickle red blood cell adhesion to laminin by hydroxyurea is associated with inhibition of Lu/BCAM protein phosphorylation. *Blood*, *116*(12), 2152-2159. https://doi.org/10.1182/blood-2009-12-257444

Batoon, L., Millard, S. M., Wullschleger, M. E., Preda, C., Wu, A. C., Kaur, S., Tseng, H. W., Hume, D. A., Levesque, J. P., Raggatt, L. J., & Pettit, A. R. (2019). CD169(+) macrophages are critical for osteoblast maintenance and promote intramembranous and endochondral ossification during bone repair. *Biomaterials*, *196*, 51-66. https://doi.org/10.1016/j.biomaterials.2017.10.033

Bedoui, S., Herold, M. J., & Strasser, A. (2020). Emerging connectivity of programmed cell death pathways and its physiological implications. *Nat Rev Mol Cell Biol*, *21*(11), 678-695. https://doi.org/10.1038/s41580-020-0270-8

Belcher, J. D., Chen, C., Nguyen, J., Milbauer, L., Abdulla, F., Alayash, A. I., Smith, A., Nath, K. A., Hebbel, R. P., & Vercellotti, G. M. (2014). Heme triggers TLR4 signaling leading to endothelial cell activation and vaso-occlusion in murine sickle cell disease. *Blood*, *123*(3), 377-390. https://doi.org/https://doi.org/10.1182/blood-2013-04-495887

Bell, A. J., Satchwell, T. J., Heesom, K. J., Hawley, B. R., Kupzig, S., Hazell, M., Mushens, R., Herman, A., & Toye, A. M. (2013). Protein distribution during human erythroblast enucleation in vitro. *PLoS One*, *8*(4), e60300. https://doi.org/10.1371/journal.pone.0060300

Bellairs, R. (1961). Cell death in chick embryos as studied by electron microscopy. *J Anat*, *95*(Pt 1), 54-60.53.

Bender, M. A., & Carlberg, K. (1993). Sickle Cell Disease. In M. P. Adam, G. M. Mirzaa, R. A. Pagon, S. E. Wallace, L. J. H. Bean, K. W. Gripp, & A. Amemiya (Eds.), *GeneReviews(®)*. University of Washington, Seattle

Bennett, L. F., Liao, C., & Paulson, R. F. (2018). Stress Erythropoiesis Model Systems. *Methods Mol Biol*, *1698*, 91-102. https://doi.org/10.1007/978-1-4939-7428-3_5

Bennett, L. F., Liao, C., Quickel, M. D., Yeoh, B. S., Vijay-Kumar, M., Hankey-Giblin, P., Prabhu, K. S., & Paulson, R. F. (2019). Inflammation induces stress erythropoiesis through heme-dependent activation of SPI-C. *Sci Signal*, *12*(598). https://doi.org/10.1126/scisignal.aap7336

Bennewitz, M. F., Jimenez, M. A., Vats, R., Tutuncuoglu, E., Jonassaint, J., Kato, G. J., Gladwin, M. T., & Sundd, P. (2017). Lung vaso-occlusion in sickle cell disease mediated by arteriolar neutrophil-platelet microemboli. *JCI Insight*, *2*(1), e89761. https://doi.org/10.1172/jci.insight.89761

Benz, C., Copley, M. R., Kent, D. G., Wohrer, S., Cortes, A., Aghaeepour, N., Ma, E., Mader, H., Rowe, K., Day, C., Treloar, D., Brinkman, R. R., & Eaves, C. J. (2012). Hematopoietic stem cell subtypes expand differentially during development and display distinct lymphopoietic programs. *Cell Stem Cell*, *10*(3), 273-283. https://doi.org/10.1016/j.stem.2012.02.007

Bernaudin, F., Socie, G., Kuentz, M., Chevret, S., Duval, M., Bertrand, Y., Vannier, J. P., Yakouben, K., Thuret, I., Bordigoni, P., Fischer, A., Lutz, P., Stephan, J. L., Dhedin, N., Plouvier, E., Margueritte, G., Bories, D., Verlhac, S., Esperou, H., . . . Gluckman, E. (2007). Long-term results of related myeloablative stem-cell transplantation to cure sickle cell disease. *Blood*, *110*(7), 2749-2756. https://doi.org/10.1182/blood-2007-03-079665

Berry, D. L., & Baehrecke, E. H. (2007). Growth arrest and autophagy are required for salivary gland cell degradation in Drosophila. *Cell*, *131*(6), 1137-1148. https://doi.org/10.1016/j.cell.2007.10.048

Bersuker, K., Hendricks, J. M., Li, Z., Magtanong, L., Ford, B., Tang, P. H., Roberts, M. A., Tong, B., Maimone, T. J., Zoncu, R., Bassik, M. C., Nomura, D. K., Dixon, S. J., & Olzmann, J. A. (2019). The CoQ oxidoreductase FSP1 acts parallel to GPX4 to inhibit ferroptosis. *Nature*, *575*(7784), 688-692. https://doi.org/10.1038/s41586-019-1705-2

Bessis, M., & Breton-Gorius, J. (1962). [Differences between normal and pathologic sideroblasts. Study with the electron microscope]. *Nouv Rev Fr Hematol*, *2*, 629-634.

Blouin, M. J., De Paepe, M. E., & Trudel, M. (1999). Altered hematopoiesis in murine sickle cell disease. *Blood*, *94*(4), 1451-1459. https://www.ncbi.nlm.nih.gov/pubmed/10438733

Boehm, D., Mazurier, C., Giarratana, M. C., Darghouth, D., Faussat, A. M., Harmand, L., & Douay, L. (2013). Caspase-3 is involved in the signalling in erythroid differentiation by targeting late progenitors. *PLoS One*, *8*(5), e62303. https://doi.org/10.1371/journal.pone.0062303

Bohmer, R. M. (2004). IL-3-dependent early erythropoiesis is stimulated by autocrine transforming growth factor beta. *Stem Cells*, *22*(2), 216-224. https://doi.org/10.1634/stemcells.22-2-216

Bolaños-Meade, J., Fuchs, E. J., Luznik, L., Lanzkron, S. M., Gamper, C. J., Jones, R. J., & Brodsky, R. A. (2012). HLA-haploidentical bone marrow transplantation with posttransplant cyclophosphamide expands the donor pool for patients with sickle cell disease. *Blood*, *120*(22), 4285-4291. https://doi.org/10.1182/blood-2012-07-438408

Bonig, H., Priestley, G. V., & Papayannopoulou, T. (2006). Hierarchy of molecular-pathway usage in bone marrow homing and its shift by cytokines. *Blood*, *107*(1), 79-86. https://doi.org/10.1182/blood-2005-05-2023

Borg, J., Papadopoulos, P., Georgitsi, M., Gutiérrez, L., Grech, G., Fanis, P., Phylactides, M., Verkerk, A. J., van der Spek, P. J., Scerri, C. A., Cassar, W., Galdies, R., van Ijcken, W., Ozgür, Z., Gillemans, N., Hou, J., Bugeja, M., Grosveld, F. G., von Lindern, M., . . . Philipsen, S. (2010). Haploinsufficiency for the erythroid transcription factor KLF1 causes hereditary persistence of fetal hemoglobin. *Nat Genet*, *42*(9), 801-805. https://doi.org/10.1038/ng.630

Boyer, S. H., Belding, T. K., Margolet, L., & Noyes, A. N. (1975). Fetal hemoglobin restriction to a few erythrocytes (F cells) in normal human adults. *Science*, *188*(4186), 361-363. https://doi.org/10.1126/science.804182

Boyer, S. H., Belding, T. K., Margolte, L., Noyes, A. N., Burke, P. J., & Bell, W. R. (1975). Variations in the frequency of fetal hemoglobin-bearing erythrocytes (F-cells) in well adults, pregnant women, and adult leukemics. *Johns Hopkins Med J*, *137*(3), 105-115.

Boyer, S. H., Margolet, L., Boyer, M. L., Huisman, T. H., Schroeder, W. A., Wood, W. G., Weatherall, D. J., Clegg, J. B., & Cartner, R. (1977). Inheritance of F cell frequency in heterocellular hereditary persistence of fetal hemoglobin: an example of allelic exclusion. *Am J Hum Genet*, *29*(3), 256-271.

Bozza, M. T., & Jeney, V. (2020). Pro-inflammatory Actions of Heme and Other Hemoglobin-Derived DAMPs. *Front Immunol*, *11*, 1323. https://doi.org/10.3389/fimmu.2020.01323

Bradford, C., Miodownik, H., Thomas, M., Ogu, U. O., & Minniti, C. P. (2022). Patient-focused inquiry on hydroxyurea therapy adherence and reasons for discontinuation in adults with sickle cell disease. *Am J Hematol*, *97*(3), E93-e95. https://doi.org/10.1002/ajh.26438

Brigelius-Flohé, R., & Maiorino, M. (2013). Glutathione peroxidases. *Biochim Biophys Acta*, *1830*(5), 3289-3303. https://doi.org/10.1016/j.bbagen.2012.11.020

Brinkman, E. K., Chen, T., Amendola, M., & van Steensel, B. (2014). Easy quantitative assessment of genome editing by sequence trace decomposition. *Nucleic Acids Res*, *42*(22), e168. https://doi.org/10.1093/nar/gku936

Brittenham, G. M., Schechter, A. N., & Noguchi, C. T. (1985). Hemoglobin S polymerization: primary determinant of the hemolytic and clinical severity of the sickling syndromes. *Blood*, *65*(1), 183-189.

Broudy, V. C. (1997). Stem cell factor and hematopoiesis. *Blood*, *90*(4), 1345-1364.

Brousse, V., Makani, J., & Rees, D. C. (2014). Management of sickle cell disease in the community. *Bmj*, *348*, g1765. https://doi.org/10.1136/bmj.g1765

Browne, P., Shalev, O., & Hebbel, R. P. (1998). The molecular pathobiology of cell membrane iron: the sickle red cell as a model. *Free Radic Biol Med*, *24*(6), 1040-1048. https://doi.org/10.1016/s0891-5849(97)00391-2

Broxmeyer, H. E. (2013). Erythropoietin: multiple targets, actions, and modifying influences for biological and clinical consideration. *J Exp Med*, *210*(2), 205-208. https://doi.org/10.1084/jem.20122760

Brunson, A., Keegan, T. H. M., Bang, H., Mahajan, A., Paulukonis, S., & Wun, T. (2017). Increased risk of leukemia among sickle cell disease patients in California. *Blood*, *130*(13), 1597-1599. https://doi.org/10.1182/blood-2017-05-783233

Bunn, H. F. (1997). Pathogenesis and treatment of sickle cell disease. *N Engl J Med*, *337*(11), 762-769. https://doi.org/10.1056/nejm199709113371107

Burch, J. S., Marcero, J. R., Maschek, J. A., Cox, J. E., Jackson, L. K., Medlock, A. E., Phillips, J. D., & Dailey, H. A., Jr. (2018). Glutamine via α-ketoglutarate dehydrogenase provides succinyl-CoA for heme synthesis during erythropoiesis. *Blood*, *132*(10), 987-998. https://doi.org/10.1182/blood-2018-01-829036

Cabantchik, Z. I. (2014). Labile iron in cells and body fluids: physiology, pathology, and pharmacology. *Front Pharmacol*, *5*, 45. https://doi.org/10.3389/fphar.2014.00045

Cao, J. Y., Poddar, A., Magtanong, L., Lumb, J. H., Mileur, T. R., Reid, M. A., Dovey, C. M., Wang, J., Locasale, J. W., Stone, E., Cole, S. P. C., Carette, J. E., & Dixon, S. J. (2019). A Genome-wide Haploid Genetic Screen Identifies Regulators of Glutathione Abundance and Ferroptosis Sensitivity. *Cell Rep*, *26*(6), 1544-1556.e1548. https://doi.org/10.1016/j.celrep.2019.01.043

Cao, W., Fan, W., Wang, F., Zhang, Y., Wu, G., Shi, X., Shi, J. x., Gao, F., Yan, M., Guo, R., Li, Y., Li, W., Du, C., & Jiang, Z. (2022). GM-CSF impairs erythropoiesis by disrupting erythroblastic island formation via macrophages. *Journal of Translational Medicine*, *20*(1), 11. https://doi.org/10.1186/s12967-021-03214-5

Capellera-Garcia, S., Pulecio, J., Dhulipala, K., Siva, K., Rayon-Estrada, V., Singbrant, S., Sommarin, M. N., Walkley, C. R., Soneji, S., Karlsson, G., Raya, Á., Sankaran, V. G., & Flygare, J. (2016). Defining the Minimal Factors Required for Erythropoiesis through Direct Lineage Conversion. *Cell Rep*, *15*(11), 2550-2562. https://doi.org/10.1016/j.celrep.2016.05.027

Catala, A., Youssef, L. A., Reisz, J. A., Dzieciatkowska, M., Powers, N. E., Marchetti, C., Karafin, M., Zimring, J. C., Hudson, K. E., Hansen, K. C., Spitalnik, S. L., & D'Alessandro, A. (2020). Metabolic Reprogramming of Mouse Bone Marrow Derived Macrophages Following Erythrophagocytosis. *Front Physiol*, *11*, 396. https://doi.org/10.3389/fphys.2020.00396

Cavazzana-Calvo, M., Payen, E., Negre, O., Wang, G., Hehir, K., Fusil, F., Down, J., Denaro, M., Brady, T., Westerman, K., Cavallesco, R., Gillet-Legrand, B., Caccavelli, L., Sgarra, R., Maouche-Chrétien, L., Bernaudin, F., Girot, R., Dorazio, R., Mulder, G.-J., . . . Leboulch, P. (2010). Transfusion independence and HMGA2 activation after gene therapy of human β-thalassaemia. *Nature*, *467*(7313), 318-322. https://doi.org/10.1038/nature09328

Cenariu, D., Iluta, S., Zimta, A. A., Petrushev, B., Qian, L., Dirzu, N., Tomuleasa, C., Bumbea, H., & Zaharie, F. (2021). Extramedullary Hematopoiesis of the Liver and Spleen. *J Clin Med*, *10*(24). https://doi.org/10.3390/jcm10245831

Centis, F., Tabellini, L., Lucarelli, G., Buffi, O., Tonucci, P., Persini, B., Annibali, M., Emiliani, R., Iliescu, A., Rapa, S., Rossi, R., Ma, L., Angelucci, E., & Schrier, S. L. (2000). The importance of erythroid expansion in determining the extent of apoptosis in erythroid precursors in patients with β-thalassemia major. *Blood*, *96*(10), 3624-3629. https://doi.org/https://doi.org/10.1182/blood.V96.10.3624

Chaar, V., Laurance, S., Lapoumeroulie, C., Cochet, S., De Grandis, M., Colin, Y., Elion, J., Le Van Kim, C., & El Nemer, W. (2014). Hydroxycarbamide decreases sickle reticulocyte adhesion to resting endothelium by inhibiting endothelial lutheran/basal cell adhesion molecule (Lu/BCAM) through phosphodiesterase 4A activation. *J Biol Chem*, *289*(16), 11512-11521. https://doi.org/10.1074/jbc.M113.506121

Chang, M. K., Raggatt, L. J., Alexander, K. A., Kuliwaba, J. S., Fazzalari, N. L., Schroder, K., Maylin, E. R., Ripoll, V. M., Hume, D. A., & Pettit, A. R. (2008). Osteal tissue macrophages are intercalated throughout human and mouse bone lining tissues and regulate osteoblast function in vitro and in vivo. *J Immunol*, *181*(2), 1232-1244. https://doi.org/10.4049/jimmunol.181.2.1232

Charache, S., Barton, F. B., Moore, R. D., Terrin, M. L., Steinberg, M. H., Dover, G. J., Ballas, S. K., McMahon, R. P., Castro, O., & Orringer, E. P. (1996). Hydroxyurea and sickle cell anemia. Clinical utility of a myelosuppressive "switching" agent. The Multicenter Study of Hydroxyurea in Sickle Cell Anemia. *Medicine (Baltimore)*, *75*(6), 300-326. https://doi.org/10.1097/00005792-199611000-00002

Chasis, J. A., & Mohandas, N. (2008). Erythroblastic islands: niches for erythropoiesis. *Blood*, *112*(3), 470-478. https://doi.org/10.1182/blood-2008-03-077883

Chasis, J. A., & Schrier, S. L. (1989). Membrane deformability and the capacity for shape change in the erythrocyte. *Blood*, *74*(7), 2562-2568.

Chen , C., Liu , Y., Liu , R., Ikenoue , T., Guan , K.-L., Liu , Y., & Zheng , P. (2008). TSC–mTOR maintains quiescence and function of hematopoietic stem cells by repressing mitochondrial biogenesis and reactive oxygen species. *Journal of Experimental Medicine*, *205*(10), 2397-2408. https://doi.org/10.1084/jem.20081297

Chen, D., Tavana, O., Chu, B., Erber, L., Chen, Y., Baer, R., & Gu, W. (2017). NRF2 Is a Major Target of ARF in p53-Independent Tumor Suppression. *Mol Cell*, *68*(1), 224-232.e224. https://doi.org/10.1016/j.molcel.2017.09.009

Chen, K., Jiao, Y., Liu, L., Huang, M., He, C., He, W., Hou, J., Yang, M., Luo, X., & Li, C. (2020). Communications Between Bone Marrow Macrophages and Bone Cells in Bone Remodeling. *Frontiers in Cell and Developmental Biology*, *8*. https://doi.org/10.3389/fcell.2020.598263

Chen, X., Yu, C., Kang, R., & Tang, D. (2020). Iron Metabolism in Ferroptosis. *Front Cell Dev Biol*, *8*, 590226. https://doi.org/10.3389/fcell.2020.590226

Cheng, Y., Wu, W., Kumar, S. A., Yu, D., Deng, W., Tripic, T., King, D. C., Chen, K. B., Zhang, Y., Drautz, D., Giardine, B., Schuster, S. C., Miller, W., Chiaromonte, F., Zhang, Y., Blobel, G. A., Weiss, M. J., & Hardison, R. C. (2009). Erythroid GATA1 function revealed by genome-wide analysis of transcription factor occupancy, histone modifications, and mRNA expression. *Genome Res*, *19*(12), 2172-2184. https://doi.org/10.1101/gr.098921.109

Cheng, Z., & Li, Y. (2007). What is responsible for the initiating chemistry of iron-mediated lipid peroxidation: an update. *Chem Rev*, *107*(3), 748-766. https://doi.org/10.1021/cr040077w

Chow, A., Huggins, M., Ahmed, J., Hashimoto, D., Lucas, D., Kunisaki, Y., Pinho, S., Leboeuf, M., Noizat, C., van Rooijen, N., Tanaka, M., Zhao, Z. J., Bergman, A., Merad, M., & Frenette, P. S. (2013a). CD169(+) macrophages provide a niche promoting erythropoiesis under homeostasis and stress. *Nat Med*, *19*(4), 429-436. https://doi.org/10.1038/nm.3057

Chow, A., Huggins, M., Ahmed, J., Hashimoto, D., Lucas, D., Kunisaki, Y., Pinho, S., Leboeuf, M., Noizat, C., van Rooijen, N., Tanaka, M., Zhao, Z. J., Bergman, A., Merad, M., & Frenette, P. S. (2013b). CD169^{+} macrophages provide a niche promoting erythropoiesis under homeostasis and stress. *Nat Med*, *19*(4), 429-436. https://doi.org/10.1038/nm.3057

Chow, A., Lucas, D., Hidalgo, A., Mendez-Ferrer, S., Hashimoto, D., Scheiermann, C., Battista, M., Leboeuf, M., Prophete, C., van Rooijen, N., Tanaka, M., Merad, M., & Frenette, P. S. (2011). Bone marrow CD169+ macrophages promote the retention of hematopoietic stem and progenitor cells in the mesenchymal stem cell niche. *J Exp Med*, *208*(2), 261-271. https://doi.org/10.1084/jem.20101688

Chu, B., Kon, N., Chen, D., Li, T., Liu, T., Jiang, L., Song, S., Tavana, O., & Gu, W. (2019). ALOX12 is required for p53-mediated tumour suppression through a distinct ferroptosis pathway. *Nature Cell Biology*, *21*(5), 579-591. https://doi.org/10.1038/s41556-019-0305-6

Chung, J., Bauer, D. E., Ghamari, A., Nizzi, C. P., Deck, K. M., Kingsley, P. D., Yien, Y. Y., Huston, N. C., Chen, C., Schultz, I. J., Dalton, A. J., Wittig, J. G., Palis, J., Orkin, S. H., Lodish, H. F., Eisenstein, R. S., Cantor, A. B., & Paw, B. H. (2015). The mTORC1/4E-BP pathway coordinates hemoglobin production with L-leucine availability. *Sci Signal*, *8*(372), ra34. https://doi.org/10.1126/scisignal.aaa5903

Ciurea, S. O., & Andersson, B. S. (2009). Busulfan in Hematopoietic Stem Cell Transplantation. *Biology of Blood and Marrow Transplantation*, *15*(5), 523-536. https://doi.org/https://doi.org/10.1016/j.bbmt.2008.12.489

Cohnheim, J. (1889). *Lectures on General Pathology*. New Sydenham Society.

Cokic, V. P., Smith, R. D., Beleslin-Cokic, B. B., Njoroge, J. M., Miller, J. L., Gladwin, M. T., & Schechter, A. N. (2003). Hydroxyurea induces fetal hemoglobin by the nitric oxide-dependent activation of soluble guanylyl cyclase. *J Clin Invest*, *111*(2), 231-239. https://doi.org/10.1172/jci16672

Constantino, B. T., & Cogionis, B. (2000). Nucleated RBCs—significance in the peripheral blood film. *Laboratory Medicine*, *31*(4), 223-229.

Couque, N., Girard, D., Ducrocq, R., Boizeau, P., Haouari, Z., Missud, F., Holvoet, L., Ithier, G., Belloy, M., Odièvre, M. H., Benemou, M., Benhaim, P., Retali, B., Bensaid, P., Monier, B., Brousse, V., Amira, R., Orzechowski, C., Lesprit, E., . . . Benkerrou, M. (2016). Improvement of medical care in a cohort of newborns with sickle-cell disease in North Paris: impact of national guidelines. *Br J Haematol*, *173*(6), 927-937. https://doi.org/10.1111/bjh.14015

Crocker, P. R., Werb, Z., Gordon, S., & Bainton, D. F. (1990). Ultrastructural localization of a macrophage-restricted sialic acid binding hemagglutinin, SER, in macrophage-hematopoietic cell clusters. *Blood*, *76*(6), 1131-1138.

Dai, C., Chung, I. J., Jiang, S., Price, J. O., & Krantz, S. B. (2003). Reduction of cell cycle progression in human erythroid progenitor cells treated with tumour necrosis factor alpha occurs with reduced CDK6 and is partially reversed by CDK6 transduction. *Br J Haematol*, *121*(6), 919-927. https://doi.org/10.1046/j.1365-2141.2003.04367.x

Dalleau, S., Baradat, M., Guéraud, F., & Huc, L. (2013). Cell death and diseases related to oxidative stress: 4-hydroxynonenal (HNE) in the balance. *Cell Death Differ*, *20*(12), 1615-1630. https://doi.org/10.1038/cdd.2013.138

Danise, P., Maconi, M., Barrella, F., Di Palma, A., Avino, D., Rovetti, A., Gioia, M., & Amendola, G. (2011). Evaluation of nucleated red blood cells in the peripheral blood of hematological diseases. *Clin Chem Lab Med*, *50*(2), 357-360. https://doi.org/10.1515/cclm.2011.766

de Back, D. Z., Kostova, E. B., van Kraaij, M., van den Berg, T. K., & van Bruggen, R. (2014). Of macrophages and red blood cells; a complex love story. *Front Physiol*, *5*, 9. https://doi.org/10.3389/fphys.2014.00009

De Brabander, M., Van Belle, H., Aerts, F., Van De Veire, R., & Geuens, G. (1979). Protective effect of levamisole and its sulfhydryl metabolite OMPI against cell death induced by glutathione depletion. *Int J Immunopharmacol*, *1*(2), 93-100. https://doi.org/10.1016/0192-0561(79)90011-0

De Maria, R., Testa, U., Luchetti, L., Zeuner, A., Stassi, G., Pelosi, E., Riccioni, R., Felli, N., Samoggia, P., & Peschle, C. (1999). Apoptotic role of Fas/Fas ligand system in the regulation of erythropoiesis. *Blood*, *93*(3), 796-803.

de Montalembert, M., Brousse, V., Chakravorty, S., Pagliuca, A., Porter, J., Telfer, P., Vora, A., & Rees, D. C. (2017). Are the risks of treatment to cure a child with severe sickle cell disease too high? *Bmj*, *359*, j5250. https://doi.org/10.1136/bmj.j5250

Denney, L., Kok, W. L., Cole, S. L., Sanderson, S., McMichael, A. J., & Ho, L. P. (2012). Activation of invariant NKT cells in early phase of experimental autoimmune encephalomyelitis results in differentiation of Ly6Chi inflammatory monocyte to M2 macrophages and improved outcome. *J Immunol*, *189*(2), 551-557. https://doi.org/10.4049/jimmunol.1103608

Dixon, S. J., Lemberg, K. M., Lamprecht, M. R., Skouta, R., Zaitsev, E. M., Gleason, C. E., Patel, D. N., Bauer, A. J., Cantley, A. M., Yang, W. S., Morrison, B., 3rd, & Stockwell, B. R. (2012). Ferroptosis: an iron-dependent form of nonapoptotic cell death. *Cell*, *149*(5), 1060-1072. https://doi.org/10.1016/j.cell.2012.03.042

Dixon, S. J., Patel, D. N., Welsch, M., Skouta, R., Lee, E. D., Hayano, M., Thomas, A. G., Gleason, C. E., Tatonetti, N. P., Slusher, B. S., & Stockwell, B. R. (2014). Pharmacological inhibition of cystine-glutamate exchange induces endoplasmic reticulum stress and ferroptosis. *Elife*, *3*, e02523. https://doi.org/10.7554/eLife.02523

Dixon, S. J., & Pratt, D. A. (2023). Ferroptosis: A flexible constellation of related biochemical mechanisms. *Mol Cell*, *83*(7), 1030-1042. https://doi.org/10.1016/j.molcel.2023.03.005

Dixon, S. J., Winter, G. E., Musavi, L. S., Lee, E. D., Snijder, B., Rebsamen, M., Superti-Furga, G., & Stockwell, B. R. (2015). Human Haploid Cell Genetics Reveals Roles for Lipid Metabolism Genes in Nonapoptotic Cell Death. *ACS Chem Biol*, *10*(7), 1604-1609. https://doi.org/10.1021/acschembio.5b00245

Dodson, M., Castro-Portuguez, R., & Zhang, D. D. (2019). NRF2 plays a critical role in mitigating lipid peroxidation and ferroptosis. *Redox Biol*, *23*, 101107. https://doi.org/10.1016/j.redox.2019.101107

Doll, S., Proneth, B., Tyurina, Y. Y., Panzilius, E., Kobayashi, S., Ingold, I., Irmler, M., Beckers, J., Aichler, M., Walch, A., Prokisch, H., Trumbach, D., Mao, G., Qu, F., Bayir, H., Fullekrug, J., Scheel, C. H., Wurst, W., Schick, J. A., . . . Conrad, M. (2017). ACSL4 dictates ferroptosis sensitivity by shaping cellular lipid composition. *Nat Chem Biol*, *13*(1), 91-98. https://doi.org/10.1038/nchembio.2239

Dolma, S., Lessnick, S. L., Hahn, W. C., & Stockwell, B. R. (2003). Identification of genotype-selective antitumor agents using synthetic lethal chemical screening in engineered human tumor cells. *Cancer Cell*, *3*(3), 285-296. https://doi.org/10.1016/s1535-6108(03)00050-3

Doty, R. T., Fan, X., Young, D. J., Liang, J., Singh, K., Pakbaz, Z., Desmond, R., Young-Baird, S. K., Chandrasekharappa, S. C., Donovan, F. X., Phelps, S. R., Winkler, T., Dunbar, C. E., & Abkowitz, J. L. (2022). Studies of a mosaic patient with DBA and chimeric mice reveal erythroid cell-extrinsic contributions to erythropoiesis. *Blood*, *139*(23), 3439-3449. https://doi.org/10.1182/blood.2021013507

Doulatov, S., Notta, F., Eppert, K., Nguyen, L. T., Ohashi, P. S., & Dick, J. E. (2010). Revised map of the human progenitor hierarchy shows the origin of macrophages and dendritic cells in early lymphoid development. *Nature Immunology*, *11*(7), 585-593. https://doi.org/10.1038/ni.1889

Doulatov, S., Notta, F., Laurenti, E., & Dick, John E. (2012). Hematopoiesis: A Human Perspective. *Cell Stem Cell*, *10*(2), 120-136. https://doi.org/https://doi.org/10.1016/j.stem.2012.01.006

Dover, G. J., Boyer, S. H., Charache, S., & Heintzelman, K. (1978). Individual variation in the production and survival of F cells in sickle-cell disease. *N Engl J Med*, *299*(26), 1428-1435. https://doi.org/10.1056/nejm197812282992603

Drakopoulou, E., Georgomanoli, M., Lederer, C. W., Kleanthous, M., Costa, C., Bernadin, O., Cosset, F. L., Voskaridou, E., Verhoeyen, E., Papanikolaou, E., & Anagnou, N. P. (2019). A Novel BaEVRless-Pseudotyped γ-Globin Lentiviral Vector Drives High and Stable Fetal Hemoglobin Expression and Improves Thalassemic Erythropoiesis In Vitro. *Hum Gene Ther*, *30*(5), 601-617. https://doi.org/10.1089/hum.2018.022

Dulay, A. T., Buhimschi, I. A., Zhao, G., Luo, G., Abdel-Razeq, S., Cackovic, M., Rosenberg, V. A., Pettker, C. M., Thung, S. F., Bahtiyar, M. O., Bhandari, V., & Buhimschi, C. S. (2008). Nucleated red blood cells are a direct response to mediators of inflammation in newborns with early-onset neonatal sepsis. *Am J Obstet Gynecol*, *198*(4), 426.e421-429. https://doi.org/10.1016/j.ajog.2008.01.040

Dulmovits, B. M., Appiah-Kubi, A. O., Papoin, J., Hale, J., He, M., Al-Abed, Y., Didier, S., Gould, M., Husain-Krautter, S., Singh, S. A., Chan, K. W., Vlachos, A., Allen, S. L., Taylor, N., Marambaud, P., An, X., Gallagher, P. G., Mohandas, N., Lipton, J. M., . . . Blanc, L. (2016). Pomalidomide reverses γ-globin silencing through the transcriptional reprogramming of adult hematopoietic progenitors. *Blood*, *127*(11), 1481-1492. https://doi.org/10.1182/blood-2015-09-667923

Dupuis, L., Chauvet, M., Bourdelier, E., Dussiot, M., Belmatoug, N., Le Van Kim, C., Chene, A., & Franco, M. (2022). Phagocytosis of Erythrocytes from Gaucher Patients Induces Phenotypic Modifications in Macrophages, Driving Them toward Gaucher Cells. *Int J Mol Sci*, *23*(14). https://doi.org/10.3390/ijms23147640

Dutra, F. F., & Bozza, M. T. (2014). Heme on innate immunity and inflammation. *Front Pharmacol*, *5*, 115. https://doi.org/10.3389/fphar.2014.00115

Dykstra, B., Kent, D., Bowie, M., McCaffrey, L., Hamilton, M., Lyons, K., Lee, S. J., Brinkman, R., & Eaves, C. (2007). Long-term propagation of distinct hematopoietic differentiation programs in vivo. *Cell Stem Cell*, *1*(2), 218-229. https://doi.org/10.1016/j.stem.2007.05.015

Eagle, H. (1955a). Nutrition needs of mammalian cells in tissue culture. *Science*, *122*(3168), 501-514. https://doi.org/10.1126/science.122.3168.501

Eagle, H. (1955b). The specific amino acid requirements of a human carcinoma cell (Stain HeLa) in tissue culture. *J Exp Med*, *102*(1), 37-48. https://doi.org/10.1084/jem.102.1.37

Eagle, H. (1959). Amino acid metabolism in mammalian cell cultures. *Science*, *130*(3373), 432-437. https://doi.org/10.1126/science.130.3373.432

Eagle, H., Piez, K. A., & Oyama, V. I. (1961). The biosynthesis of cystine in human cell cultures. *J Biol Chem*, *236*, 1425-1428.

Eaves, C., & Lambie, K. (1995). *Atlas of human hematopoietic colonies : an introduction to the recognition of colonies produced by human hematopoietic progenitor cells cultured in methylcellulose media*. StemCell Techn. Inc.

Ehninger, A., & Trumpp, A. (2011). The bone marrow stem cell niche grows up: mesenchymal stem cells and macrophages move in. *J Exp Med*, *208*(3), 421-428. https://doi.org/10.1084/jem.20110132

El Hoss, S., Cochet, S., Godard, A., Yan, H., Dussiot, M., Frati, G., Boutonnat-Faucher, B., Laurance, S., Renaud, O., Joseph, L., Miccio, A., Brousse, V., Narla, M., & El Nemer, W. (2021). Fetal hemoglobin rescues ineffective erythropoiesis in sickle cell disease. *Haematologica*, *106*(10), 2707-2719. https://doi.org/10.3324/haematol.2020.265462

El Hoss, S., El Nemer, W., & Rees, D. C. (2022). Precision Medicine and Sickle Cell Disease. *Hemasphere*, *6*(9), e762. https://doi.org/10.1097/hs9.0000000000000762

Elenga, N., Loko, G., Etienne-Julan, M., Al-Okka, R., Adel, A. M., & Yassin, M. A. (2023). "Long-term efficacy and safety of L-glutamine in preventing sickle cell disease-related acute complications and hemolysis in pediatric and adult patients-Real-world, observational study". *Eur J Haematol*, *110*(6), 772-773. https://doi.org/10.1111/ejh.13939

Elford, H. L. (1968). Effect of hydroxyurea on ribonucleotide reductase. *Biochem Biophys Res Commun*, *33*(1), 129-135. https://doi.org/10.1016/0006-291x(68)90266-0

Esrick, E. B., Lehmann, L. E., Biffi, A., Achebe, M., Brendel, C., Ciuculescu, M. F., Daley, H., MacKinnon, B., Morris, E., Federico, A., Abriss, D., Boardman, K., Khelladi, R., Shaw, K., Negre, H., Negre, O., Nikiforow, S., Ritz, J., Pai, S. Y., . . . Williams, D. A. (2021). Post-Transcriptional Genetic Silencing of BCL11A to Treat Sickle Cell Disease. *N Engl J Med*, *384*(3), 205-215. https://doi.org/10.1056/NEJMoa2029392

Estepp, J. H., Kalpatthi, R., Woods, G., Trompeter, S., Liem, R. I., Sims, K., Inati, A., Inusa, B. P. D., Campbell, A., Piccone, C., Abboud, M. R., Smith-Whitley, K., Dixon, S., Tonda, M., Washington, C., Griffin, N. M., & Brown, C. (2022). Safety and efficacy of voxelotor in pediatric patients with sickle cell disease aged 4 to 11 years. *Pediatr Blood Cancer*, *69*(8), e29716. https://doi.org/10.1002/pbc.29716

Fabriek, B. O., Polfliet, M. M., Vloet, R. P., van der Schors, R. C., Ligtenberg, A. J., Weaver, L. K., Geest, C., Matsuno, K., Moestrup, S. K., Dijkstra, C. D., & van den Berg, T. K. (2007). The macrophage CD163 surface glycoprotein is an erythroblast adhesion receptor. *Blood*, *109*(12), 5223-5229. https://doi.org/10.1182/blood-2006-08-036467

Fabry, M. E., Nagel, R. L., Pachnis, A., Suzuka, S. M., & Costantini, F. (1992). High expression of human beta S- and alpha-globins in transgenic mice: hemoglobin composition and hematological consequences. *Proc Natl Acad Sci U S A*, *89*(24), 12150-12154. https://doi.org/10.1073/pnas.89.24.12150

Fabry, M. E., Sengupta, A., Suzuka, S. M., Costantini, F., Rubin, E. M., Hofrichter, J., Christoph, G., Manci, E., Culberson, D., Factor, S. M., & Nagel, R. L. (1995). A second generation transgenic mouse model expressing both hemoglobin S (HbS) and HbS-Antilles results in increased phenotypic severity. *Blood*, *86*(6), 2419-2428.

Fabry, M. E., Suzuka, S. M., Weinberg, R. S., Lawrence, C., Factor, S. M., Gilman, J. G., Costantini, F., & Nagel, R. L. (2001). Second generation knockout sickle mice: the effect of HbF. *Blood*, *97*(2), 410-418. https://doi.org/https://doi.org/10.1182/blood.V97.2.410

Falchi, M., Varricchio, L., Martelli, F., Masiello, F., Federici, G., Zingariello, M., Girelli, G., Whitsett, C., Petricoin, E. F., 3rd, Moestrup, S. K., Zeuner, A., & Migliaccio, A. R. (2015). Dexamethasone targeted directly to macrophages induces macrophage niches that promote erythroid expansion. *Haematologica*, *100*(2), 178-187. https://doi.org/10.3324/haematol.2014.114405

Fang, X., Ardehali, H., Min, J., & Wang, F. (2023). The molecular and metabolic landscape of iron and ferroptosis in cardiovascular disease. *Nature Reviews Cardiology*, *20*(1), 7-23. https://doi.org/10.1038/s41569-022-00735-4

Fang, X., Cai, Z., Wang, H., Han, D., Cheng, Q., Zhang, P., Gao, F., Yu, Y., Song, Z., Wu, Q., An, P., Huang, S., Pan, J., Chen, H. Z., Chen, J., Linkermann, A., Min, J., & Wang, F. (2020). Loss of Cardiac Ferritin H Facilitates Cardiomyopathy via Slc7a11-Mediated Ferroptosis. *Circ Res*, *127*(4), 486-501. https://doi.org/10.1161/circresaha.120.316509

Fang, X., Wang, H., Han, D., Xie, E., Yang, X., Wei, J., Gu, S., Gao, F., Zhu, N., Yin, X., Cheng, Q., Zhang, P., Dai, W., Chen, J., Yang, F., Yang, H. T., Linkermann, A., Gu, W., Min, J., & Wang, F. (2019). Ferroptosis as a target for protection against cardiomyopathy. *Proc Natl Acad Sci U S A*, *116*(7), 2672-2680. https://doi.org/10.1073/pnas.1821022116

Feng, X., Wang, S., Sun, Z., Dong, H., Yu, H., Huang, M., & Gao, X. (2021). Ferroptosis Enhanced Diabetic Renal Tubular Injury via HIF-1α/HO-1 Pathway in db/db Mice. *Front Endocrinol (Lausanne)*, *12*, 626390. https://doi.org/10.3389/fendo.2021.626390

Fibach, E., Manor, D., Oppenheim, A., & Rachmilewitz, E. A. (1989). Proliferation and maturation of human erythroid progenitors in liquid culture. *Blood*, *73*(1), 100-103.

Figueiredo, R. T., Fernandez, P. L., Mourao-Sa, D. S., Porto, B. N., Dutra, F. F., Alves, L. S., Oliveira, M. F., Oliveira, P. L., Graça-Souza, A. V., & Bozza, M. T. (2007). Characterization of Heme as Activator of Toll-like Receptor 4*. *Journal of Biological Chemistry*, *282*(28), 20221-20229. https://doi.org/https://doi.org/10.1074/jbc.M610737200

Finch, C. A., Lee, M. Y., & Leonard, J. M. (1982). Continuous RBC transfusions in a patient with sickle cell disease. *Arch Intern Med*, *142*(2), 279-282.

Fitzhugh, C. D., Cordes, S., Taylor, T., Coles, W., Roskom, K., Link, M., Hsieh, M. M., & Tisdale, J. F. (2017). At least 20% donor myeloid chimerism is necessary to reverse the sickle phenotype after allogeneic HSCT. *Blood*, *130*(17), 1946-1948. https://doi.org/10.1182/blood-2017-03-772392

Flemming, W. (1885). *Ueber die Bildung von Richtungsfiguren in Säugethiereiern beim Untergang Graaf'scher Follikel*. [publisher not identified].

Foell, J., Pfirstinger, B., Rehe, K., Wolff, D., Holler, E., & Corbacioglu, S. (2017). Haploidentical stem cell transplantation with CD3(+)-/CD19(+)- depleted peripheral stem cells for patients with advanced stage sickle cell disease and no alternative donor: results of a pilot study. *Bone Marrow Transplant*, *52*(6), 938-940. https://doi.org/10.1038/bmt.2017.49

Franco, R. S., Lohmann, J., Silberstein, E. B., Mayfield-Pratt, G., Palascak, M., Nemeth, T. A., Joiner, C. H., Weiner, M., & Rucknagel, D. L. (1998). Time-dependent changes in the density and hemoglobin F content of biotin-labeled sickle cells. *J Clin Invest*, *101*(12), 2730-2740. https://doi.org/10.1172/jci2484

Franco, R. S., Yasin, Z., Palascak, M. B., Ciraolo, P., Joiner, C. H., & Rucknagel, D. L. (2006). The effect of fetal hemoglobin on the survival characteristics of sickle cells. *Blood*, *108*(3), 1073-1076. https://doi.org/10.1182/blood-2005-09-008318

Frangoul, H., Altshuler, D., Cappellini, M. D., Chen, Y. S., Domm, J., Eustace, B. K., Foell, J., de la Fuente, J., Grupp, S., Handgretinger, R., Ho, T. W., Kattamis, A., Kernytsky, A., Lekstrom-Himes, J., Li, A. M., Locatelli, F., Mapara, M. Y., de Montalembert, M., Rondelli, D., . . . Corbacioglu, S. (2021). CRISPR-Cas9 Gene Editing for Sickle Cell Disease and β-Thalassemia. *N Engl J Med*, *384*(3), 252-260. https://doi.org/10.1056/NEJMoa2031054

Franks, T. M., Haugabook, S. J., Ottinger, E. A., Vermillion, M. S., Pawlik, K. M., Townes, T. M., & Rogers, C. S. (2020). Engineering, Generation and Preliminary Characterization of a Humanized Porcine Sickle Cell Disease Animal Model. *bioRxiv*, 2020.2009. 2015.291864.

Frazer, D. M., & Anderson, G. J. (2014). The regulation of iron transport. *Biofactors*, *40*(2), 206-214. https://doi.org/10.1002/biof.1148

Freyssinier, J. M., Lecoq-Lafon, C., Amsellem, S., Picard, F., Ducrocq, R., Mayeux, P., Lacombe, C., & Fichelson, S. (1999). Purification, amplification and characterization of a population of human erythroid progenitors. *Br J Haematol*, *106*(4), 912-922. https://doi.org/10.1046/j.1365-2141.1999.01639.x

Friedmann Angeli, J. P., Schneider, M., Proneth, B., Tyurina, Y. Y., Tyurin, V. A., Hammond, V. J., Herbach, N., Aichler, M., Walch, A., Eggenhofer, E., Basavarajappa, D., Rådmark, O., Kobayashi, S., Seibt, T., Beck, H., Neff, F., Esposito, I., Wanke, R., Förster, H., . . . Conrad, M. (2014). Inactivation of the ferroptosis regulator Gpx4 triggers acute renal failure in mice. *Nat Cell Biol*, *16*(12), 1180-1191. https://doi.org/10.1038/ncb3064

Frontelo, P., Manwani, D., Galdass, M., Karsunky, H., Lohmann, F., Gallagher, P. G., & Bieker, J. J. (2007). Novel role for EKLF in megakaryocyte lineage commitment. *Blood*, *110*(12), 3871-3880. https://doi.org/10.1182/blood-2007-03-082065

Galanello, R., Sanna, S., Perseu, L., Sollaino, M. C., Satta, S., Lai, M. E., Barella, S., Uda, M., Usala, G., Abecasis, G. R., & Cao, A. (2009). Amelioration of Sardinian beta0 thalassemia by genetic modifiers. *Blood*, *114*(18), 3935-3937. https://doi.org/10.1182/blood-2009-04-217901

Galanello, R., Veith, R., Papayannopoulou, T., & Stamatoyannopoulos, G. (1985). Pharmacologic stimulation of Hb F in patients with sickle cell anemia. *Prog Clin Biol Res*, *191*, 433-445.

Gallivan, A., Kanu, A., Alejandro, M., Zekaryas, N., Horneman, H., Ramasamy, J., Hong, L., Lavelle, D., Diamond, A., Molokie, R. E., Vichinsky, E. P., & Rivers, A. (2022). Reticulocytosis from Stress Erythropoiesis Is a Major Source of Erythrocyte Mitochondrial Retention, Oxygen Consumption and Reactive Oxygen Species in a SCD Mouse Model. *Blood*, *140*(Supplement 1), 8239-8240. https://doi.org/10.1182/blood-2022-160481

Galluzzi, L., Bravo-San Pedro, J. M., Vitale, I., Aaronson, S. A., Abrams, J. M., Adam, D., Alnemri, E. S., Altucci, L., Andrews, D., Annicchiarico-Petruzzelli, M., Baehrecke, E. H., Bazan, N. G., Bertrand, M. J., Bianchi, K., Blagosklonny, M. V., Blomgren, K., Borner, C., Bredesen, D. E., Brenner, C., . . . Kroemer, G. (2015). Essential versus accessory aspects of cell death: recommendations of the NCCD 2015. *Cell Death & Differentiation*, *22*(1), 58-73. https://doi.org/10.1038/cdd.2014.137

Galluzzi, L., Vitale, I., Aaronson, S. A., Abrams, J. M., Adam, D., Agostinis, P., Alnemri, E. S., Altucci, L., Amelio, I., Andrews, D. W., Annicchiarico-Petruzzelli, M., Antonov, A. V., Arama, E., Baehrecke, E. H., Barlev, N. A., Bazan, N. G., Bernassola, F., Bertrand, M. J. M., Bianchi, K., . . . Kroemer, G. (2018). Molecular mechanisms of cell death: recommendations of the Nomenclature Committee on Cell Death 2018. *Cell Death & Differentiation*, *25*(3), 486-541. https://doi.org/10.1038/s41418-017-0012-4

Galluzzi, L., Vitale, I., Abrams, J. M., Alnemri, E. S., Baehrecke, E. H., Blagosklonny, M. V., Dawson, T. M., Dawson, V. L., El-Deiry, W. S., Fulda, S., Gottlieb, E., Green, D. R., Hengartner, M. O., Kepp, O., Knight, R. A., Kumar, S., Lipton, S. A., Lu, X., Madeo, F., . . . Kroemer, G. (2012). Molecular definitions of cell death subroutines: recommendations of the Nomenclature Committee on Cell Death 2012. *Cell Death Differ*, *19*(1), 107-120. https://doi.org/10.1038/cdd.2011.96

Gambero, S., Canalli, A. A., Traina, F., Albuquerque, D. M., Saad, S. T., Costa, F. F., & Conran, N. (2007). Therapy with hydroxyurea is associated with reduced adhesion molecule gene and protein expression in sickle red cells with a concomitant reduction in adhesive properties. *Eur J Haematol*, *78*(2), 144-151. https://doi.org/10.1111/j.1600-0609.2006.00788.x

Gao, M., Monian, P., Quadri, N., Ramasamy, R., & Jiang, X. (2015). Glutaminolysis and Transferrin Regulate Ferroptosis. *Mol Cell*, *59*(2), 298-308. https://doi.org/10.1016/j.molcel.2015.06.011

Gardner, K., Douiri, A., Drasar, E., Allman, M., Mwirigi, A., Awogbade, M., & Thein, S. L. (2016). Survival in adults with sickle cell disease in a high-income setting. *Blood*, *128*(10), 1436-1438. https://doi.org/https://doi.org/10.1182/blood-2016-05-716910

Garrido, V. T., Proença-Ferreira, R., Dominical, V. M., Traina, F., Bezerra, M. A., de Mello, M. R., Colella, M. P., Araújo, A. S., Saad, S. T., Costa, F. F., & Conran, N. (2012). Elevated plasma levels and platelet-associated expression of the pro-thrombotic and pro-inflammatory protein, TNFSF14 (LIGHT), in sickle cell disease. *Br J Haematol*, *158*(6), 788-797. https://doi.org/10.1111/j.1365-2141.2012.09218.x

Gautier, E.-F., Ducamp, S., Leduc, M., Salnot, V., Guillonneau, F., Dussiot, M., Hale, J., Giarratana, M.-C., Raimbault, A., Douay, L., Lacombe, C., Mohandas, N., Verdier, F., Zermati, Y., & Mayeux, P. (2016). Comprehensive Proteomic Analysis of Human Erythropoiesis. *Cell Reports*, *16*(5), 1470-1484. https://doi.org/https://doi.org/10.1016/j.celrep.2016.06.085

Gautier, E. L., Shay, T., Miller, J., Greter, M., Jakubzick, C., Ivanov, S., Helft, J., Chow, A., Elpek, K. G., Gordonov, S., Mazloom, A. R., Ma'ayan, A., Chua, W. J., Hansen, T. H., Turley, S. J., Merad, M., & Randolph, G. J. (2012). Gene-expression profiles and transcriptional regulatory pathways that underlie the identity and diversity of mouse tissue macrophages. *Nat Immunol*, *13*(11), 1118-1128. https://doi.org/10.1038/ni.2419

Giarratana, M. C., Kobari, L., Lapillonne, H., Chalmers, D., Kiger, L., Cynober, T., Marden, M. C., Wajcman, H., & Douay, L. (2005). Ex vivo generation of fully mature human red blood cells from hematopoietic stem cells. *Nat Biotechnol*, *23*(1), 69-74. https://doi.org/10.1038/nbt1047

Giarratana, M. C., Rouard, H., Dumont, A., Kiger, L., Safeukui, I., Le Pennec, P. Y., François, S., Trugnan, G., Peyrard, T., Marie, T., Jolly, S., Hebert, N., Mazurier, C., Mario, N., Harmand, L., Lapillonne, H., Devaux, J. Y., & Douay, L. (2011). Proof of principle for transfusion of in vitro-generated red blood cells. *Blood*, *118*(19), 5071-5079. https://doi.org/10.1182/blood-2011-06-362038

Ginhoux, F., & Guilliams, M. (2016). Tissue-Resident Macrophage Ontogeny and Homeostasis. *Immunity*, *44*(3), 439-449. https://doi.org/10.1016/j.immuni.2016.02.024

Gladwin, M. T., & Ofori-Acquah, S. F. (2014). Erythroid DAMPs drive inflammation in SCD. *Blood*, *123*(24), 3689-3690. https://doi.org/https://doi.org/10.1182/blood-2014-03-563874

Gnanapragasam, M. N., McGrath, K. E., Catherman, S., Xue, L., Palis, J., & Bieker, J. J. (2016). EKLF/KLF1-regulated cell cycle exit is essential for erythroblast enucleation. *Blood*, *128*(12), 1631-1641. https://doi.org/10.1182/blood-2016-03-706671

Goldschmidt, R. (1914). *Archiv für Zellforschung* (Vol. Bd.12 (1914)). W. Engelmann. https://www.biodiversitylibrary.org/item/218177

Gomez Perdiguero, E., Klapproth, K., Schulz, C., Busch, K., Azzoni, E., Crozet, L., Garner, H., Trouillet, C., de Bruijn, M. F., Geissmann, F., & Rodewald, H. R. (2015). Tissue-resident macrophages originate from yolk-sac-derived erythro-myeloid progenitors. *Nature*, *518*(7540), 547-551. https://doi.org/10.1038/nature13989

Gonzalez-Menendez, P., Phadke, I., Olive, M. E., Joly, A., Papoin, J., Yan, H., Galtier, J., Platon, J., Kang, S. W. S., McGraw, K. L., Daumur, M., Pouzolles, M., Kondo, T., Boireau, S., Paul, F., Young, D. J., Lamure, S., Mirmira, R. G., Narla, A., . . . Taylor, N. (2023). Arginine metabolism regulates human erythroid differentiation through hypusination of eIF5A. *Blood*, *141*(20), 2520-2536. https://doi.org/10.1182/blood.2022017584

Gonzalez-Menendez, P., Romano, M., Yan, H., Deshmukh, R., Papoin, J., Oburoglu, L., Daumur, M., Dumé, A. S., Phadke, I., Mongellaz, C., Qu, X., Bories, P. N., Fontenay, M., An, X., Dardalhon, V., Sitbon, M., Zimmermann, V. S., Gallagher, P. G., Tardito, S., . . . Kinet, S. (2021). An IDH1-vitamin C crosstalk drives human erythroid development by inhibiting pro-oxidant mitochondrial metabolism. *Cell Rep*, *34*(5), 108723. https://doi.org/10.1016/j.celrep.2021.108723

Gout, P. W., Buckley, A. R., Simms, C. R., & Bruchovsky, N. (2001). Sulfasalazine, a potent suppressor of lymphoma growth by inhibition of the x(c)- cystine transporter: a new action for an old drug. *Leukemia*, *15*(10), 1633-1640. https://doi.org/10.1038/sj.leu.2402238

Granick, S., & Levere, R. D. (1964). HEME SYNTHESIS IN ERYTHROID CELLS. *Prog Hematol*, *4*, 1-47.

Grasso, J. A., Sullivan, A. L., & Sullivan, L. W. (1975). Ultrastructural studies of the bone marrow in sickle cell anaemia. I. The structure of sickled erythrocytes and reticulocytes and their phagocytic destruction. *Br J Haematol*, *31*(2), 135-148. https://doi.org/10.1111/j.1365-2141.1975.tb00844.x

Greaney, A. J., Maier, N. K., Leppla, S. H., & Moayeri, M. (2016). Sulforaphane inhibits multiple inflammasomes through an Nrf2-independent mechanism. *J Leukoc Biol*, *99*(1), 189-199. https://doi.org/10.1189/jlb.3A0415-155RR

Grenier, J. M. P., Delahaye, M. C., Mancini, S. J. C., & Aurrand-Lions, M. (2021). Flow Cytometry Analysis of Mouse Hematopoietic Stem and Multipotent Progenitor Cells. *Methods Mol Biol*, *2308*, 73-81. https://doi.org/10.1007/978-1-0716-1425-9_6

Griffiths, R. E., Kupzig, S., Cogan, N., Mankelow, T. J., Betin, V. M., Trakarnsanga, K., Massey, E. J., Lane, J. D., Parsons, S. F., & Anstee, D. J. (2012). Maturing reticulocytes internalize plasma membrane in glycophorin A-containing vesicles that fuse with autophagosomes before exocytosis. *Blood*, *119*(26), 6296-6306. https://doi.org/10.1182/blood-2011-09-376475

Griffiths, R. E., Kupzig, S., Cogan, N., Mankelow, T. J., Betin, V. M., Trakarnsanga, K., Massey, E. J., Parsons, S. F., Anstee, D. J., & Lane, J. D. (2012). The ins and outs of human reticulocyte maturation: autophagy and the endosome/exosome pathway. *Autophagy*, *8*(7), 1150-1151. https://doi.org/10.4161/auto.20648

Grosse, S. D., Odame, I., Atrash, H. K., Amendah, D. D., Piel, F. B., & Williams, T. N. (2011). Sickle cell disease in Africa: a neglected cause of early childhood mortality. *Am J Prev Med*, *41*(6 Suppl 4), S398-405. https://doi.org/10.1016/j.amepre.2011.09.013

Guilliams, M., & Scott, C. L. (2017). Does niche competition determine the origin of tissue-resident macrophages? *Nat Rev Immunol*, *17*(7), 451-460. https://doi.org/10.1038/nri.2017.42

Guilliams, M., Thierry, G. R., Bonnardel, J., & Bajenoff, M. (2020). Establishment and Maintenance of the Macrophage Niche. *Immunity*, *52*(3), 434-451. https://doi.org/10.1016/j.immuni.2020.02.015

Gutiérrez, L., Tsukamoto, S., Suzuki, M., Yamamoto-Mukai, H., Yamamoto, M., Philipsen, S., & Ohneda, K. (2008). Ablation of Gata1 in adult mice results in aplastic crisis, revealing its essential role in steady-state and stress erythropoiesis. *Blood*, *111*(8), 4375-4385. https://doi.org/10.1182/blood-2007-09-115121

Hampton-O'Neil, L. A., Severn, C. E., Cross, S. J., Gurung, S., Nobes, C. D., & Toye, A. M. (2020). Ephrin/Eph receptor interaction facilitates macrophage recognition of differentiating human erythroblasts. *Haematologica*, *105*(4), 914-924. https://doi.org/10.3324/haematol.2018.215160

Han, F., Li, S., Yang, Y., & Bai, Z. (2021). Interleukin-6 promotes ferroptosis in bronchial epithelial cells by inducing reactive oxygen species-dependent lipid peroxidation and disrupting iron homeostasis. *Bioengineered*, *12*(1), 5279-5288. https://doi.org/10.1080/21655979.2021.1964158

Han, S. Y., Lee, E. M., Lee, J., Lee, H., Kwon, A. M., Ryu, K. Y., Choi, W. S., & Baek, E. J. (2021). Red cell manufacturing using parallel stirred-tank bioreactors at the final stages of differentiation enhances reticulocyte maturation. *Biotechnol Bioeng*, *118*(5), 1763-1778. https://doi.org/10.1002/bit.27691

Handa, P., Thomas, S., Morgan-Stevenson, V., Maliken, B. D., Gochanour, E., Boukhar, S., Yeh, M. M., & Kowdley, K. V. (2019). Iron alters macrophage polarization status and leads to steatohepatitis and fibrogenesis. *J Leukoc Biol*, *105*(5), 1015-1026. https://doi.org/10.1002/JLB.3A0318-108R

Hanspal, M., & Hanspal, J. S. (1994). The association of erythroblasts with macrophages promotes erythroid proliferation and maturation: a 30-kD heparin-binding protein is involved in this contact. *Blood*, *84*(10), 3494-3504.

Hanspal, M., Smockova, Y., & Uong, Q. (1998). Molecular identification and functional characterization of a novel protein that mediates the attachment of erythroblasts to macrophages. *Blood*, *92*(8), 2940-2950.

Hao, S., Yu, J., He, W., Huang, Q., Zhao, Y., Liang, B., Zhang, S., Wen, Z., Dong, S., Rao, J., Liao, W., & Shi, M. (2017). Cysteine Dioxygenase 1 Mediates Erastin-Induced Ferroptosis in Human Gastric Cancer Cells. *Neoplasia*, *19*(12), 1022-1032. https://doi.org/10.1016/j.neo.2017.10.005

Hasegawa, S., Rodgers, G. P., Dwyer, N., Noguchi, C. T., Blanchette-Mackie, E. J., Uyesaka, N., Schechter, A. N., & Fibach, E. (1998). Sickling of nucleated erythroid precursors from patients with sickle cell anemia. *Exp Hematol*, *26*(4), 314-319. https://www.ncbi.nlm.nih.gov/pubmed/9546314

Hashimoto, D., Chow, A., Noizat, C., Teo, P., Beasley, M. B., Leboeuf, M., Becker, C. D., See, P., Price, J., Lucas, D., Greter, M., Mortha, A., Boyer, S. W., Forsberg, E. C., Tanaka, M., van Rooijen, N.,

Garcia-Sastre, A., Stanley, E. R., Ginhoux, F., . . . Merad, M. (2013). Tissue-resident macrophages self-maintain locally throughout adult life with minimal contribution from circulating monocytes. *Immunity*, *38*(4), 792-804. https://doi.org/10.1016/j.immuni.2013.04.004

Hassannia, B., Wiernicki, B., Ingold, I., Qu, F., Van Herck, S., Tyurina, Y. Y., Bayır, H., Abhari, B. A., Angeli, J. P. F., Choi, S. M., Meul, E., Heyninck, K., Declerck, K., Chirumamilla, C. S., Lahtela-Kakkonen, M., Van Camp, G., Krysko, D. V., Ekert, P. G., Fulda, S., . . . Vanden Berghe, T. (2018). Nano-targeted induction of dual ferroptotic mechanisms eradicates high-risk neuroblastoma. *J Clin Invest*, *128*(8), 3341-3355. https://doi.org/10.1172/jci99032

Hattangadi, S. M., Wong, P., Zhang, L., Flygare, J., & Lodish, H. F. (2011). From stem cell to red cell: regulation of erythropoiesis at multiple levels by multiple proteins, RNAs, and chromatin modifications. *Blood*, *118*(24), 6258-6268. https://doi.org/10.1182/blood-2011-07-356006

Haywood, C., Jr., Beach, M. C., Bediako, S., Carroll, C. P., Lattimer, L., Jarrett, D., & Lanzkron, S. (2011). Examining the characteristics and beliefs of hydroxyurea users and nonusers among adults with sickle cell disease. *Am J Hematol*, *86*(1), 85-87. https://doi.org/10.1002/ajh.21883

Hebbel, R. P., & Key, N. S. (2016). Microparticles in sickle cell anaemia: promise and pitfalls. *Br J Haematol*, *174*(1), 16-29. https://doi.org/10.1111/bjh.14112

Hebbel, R. P., & Vercellotti, G. M. (1997). The endothelial biology of sickle cell disease. *J Lab Clin Med*, *129*(3), 288-293. https://doi.org/10.1016/s0022-2143(97)90176-1

Heideveld, E., Hampton-O'Neil, L. A., Cross, S. J., van Alphen, F. P. J., van den Biggelaar, M., Toye, A. M., & van den Akker, E. (2018). Glucocorticoids induce differentiation of monocytes towards macrophages that share functional and phenotypical aspects with erythroblastic island macrophages. *Haematologica*, *103*(3), 395-405. https://doi.org/10.3324/haematol.2017.179341

Heideveld, E., & van den Akker, E. (2017). Digesting the role of bone marrow macrophages on hematopoiesis. *Immunobiology*, *222*(6), 814-822. https://doi.org/10.1016/j.imbio.2016.11.007

Herrick, J. B. (2001). Peculiar elongated and sickle-shaped red blood corpuscles in a case of severe anemia. 1910. *Yale J Biol Med*, *74*(3), 179-184.

Hershko, C. (2010). Pathogenesis and management of iron toxicity in thalassemia. *Ann N Y Acad Sci*, *1202*, 1-9. https://doi.org/10.1111/j.1749-6632.2010.05544.x

Heshusius, S., Heideveld, E., Burger, P., Thiel-Valkhof, M., Sellink, E., Varga, E., Ovchynnikova, E., Visser, A., Martens, J. H. A., von Lindern, M., & van den Akker, E. (2019). Large-scale in vitro production of red blood cells from human peripheral blood mononuclear cells. *Blood Adv*, *3*(21), 3337-3350. https://doi.org/10.1182/bloodadvances.2019000689

Hirschhorn, T., & Stockwell, B. R. (2019). The development of the concept of ferroptosis. *Free Radic Biol Med*, *133*, 130-143. https://doi.org/10.1016/j.freeradbiomed.2018.09.043

Hou, W., Xie, Y., Song, X., Sun, X., Lotze, M. T., Zeh, H. J., 3rd, Kang, R., & Tang, D. (2016). Autophagy promotes ferroptosis by degradation of ferritin. *Autophagy*, *12*(8), 1425-1428. https://doi.org/10.1080/15548627.2016.1187366

Housler, G. J., Miki, T., Schmelzer, E., Pekor, C., Zhang, X., Kang, L., Voskinarian-Berse, V., Abbot, S., Zeilinger, K., & Gerlach, J. C. (2012). Compartmental hollow fiber capillary membrane-based bioreactor technology for in vitro studies on red blood cell lineage direction of hematopoietic stem cells. *Tissue Eng Part C Methods*, *18*(2), 133-142. https://doi.org/10.1089/ten.TEC.2011.0305

Howard, J., Ataga, K. I., Brown, R. C., Achebe, M., Nduba, V., El-Beshlawy, A., Hassab, H., Agodoa, I., Tonda, M., Gray, S., Lehrer-Graiwer, J., & Vichinsky, E. (2021). Voxelotor in adolescents and adults with sickle cell disease (HOPE): long-term follow-up results of an international, randomised, double-blind, placebo-controlled, phase 3 trial. *Lancet Haematol*, *8*(5), e323-e333. https://doi.org/10.1016/s2352-3026(21)00059-4

Howard, J., Hemmaway, C. J., Telfer, P., Layton, D. M., Porter, J., Awogbade, M., Mant, T., Gretler, D. D., Dufu, K., Hutchaleelaha, A., Patel, M., Siu, V., Dixon, S., Landsman, N., Tonda, M., & Lehrer-Graiwer, J. (2019). A phase 1/2 ascending dose study and open-label extension study of

voxelotor in patients with sickle cell disease. *Blood*, *133*(17), 1865-1875. https://doi.org/10.1182/blood-2018-08-868893

Hu, D., & Shilatifard, A. (2016). Epigenetics of hematopoiesis and hematological malignancies. *Genes Dev*, *30*(18), 2021-2041. https://doi.org/10.1101/gad.284109.116

Hu, J., Liu, J., Xue, F., Halverson, G., Reid, M., Guo, A., Chen, L., Raza, A., Galili, N., Jaffray, J., Lane, J., Chasis, J. A., Taylor, N., Mohandas, N., & An, X. (2013). Isolation and functional characterization of human erythroblasts at distinct stages: implications for understanding of normal and disordered erythropoiesis in vivo. *Blood*, *121*(16), 3246-3253. https://doi.org/10.1182/blood-2013-01-476390

Huang, J., Sommers, E. M., Kim-Shapiro, D. B., & King, S. B. (2002). Horseradish peroxidase catalyzed nitric oxide formation from hydroxyurea. *J Am Chem Soc*, *124*(13), 3473-3480. https://doi.org/10.1021/ja012271v

Huang, N.-J., Lin, Y.-C., Lin, C.-Y., Pishesha, N., Lewis, C. A., Freinkman, E., Farquharson, C., Millán, J. L., & Lodish, H. (2018). Enhanced phosphocholine metabolism is essential for terminal erythropoiesis. *Blood*, *131*(26), 2955-2966. https://doi.org/10.1182/blood-2018-03-838516

Hur, J., Choi, J. I., Lee, H., Nham, P., Kim, T. W., Chae, C. W., Yun, J. Y., Kang, J. A., Kang, J., Lee, S. E., Yoon, C. H., Boo, K., Ham, S., Roh, T. Y., Jun, J. K., Lee, H., Baek, S. H., & Kim, H. S. (2016). CD82/KAI1 Maintains the Dormancy of Long-Term Hematopoietic Stem Cells through Interaction with DARC-Expressing Macrophages. *Cell Stem Cell*, *18*(4), 508-521. https://doi.org/10.1016/j.stem.2016.01.013

Imai, H., Hakkaku, N., Iwamoto, R., Suzuki, J., Suzuki, T., Tajima, Y., Konishi, K., Minami, S., Ichinose, S., Ishizaka, K., Shioda, S., Arata, S., Nishimura, M., Naito, S., & Nakagawa, Y. (2009). Depletion of selenoprotein GPx4 in spermatocytes causes male infertility in mice. *J Biol Chem*, *284*(47), 32522-32532. https://doi.org/10.1074/jbc.M109.016139

Imai, H., Hirao, F., Sakamoto, T., Sekine, K., Mizukura, Y., Saito, M., Kitamoto, T., Hayasaka, M., Hanaoka, K., & Nakagawa, Y. (2003). Early embryonic lethality caused by targeted disruption of the mouse PHGPx gene. *Biochem Biophys Res Commun*, *305*(2), 278-286. https://doi.org/10.1016/s0006-291x(03)00734-4

Inusa, B. P. D., Hsu, L. L., Kohli, N., Patel, A., Ominu-Evbota, K., Anie, K. A., & Atoyebi, W. (2019). Sickle Cell Disease—Genetics, Pathophysiology, Clinical Presentation and Treatment. *International Journal of Neonatal Screening*, *5*(2).

Ito, K., Carracedo, A., Weiss, D., Arai, F., Ala, U., Avigan, D. E., Schafer, Z. T., Evans, R. M., Suda, T., Lee, C. H., & Pandolfi, P. P. (2012). A PML–PPAR-δ pathway for fatty acid oxidation regulates hematopoietic stem cell maintenance. *Nat Med*, *18*(9), 1350-1358. https://doi.org/10.1038/nm.2882

Jacobs-Helber, S. M., Penta, K., Sun, Z., Lawson, A., & Sawyer, S. T. (1997). Distinct signaling from stem cell factor and erythropoietin in HCD57 cells. *J Biol Chem*, *272*(11), 6850-6853. https://doi.org/10.1074/jbc.272.11.6850

Jacobsen, R. N., Forristal, C. E., Raggatt, L. J., Nowlan, B., Barbier, V., Kaur, S., van Rooijen, N., Winkler, I. G., Pettit, A. R., & Levesque, J. P. (2014). Mobilization with granulocyte colony-stimulating factor blocks medullar erythropoiesis by depleting F4/80(+)VCAM1(+)CD169(+)ER-HR3(+)Ly6G(+) erythroid island macrophages in the mouse. *Exp Hematol*, *42*(7), 547-561.e544. https://doi.org/10.1016/j.exphem.2014.03.009

Jafri, F., Seong, G., Jang, T., Cimpeanu, E., Poplawska, M., Dutta, D., & Lim, S. (2022). L-glutamine for sickle cell disease: more than reducing redox. *Annals of Hematology*, *101*, 1-10. https://doi.org/10.1007/s00277-022-04867-y

Jelkmann, W. (2004). Molecular biology of erythropoietin. *Intern Med*, *43*(8), 649-659. https://doi.org/10.2169/internalmedicine.43.649

Jewell, J. L., Russell, R. C., & Guan, K. L. (2013). Amino acid signalling upstream of mTOR. *Nat Rev Mol Cell Biol*, *14*(3), 133-139. https://doi.org/10.1038/nrm3522

Jiang, L., Kon, N., Li, T., Wang, S. J., Su, T., Hibshoosh, H., Baer, R., & Gu, W. (2015). Ferroptosis as a p53-mediated activity during tumour suppression. *Nature*, *520*(7545), 57-62. https://doi.org/10.1038/nature14344

Jiang, X., Stockwell, B. R., & Conrad, M. (2021). Ferroptosis: mechanisms, biology and role in disease. *Nature Reviews Molecular Cell Biology*, *22*(4), 266-282. https://doi.org/10.1038/s41580-020-00324-8

Jung, H. S., Shimizu-Albergine, M., Shen, X., Kramer, F., Shao, D., Vivekanandan-Giri, A., Pennathur, S., Tian, R., Kanter, J. E., & Bornfeldt, K. E. (2020). TNF-α induces acyl-CoA synthetase 3 to promote lipid droplet formation in human endothelial cells. *J Lipid Res*, *61*(1), 33-44. https://doi.org/10.1194/jlr.RA119000256

Juwah, A. I., Nlemadim, E. U., & Kaine, W. (2004). Types of anaemic crises in paediatric patients with sickle cell anaemia seen in Enugu, Nigeria. *Arch Dis Child*, *89*(6), 572-576. https://doi.org/10.1136/adc.2003.037374

Kamimura, S., Smith, M., Vogel, S., Almeida, L. E. F., Thein, S. L., & Quezado, Z. M. N. (2023). Mouse models of sickle cell disease: Imperfect and yet very informative. *Blood Cells, Molecules, and Diseases*, 102776. https://doi.org/https://doi.org/10.1016/j.bcmd.2023.102776

Kaneko, H., Shimizu, R., & Yamamoto, M. (2010). GATA factor switching during erythroid differentiation. *Curr Opin Hematol*, *17*(3), 163-168. https://doi.org/10.1097/MOH.0b013e32833800b8

Kang, J., Jeong, M. G., Oh, S., Jang, E. J., Kim, H. K., & Hwang, E. S. (2014). A FoxO1-dependent, but NRF2-independent induction of heme oxygenase-1 during muscle atrophy. *FEBS Lett*, *588*(1), 79-85. https://doi.org/10.1016/j.febslet.2013.11.009

Kang, Y. P., Mockabee-Macias, A., Jiang, C., Falzone, A., Prieto-Farigua, N., Stone, E., Harris, I. S., & DeNicola, G. M. (2021). Non-canonical Glutamate-Cysteine Ligase Activity Protects against Ferroptosis. *Cell Metab*, *33*(1), 174-189.e177. https://doi.org/10.1016/j.cmet.2020.12.007

Kanter, J., Walters, M. C., Krishnamurti, L., Mapara, M. Y., Kwiatkowski, J. L., Rifkin-Zenenberg, S., Aygun, B., Kasow, K. A., Pierciey, F. J., Jr., Bonner, M., Miller, A., Zhang, X., Lynch, J., Kim, D., Ribeil, J. A., Asmal, M., Goyal, S., Thompson, A. A., & Tisdale, J. F. (2022). Biologic and Clinical Efficacy of LentiGlobin for Sickle Cell Disease. *N Engl J Med*, *386*(7), 617-628. https://doi.org/10.1056/NEJMoa2117175

Kao, J. K., Wang, S. C., Ho, L. W., Huang, S. W., Lee, C. H., Lee, M. S., Yang, R. C., & Shieh, J. J. (2020). M2-like polarization of THP-1 monocyte-derived macrophages under chronic iron overload. *Ann Hematol*, *99*(3), 431-441. https://doi.org/10.1007/s00277-020-03916-8

Kapralov, A. A., Yang, Q., Dar, H. H., Tyurina, Y. Y., Anthonymuthu, T. S., Kim, R., St Croix, C. M., Mikulska-Ruminska, K., Liu, B., Shrivastava, I. H., Tyurin, V. A., Ting, H. C., Wu, Y. L., Gao, Y., Shurin, G. V., Artyukhova, M. A., Ponomareva, L. A., Timashev, P. S., Domingues, R. M., . . . Kagan, V. E. (2020). Redox lipid reprogramming commands susceptibility of macrophages and microglia to ferroptotic death. *Nat Chem Biol*, *16*(3), 278-290. https://doi.org/10.1038/s41589-019-0462-8

Karakukcu, M., Karakukcu, C., Unal, E., Ozturk, A., Ciraci, Z., Patiroglu, T., & Ozdemir, M. A. (2015). The Importance of Nucleated Red Blood Cells in Patients with Beta Thalassemia Major and Comparison of Two Automated Systems with Manual Microscopy and Flow Cytometry. *Clin Lab*, *61*(9), 1289-1295. https://doi.org/10.7754/clin.lab.2015.141250

Kaul, D. K., Finnegan, E., & Barabino, G. A. (2009). Sickle red cell-endothelium interactions. *Microcirculation*, *16*(1), 97-111. https://doi.org/10.1080/10739680802279394

Kaul, D. K., & Hebbel, R. P. (2000). Hypoxia/reoxygenation causes inflammatory response in transgenic sickle mice but not in normal mice. *J Clin Invest*, *106*(3), 411-420. https://doi.org/10.1172/jci9225

Kaur, S., Raggatt, L. J., Batoon, L., Hume, D. A., Levesque, J. P., & Pettit, A. R. (2017). Role of bone marrow macrophages in controlling homeostasis and repair in bone and bone marrow niches. *Semin Cell Dev Biol*, *61*, 12-21. https://doi.org/10.1016/j.semcdb.2016.08.009

Kaur, S., Raggatt, L. J., Millard, S. M., Wu, A. C., Batoon, L., Jacobsen, R. N., Winkler, I. G., MacDonald, K. P., Perkins, A. C., Hume, D. A., Levesque, J. P., & Pettit, A. R. (2018). Self-repopulating recipient

bone marrow resident macrophages promote long-term hematopoietic stem cell engraftment. *Blood*, *132*(7), 735-749. https://doi.org/10.1182/blood-2018-01-829663

Kawane, K., Fukuyama, H., Kondoh, G., Takeda, J., Ohsawa, Y., Uchiyama, Y., & Nagata, S. (2001). Requirement of DNase II for definitive erythropoiesis in the mouse fetal liver. *Science*, *292*(5521), 1546-1549. https://doi.org/10.1126/science.292.5521.1546

Kerr, J. F. (1965). A histochemical study of hypertrophy and ischaemic injury of rat liver with special reference to changes in lysosomes. *J Pathol Bacteriol*, *90*(2), 419-435. https://doi.org/10.1002/path.1700900210

Kerr, J. F., Wyllie, A. H., & Currie, A. R. (1972). Apoptosis: a basic biological phenomenon with wide-ranging implications in tissue kinetics. *Br J Cancer*, *26*(4), 239-257. https://doi.org/10.1038/bjc.1972.33

Kim, J. W., Kim, M.-J., Han, T.-H., Lee, J.-Y., Kim, S., Kim, H., Oh, K.-J., Kim, W. K., Han, B.-S., Bae, K.-H., Ban, H. S., Bae, S. H., Lee, S. C., Lee, H., & Lee, E.-W. (2023). FSP1 confers ferroptosis resistance in KEAP1 mutant non-small cell lung carcinoma in NRF2-dependent and -independent manner. *Cell Death & Disease*, *14*(8), 567. https://doi.org/10.1038/s41419-023-06070-x

Ko, L. J., & Engel, J. D. (1993). DNA-binding specificities of the GATA transcription factor family. *Mol Cell Biol*, *13*(7), 4011-4022. https://doi.org/10.1128/mcb.13.7.4011-4022.1993

Koehl, B., Vrignaud, C., Mikdar, M., Nair, T. S., Yang, L., Landry, S., Laiguillon, G., Giroux-Lathuile, C., Anselme-Martin, S., El Kenz, H., Hermine, O., Mohandas, N., Cartron, J. P., Colin, Y., Detante, O., Marlu, R., Le Van Kim, C., Carey, T. E., Azouzi, S., & Peyrard, T. (2023). Lack of the human choline transporter-like protein SLC44A2 causes hearing impairment and a rare red blood phenotype. *EMBO Mol Med*, *15*(3), e16320. https://doi.org/10.15252/emmm.202216320

Kokkinopoulos, I., Banos, A., Grigoriou, M., Filia, A., Manolakou, T., Alissafi, T., Malissovas, N., Mitroulis, I., Verginis, P., & Boumpas, D. T. (2021). Patrolling human SLE haematopoietic progenitors demonstrate enhanced extramedullary colonisation; implications for peripheral tissue injury. *Sci Rep*, *11*(1), 15759. https://doi.org/10.1038/s41598-021-95224-y

Kondo, M., Weissman, I. L., & Akashi, K. (1997). Identification of Clonogenic Common Lymphoid Progenitors in Mouse Bone Marrow. *Cell*, *91*(5), 661-672. https://doi.org/https://doi.org/10.1016/S0092-8674(00)80453-5

Koppula, P., Zhuang, L., & Gan, B. (2021). Cystine transporter SLC7A11/xCT in cancer: ferroptosis, nutrient dependency, and cancer therapy. *Protein Cell*, *12*(8), 599-620. https://doi.org/10.1007/s13238-020-00789-5

Koury, M. J., & Bondurant, M. C. (1988). Maintenance by erythropoietin of viability and maturation of murine erythroid precursor cells. *J Cell Physiol*, *137*(1), 65-74. https://doi.org/10.1002/jcp.1041370108

Koury, M. J., & Bondurant, M. C. (1990). Erythropoietin retards DNA breakdown and prevents programmed death in erythroid progenitor cells. *Science*, *248*(4953), 378-381. https://doi.org/10.1126/science.2326648

Kovtunovych, G., Eckhaus, M. A., Ghosh, M. C., Ollivierre-Wilson, H., & Rouault, T. A. (2010). Dysfunction of the heme recycling system in heme oxygenase 1-deficient mice: effects on macrophage viability and tissue iron distribution. *Blood*, *116*(26), 6054-6062. https://doi.org/10.1182/blood-2010-03-272138

Krishnamurti, L., Neuberg, D. S., Sullivan, K. M., Kamani, N. R., Abraham, A., Campigotto, F., Zhang, W., Dahdoul, T., De Castro, L., Parikh, S., Bakshi, N., Haight, A., Hassell, K. L., Loving, R., Rosenthal, J., Smith, S. L., Smith, W., Spearman, M., Stevenson, K., . . . Walters, M. C. (2019). Bone marrow transplantation for adolescents and young adults with sickle cell disease: Results of a prospective multicenter pilot study. *Am J Hematol*, *94*(4), 446-454. https://doi.org/10.1002/ajh.25401

Kroemer, G., El-Deiry, W. S., Golstein, P., Peter, M. E., Vaux, D., Vandenabeele, P., Zhivotovsky, B., Blagosklonny, M. V., Malorni, W., Knight, R. A., Piacentini, M., Nagata, S., & Melino, G. (2005). Classification of cell death: recommendations of the Nomenclature Committee on Cell Death. *Cell Death Differ*, *12 Suppl 2*, 1463-1467. https://doi.org/10.1038/sj.cdd.4401724

Kroemer, G., Galluzzi, L., Vandenabeele, P., Abrams, J., Alnemri, E. S., Baehrecke, E. H., Blagosklonny, M. V., El-Deiry, W. S., Golstein, P., Green, D. R., Hengartner, M., Knight, R. A., Kumar, S., Lipton, S. A., Malorni, W., Nuñez, G., Peter, M. E., Tschopp, J., Yuan, J., . . . Melino, G. (2009). Classification of cell death: recommendations of the Nomenclature Committee on Cell Death 2009. *Cell Death Differ*, *16*(1), 3-11. https://doi.org/10.1038/cdd.2008.150

Kuczynski, C. E., Perisse, I. V., Regouski, M., Alipour, E., LaPradd, C., Liu, Y., Beaty, M. W., Kim-Shapiro, D. B., Atala, A., Polejaeva, I., Porada, C. D., & Almeida-Porada, M. G. (2022). Novel Sheep Model of Sickle Cell Disease Reproduces Human Clinical and Laboratory Parameters. *Blood*, *140*, 8220. https://doi.org/https://doi.org/10.1182/blood-2022-168050

Kuert, S., Holland-Letz, T., Friese, J., & Stachon, A. (2011). Association of nucleated red blood cells in blood and arterial oxygen partial tension. *Clin Chem Lab Med*, *49*(2), 257-263. https://doi.org/10.1515/cclm.2011.041

Kuhrt, D., & Wojchowski, D. M. (2015). Emerging EPO and EPO receptor regulators and signal transducers. *Blood*, *125*(23), 3536-3541. https://doi.org/10.1182/blood-2014-11-575357

Kupzig, S., Parsons, S. F., Curnow, E., Anstee, D. J., & Blair, A. (2017). Superior survival of ex vivo cultured human reticulocytes following transfusion into mice. *Haematologica*, *102*(3), 476-483. https://doi.org/10.3324/haematol.2016.154443

Kwon, M. Y., Park, E., Lee, S. J., & Chung, S. W. (2015). Heme oxygenase-1 accelerates erastin-induced ferroptotic cell death. *Oncotarget*, *6*(27), 24393-24403. https://doi.org/10.18632/oncotarget.5162

Lam, G. Y., Huang, J., & Brumell, J. H. (2010). The many roles of NOX2 NADPH oxidase-derived ROS in immunity. *Semin Immunopathol*, *32*(4), 415-430. https://doi.org/10.1007/s00281-010-0221-0

Laster, S. M., Wood, J. G., & Gooding, L. R. (1988). Tumor necrosis factor can induce both apoptic and necrotic forms of cell lysis. *J Immunol*, *141*(8), 2629-2634.

Lavin, Y., Winter, D., Blecher-Gonen, R., David, E., Keren-Shaul, H., Merad, M., Jung, S., & Amit, I. (2014). Tissue-resident macrophage enhancer landscapes are shaped by the local microenvironment. *Cell*, *159*(6), 1312-1326. https://doi.org/10.1016/j.cell.2014.11.018

Leberbauer, C., Boulme, F., Unfried, G., Huber, J., Beug, H., & Mullner, E. W. (2005). Different steroids co-regulate long-term expansion versus terminal differentiation in primary human erythroid progenitors. *Blood*, *105*(1), 85-94. https://doi.org/10.1182/blood-2004-03-1002

Lee, H., Zandkarimi, F., Zhang, Y., Meena, J. K., Kim, J., Zhuang, L., Tyagi, S., Ma, L., Westbrook, T. F., Steinberg, G. R., Nakada, D., Stockwell, B. R., & Gan, B. (2020). Energy-stress-mediated AMPK activation inhibits ferroptosis. *Nat Cell Biol*, *22*(2), 225-234. https://doi.org/10.1038/s41556-020-0461-8

Lee, J. C., Gimm, J. A., Lo, A. J., Koury, M. J., Krauss, S. W., Mohandas, N., & Chasis, J. A. (2004). Mechanism of protein sorting during erythroblast enucleation: role of cytoskeletal connectivity. *Blood*, *103*(5), 1912-1919. https://doi.org/10.1182/blood-2003-03-0928

Lee, S. H., Crocker, P. R., Westaby, S., Key, N., Mason, D. Y., Gordon, S., & Weatherall, D. J. (1988). Isolation and immunocytochemical characterization of human bone marrow stromal macrophages in hemopoietic clusters. *J Exp Med*, *168*(3), 1193-1198. https://doi.org/10.1084/jem.168.3.1193

Leecharoenkiat, K., Lithanatudom, P., Sornjai, W., & Smith, D. R. (2016). Iron dysregulation in beta-thalassemia. *Asian Pac J Trop Med*, *9*(11), 1035-1043. https://doi.org/10.1016/j.apjtm.2016.07.035

Leibovitch, J. N., Tambe, A. V., Cimpeanu, E., Poplawska, M., Jafri, F., Dutta, D., & Lim, S. H. (2022). l-glutamine, crizanlizumab, voxelotor, and cell-based therapy for adult sickle cell disease: Hype or hope? *Blood Reviews*, *53*, 100925. https://doi.org/https://doi.org/10.1016/j.blre.2021.100925

Leimberg, M. J., Prus, E., Konijn, A. M., & Fibach, E. (2008). Macrophages function as a ferritin iron source for cultured human erythroid precursors. *J Cell Biochem*, *103*(4), 1211-1218. https://doi.org/10.1002/jcb.21499

Leleu, H., Arlet, J. B., Habibi, A., Etienne-Julan, M., Khellaf, M., Adjibi, Y., Pirenne, F., Pitel, M., Granghaud, A., Sinniah, C., De Montalembert, M., & Galacteros, F. (2021). Epidemiology and disease burden of sickle cell disease in France: A descriptive study based on a French nationwide claim database. *PLoS One*, *16*(7), e0253986. https://doi.org/10.1371/journal.pone.0253986

Lemmon, M. A., & Schlessinger, J. (2010). Cell signaling by receptor tyrosine kinases. *Cell*, *141*(7), 1117-1134. https://doi.org/10.1016/j.cell.2010.06.011

Leonard, A., Bonifacino, A., Dominical, V. M., Luo, M., Haro-Mora, J. J., Demirci, S., Uchida, N., Pierciey, F. J., Jr., & Tisdale, J. F. (2019). Bone marrow characterization in sickle cell disease: inflammation and stress erythropoiesis lead to suboptimal CD34 recovery. *Br J Haematol*, *186*(2), 286-299. https://doi.org/10.1111/bjh.15902

Li, J., Hale, J., Bhagia, P., Xue, F., Chen, L., Jaffray, J., Yan, H., Lane, J., Gallagher, P. G., Mohandas, N., Liu, J., & An, X. (2014). Isolation and transcriptome analyses of human erythroid progenitors: BFU-E and CFU-E. *Blood*, *124*(24), 3636-3645. https://doi.org/10.1182/blood-2014-07-588806

Li, L., Hao, Y., Zhao, Y., Wang, H., Zhao, X., Jiang, Y., & Gao, F. (2018). Ferroptosis is associated with oxygen-glucose deprivation/reoxygenation-induced Sertoli cell death. *Int J Mol Med*, *41*(5), 3051-3062. https://doi.org/10.3892/ijmm.2018.3469

Li, Q., Han, X., Lan, X., Gao, Y., Wan, J., Durham, F., Cheng, T., Yang, J., Wang, Z., Jiang, C., Ying, M., Koehler, R. C., Stockwell, B. R., & Wang, J. (2017). Inhibition of neuronal ferroptosis protects hemorrhagic brain. *JCI Insight*, *2*(7), e90777. https://doi.org/10.1172/jci.insight.90777

Li, W., Wang, Y., Zhao, H., Zhang, H., Xu, Y., Wang, S., Guo, X., Huang, Y., Zhang, S., Han, Y., Wu, X., Rice, C. M., Huang, G., Gallagher, P. G., Mendelson, A., Yazdanbakhsh, K., Liu, J., Chen, L., & An, X. (2019). Identification and transcriptome analysis of erythroblastic island macrophages. *Blood*, *134*(5), 480-491. https://doi.org/10.1182/blood.2019000430

Li, Y., Maule, J., Neff, J. L., McCall, C. M., Rapisardo, S., Lagoo, A. S., Yang, L. H., Crawford, R. D., Zhao, Y., & Wang, E. (2019). Myeloid neoplasms in the setting of sickle cell disease: an intrinsic association with the underlying condition rather than a coincidence; report of 4 cases and review of the literature. *Mod Pathol*, *32*(12), 1712-1726. https://doi.org/10.1038/s41379-019-0325-6

Liang, H., Yoo, S. E., Na, R., Walter, C. A., Richardson, A., & Ran, Q. (2009). Short form glutathione peroxidase 4 is the essential isoform required for survival and somatic mitochondrial functions. *J Biol Chem*, *284*(45), 30836-30844. https://doi.org/10.1074/jbc.M109.032839

Liang, R., Menon, V., Qiu, J., Arif, T., Renuse, S., Lin, M., Nowak, R., Hartmann, B., Tzavaras, N., Benson, D. L., Chipuk, J. E., Fribourg, M., Pandey, A., Fowler, V., & Ghaffari, S. (2021). Mitochondrial localization and moderated activity are key to murine erythroid enucleation. *Blood Adv*, *5*(10), 2490-2504. https://doi.org/10.1182/bloodadvances.2021004259

Liao, C., Prabhu, K. S., & Paulson, R. F. (2018). Monocyte-derived macrophages expand the murine stress erythropoietic niche during the recovery from anemia. *Blood*, *132*(24), 2580-2593. https://doi.org/10.1182/blood-2018-06-856831

Lim, J. K. M., Delaidelli, A., Minaker, S. W., Zhang, H. F., Colovic, M., Yang, H., Negri, G. L., von Karstedt, S., Lockwood, W. W., Schaffer, P., Leprivier, G., & Sorensen, P. H. (2019). Cystine/glutamate antiporter xCT (SLC7A11) facilitates oncogenic RAS transformation by preserving intracellular redox balance. *Proc Natl Acad Sci U S A*, *116*(19), 9433-9442. https://doi.org/10.1073/pnas.1821323116

Liu, W., Ostberg, N., Yalcinkaya, M., Dou, H., Endo-Umeda, K., Tang, Y., Hou, X., Xiao, T., Fidler, T. P., Abramowicz, S., Yang, Y. G., Soehnlein, O., Tall, A. R., & Wang, N. (2022). Erythroid lineage Jak2V617F expression promotes atherosclerosis through erythrophagocytosis and macrophage ferroptosis. *J Clin Invest*, *132*(13). https://doi.org/10.1172/JCI155724

Liu, W., Östberg, N., Yalcinkaya, M., Dou, H., Endo-Umeda, K., Tang, Y., Hou, X., Xiao, T., Fidler, T. P., Abramowicz, S., Yang, Y. G., Soehnlein, O., Tall, A. R., & Wang, N. (2022). Erythroid lineage Jak2V617F expression promotes atherosclerosis through erythrophagocytosis and macrophage ferroptosis. *J Clin Invest*, *132*(13). https://doi.org/10.1172/jci155724

Liu, X., Zhang, Y., Ni, M., Cao, H., Signer, R. A. J., Li, D., Li, M., Gu, Z., Hu, Z., Dickerson, K. E., Weinberg, S. E., Chandel, N. S., DeBerardinis, R. J., Zhou, F., Shao, Z., & Xu, J. (2017). Regulation of mitochondrial biogenesis in erythropoiesis by mTORC1-mediated protein translation. *Nat Cell Biol*, *19*(6), 626-638. https://doi.org/10.1038/ncb3527

Liu, Y., Zhong, H., Bao, W., Mendelson, A., An, X., Shi, P., Chou, S. T., Manwani, D., & Yazdanbakhsh, K. (2019). Patrolling monocytes scavenge endothelial-adherent sickle RBCs: a novel mechanism of inhibition of vaso-occlusion in SCD. *Blood*, *134*(7), 579-590. https://doi.org/10.1182/blood.2019000172

Lizarralde Iragorri, M. A., El Hoss, S., Brousse, V., Lefevre, S. D., Dussiot, M., Xu, T., Ferreira, A. R., Lamarre, Y., Silva Pinto, A. C., Kashima, S., Lapouméroulie, C., Covas, D. T., Le Van Kim, C., Colin, Y., Elion, J., Français, O., Le Pioufle, B., & El Nemer, W. (2018). A microfluidic approach to study the effect of mechanical stress on erythrocytes in sickle cell disease. *Lab Chip*, *18*(19), 2975-2984. https://doi.org/10.1039/c8lc00637g

Lopez-Yrigoyen, M., Yang, C.-T., Fidanza, A., Cassetta, L., Taylor, A. H., McCahill, A., Sellink, E., von Lindern, M., van den Akker, E., Mountford, J. C., Pollard, J. W., & Forrester, L. M. (2019). Genetic programming of macrophages generates an in vitro model for the human erythroid island niche. *Nature Communications*, *10*(1), 881. https://doi.org/10.1038/s41467-019-08705-0

Lopez-Yrigoyen, M., Yang, C. T., Fidanza, A., Cassetta, L., Taylor, A. H., McCahill, A., Sellink, E., von Lindern, M., van den Akker, E., Mountford, J. C., Pollard, J. W., & Forrester, L. M. (2019). Genetic programming of macrophages generates an in vitro model for the human erythroid island niche. *Nat Commun*, *10*(1), 881. https://doi.org/10.1038/s41467-019-08705-0

Lou, T. F., Singh, M., Mackie, A., Li, W., & Pace, B. S. (2009). Hydroxyurea generates nitric oxide in human erythroid cells: mechanisms for gamma-globin gene activation. *Exp Biol Med (Maywood)*, *234*(11), 1374-1382. https://doi.org/10.3181/0811-rm-339

Louandre, C., Ezzoukhry, Z., Godin, C., Barbare, J. C., Mazière, J. C., Chauffert, B., & Galmiche, A. (2013). Iron-dependent cell death of hepatocellular carcinoma cells exposed to sorafenib. *Int J Cancer*, *133*(7), 1732-1742. https://doi.org/10.1002/ijc.28159

Luo, S. T., Zhang, D. M., Qin, Q., Lu, L., Luo, M., Guo, F. C., Shi, H. S., Jiang, L., Shao, B., Li, M., Yang, H. S., & Wei, Y. Q. (2017). The Promotion of Erythropoiesis via the Regulation of Reactive Oxygen Species by Lactic Acid. *Sci Rep*, *7*, 38105. https://doi.org/10.1038/srep38105

Lux, C. T., Pattabhi, S., Berger, M., Nourigat, C., Flowers, D. A., Negre, O., Humbert, O., Yang, J. G., Lee, C., Jacoby, K., Bernstein, I., Kiem, H.-P., Scharenberg, A., & Rawlings, D. J. (2019). TALEN-Mediated Gene Editing of HBG in Human Hematopoietic Stem Cells Leads to Therapeutic Fetal Hemoglobin Induction. *Molecular Therapy - Methods & Clinical Development*, *12*, 175-183. https://doi.org/https://doi.org/10.1016/j.omtm.2018.12.008

Magrin, E., Miccio, A., & Cavazzana, M. (2019). Lentiviral and genome-editing strategies for the treatment of β-hemoglobinopathies. *Blood*, *134*(15), 1203-1213. https://doi.org/10.1182/blood.2019000949

Magtanong, L., Ko, P. J., To, M., Cao, J. Y., Forcina, G. C., Tarangelo, A., Ward, C. C., Cho, K., Patti, G. J., Nomura, D. K., Olzmann, J. A., & Dixon, S. J. (2019). Exogenous Monounsaturated Fatty Acids Promote a Ferroptosis-Resistant Cell State. *Cell Chem Biol*, *26*(3), 420-432.e429. https://doi.org/10.1016/j.chembiol.2018.11.016

Magtanong, L., Mueller, G. D., Williams, K. J., Billmann, M., Chan, K., Armenta, D. A., Pope, L. E., Moffat, J., Boone, C., Myers, C. L., Olzmann, J. A., Bensinger, S. J., & Dixon, S. J. (2022). Context-dependent regulation of ferroptosis sensitivity. *Cell Chem Biol*, *29*(9), 1409-1418.e1406. https://doi.org/10.1016/j.chembiol.2022.06.004

Maier-Redelsperger, M., Noguchi, C. T., de Montalembert, M., Rodgers, G. P., Schechter, A. N., Gourbil, A., Blanchard, D., Jais, J. P., Ducrocq, R., Peltier, J. Y., & et al. (1994). Variation in fetal hemoglobin parameters and predicted hemoglobin S polymerization in sickle cell children in the first two years of life: Parisian Prospective Study on Sickle Cell Disease. *Blood*, *84*(9), 3182-3188.

Majeti, R., Park, C. Y., & Weissman, I. L. (2007). Identification of a Hierarchy of Multipotent Hematopoietic Progenitors in Human Cord Blood. *Cell Stem Cell*, *1*(6), 635-645. https://doi.org/https://doi.org/10.1016/j.stem.2007.10.001

Majmundar, A. J., Wong, W. J., & Simon, M. C. (2010). Hypoxia-inducible factors and the response to hypoxic stress. *Mol Cell*, *40*(2), 294-309. https://doi.org/10.1016/j.molcel.2010.09.022

Manci, E. A., Hillery, C. A., Bodian, C. A., Zhang, Z. G., Lutty, G. A., & Coller, B. S. (2006). Pathology of Berkeley sickle cell mice: similarities and differences with human sickle cell disease. *Blood*, *107*(4), 1651-1658. https://doi.org/10.1182/blood-2005-07-2839

Mankelow, T. J., Spring, F. A., Parsons, S. F., Brady, R. L., Mohandas, N., Chasis, J. A., & Anstee, D. J. (2004). Identification of critical amino-acid residues on the erythroid intercellular adhesion molecule-4 (ICAM-4) mediating adhesion to alpha V integrins. *Blood*, *103*(4), 1503-1508. https://doi.org/10.1182/blood-2003-08-2792

Mantel, C., Messina-Graham, S., & Broxmeyer, H. E. (2010). Upregulation of nascent mitochondrial biogenesis in mouse hematopoietic stem cells parallels upregulation of CD34 and loss of pluripotency: a potential strategy for reducing oxidative risk in stem cells. *Cell Cycle*, *9*(10), 2008-2017. https://doi.org/10.4161/cc.9.10.11733

Mantel, C. R., O'Leary, H. A., Chitteti, B. R., Huang, X., Cooper, S., Hangoc, G., Brustovetsky, N., Srour, E. F., Lee, M. R., Messina-Graham, S., Haas, D. M., Falah, N., Kapur, R., Pelus, L. M., Bardeesy, N., Fitamant, J., Ivan, M., Kim, K. S., & Broxmeyer, H. E. (2015). Enhancing Hematopoietic Stem Cell Transplantation Efficacy by Mitigating Oxygen Shock. *Cell*, *161*(7), 1553-1565. https://doi.org/10.1016/j.cell.2015.04.054

Mantovani, A., Sica, A., Sozzani, S., Allavena, P., Vecchi, A., & Locati, M. (2004). The chemokine system in diverse forms of macrophage activation and polarization. *Trends Immunol*, *25*(12), 677-686. https://doi.org/10.1016/j.it.2004.09.015

Mañú Pereira, M. D. M., Colombatti, R., Alvarez, F., Bartolucci, P., Bento, C., Brunetta, A. L., Cela, E., Christou, S., Collado, A., de Montalembert, M., Dedeken, L., Fenaux, P., Galacteros, F., Glenthøj, A., Gutiérrez Valle, V., Kattamis, A., Kunz, J., Lobitz, S., McMahon, C., . . . Gulbis, B. (2023). Sickle cell disease landscape and challenges in the EU: the ERN-EuroBloodNet perspective. *Lancet Haematol*, *10*(8), e687-e694. https://doi.org/10.1016/s2352-3026(23)00182-5

Maria, N. I., Papoin, J., Raparia, C., Sun, Z., Josselsohn, R., Lu, A., Katerji, H., Syeda, M. M., Polsky, D., Paulson, R., Kalfa, T., Barnes, B. J., Zhang, W., Blanc, L., & Davidson, A. (2023). Human TLR8 induces inflammatory bone marrow erythromyeloblastic islands and anemia in SLE-prone mice. *Life Sci Alliance*, *6*(10). https://doi.org/10.26508/lsa.202302241

Mãrtensson, J., & Meister, A. (1991). Glutathione deficiency decreases tissue ascorbate levels in newborn rats: ascorbate spares glutathione and protects. *Proc Natl Acad Sci U S A*, *88*(11), 4656-4660. https://doi.org/10.1073/pnas.88.11.4656

Martinez, F. O., & Gordon, S. (2014). The M1 and M2 paradigm of macrophage activation: time for reassessment. *F1000Prime Rep*, *6*, 13. https://doi.org/10.12703/p6-13

Martyn, G. E., Wienert, B., Yang, L., Shah, M., Norton, L. J., Burdach, J., Kurita, R., Nakamura, Y., Pearson, R. C. M., Funnell, A. P. W., Quinlan, K. G. R., & Crossley, M. (2018). Natural regulatory mutations elevate the fetal globin gene via disruption of BCL11A or ZBTB7A binding. *Nature Genetics*, *50*(4), 498-503. https://doi.org/10.1038/s41588-018-0085-0

Masiuk, K. E., Zhang, R., Osborne, K., Hollis, R. P., Campo-Fernandez, B., & Kohn, D. B. (2019). PGE2 and Poloxamer Synperonic F108 Enhance Transduction of Human HSPCs with a β-Globin Lentiviral Vector. *Mol Ther Methods Clin Dev*, *13*, 390-398. https://doi.org/10.1016/j.omtm.2019.03.005

May, A., & Forrester, L. M. (2020). The erythroblastic island niche: modeling in health, stress, and disease. *Experimental Hematology*, *91*, 10-21. https://doi.org/https://doi.org/10.1016/j.exphem.2020.09.185

McArthur, J. G., Svenstrup, N., Chen, C., Fricot, A., Carvalho, C., Nguyen, J., Nguyen, P., Parachikova, A., Abdulla, F., Vercellotti, G. M., Hermine, O., Edwards, D., Ribeil, J. A., Belcher, J. D., & Maciel, T. T. (2020). A novel, highly potent and selective phosphodiesterase-9 inhibitor for the treatment

of sickle cell disease. *Haematologica*, *105*(3), 623-631. https://doi.org/10.3324/haematol.2018.213462

McBean, G. J. (2012). The transsulfuration pathway: a source of cysteine for glutathione in astrocytes. *Amino Acids*, *42*(1), 199-205. https://doi.org/10.1007/s00726-011-0864-8

McCabe, A., & MacNamara, K. C. (2016). Macrophages: Key regulators of steady-state and demand-adapted hematopoiesis. *Exp Hematol*, *44*(4), 213-222. https://doi.org/10.1016/j.exphem.2016.01.003

McGrath, K. E., Kingsley, P. D., Koniski, A. D., Porter, R. L., Bushnell, T. P., & Palis, J. (2008). Enucleation of primitive erythroid cells generates a transient population of "pyrenocytes" in the mammalian fetus. *Blood*, *111*(4), 2409-2417. https://doi.org/10.1182/blood-2007-08-107581

Meiler, S. E., Wade, M., Kutlar, F., Yerigenahally, S. D., Xue, Y., Moutouh-de Parseval, L. A., Corral, L. G., Swerdlow, P. S., & Kutlar, A. (2011). Pomalidomide augments fetal hemoglobin production without the myelosuppressive effects of hydroxyurea in transgenic sickle cell mice. *Blood*, *118*(4), 1109-1112. https://doi.org/10.1182/blood-2010-11-319137

Mendonça, R., Silveira, A. A., & Conran, N. (2016). Red cell DAMPs and inflammation. *Inflamm Res*, *65*(9), 665-678. https://doi.org/10.1007/s00011-016-0955-9

Menendez-Gonzalez, J. B., Vukovic, M., Abdelfattah, A., Saleh, L., Almotiri, A., Thomas, L. A., Agirre-Lizaso, A., Azevedo, A., Menezes, A. C., Tornillo, G., Edkins, S., Kong, K., Giles, P., Anjos-Afonso, F., Tonks, A., Boyd, A. S., Kranc, K. R., & Rodrigues, N. P. (2019). Gata2 as a Crucial Regulator of Stem Cells in Adult Hematopoiesis and Acute Myeloid Leukemia. *Stem Cell Reports*, *13*(2), 291-306. https://doi.org/10.1016/j.stemcr.2019.07.005

Menon, A. V., Liu, J., Tsai, H. P., Zeng, L., Yang, S., Asnani, A., & Kim, J. (2022). Excess heme upregulates heme oxygenase 1 and promotes cardiac ferroptosis in mice with sickle cell disease. *Blood*, *139*(6), 936-941. https://doi.org/10.1182/blood.2020008455

Mercier, F. E., & Scadden, D. T. (2015). Not All Created Equal: Lineage Hard-Wiring in the Production of Blood. *Cell*, *163*(7), 1568-1570. https://doi.org/10.1016/j.cell.2015.12.013

Mercille, S., & Massie, B. (1994). Induction of apoptosis in nutrient-deprived cultures of hybridoma and myeloma cells. *Biotechnol Bioeng*, *44*(9), 1140-1154. https://doi.org/10.1002/bit.260440916

Metcalf, B., Chuang, C., Dufu, K., Patel, M. P., Silva-Garcia, A., Johnson, C., Lu, Q., Partridge, J. R., Patskovska, L., Patskovsky, Y., Almo, S. C., Jacobson, M. P., Hua, L., Xu, Q., Gwaltney, S. L., 2nd, Yee, C., Harris, J., Morgan, B. P., James, J., . . . Li, Z. (2017). Discovery of GBT440, an Orally Bioavailable R-State Stabilizer of Sickle Cell Hemoglobin. *ACS Med Chem Lett*, *8*(3), 321-326. https://doi.org/10.1021/acsmedchemlett.6b00491

Migliaccio, G., Di Pietro, R., di Giacomo, V., Di Baldassarre, A., Migliaccio, A. R., Maccioni, L., Galanello, R., & Papayannopoulou, T. (2002). In vitro mass production of human erythroid cells from the blood of normal donors and of thalassemic patients. *Blood Cells Mol Dis*, *28*(2), 169-180. https://doi.org/10.1006/bcmd.2002.0502

Miharada, K., Hiroyama, T., Sudo, K., Nagasawa, T., & Nakamura, Y. (2006). Refinement of cytokine use in the in vitro expansion of erythroid cells. *Hum Cell*, *19*(1), 30-37. https://doi.org/10.1111/j.1749-0774.2005.00005.x

Miller, I. J., & Bieker, J. J. (1993). A novel, erythroid cell-specific murine transcription factor that binds to the CACCC element and is related to the Krüppel family of nuclear proteins. *Mol Cell Biol*, *13*(5), 2776-2786. https://doi.org/10.1128/mcb.13.5.2776-2786.1993

Millot, S., Andrieu, V., Letteron, P., Lyoumi, S., Hurtado-Nedelec, M., Karim, Z., Thibaudeau, O., Bennada, S., Charrier, J. L., Lasocki, S., & Beaumont, C. (2010). Erythropoietin stimulates spleen BMP4-dependent stress erythropoiesis and partially corrects anemia in a mouse model of generalized inflammation. *Blood*, *116*(26), 6072-6081. https://doi.org/10.1182/blood-2010-04-281840

Mills, C. D., Kincaid, K., Alt, J. M., Heilman, M. J., & Hill, A. M. (2000). M-1/M-2 macrophages and the Th1/Th2 paradigm. *J Immunol*, *164*(12), 6166-6173. https://doi.org/10.4049/jimmunol.164.12.6166

Minniti, C. P., Tolu, S. S., Wang, K., Yan, Z., Robert, K., Zhang, S., Crouch, A. S., Uehlinger, J., Manwani, D., & Bouhassira, E. E. (2020). HbF Levels in Sickle Cell Disease Are Associated with Proportion of Circulating Hematopoietic Stem and Progenitor Cells and CC-Chemokines. *Cells*, *9*(10). https://doi.org/10.3390/cells9102199

Mitchell, J. R., Jollow, D. J., Potter, W. Z., Gillette, J. R., & Brodie, B. B. (1973). Acetaminophen-induced hepatic necrosis. IV. Protective role of glutathione. *J Pharmacol Exp Ther*, *187*(1), 211-217.

Miyamoto, K., Araki, K. Y., Naka, K., Arai, F., Takubo, K., Yamazaki, S., Matsuoka, S., Miyamoto, T., Ito, K., Ohmura, M., Chen, C., Hosokawa, K., Nakauchi, H., Nakayama, K., Nakayama, K. I., Harada, M., Motoyama, N., Suda, T., & Hirao, A. (2007). Foxo3a is essential for maintenance of the hematopoietic stem cell pool. *Cell Stem Cell*, *1*(1), 101-112. https://doi.org/10.1016/j.stem.2007.02.001

Miyanishi, M., Tada, K., Koike, M., Uchiyama, Y., Kitamura, T., & Nagata, S. (2007). Identification of Tim4 as a phosphatidylserine receptor. *Nature*, *450*(7168), 435-439. https://doi.org/10.1038/nature06307

Mohamad, S. F., Xu, L., Ghosh, J., Childress, P. J., Abeysekera, I., Himes, E. R., Wu, H., Alvarez, M. B., Davis, K. M., Aguilar-Perez, A., Hong, J. M., Bruzzaniti, A., Kacena, M. A., & Srour, E. F. (2017). Osteomacs interact with megakaryocytes and osteoblasts to regulate murine hematopoietic stem cell function. *Blood Adv*, *1*(26), 2520-2528. https://doi.org/10.1182/bloodadvances.2017011304

Mohandas, N., & Prenant, M. (1978). Three-dimensional model of bone marrow. *Blood*, *51*(4), 633-643. https://www.ncbi.nlm.nih.gov/pubmed/630113

Mohyeldin, A., Garzón-Muvdi, T., & Quiñones-Hinojosa, A. (2010). Oxygen in stem cell biology: a critical component of the stem cell niche. *Cell Stem Cell*, *7*(2), 150-161. https://doi.org/10.1016/j.stem.2010.07.007

Montel-Hagen, A., Blanc, L., Boyer-Clavel, M., Jacquet, C., Vidal, M., Sitbon, M., & Taylor, N. (2008). The Glut1 and Glut4 glucose transporters are differentially expressed during perinatal and postnatal erythropoiesis. *Blood*, *112*(12), 4729-4738. https://doi.org/10.1182/blood-2008-05-159269

Moras, M., Lefevre, S. D., & Ostuni, M. A. (2017). From Erythroblasts to Mature Red Blood Cells: Organelle Clearance in Mammals. *Front Physiol*, *8*, 1076. https://doi.org/10.3389/fphys.2017.01076

Moriguchi, T., & Yamamoto, M. (2014). A regulatory network governing Gata1 and Gata2 gene transcription orchestrates erythroid lineage differentiation. *Int J Hematol*, *100*(5), 417-424. https://doi.org/10.1007/s12185-014-1568-0

Morris, C. R., Kato, G. J., Poljakovic, M., Wang, X., Blackwelder, W. C., Sachdev, V., Hazen, S. L., Vichinsky, E. P., Morris, S. M., Jr., & Gladwin, M. T. (2005). Dysregulated arginine metabolism, hemolysis-associated pulmonary hypertension, and mortality in sickle cell disease. *Jama*, *294*(1), 81-90. https://doi.org/10.1001/jama.294.1.81

Moutouh-de Parseval, L. A., Verhelle, D., Glezer, E., Jensen-Pergakes, K., Ferguson, G. D., Corral, L. G., Morris, C. L., Muller, G., Brady, H., & Chan, K. (2008). Pomalidomide and lenalidomide regulate erythropoiesis and fetal hemoglobin production in human CD34+ cells. *J Clin Invest*, *118*(1), 248-258. https://doi.org/10.1172/jci32322

Mueckler, M. (1994). Facilitative glucose transporters. *Eur J Biochem*, *219*(3), 713-725. https://doi.org/10.1111/j.1432-1033.1994.tb18550.x

Mukherjee, K., Xue, L., Planutis, A., Gnanapragasam, M. N., Chess, A., & Bieker, J. J. (2021). EKLF/KLF1 expression defines a unique macrophage subset during mouse erythropoiesis. *Elife*, *10*. https://doi.org/10.7554/eLife.61070

Muller-Sieburg, C. E., Cho, R. H., Karlsson, L., Huang, J. F., & Sieburg, H. B. (2004). Myeloid-biased hematopoietic stem cells have extensive self-renewal capacity but generate diminished lymphoid progeny with impaired IL-7 responsiveness. *Blood*, *103*(11), 4111-4118. https://doi.org/10.1182/blood-2003-10-3448

Müller-Sieburg, C. E., Cho, R. H., Thoman, M., Adkins, B., & Sieburg, H. B. (2002). Deterministic regulation of hematopoietic stem cell self-renewal and differentiation. *Blood*, *100*(4), 1302-1309.

Murray, P. J. (2017). Macrophage Polarization. *Annu Rev Physiol*, *79*, 541-566. https://doi.org/10.1146/annurev-physiol-022516-034339

Nagel, R. L. (1998). A knockout of a transgenic mouse--animal models of sickle cell anemia. *N Engl J Med*, *339*(3), 194-195. https://doi.org/10.1056/nejm199807163390310

Nahrendorf, M., & Swirski, F. K. (2016). Abandoning M1/M2 for a Network Model of Macrophage Function. *Circ Res*, *119*(3), 414-417. https://doi.org/10.1161/circresaha.116.309194

Neildez-Nguyen, T. M., Wajcman, H., Marden, M. C., Bensidhoum, M., Moncollin, V., Giarratana, M. C., Kobari, L., Thierry, D., & Douay, L. (2002). Human erythroid cells produced ex vivo at large scale differentiate into red blood cells in vivo. *Nat Biotechnol*, *20*(5), 467-472. https://doi.org/10.1038/nbt0502-467

Nemeth, E., & Ganz, T. (2014). Anemia of inflammation. *Hematol Oncol Clin North Am*, *28*(4), 671-681, vi. https://doi.org/10.1016/j.hoc.2014.04.005

Netsrithong, R., Suwanpitak, S., Boonkaew, B., Trakarnsanga, K., Chang, L. J., Tipgomut, C., Vatanashevanopakorn, C., Pattanapanyasat, K., & Wattanapanitch, M. (2020). Multilineage differentiation potential of hematoendothelial progenitors derived from human induced pluripotent stem cells. *Stem Cell Res Ther*, *11*(1), 481. https://doi.org/10.1186/s13287-020-01997-w

Neumayr, L. D., Hoppe, C. C., & Brown, C. (2019). Sickle cell disease: current treatment and emerging therapies. *Am J Manag Care*, *25*(18 Suppl), S335-s343.

Newby, G. A., Yen, J. S., Woodard, K. J., Mayuranathan, T., Lazzarotto, C. R., Li, Y., Sheppard-Tillman, H., Porter, S. N., Yao, Y., Mayberry, K., Everette, K. A., Jang, Y., Podracky, C. J., Thaman, E., Lechauve, C., Sharma, A., Henderson, J. M., Richter, M. F., Zhao, K. T., . . . Liu, D. R. (2021). Base editing of haematopoietic stem cells rescues sickle cell disease in mice. *Nature*, *595*(7866), 295-302. https://doi.org/10.1038/s41586-021-03609-w

Nicotera, P., & Melino, G. (2004). Regulation of the apoptosis-necrosis switch. *Oncogene*, *23*(16), 2757-2765. https://doi.org/10.1038/sj.onc.1207559

Niedernhofer, L. J., Daniels, J. S., Rouzer, C. A., Greene, R. E., & Marnett, L. J. (2003). Malondialdehyde, a product of lipid peroxidation, is mutagenic in human cells. *J Biol Chem*, *278*(33), 31426-31433. https://doi.org/10.1074/jbc.M212549200

Niihara, Y., Matsui, N. M., Shen, Y. M., Akiyama, D. A., Johnson, C. S., Sunga, M. A., Magpayo, J., Embury, S. H., Kalra, V. K., Cho, S. H., & Tanaka, K. R. (2005). L-glutamine therapy reduces endothelial adhesion of sickle red blood cells to human umbilical vein endothelial cells. *BMC Blood Disord*, *5*, 4. https://doi.org/10.1186/1471-2326-5-4

Niihara, Y., Miller, S. T., Kanter, J., Lanzkron, S., Smith, W. R., Hsu, L. L., Gordeuk, V. R., Viswanathan, K., Sarnaik, S., Osunkwo, I., Guillaume, E., Sadanandan, S., Sieger, L., Lasky, J. L., Panosyan, E. H., Blake, O. A., New, T. N., Bellevue, R., Tran, L. T., . . . Vichinsky, E. P. (2018). A Phase 3 Trial of l-Glutamine in Sickle Cell Disease. *N Engl J Med*, *379*(3), 226-235. https://doi.org/10.1056/NEJMoa1715971

Niihara, Y., Zerez, C. R., Akiyama, D. S., & Tanaka, K. R. (1998). Oral L-glutamine therapy for sickle cell anemia: I. Subjective clinical improvement and favorable change in red cell NAD redox potential. *Am J Hematol*, *58*(2), 117-121. https://doi.org/10.1002/(sici)1096-8652(199806)58:2<117::aid-ajh5>3.0.co;2-v

Nocka, K., Majumder, S., Chabot, B., Ray, P., Cervone, M., Bernstein, A., & Besmer, P. (1989). Expression of c-kit gene products in known cellular targets of W mutations in normal and W mutant mice--evidence for an impaired c-kit kinase in mutant mice. *Genes Dev*, *3*(6), 816-826. https://doi.org/10.1101/gad.3.6.816

Noguchi, C. T., Rodgers, G. P., & Schechter, A. N. (1989). Intracellular polymerization. Disease severity and therapeutic predictions. *Ann N Y Acad Sci*, *565*, 75-82. https://doi.org/10.1111/j.1749-6632.1989.tb24152.x

Notta, F., Doulatov, S., Laurenti, E., Poeppl, A., Jurisica, I., & Dick, J. E. (2011). Isolation of single human hematopoietic stem cells capable of long-term multilineage engraftment. *Science*, *333*(6039), 218-221. https://doi.org/10.1126/science.1201219

Notta, F., Zandi, S., Takayama, N., Dobson, S., Gan, O. I., Wilson, G., Kaufmann, K. B., McLeod, J., Laurenti, E., Dunant, C. F., McPherson, J. D., Stein, L. D., Dror, Y., & Dick, J. E. (2016). Distinct routes of lineage development reshape the human blood hierarchy across ontogeny. *Science*, *351*(6269), aab2116. https://doi.org/10.1126/science.aab2116

Novershtern, N., Subramanian, A., Lawton, L. N., Mak, R. H., Haining, W. N., McConkey, M. E., Habib, N., Yosef, N., Chang, C. Y., Shay, T., Frampton, G. M., Drake, A. C., Leskov, I., Nilsson, B., Preffer, F., Dombkowski, D., Evans, J. W., Liefeld, T., Smutko, J. S., . . . Ebert, B. L. (2011). Densely interconnected transcriptional circuits control cell states in human hematopoiesis. *Cell*, *144*(2), 296-309. https://doi.org/10.1016/j.cell.2011.01.004

Nyffenegger, N., Zennadi, R., Kalleda, N., Flace, A., Ingoglia, G., Buzzi, R. M., Doucerain, C., Buehler, P. W., Schaer, D. J., Dürrenberger, F., & Manolova, V. (2022). The oral ferroportin inhibitor vamifeport improves hemodynamics in a mouse model of sickle cell disease. *Blood*, *140*(7), 769-781. https://doi.org/https://doi.org/10.1182/blood.2021014716

Oburoglu, L., Romano, M., Taylor, N., & Kinet, S. (2016). Metabolic regulation of hematopoietic stem cell commitment and erythroid differentiation. *Curr Opin Hematol*, *23*(3), 198-205. https://doi.org/10.1097/moh.0000000000000234

Oburoglu, L., Tardito, S., Fritz, V., de Barros, S. C., Merida, P., Craveiro, M., Mamede, J., Cretenet, G., Mongellaz, C., An, X., Klysz, D., Touhami, J., Boyer-Clavel, M., Battini, J. L., Dardalhon, V., Zimmermann, V. S., Mohandas, N., Gottlieb, E., Sitbon, M., . . . Taylor, N. (2014). Glucose and glutamine metabolism regulate human hematopoietic stem cell lineage specification. *Cell Stem Cell*, *15*(2), 169-184. https://doi.org/10.1016/j.stem.2014.06.002

Odièvre, M. H., Verger, E., Silva-Pinto, A. C., & Elion, J. (2011). Pathophysiological insights in sickle cell disease. *Indian J Med Res*, *134*(4), 532-537.

Ofori-Acquah, S. F., Hazra, R., Orikogbo, O. O., Crosby, D., Flage, B., Ackah, E. B., Lenhart, D., Tan, R. J., Vitturi, D. A., Paintsil, V., Owusu-Dabo, E., & Ghosh, S. (2020). Hemopexin deficiency promotes acute kidney injury in sickle cell disease. *Blood*, *135*(13), 1044-1048. https://doi.org/10.1182/blood.2019002653

Oksenberg, D., Dufu, K., Patel, M. P., Chuang, C., Li, Z., Xu, Q., Silva-Garcia, A., Zhou, C., Hutchaleelaha, A., Patskovska, L., Patskovsky, Y., Almo, S. C., Sinha, U., Metcalf, B. W., & Archer, D. R. (2016). GBT440 increases haemoglobin oxygen affinity, reduces sickling and prolongs RBC half-life in a murine model of sickle cell disease. *Br J Haematol*, *175*(1), 141-153. https://doi.org/10.1111/bjh.14214

Olivier, E. N., Marenah, L., McCahill, A., Condie, A., Cowan, S., & Mountford, J. C. (2016). High-Efficiency Serum-Free Feeder-Free Erythroid Differentiation of Human Pluripotent Stem Cells Using Small Molecules. *Stem Cells Transl Med*, *5*(10), 1394-1405. https://doi.org/10.5966/sctm.2015-0371

Orkin, S. H. (1992). GATA-binding transcription factors in hematopoietic cells. *Blood*, *80*(3), 575-581.

Orkin, S. H. (2000). Diversification of haematopoietic stem cells to specific lineages. *Nat Rev Genet*, *1*(1), 57-64. https://doi.org/10.1038/35049577

Ouled-Haddou, H., Messaoudi, K., Demont, Y., Lopes Dos Santos, R., Carola, C., Caulier, A., Vong, P., Jankovsky, N., Lebon, D., Willaume, A., Demagny, J., Boyer, T., Marolleau, J. P., Rochette, J., & Garçon, L. (2020). A new role of glutathione peroxidase 4 during human erythroblast enucleation. *Blood Adv*, *4*(22), 5666-5680. https://doi.org/10.1182/bloodadvances.2020003100

Ovchynnikova, E., Aglialoro, F., von Lindern, M., & van den Akker, E. (2018). The Shape Shifting Story of Reticulocyte Maturation. *Front Physiol*, *9*, 829. https://doi.org/10.3389/fphys.2018.00829

Paikari, A., & Sheehan, V. A. (2018). Fetal haemoglobin induction in sickle cell disease. *Br J Haematol*, *180*(2), 189-200. https://doi.org/10.1111/bjh.15021

Palis, J. (2014). Primitive and definitive erythropoiesis in mammals. *Front Physiol*, *5*, 3. https://doi.org/10.3389/fphys.2014.00003

Panday, A., Sahoo, M. K., Osorio, D., & Batra, S. (2015). NADPH oxidases: an overview from structure to innate immunity-associated pathologies. *Cell Mol Immunol*, *12*(1), 5-23. https://doi.org/10.1038/cmi.2014.89

Park, S. Y., Matte, A., Jung, Y., Ryu, J., Anand, W. B., Han, E. Y., Liu, M., Carbone, C., Melisi, D., Nagasawa, T., Locascio, J. J., Lin, C. P., Silberstein, L. E., & De Franceschi, L. (2020). Pathologic angiogenesis in the bone marrow of humanized sickle cell mice is reversed by blood transfusion. *Blood*, *135*(23), 2071-2084. https://doi.org/10.1182/blood.2019002227

Pászty, C., Brion, C. M., Manci, E., Witkowska, H. E., Stevens, M. E., Mohandas, N., & Rubin, E. M. (1997). Transgenic knockout mice with exclusively human sickle hemoglobin and sickle cell disease. *Science*, *278*(5339), 876-878. https://doi.org/10.1126/science.278.5339.876

Pauling, L., Itano, H. A., & et al. (1949). Sickle cell anemia a molecular disease. *Science*, *110*(2865), 543-548. https://doi.org/10.1126/science.110.2865.543

Pérez, C. (1910). *Recherches histologiques sur la métamorphose des Muscides (Calliphora erythrocephala Mg.)*.

Piattini, F., Matsushita, M., Muri, J., Bretscher, P., Feng, X., Freigang, S., Dalli, J., Schneider, C., & Kopf, M. (2021). Differential sensitivity of inflammatory macrophages and alternatively activated macrophages to ferroptosis. *Eur J Immunol*, *51*(10), 2417-2429. https://doi.org/10.1002/eji.202049114

Piel, F. B., Patil, A. P., Howes, R. E., Nyangiri, O. A., Gething, P. W., Dewi, M., Temperley, W. H., Williams, T. N., Weatherall, D. J., & Hay, S. I. (2013). Global epidemiology of sickle haemoglobin in neonates: a contemporary geostatistical model-based map and population estimates. *Lancet*, *381*(9861), 142-151. https://doi.org/10.1016/s0140-6736(12)61229-x

Piel, F. B., Rees, D. C., DeBaun, M. R., Nnodu, O., Ranque, B., Thompson, A. A., Ware, R. E., Abboud, M. R., Abraham, A., Ambrose, E. E., Andemariam, B., Colah, R., Colombatti, R., Conran, N., Costa, F. F., Cronin, R. M., de Montalembert, M., Elion, J., Esrick, E., . . . Ohene-Frempong, K. (2023). Defining global strategies to improve outcomes in sickle cell disease: a Lancet Haematology Commission. *Lancet Haematol*, *10*(8), e633-e686. https://doi.org/10.1016/s2352-3026(23)00096-0

Piel, F. B., Steinberg, M. H., & Rees, D. C. (2017). Sickle Cell Disease. *N Engl J Med*, *377*(3), 305. https://doi.org/10.1056/NEJMc1706325

Platt, O. S., Brambilla, D. J., Rosse, W. F., Milner, P. F., Castro, O., Steinberg, M. H., & Klug, P. P. (1994). Mortality in sickle cell disease. Life expectancy and risk factors for early death. *N Engl J Med*, *330*(23), 1639-1644. https://doi.org/10.1056/nejm199406093302303

Popescu, D. M., Botting, R. A., Stephenson, E., Green, K., Webb, S., Jardine, L., Calderbank, E. F., Polanski, K., Goh, I., Efremova, M., Acres, M., Maunder, D., Vegh, P., Gitton, Y., Park, J. E., Vento-Tormo, R., Miao, Z., Dixon, D., Rowell, R., . . . Haniffa, M. (2019). Decoding human fetal liver haematopoiesis. *Nature*, *574*(7778), 365-371. https://doi.org/10.1038/s41586-019-1652-y

Popp, R. A., Popp, D. M., Shinpock, S. G., Yang, M. Y., Mural, J. G., Aguinaga, M. P., Kopsombut, P., Roa, P. D., Turner, E. A., & Rubin, E. M. (1997). A transgenic mouse model of hemoglobin S Antilles disease. *Blood*, *89*(11), 4204-4212.

Porcher, C., Chagraoui, H., & Kristiansen, M. S. (2017). SCL/TAL1: a multifaceted regulator from blood development to disease. *Blood*, *129*(15), 2051-2060. https://doi.org/10.1182/blood-2016-12-754051

Porcu, S., Manchinu, M. F., Marongiu, M. F., Sogos, V., Poddie, D., Asunis, I., Porcu, L., Marini, M. G., Moi, P., Cao, A., Grosveld, F., & Ristaldi, M. S. (2011). Klf1 affects DNase II-alpha expression in the central macrophage of a fetal liver erythroblastic island: a non-cell-autonomous role in definitive erythropoiesis. *Mol Cell Biol*, *31*(19), 4144-4154. https://doi.org/10.1128/mcb.05532-11

Porter, J. B., Cappellini, M. D., Kattamis, A., Viprakasit, V., Musallam, K. M., Zhu, Z., & Taher, A. T. (2017). Iron overload across the spectrum of non-transfusion-dependent thalassaemias: role of erythropoiesis, splenectomy and transfusions. *Br J Haematol*, *176*(2), 288-299. https://doi.org/10.1111/bjh.14373

Porter, N. A., Wolf, R. A., Yarbro, E. M., & Weenen, H. (1979). The autoxidation of arachidonic acid: formation of the proposed SRS-A intermediate. *Biochem Biophys Res Commun*, *89*(4), 1058-1064. https://doi.org/10.1016/0006-291x(79)92115-6

Poss, K. D., & Tonegawa, S. (1997). Heme oxygenase 1 is required for mammalian iron reutilization. *Proc Natl Acad Sci U S A*, *94*(20), 10919-10924. https://doi.org/10.1073/pnas.94.20.10919

Powars, D. R., Weiss, J. N., Chan, L. S., & Schroeder, W. A. (1984). Is there a threshold level of fetal hemoglobin that ameliorates morbidity in sickle cell anemia? *Blood*, *63*(4), 921-926.

Pradhan, P., Vijayan, V., Gueler, F., & Immenschuh, S. (2020). Interplay of Heme with Macrophages in Homeostasis and Inflammation. *Int J Mol Sci*, *21*(3). https://doi.org/10.3390/ijms21030740

Pule, G. D., Mowla, S., Novitzky, N., & Wonkam, A. (2016). Hydroxyurea down-regulates BCL11A, KLF-1 and MYB through miRNA-mediated actions to induce γ-globin expression: implications for new therapeutic approaches of sickle cell disease. *Clin Transl Med*, *5*(1), 15. https://doi.org/10.1186/s40169-016-0092-7

Puylaert, P., Roth, L., Van Praet, M., Pintelon, I., Dumitrascu, C., van Nuijs, A., Klejborowska, G., Guns, P. J., Berghe, T. V., Augustyns, K., De Meyer, G. R. Y., & Martinet, W. (2023). Effect of erythrophagocytosis-induced ferroptosis during angiogenesis in atherosclerotic plaques. *Angiogenesis*. https://doi.org/10.1007/s10456-023-09877-6

Raic, A., Rödling, L., Kalbacher, H., & Lee-Thedieck, C. (2014). Biomimetic macroporous PEG hydrogels as 3D scaffolds for the multiplication of human hematopoietic stem and progenitor cells. *Biomaterials*, *35*(3), 929-940. https://doi.org/https://doi.org/10.1016/j.biomaterials.2013.10.038

Ramos, P., Casu, C., Gardenghi, S., Breda, L., Crielaard, B. J., Guy, E., Marongiu, M. F., Gupta, R., Levine, R. L., Abdel-Wahab, O., Ebert, B. L., Van Rooijen, N., Ghaffari, S., Grady, R. W., Giardina, P. J., & Rivella, S. (2013). Macrophages support pathological erythropoiesis in polycythemia vera and β-thalassemia. *Nat Med*, *19*(4), 437-445. https://doi.org/10.1038/nm.3126

Ratan, R. R., Lee, P. J., & Baraban, J. M. (1996). Serum deprivation inhibits glutathione depletion-induced death in embryonic cortical neurons: evidence against oxidative stress as a final common mediator of neuronal apoptosis. *Neurochem Int*, *29*(2), 153-157. https://doi.org/10.1016/0197-0186(95)00115-8

Ratcliffe, E., Glen, K. E., Workman, V. L., Stacey, A. J., & Thomas, R. J. (2012). A novel automated bioreactor for scalable process optimisation of haematopoietic stem cell culture. *J Biotechnol*, *161*(3), 387-390. https://doi.org/10.1016/j.jbiotec.2012.06.025

Rees, D. C., Williams, T. N., & Gladwin, M. T. (2010). Sickle-cell disease. *The Lancet*, *376*(9757), 2018-2031. https://doi.org/https://doi.org/10.1016/S0140-6736(10)61029-X

Rhoda, M.-D., Domenget, C., Vidaud, M., Bardakdjian-Michau, J., Rouyer-Fessard, P., Rosa, J., & Beuzard, Y. (1988). Mouse α chains inhibit polymerization of hemoglobin induced by human βS or βS Antilles chains. *Biochimica et Biophysica Acta (BBA) - Protein Structure and Molecular Enzymology*, *952*, 208-212. https://doi.org/https://doi.org/10.1016/0167-4838(88)90117-3

Ribeil, J. A., Arlet, J. B., Dussiot, M., Moura, I. C., Courtois, G., & Hermine, O. (2013). Ineffective erythropoiesis in β -thalassemia. *ScientificWorldJournal*, *2013*, 394295. https://doi.org/10.1155/2013/394295

Ribeil, J. A., Hacein-Bey-Abina, S., Payen, E., Magnani, A., Semeraro, M., Magrin, E., Caccavelli, L., Neven, B., Bourget, P., El Nemer, W., Bartolucci, P., Weber, L., Puy, H., Meritet, J. F., Grevent, D., Beuzard, Y., Chrétien, S., Lefebvre, T., Ross, R. W., . . . Cavazzana, M. (2017). Gene Therapy in a Patient with Sickle Cell Disease. *N Engl J Med*, *376*(9), 848-855. https://doi.org/10.1056/NEJMoa1609677

Ribeil, J. A., Zermati, Y., Vandekerckhove, J., Cathelin, S., Kersual, J., Dussiot, M., Coulon, S., Moura, I. C., Zeuner, A., Kirkegaard-Sørensen, T., Varet, B., Solary, E., Garrido, C., & Hermine, O. (2007). Hsp70 regulates erythropoiesis by preventing caspase-3-mediated cleavage of GATA-1. *Nature*, *445*(7123), 102-105. https://doi.org/10.1038/nature05378

Rogers, H. M., Yu, X., Wen, J., Smith, R., Fibach, E., & Noguchi, C. T. (2008). Hypoxia alters progression of the erythroid program. *Exp Hematol*, *36*(1), 17-27. https://doi.org/10.1016/j.exphem.2007.08.014

Romano, L., Seu, K. G., Blanc, L., & Kalfa, T. A. (2023). Crosstalk between terminal erythropoiesis and granulopoiesis within their common niche: the erythromyeloblastic island. *Curr Opin Hematol*, *30*(4), 99-105. https://doi.org/10.1097/moh.0000000000000767

Romano, L., Seu, K. G., Papoin, J., Muench, D. E., Konstantinidis, D., Olsson, A., Schlum, K., Chetal, K., Chasis, J. A., Mohandas, N., Barnes, B. J., Zheng, Y., Grimes, H. L., Salomonis, N., Blanc, L., & Kalfa, T. A. (2022). Erythroblastic islands foster granulopoiesis in parallel to terminal erythropoiesis. *Blood*, *140*(14), 1621-1634. https://doi.org/10.1182/blood.2022015724

Rosin, C., Bates, T. E., & Skaper, S. D. (2004). Excitatory amino acid induced oligodendrocyte cell death in vitro: receptor-dependent and -independent mechanisms. *J Neurochem*, *90*(5), 1173-1185. https://doi.org/10.1111/j.1471-4159.2004.02584.x

Ross, D., & Siegel, D. (2017). Functions of NQO1 in Cellular Protection and CoQ(10) Metabolism and its Potential Role as a Redox Sensitive Molecular Switch. *Front Physiol*, *8*, 595. https://doi.org/10.3389/fphys.2017.00595

Roszer, T. (2015). Understanding the Mysterious M2 Macrophage through Activation Markers and Effector Mechanisms. *Mediators Inflamm*, *2015*, 816460. https://doi.org/10.1155/2015/816460

Rouzer, C. A., & Marnett, L. J. (2003). Mechanism of free radical oxygenation of polyunsaturated fatty acids by cyclooxygenases. *Chem Rev*, *103*(6), 2239-2304. https://doi.org/10.1021/cr000068x

Rubin, E. M., Witkowska, H. E., Spangler, E., Curtin, P., Lubin, B. H., Mohandas, N., & Clift, S. M. (1991). Hypoxia-induced in vivo sickling of transgenic mouse red cells. *J Clin Invest*, *87*(2), 639-647. https://doi.org/10.1172/jci115041

Ryan, T. M., Ciavatta, D. J., & Townes, T. M. (1997). Knockout-transgenic mouse model of sickle cell disease. *Science*, *278*(5339), 873-876. https://doi.org/10.1126/science.278.5339.873

Sadahira, Y., Yoshino, T., & Monobe, Y. (1995). Very late activation antigen 4-vascular cell adhesion molecule 1 interaction is involved in the formation of erythroblastic islands. *J Exp Med*, *181*(1), 411-415. https://doi.org/10.1084/jem.181.1.411

Sawada, K., Krantz, S. B., Dessypris, E. N., Koury, S. T., & Sawyer, S. T. (1989). Human colony-forming units-erythroid do not require accessory cells, but do require direct interaction with insulin-like growth factor I and/or insulin for erythroid development. *J Clin Invest*, *83*(5), 1701-1709. https://doi.org/10.1172/jci114070

Schallmeiner, E., Oksanen, E., Ericsson, O., Spångberg, L., Eriksson, S., Stenman, U. H., Pettersson, K., & Landegren, U. (2007). Sensitive protein detection via triple-binder proximity ligation assays. *Nat Methods*, *4*(2), 135-137. https://doi.org/10.1038/nmeth974

Schindelin, J., Arganda-Carreras, I., Frise, E., Kaynig, V., Longair, M., Pietzsch, T., Preibisch, S., Rueden, C., Saalfeld, S., Schmid, B., Tinevez, J. Y., White, D. J., Hartenstein, V., Eliceiri, K., Tomancak, P., & Cardona, A. (2012). Fiji: an open-source platform for biological-image analysis. *Nat Methods*, *9*(7), 676-682. https://doi.org/10.1038/nmeth.2019

Schippel, N., & Sharma, S. (2023). Dynamics of human hematopoietic stem and progenitor cell differentiation to the erythroid lineage. *Exp Hematol*, *123*, 1-17. https://doi.org/10.1016/j.exphem.2023.05.001

Schubert, D., Kimura, H., & Maher, P. (1992). Growth factors and vitamin E modify neuronal glutamate toxicity. *Proc Natl Acad Sci U S A*, *89*(17), 8264-8267. https://doi.org/10.1073/pnas.89.17.8264

Schuckelt, R., Brigelius-Flohé, R., Maiorino, M., Roveri, A., Reumkens, J., Strassburger, W., Ursini, F., Wolf, B., & Flohé, L. (1991). Phospholipid hydroperoxide glutathione peroxidase is a selenoenzyme distinct from the classical glutathione peroxidase as evident from cDNA and amino acid sequencing. *Free Radic Res Commun*, *14*(5-6), 343-361. https://doi.org/10.3109/10715769109093424

Schulz, C., Gomez Perdiguero, E., Chorro, L., Szabo-Rogers, H., Cagnard, N., Kierdorf, K., Prinz, M., Wu, B., Jacobsen, S. E., Pollard, J. W., Frampton, J., Liu, K. J., & Geissmann, F. (2012). A lineage of

myeloid cells independent of Myb and hematopoietic stem cells. *Science*, *336*(6077), 86-90. https://doi.org/10.1126/science.1219179

Schweichel, J. U., & Merker, H. J. (1973). The morphology of various types of cell death in prenatal tissues. *Teratology*, *7*(3), 253-266. https://doi.org/10.1002/tera.1420070306

Scott, C. L., Zheng, F., De Baetselier, P., Martens, L., Saeys, Y., De Prijck, S., Lippens, S., Abels, C., Schoonooghe, S., Raes, G., Devoogdt, N., Lambrecht, B. N., Beschin, A., & Guilliams, M. (2016). Bone marrow-derived monocytes give rise to self-renewing and fully differentiated Kupffer cells. *Nat Commun*, *7*, 10321. https://doi.org/10.1038/ncomms10321

Seminog, O. O., Ogunlaja, O. I., Yeates, D., & Goldacre, M. J. (2016). Risk of individual malignant neoplasms in patients with sickle cell disease: English national record linkage study. *J R Soc Med*, *109*(8), 303-309. https://doi.org/10.1177/0141076816651037

Sengupta, A., Lichti, U. F., Carlson, B. A., Cataisson, C., Ryscavage, A. O., Mikulec, C., Conrad, M., Fischer, S. M., Hatfield, D. L., & Yuspa, S. H. (2013). Targeted disruption of glutathione peroxidase 4 in mouse skin epithelial cells impairs postnatal hair follicle morphogenesis that is partially rescued through inhibition of COX-2. *J Invest Dermatol*, *133*(7), 1731-1741. https://doi.org/10.1038/jid.2013.52

Sesti-Costa, R., Costa, F. F., & Conran, N. (2023). Role of Macrophages in Sickle Cell Disease Erythrophagocytosis and Erythropoiesis. *Int J Mol Sci*, *24*(7). https://doi.org/10.3390/ijms24076333

Seu, K. G., Papoin, J., Fessler, R., Hom, J., Huang, G., Mohandas, N., Blanc, L., & Kalfa, T. A. (2017). Unraveling Macrophage Heterogeneity in Erythroblastic Islands. *Front Immunol*, *8*, 1140. https://doi.org/10.3389/fimmu.2017.01140

Severn, C. E., Eissa, A. M., Langford, C. R., Parker, A., Walker, M., Dobbe, J. G. G., Streekstra, G. J., Cameron, N. R., & Toye, A. M. (2019). Ex vivo culture of adult CD34(+) stem cells using functional highly porous polymer scaffolds to establish biomimicry of the bone marrow niche. *Biomaterials*, *225*, 119533. https://doi.org/10.1016/j.biomaterials.2019.119533

Severn, C. E., & Toye, A. M. (2018). The challenge of growing enough reticulocytes for transfusion. *ISBT Science Series*, *13*(1), 80-86. https://doi.org/https://doi.org/10.1111/voxs.12374

Sewchand, L. S., Johnson, C. S., & Meiselman, H. J. (1983). The effect of fetal hemoglobin on the sickling dynamics of SS erythrocytes. *Blood Cells*, *9*(1), 147-166.

Sharma, R., Antypiuk, A., Vance, S. Z., Manwani, D., Pearce, Q., Cox, J. E., An, X., Yazdanbakhsh, K., & Vinchi, F. (2023). Macrophage metabolic rewiring improves heme-suppressed efferocytosis and tissue damage in sickle cell disease. *Blood*, *141*(25), 3091-3108. https://doi.org/10.1182/blood.2022018026

Shay, J. W., & Wright, W. E. (2000). Hayflick, his limit, and cellular ageing. *Nat Rev Mol Cell Biol*, *1*(1), 72-76. https://doi.org/10.1038/35036093

Shet, A. S., Lizarralde-Iragorri, M. A., & Naik, R. P. (2020). The molecular basis for the prothrombotic state in sickle cell disease. *Haematologica*, *105*(10), 2368-2379. https://doi.org/10.3324/haematol.2019.239350

Shin, D., Kim, E. H., Lee, J., & Roh, J. L. (2018). Nrf2 inhibition reverses resistance to GPX4 inhibitor-induced ferroptosis in head and neck cancer. *Free Radic Biol Med*, *129*, 454-462. https://doi.org/10.1016/j.freeradbiomed.2018.10.426

Shinar, E., Rachmilewitz, E. A., & Lux, S. E. (1989). Differing erythrocyte membrane skeletal protein defects in alpha and beta thalassemia. *J Clin Invest*, *83*(2), 404-410. https://doi.org/10.1172/jci113898

Shrestha, A., Chi, M., Wagner, K., Malik, A., Korpik, J., Drake, A., Fulzele, K., Guichard, S., & Malik, P. (2021). FT-4202, an oral PKR activator, has potent antisickling effects and improves RBC survival and Hb levels in SCA mice. *Blood Adv*, *5*(9), 2385-2390. https://doi.org/10.1182/bloodadvances.2020003604

Shui, S., Zhao, Z., Wang, H., Conrad, M., & Liu, G. (2021). Non-enzymatic lipid peroxidation initiated by photodynamic therapy drives a distinct ferroptosis-like cell death pathway. *Redox Biol*, *45*, 102056. https://doi.org/10.1016/j.redox.2021.102056

Silva, M., Grillot, D., Benito, A., Richard, C., Nunez, G., & Fernandez-Luna, J. L. (1996). Erythropoietin can promote erythroid progenitor survival by repressing apoptosis through Bcl-XL and Bcl-2. *Blood*, *88*(5), 1576-1582. https://www.ncbi.nlm.nih.gov/pubmed/8781412

Singhal, R., Mitta, S. R., Das, N. K., Kerk, S. A., Sajjakulnukit, P., Solanki, S., Andren, A., Kumar, R., Olive, K. P., Banerjee, R., Lyssiotis, C. A., & Shah, Y. M. (2021). HIF-2α activation potentiates oxidative cell death in colorectal cancers by increasing cellular iron. *J Clin Invest*, *131*(12). https://doi.org/10.1172/jci143691

Solovey, A., Lin, Y., Browne, P., Choong, S., Wayner, E., & Hebbel, R. P. (1997). Circulating activated endothelial cells in sickle cell anemia. *N Engl J Med*, *337*(22), 1584-1590. https://doi.org/10.1056/nejm199711273372203

Song, X., Xie, Y., Kang, R., Hou, W., Sun, X., Epperly, M. W., Greenberger, J. S., & Tang, D. (2016). FANCD2 protects against bone marrow injury from ferroptosis. *Biochem Biophys Res Commun*, *480*(3), 443-449. https://doi.org/10.1016/j.bbrc.2016.10.068

Soni, S., Bala, S., Gwynn, B., Sahr, K. E., Peters, L. L., & Hanspal, M. (2006). Absence of erythroblast macrophage protein (Emp) leads to failure of erythroblast nuclear extrusion. *J Biol Chem*, *281*(29), 20181-20189. https://doi.org/10.1074/jbc.M603226200

Soni, S., Bala, S., & Hanspal, M. (2008). Requirement for erythroblast-macrophage protein (Emp) in definitive erythropoiesis. *Blood Cells Mol Dis*, *41*(2), 141-147. https://doi.org/10.1016/j.bcmd.2008.03.008

Spivak, J. L., Pham, T., Isaacs, M., & Hankins, W. D. (1991). Erythropoietin is both a mitogen and a survival factor. *Blood*, *77*(6), 1228-1233. https://www.ncbi.nlm.nih.gov/pubmed/1705834

Spring, F. A., Griffiths, R. E., Mankelow, T. J., Agnew, C., Parsons, S. F., Chasis, J. A., & Anstee, D. J. (2013). Tetraspanins CD81 and CD82 facilitate alpha4beta1-mediated adhesion of human erythroblasts to vascular cell adhesion molecule-1. *PLoS One*, *8*(5), e62654. https://doi.org/10.1371/journal.pone.0062654

Stamatoyannopoulos, G., Veith, R., Galanello, R., & Papayannopoulou, T. (1985). Hb F production in stressed erythropoiesis: observations and kinetic models. *Ann N Y Acad Sci*, *445*, 188-197. https://doi.org/10.1111/j.1749-6632.1985.tb17188.x

Stephenson, J. R., Axelrad, A. A., McLeod, D. L., & Shreeve, M. M. (1971). Induction of Colonies of Hemoglobin-Synthesizing Cells by Erythropoietin In Vitro. *Proceedings of the National Academy of Sciences*, *68*(7), 1542-1546. https://doi.org/doi:10.1073/pnas.68.7.1542

Storti, F., Santambrogio, S., Crowther, L. M., Otto, T., Abreu-Rodríguez, I., Kaufmann, M., Hu, C. J., Dame, C., Fandrey, J., Wenger, R. H., & Hoogewijs, D. (2014). A novel distal upstream hypoxia response element regulating oxygen-dependent erythropoietin gene expression. *Haematologica*, *99*(4), e45-48. https://doi.org/10.3324/haematol.2013.102707

Suda, T., Takubo, K., & Semenza, G. L. (2011). Metabolic regulation of hematopoietic stem cells in the hypoxic niche. *Cell Stem Cell*, *9*(4), 298-310. https://doi.org/10.1016/j.stem.2011.09.010

Sui, X., Krantz, S. B., & Zhao, Z. J. (2000). Stem cell factor and erythropoietin inhibit apoptosis of human erythroid progenitor cells through different signalling pathways. *Br J Haematol*, *110*(1), 63-70. https://doi.org/10.1046/j.1365-2141.2000.02145.x

Sun, X., Ou, Z., Chen, R., Niu, X., Chen, D., Kang, R., & Tang, D. (2016). Activation of the p62-Keap1-NRF2 pathway protects against ferroptosis in hepatocellular carcinoma cells. *Hepatology*, *63*(1), 173-184. https://doi.org/10.1002/hep.28251

Sunami, K., Yamane, H., Konishi, K., Iguchi, H., Nakagawa, T., Shibata, S., Takayama, M., & Nakai, Y. (1998). Role of amino acids in cochlear degeneration: deprivation of cystine induces death of cochlear hair cells of guinea pigs in vitro. *Acta Otolaryngol Suppl*, *538*, 19-21. https://doi.org/10.1080/00016489850182675-2

Suttner, D. M., & Dennery, P. A. (1999). Reversal of HO-1 related cytoprotection with increased expression is due to reactive iron. *Faseb j*, *13*(13), 1800-1809. https://doi.org/10.1096/fasebj.13.13.1800

Takahashi, K., Donovan, M. J., Rogers, R. A., & Ezekowitz, R. A. (1998). Distribution of murine mannose receptor expression from early embryogenesis through to adulthood. *Cell Tissue Res*, *292*(2), 311-323. https://doi.org/10.1007/s004410051062

Takubo, K., Nagamatsu, G., Kobayashi, C. I., Nakamura-Ishizu, A., Kobayashi, H., Ikeda, E., Goda, N., Rahimi, Y., Johnson, R. S., Soga, T., Hirao, A., Suematsu, M., & Suda, T. (2013). Regulation of glycolysis by Pdk functions as a metabolic checkpoint for cell cycle quiescence in hematopoietic stem cells. *Cell Stem Cell*, *12*(1), 49-61. https://doi.org/10.1016/j.stem.2012.10.011

Tan, S., Schubert, D., & Maher, P. (2001). Oxytosis: A novel form of programmed cell death. *Curr Top Med Chem*, *1*(6), 497-506. https://doi.org/10.2174/1568026013394741

Tay, J., Bisht, K., McGirr, C., Millard, S. M., Pettit, A. R., Winkler, I. G., & Levesque, J. P. (2020). Imaging flow cytometry reveals that granulocyte colony-stimulating factor treatment causes loss of erythroblastic islands in the mouse bone marrow. *Exp Hematol*, *82*, 33-42. https://doi.org/10.1016/j.exphem.2020.02.003

Thomson, A. M., McHugh, T. A., Oron, A. P., Teply, C., Lonberg, N., Vilchis Tella, V., Wilner, L. B., Fuller, K., Hagins, H., Aboagye, R. G., Aboye, M. B., Abu-Gharbieh, E., Abu-Zaid, A., Addo, I. Y., Ahinkorah, B. O., Ahmad, A., AlRyalat, S. A. S., Amu, H., Aravkin, A. Y., . . . Kassebaum, N. J. (2023). Global, regional, and national prevalence and mortality burden of sickle cell disease, 2000–2021: a systematic analysis from the Global Burden of Disease Study 2021. *The Lancet Haematology*, *10*(8), e585-e599. https://doi.org/https://doi.org/10.1016/S2352-3026(23)00118-7

Tierney, J. B., Kharkrang, M., & La Flamme, A. C. (2009). Type II-activated macrophages suppress the development of experimental autoimmune encephalomyelitis. *Immunol Cell Biol*, *87*(3), 235-240. https://doi.org/10.1038/icb.2008.99

Timmins, N. E., Athanasas, S., Günther, M., Buntine, P., & Nielsen, L. K. (2011). Ultra-high-yield manufacture of red blood cells from hematopoietic stem cells. *Tissue Eng Part C Methods*, *17*(11), 1131-1137. https://doi.org/10.1089/ten.TEC.2011.0207

Tirelli, V., Ghinassi, B., Migliaccio, A. R., Whitsett, C., Masiello, F., Sanchez, M., & Migliaccio, G. (2011). Phenotypic definition of the progenitor cells with erythroid differentiation potential present in human adult blood. *Stem Cells Int*, *2011*, 602483. https://doi.org/10.4061/2011/602483

Toda, S., Segawa, K., & Nagata, S. (2014). MerTK-mediated engulfment of pyrenocytes by central macrophages in erythroblastic islands. *Blood*, *123*(25), 3963-3971. https://doi.org/10.1182/blood-2014-01-547976

Tolu, S. S., Wang, K., Yan, Z., Zhang, S., Roberts, K., Crouch, A. S., Sebastian, G., Chaitowitz, M., Fornari, E. D., Schwechter, E. M., Uehlinger, J., Manwani, D., Minniti, C. P., & Bouhassira, E. E. (2020). Characterization of Hematopoiesis in Sickle Cell Disease by Prospective Isolation of Stem and Progenitor Cells. *Cells*, *9*(10). https://doi.org/10.3390/cells9102159

Tordjman, R., Delaire, S., Plouet, J., Ting, S., Gaulard, P., Fichelson, S., Romeo, P. H., & Lemarchandel, V. (2001). Erythroblasts are a source of angiogenic factors. *Blood*, *97*(7), 1968-1974. https://doi.org/10.1182/blood.v97.7.1968

Tran, H., Sagi, V., Leonce Song-Naba, W., Wang, Y., Mittal, A., Lamarre, Y., Zhang, L., & Gupta, K. (2019). Effect of chronic opioid therapy on pain and survival in a humanized mouse model of sickle cell disease. *Blood Adv*, *3*(6), 869-873. https://doi.org/10.1182/bloodadvances.2018024299

Traxler, E. A., Yao, Y., Wang, Y.-D., Woodard, K. J., Kurita, R., Nakamura, Y., Hughes, J. R., Hardison, R. C., Blobel, G. A., Li, C., & Weiss, M. J. (2016). A genome-editing strategy to treat β-hemoglobinopathies that recapitulates a mutation associated with a benign genetic condition. *Nature Medicine*, *22*(9), 987-990. https://doi.org/10.1038/nm.4170

Trucas, M., Burattini, S., Porcu, S., Simbula, M., Ristaldi, M. S., Kowalik, M. A., Serra, M. P., Gobbi, P., Battistelli, M., Perra, A., & Quartu, M. (2023). Multi-Organ Morphological Findings in a Humanized Murine Model of Sickle Cell Trait. *Int J Mol Sci*, *24*(13). https://doi.org/10.3390/ijms241310452

Trudel, M., Saadane, N., Garel, M. C., Bardakdjian-Michau, J., Blouquit, Y., Guerquin-Kern, J. L., Rouyer-Fessard, P., Vidaud, D., Pachnis, A., Roméo, P. H., & et al. (1991). Towards a transgenic mouse

model of sickle cell disease: hemoglobin SAD. *Embo j*, *10*(11), 3157-3165. https://doi.org/10.1002/j.1460-2075.1991.tb04877.x

Uchida, N., Hsieh, M. M., Raines, L., Haro-Mora, J. J., Demirci, S., Bonifacino, A. C., Krouse, A. E., Metzger, M. E., Donahue, R. E., & Tisdale, J. F. (2019). Development of a forward-oriented therapeutic lentiviral vector for hemoglobin disorders. *Nature Communications*, *10*(1), 4479. https://doi.org/10.1038/s41467-019-12456-3

Urbinati, F., Campo Fernandez, B., Masiuk, K. E., Poletti, V., Hollis, R. P., Koziol, C., Kaufman, M. L., Brown, D., Mavilio, F., & Kohn, D. B. (2018). Gene Therapy for Sickle Cell Disease: A Lentiviral Vector Comparison Study. *Hum Gene Ther*, *29*(10), 1153-1166. https://doi.org/10.1089/hum.2018.061

van de Laar, L., Saelens, W., De Prijck, S., Martens, L., Scott, C. L., Van Isterdael, G., Hoffmann, E., Beyaert, R., Saeys, Y., Lambrecht, B. N., & Guilliams, M. (2016). Yolk Sac Macrophages, Fetal Liver, and Adult Monocytes Can Colonize an Empty Niche and Develop into Functional Tissue-Resident Macrophages. *Immunity*, *44*(4), 755-768. https://doi.org/10.1016/j.immuni.2016.02.017

van den Akker, E., Satchwell, T. J., Pellegrin, S., Daniels, G., & Toye, A. M. (2010). The majority of the in vitro erythroid expansion potential resides in CD34(-) cells, outweighing the contribution of CD34(+) cells and significantly increasing the erythroblast yield from peripheral blood samples. *Haematologica*, *95*(9), 1594-1598. https://doi.org/10.3324/haematol.2009.019828

van Furth, R., & Cohn, Z. A. (1968). The origin and kinetics of mononuclear phagocytes. *J Exp Med*, *128*(3), 415-435. https://doi.org/10.1084/jem.128.3.415

Velten, L., Haas, S. F., Raffel, S., Blaszkiewicz, S., Islam, S., Hennig, B. P., Hirche, C., Lutz, C., Buss, E. C., Nowak, D., Boch, T., Hofmann, W. K., Ho, A. D., Huber, W., Trumpp, A., Essers, M. A., & Steinmetz, L. M. (2017). Human haematopoietic stem cell lineage commitment is a continuous process. *Nat Cell Biol*, *19*(4), 271-281. https://doi.org/10.1038/ncb3493

Verma, H., Lakkakula, S., & Lakkakula, B. (2018). Retrospection of the effect of hydroxyurea treatment in patients with sickle cell disease. *Acta haematologica Polonica*, *49*, 1-8. https://doi.org/10.2478/ahp-2018-0001

Vermylen, C., Cornu, G., Ferster, A., Brichard, B., Ninane, J., Ferrant, A., Zenebergh, A., Maes, P., Dhooge, C., Benoit, Y., Beguin, Y., Dresse, M. F., & Sariban, E. (1998). Haematopoietic stem cell transplantation for sickle cell anaemia: the first 50 patients transplanted in Belgium. *Bone Marrow Transplant*, *22*(1), 1-6. https://doi.org/10.1038/sj.bmt.1701291

Vichinsky, E., Hoppe, C. C., Ataga, K. I., Ware, R. E., Nduba, V., El-Beshlawy, A., Hassab, H., Achebe, M. M., Alkindi, S., Brown, R. C., Diuguid, D. L., Telfer, P., Tsitsikas, D. A., Elghandour, A., Gordeuk, V. R., Kanter, J., Abboud, M. R., Lehrer-Graiwer, J., Tonda, M., . . . Howard, J. (2019). A Phase 3 Randomized Trial of Voxelotor in Sickle Cell Disease. *N Engl J Med*, *381*(6), 509-519. https://doi.org/10.1056/NEJMoa1903212

Vinchi, F., Costa da Silva, M., Ingoglia, G., Petrillo, S., Brinkman, N., Zuercher, A., Cerwenka, A., Tolosano, E., & Muckenthaler, M. U. (2016). Hemopexin therapy reverts heme-induced proinflammatory phenotypic switching of macrophages in a mouse model of sickle cell disease. *Blood*, *127*(4), 473-486. https://doi.org/10.1182/blood-2015-08-663245

Vogt, K. C. (1842). *Untersuchungen über die Entwicklungsgeschichte der Geburtshelferkrœte (Alytes obstetricans)*. Verlag von Jent & Gassmann.

Wagner, B. A., Buettner, G. R., & Burns, C. P. (1994). Free radical-mediated lipid peroxidation in cells: oxidizability is a function of cell lipid bis-allylic hydrogen content. *Biochemistry*, *33*(15), 4449-4453. https://doi.org/10.1021/bi00181a003

Walker, A. L., Steward, S., Howard, T. A., Mortier, N., Smeltzer, M., Wang, Y. D., & Ware, R. E. (2011). Epigenetic and molecular profiles of erythroid cells after hydroxyurea treatment in sickle cell anemia. *Blood*, *118*(20), 5664-5670. https://doi.org/10.1182/blood-2011-07-368746

Walters, M. C., Patience, M., Leisenring, W., Eckman, J. R., Buchanan, G. R., Rogers, Z. R., Olivieri, N. E., Vichinsky, E., Davies, S. C., Mentzer, W. C., Powars, D., Scott, J. P., Bernaudin, F., Ohene-Frempong, K., Darbyshire, P. J., Wayne, A., Roberts, I. A., Dinndorf, P., Brandalise, S., . . . Sullivan,

K. M. (1996). Barriers to bone marrow transplantation for sickle cell anemia. *Biol Blood Marrow Transplant*, *2*(2), 100-104.

Walters, M. C., Storb, R., Patience, M., Leisenring, W., Taylor, T., Sanders, J. E., Buchanan, G. E., Rogers, Z. R., Dinndorf, P., Davies, S. C., Roberts, I. A., Dickerhoff, R., Yeager, A. M., Hsu, L., Kurtzberg, J., Ohene-Frempong, K., Bunin, N., Bernaudin, F., Wong, W. Y., . . . Sullivan, K. M. (2000). Impact of bone marrow transplantation for symptomatic sickle cell disease: an interim report. Multicenter investigation of bone marrow transplantation for sickle cell disease. *Blood*, *95*(6), 1918-1924.

Wang, H., An, P., Xie, E., Wu, Q., Fang, X., Gao, H., Zhang, Z., Li, Y., Wang, X., Zhang, J., Li, G., Yang, L., Liu, W., Min, J., & Wang, F. (2017). Characterization of ferroptosis in murine models of hemochromatosis. *Hepatology*, *66*(2), 449-465. https://doi.org/10.1002/hep.29117

Wang, H., Li, J., Follett, P. L., Zhang, Y., Cotanche, D. A., Jensen, F. E., Volpe, J. J., & Rosenberg, P. A. (2004). 12-Lipoxygenase plays a key role in cell death caused by glutathione depletion and arachidonic acid in rat oligodendrocytes. *Eur J Neurosci*, *20*(8), 2049-2058. https://doi.org/10.1111/j.1460-9568.2004.03650.x

Wang, T. X., Duan, K. L., Huang, Z. X., Xue, Z. A., Liang, J. Y., Dang, Y., Zhang, A., Xiong, Y., Ding, C., Guan, K. L., & Yuan, H. X. (2023). Tanshinone functions as a coenzyme that confers gain of function of NQO1 to suppress ferroptosis. *Life Sci Alliance*, *6*(1). https://doi.org/10.26508/lsa.202201667

Wang, Y., Yan, S., Liu, X., Deng, F., Wang, P., Yang, L., Hu, L., Huang, K., & He, J. (2022). PRMT4 promotes ferroptosis to aggravate doxorubicin-induced cardiomyopathy via inhibition of the Nrf2/GPX4 pathway. *Cell Death Differ*, *29*(10), 1982-1995. https://doi.org/10.1038/s41418-022-00990-5

Wang, Y. Q., Chang, S. Y., Wu, Q., Gou, Y. J., Jia, L., Cui, Y. M., Yu, P., Shi, Z. H., Wu, W. S., Gao, G., & Chang, Y. Z. (2016). The Protective Role of Mitochondrial Ferritin on Erastin-Induced Ferroptosis. *Front Aging Neurosci*, *8*, 308. https://doi.org/10.3389/fnagi.2016.00308

Wangen, J. R., Eidenschink Brodersen, L., Stolk, T. T., Wells, D. A., & Loken, M. R. (2014). Assessment of normal erythropoiesis by flow cytometry: important considerations for specimen preparation. *Int J Lab Hematol*, *36*(2), 184-196. https://doi.org/10.1111/ijlh.12151

Ware, R. E., & Aygun, B. (2009). Advances in the use of hydroxyurea. *Hematology Am Soc Hematol Educ Program*, 62-69. https://doi.org/10.1182/asheducation-2009.1.62

Weatherall, D. J. (2010). The inherited diseases of hemoglobin are an emerging global health burden. *Blood*, *115*(22), 4331-4336. https://doi.org/10.1182/blood-2010-01-251348

Weber, L., Frati, G., Felix, T., Hardouin, G., Casini, A., Wollenschlaeger, C., Meneghini, V., Masson, C., De Cian, A., Chalumeau, A., Mavilio, F., Amendola, M., Andre-Schmutz, I., Cereseto, A., El Nemer, W., Concordet, J. P., Giovannangeli, C., Cavazzana, M., & Miccio, A. (2020). Editing a γ-globin repressor binding site restores fetal hemoglobin synthesis and corrects the sickle cell disease phenotype. *Sci Adv*, *6*(7). https://doi.org/10.1126/sciadv.aay9392

Wei, Q., Boulais, P. E., Zhang, D., Pinho, S., Tanaka, M., & Frenette, P. S. (2019). Maea expressed by macrophages, but not erythroblasts, maintains postnatal murine bone marrow erythroblastic islands. *Blood*, *133*(11), 1222-1232. https://doi.org/10.1182/blood-2018-11-888180

Weidt, C., Niggemann, B., Kasenda, B., Drell, T. L., Zänker, K. S., & Dittmar, T. (2007). Stem cell migration: a quintessential stepping stone to successful therapy. *Curr Stem Cell Res Ther*, *2*(1), 89-103. https://doi.org/10.2174/157488807779317008

Wen, Y., Wang, Y., Chen, S., Zhou, X., Zhang, Y., Yang, D., Núñez, G., & Liu, Q. (2022). Dysregulation of Cytosolic c-di-GMP in Edwardsiella piscicida Promotes Cellular Non-Canonical Ferroptosis. *Front Cell Infect Microbiol*, *12*, 825824. https://doi.org/10.3389/fcimb.2022.825824

Wickramasinghe, S. N., & Hughes, M. (1978). Some features of bone marrow macrophages in patients with homozygous beta-thalassaemia. *Br J Haematol*, *38*(1), 23-28. https://doi.org/10.1111/j.1365-2141.1978.tb07104.x

Wiernicki, B., Dubois, H., Tyurina, Y. Y., Hassannia, B., Bayir, H., Kagan, V. E., Vandenabeele, P., Wullaert, A., & Vanden Berghe, T. (2020). Excessive phospholipid peroxidation distinguishes ferroptosis from other cell death modes including pyroptosis. *Cell Death Dis*, *11*(10), 922. https://doi.org/10.1038/s41419-020-03118-0

Winkler, I. G., Sims, N. A., Pettit, A. R., Barbier, V., Nowlan, B., Helwani, F., Poulton, I. J., van Rooijen, N., Alexander, K. A., Raggatt, L. J., & Levesque, J. P. (2010). Bone marrow macrophages maintain hematopoietic stem cell (HSC) niches and their depletion mobilizes HSCs. *Blood*, *116*(23), 4815-4828. https://doi.org/10.1182/blood-2009-11-253534

Wood, W. G., Stamatoyannopoulos, G., Lim, G., & Nute, P. E. (1975). F-cells in the adult: normal values and levels in individuals with hereditary and acquired elevations of Hb F. *Blood*, *46*(5), 671-682.

Woodard, K. J., Doerfler, P. A., Mayberry, K. D., Sharma, A., Levine, R., Yen, J., Valentine, V., Palmer, L. E., Valentine, M., & Weiss, M. J. (2022). Limitations of mouse models for sickle cell disease conferred by their human globin transgene configurations. *Dis Model Mech*, *15*(6). https://doi.org/10.1242/dmm.049463

Wu, C. J., Krishnamurti, L., Kutok, J. L., Biernacki, M., Rogers, S., Zhang, W., Antin, J. H., & Ritz, J. (2005). Evidence for ineffective erythropoiesis in severe sickle cell disease. *Blood*, *106*(10), 3639-3645. https://doi.org/10.1182/blood-2005-04-1376

Wu, G., Fang, Y. Z., Yang, S., Lupton, J. R., & Turner, N. D. (2004). Glutathione metabolism and its implications for health. *J Nutr*, *134*(3), 489-492. https://doi.org/10.1093/jn/134.3.489

Wu, J., Minikes, A. M., Gao, M., Bian, H., Li, Y., Stockwell, B. R., Chen, Z. N., & Jiang, X. (2019). Intercellular interaction dictates cancer cell ferroptosis via NF2-YAP signalling. *Nature*, *572*(7769), 402-406. https://doi.org/10.1038/s41586-019-1426-6

Wu, L. C., Sun, C. W., Ryan, T. M., Pawlik, K. M., Ren, J., & Townes, T. M. (2006). Correction of sickle cell disease by homologous recombination in embryonic stem cells. *Blood*, *108*(4), 1183-1188. https://doi.org/10.1182/blood-2006-02-004812

Wun, T., Paglieroni, T., Rangaswami, A., Franklin, P. H., Welborn, J., Cheung, A., & Tablin, F. (1998). Platelet activation in patients with sickle cell disease. *Br J Haematol*, *100*(4), 741-749. https://doi.org/10.1046/j.1365-2141.1998.00627.x

Xiang, J., Wu, D. C., Chen, Y., & Paulson, R. F. (2015). In vitro culture of stress erythroid progenitors identifies distinct progenitor populations and analogous human progenitors. *Blood*, *125*(11), 1803-1812. https://doi.org/10.1182/blood-2014-07-591453

Yachie, A., Niida, Y., Wada, T., Igarashi, N., Kaneda, H., Toma, T., Ohta, K., Kasahara, Y., & Koizumi, S. (1999). Oxidative stress causes enhanced endothelial cell injury in human heme oxygenase-1 deficiency. *J Clin Invest*, *103*(1), 129-135. https://doi.org/10.1172/jci4165

Yagoda, N., von Rechenberg, M., Zaganjor, E., Bauer, A. J., Yang, W. S., Fridman, D. J., Wolpaw, A. J., Smukste, I., Peltier, J. M., Boniface, J. J., Smith, R., Lessnick, S. L., Sahasrabudhe, S., & Stockwell, B. R. (2007). RAS-RAF-MEK-dependent oxidative cell death involving voltage-dependent anion channels. *Nature*, *447*(7146), 864-868. https://doi.org/10.1038/nature05859

Yan, H., Ali, A., Blanc, L., Narla, A., Lane, J. M., Gao, E., Papoin, J., Hale, J., Hillyer, C. D., Taylor, N., Gallagher, P. G., Raza, A., Kinet, S., & Mohandas, N. (2021). Comprehensive phenotyping of erythropoiesis in human bone marrow: Evaluation of normal and ineffective erythropoiesis. *Am J Hematol*, *96*(9), 1064-1076. https://doi.org/10.1002/ajh.26247

Yan, H., Hale, J., Jaffray, J., Li, J., Wang, Y., Huang, Y., An, X., Hillyer, C., Wang, N., Kinet, S., Taylor, N., Mohandas, N., Narla, A., & Blanc, L. (2018). Developmental differences between neonatal and adult human erythropoiesis. *Am J Hematol*, *93*(4), 494-503. https://doi.org/10.1002/ajh.25015

Yang, C., Endoh, M., Tan, D. Q., Nakamura-Ishizu, A., Takihara, Y., Matsumura, T., & Suda, T. (2021). Mitochondria transfer from early stages of erythroblasts to their macrophage niche via tunnelling nanotubes. *Br J Haematol*, *193*(6), 1260-1274. https://doi.org/10.1111/bjh.17531

Yang, W. S., SriRamaratnam, R., Welsch, M. E., Shimada, K., Skouta, R., Viswanathan, V. S., Cheah, J. H., Clemons, P. A., Shamji, A. F., Clish, C. B., Brown, L. M., Girotti, A. W., Cornish, V. W., Schreiber, S. L., & Stockwell, B. R. (2014). Regulation of ferroptotic cancer cell death by GPX4. *Cell*, *156*(1-2), 317-331. https://doi.org/10.1016/j.cell.2013.12.010

Yang, W. S., & Stockwell, B. R. (2008). Synthetic lethal screening identifies compounds activating iron-dependent, nonapoptotic cell death in oncogenic-RAS-harboring cancer cells. *Chem Biol*, *15*(3), 234-245. https://doi.org/10.1016/j.chembiol.2008.02.010

Yang, W. S., & Stockwell, B. R. (2016). Ferroptosis: Death by Lipid Peroxidation. *Trends Cell Biol*, *26*(3), 165-176. https://doi.org/10.1016/j.tcb.2015.10.014

Yang, Z., Keel, S. B., Shimamura, A., Liu, L., Gerds, A. T., Li, H. Y., Wood, B. L., Scott, B. L., & Abkowitz, J. L. (2016). Delayed globin synthesis leads to excess heme and the macrocytic anemia of Diamond Blackfan anemia and del(5q) myelodysplastic syndrome. *Sci Transl Med*, *8*(338), 338ra367. https://doi.org/10.1126/scitranslmed.aaf3006

Yant, L. J., Ran, Q., Rao, L., Van Remmen, H., Shibatani, T., Belter, J. G., Motta, L., Richardson, A., & Prolla, T. A. (2003). The selenoprotein GPX4 is essential for mouse development and protects from radiation and oxidative damage insults. *Free Radic Biol Med*, *34*(4), 496-502. https://doi.org/10.1016/s0891-5849(02)01360-6

Yeo, J. H., Cosgriff, M. P., & Fraser, S. T. (2018). Analyzing the Formation, Morphology, and Integrity of Erythroblastic Islands. *Methods Mol Biol*, *1698*, 133-152. https://doi.org/10.1007/978-1-4939-7428-3_8

Yeo, J. H., Lam, Y. W., & Fraser, S. T. (2019). Cellular dynamics of mammalian red blood cell production in the erythroblastic island niche. *Biophys Rev*, *11*(6), 873-894. https://doi.org/10.1007/s12551-019-00579-2

Yeo, J. H., McAllan, B. M., & Fraser, S. T. (2016). Scanning Electron Microscopy Reveals Two Distinct Classes of Erythroblastic Island Isolated from Adult Mammalian Bone Marrow. *Microsc Microanal*, *22*(2), 368-378. https://doi.org/10.1017/s1431927616000155

Yokoyama, T., Etoh, T., Kitagawa, H., Tsukahara, S., & Kannan, Y. (2003). Migration of erythroblastic islands toward the sinusoid as erythroid maturation proceeds in rat bone marrow. *J Vet Med Sci*, *65*(4), 449-452. https://doi.org/10.1292/jvms.65.449

Yona, S., Kim, K. W., Wolf, Y., Mildner, A., Varol, D., Breker, M., Strauss-Ayali, D., Viukov, S., Guilliams, M., Misharin, A., Hume, D. A., Perlman, H., Malissen, B., Zelzer, E., & Jung, S. (2013). Fate mapping reveals origins and dynamics of monocytes and tissue macrophages under homeostasis. *Immunity*, *38*(1), 79-91. https://doi.org/10.1016/j.immuni.2012.12.001

Youssef, L. A., Rebbaa, A., Pampou, S., Weisberg, S. P., Stockwell, B. R., Hod, E. A., & Spitalnik, S. L. (2018). Increased erythrophagocytosis induces ferroptosis in red pulp macrophages in a mouse model of transfusion. *Blood*, *131*(23), 2581-2593. https://doi.org/10.1182/blood-2017-12-822619

Yu, W. M., Liu, X., Shen, J., Jovanovic, O., Pohl, E. E., Gerson, S. L., Finkel, T., Broxmeyer, H. E., & Qu, C. K. (2013). Metabolic regulation by the mitochondrial phosphatase PTPMT1 is required for hematopoietic stem cell differentiation. *Cell Stem Cell*, *12*(1), 62-74. https://doi.org/10.1016/j.stem.2012.11.022

Yu, Y., Jiang, L., Wang, H., Shen, Z., Cheng, Q., Zhang, P., Wang, J., Wu, Q., Fang, X., Duan, L., Wang, S., Wang, K., An, P., Shao, T., Chung, R. T., Zheng, S., Min, J., & Wang, F. (2020). Hepatic transferrin plays a role in systemic iron homeostasis and liver ferroptosis. *Blood*, *136*(6), 726-739. https://doi.org/10.1182/blood.2019002907

Yuan, J., Bunyaratvej, A., Fucharoen, S., Fung, C., Shinar, E., & Schrier, S. L. (1995). The instability of the membrane skeleton in thalassemic red blood cells. *Blood*, *86*(10), 3945-3950.

Yusuf, R. Z., & Scadden, D. T. (2012). Fate through fat: lipid metabolism determines stem cell division outcome. *Cell Metab*, *16*(4), 411-413. https://doi.org/10.1016/j.cmet.2012.09.011

Zamai, L., Secchiero, P., Pierpaoli, S., Bassini, A., Papa, S., Alnemri, E. S., Guidotti, L., Vitale, M., & Zauli, G. (2000). TNF-related apoptosis-inducing ligand (TRAIL) as a negative regulator of normal human erythropoiesis. *Blood*, *95*(12), 3716-3724.

Zerez, C. R., Lachant, N. A., Lee, S. J., & Tanaka, K. R. (1988). Decreased erythrocyte nicotinamide adenine dinucleotide redox potential and abnormal pyridine nucleotide content in sickle cell disease. *Blood*, *71*(2), 512-515.

Zermati, Y., Fichelson, S., Valensi, F., Freyssinier, J. M., Rouyer-Fessard, P., Cramer, E., Guichard, J., Varet, B., & Hermine, O. (2000). Transforming growth factor inhibits erythropoiesis by blocking proliferation and accelerating differentiation of erythroid progenitors. *Exp Hematol*, *28*(8), 885-894. https://doi.org/10.1016/s0301-472x(00)00488-4

Zhang, A., Suzuki, T., Adachi, S., Naganuma, E., Suzuki, N., Hosoya, T., Itoh, K., Sporn, M. B., & Yamamoto, M. (2021). Distinct Regulations of HO-1 Gene Expression for Stress Response and Substrate Induction. *Mol Cell Biol*, *41*(11), e0023621. https://doi.org/10.1128/mcb.00236-21

Zhang, W., Gai, C., Ding, D., Wang, F., & Li, W. (2018). Targeted p53 on Small-Molecules-Induced Ferroptosis in Cancers. *Front Oncol*, *8*, 507. https://doi.org/10.3389/fonc.2018.00507

Zhang, Y., Gilmour, A., Ahn, Y. H., de la Vega, L., & Dinkova-Kostova, A. T. (2021). The isothiocyanate sulforaphane inhibits mTOR in an NRF2-independent manner. *Phytomedicine*, *86*, 153062. https://doi.org/10.1016/j.phymed.2019.153062

Zhang, Y., Paikari, A., Sumazin, P., Ginter Summarell, C. C., Crosby, J. R., Boerwinkle, E., Weiss, M. J., & Sheehan, V. A. (2018). Metformin induces FOXO3-dependent fetal hemoglobin production in human primary erythroid cells. *Blood*, *132*(3), 321-333. https://doi.org/10.1182/blood-2017-11-814335

Zhou, Y., Que, K. T., Zhang, Z., Yi, Z. J., Zhao, P. X., You, Y., Gong, J. P., & Liu, Z. J. (2018). Iron overloaded polarizes macrophage to proinflammation phenotype through ROS/acetyl-p53 pathway. *Cancer Med*, *7*(8), 4012-4022. https://doi.org/10.1002/cam4.1670

Zivot, A., Lipton, J. M., Narla, A., & Blanc, L. (2018). Erythropoiesis: insights into pathophysiology and treatments in 2017. *Mol Med*, *24*(1), 11. https://doi.org/10.1186/s10020-018-0011-z

APPENDIX

PUBLICATIONS

El Hoss S, **Godard A***, Cochet S*, Yan H, Dussiot M, Frati G, Boutonnat-Faucher B, Laurance S, Renaud O, Joseph L, Miccio A, Brousse V, Narla M, El Nemer W. **Fetal hemoglobin rescues ineffective erythropoiesis in sickle cell disease.** *Published in Haematologica in October 2021 Oct 1*. doi: 10.3324/haematol.2020.265462. PMID: 32855279; PMCID: PMC8485663.

El Nemer W, **Godard A**, El Hoss S. **Ineffective erythropoiesis in sickle cell disease: new insights and future implications.** *Published in Current Opinion in Hematology in May 2021*. doi: 10.1097/MOH.0000000000000642. PMID: 33631786.

Godard A*, Seute R*, Grimaldi A, Granier T, Chiaroni J, El Nemer W, De Grandis M. **A comparative study of two routinely used protocols for ex vivo erythroid differentiation.** *Submitted in September 2023 in Experimental Hematology & Oncology.*

ARTICLE 1

Red Cell Biology & its Disorders

ARTICLE

Fetal hemoglobin rescues ineffective erythropoiesis in sickle cell disease

Sara El Hoss,[1,2,3] Sylvie Cochet,[1,2,3,#] Auria Godard,[1,2,3,#*] Hongxia Yan,[4] Michaël Dussiot,[5] Giacomo Frati,[6,7] Bénédicte Boutonnat-Faucher,[8] Sandrine Laurance,[1,2,3] Olivier Renaud,[9,10,11,12] Laure Joseph,[13] Annarita Miccio,[6,7] Valentine Brousse,[1,2,3,8] Narla Mohandas[4] and Wassim El Nemer[1,2,3*]

[1]Université de Paris, INSERM UMRS1134, BIGR, Paris, France; [2]Institut National de la Transfusion Sanguine, Paris, France; [3]Laboratoire d'Excellence GR-Ex, Paris, France; [4]Red Cell Physiology Laboratory, New York Blood Center, New York, NY, USA; [5]Institut Imagine, INSERM U1163, CNRS UMR8254, Université de Paris, Hôpital Necker Enfants Malades, Paris, France; [6]Laboratory of Chromatin and Gene Regulation during Development, INSERM UMR1163, Paris, France; [7]Université de Paris, Imagine Institute, Paris, France; [8]Service de Pédiatrie Générale et Maladies Infectieuses, Hôpital Universitaire Necker Enfants Malades, Paris, France; [9]Institut Curie, Paris Sciences et Lettres Research University, Paris, France; [10]Institut National de la Santé et de la Recherche Médicale, INSERM U934, Paris, France;[11]Centre National de la Recherche Scientifique, INSERM UMR3215, Paris, France; [12]Cell and Tissue Imaging Facility (PICT-IBiSA), Institut Curie, Paris, France and [13]Service de Biothérapie, Hôpital Universitaire Necker Enfants Malades, Paris, France

*Present affiliation: Etablissement Français du Sang PACA-Corse, Aix Marseille Université, EFS, CNRS, ADES, "Biologie des Groupes Sanguins", Marseille, France.

#SC and AG contributed equally as co-second authors.

Ferrata Storti Foundation

Haematologica 2021
Volume 106(10):2707-2719

ABSTRACT

While ineffective erythropoiesis has long been recognized as a key contributor to anemia in thalassemia, its role in anemia of sickle cell disease (SCD) has not been critically explored. Using *in vitro* and *in vivo* derived human erythroblasts we assessed the extent of ineffective erythropoiesis in SCD. Modeling the bone marrow hypoxic environment, we found that hypoxia induces death of sickle erythroblasts starting at the polychromatic stage, positively selecting cells with high levels of fetal hemoglobin (HbF). Cell death was associated with cytoplasmic sequestration of heat shock protein 70 and was rescued by induction of HbF synthesis. Importantly, we document that in the bone marrow of SCD patients similar cell loss occurs during the final stages of terminal differentiation. Our study provides evidence for ineffective erythropoiesis in SCD and highlights an anti-apoptotic role for HbF during the terminal stages of erythroid differentiation. These findings imply that the beneficial effect on anemia of increased HbF levels is not only due to the increased life span of red cells but also a consequence of decreased ineffective erythropoiesis.

Introduction

Sickle cell disease (SCD) is an autosomal hereditary recessive disorder caused by a point mutation in the *β-globin* gene resulting in a Glu-to-Val substitution at the sixth position of the β-globin protein. The resulting abnormal hemoglobin (HbS) polymerizes under hypoxic conditions driving red blood cell (RBC) sickling.[1] SCD is a multisystem disease characterized by hemolytic anemia, high susceptibility to infections, recurrent painful vaso-occlusive crises, strokes, acute chest syndrome and organ failure.[2,3]

While the pathobiology of circulating RBC has been extensively analyzed in SCD, erythropoiesis is surprisingly poorly documented. In β-thalassemia, ineffective erythropoiesis is characterized by high levels of apoptotic erythroblasts during the late stages of terminal differentiation, due to an accumulation of free α-globin chains.[4-6] Ineffective erythropoiesis is the major cause of anemia in β-tha-

Correspondence:
WASSIM EL NEMER
wassim.el-nemer@efs.sante.fr

Received: July 1, 2020
Accepted: August 17, 2020.
Pre-published: August 27, 2020.

https://doi.org/10.3324/haematol.2020.265462

lassemia patients. In contrast, a marked decrease in the life span of circulating red cells, a feature of sickle red cells, is considered to be the major determinant of chronic anemia in SCD. It is generally surmised that ineffective erythropoiesis contributes little to anemia. There have been, however, a number of sporadic reports that suggest defective terminal erythroid differentiation in SCD. For example, erythroblasts differentiated *in vitro* or isolated from bone marrow of SCD patients were shown to sickle under hypoxic conditions.[7] Such sickling was also reported in the SAD mouse model, with altered morphology of late stage erythroid precursors within the bone marrow, as well as high levels of hemoglobin polymers and increased cell fragmentation occurring during medullary endothelial migration of reticulocytes.[8] It was presumed that sickling of erythroblasts could lead to ineffective terminal erythroid differentiation. The study of Wu *et al.* showed for the first time evidence of ineffective erythropoiesis occurring in the bone marrow of transplanted SCD patients with the preferential survival of the donor erythroid cells in a small cohort of patients.[9]

In the present study, we performed a detailed characterization of terminal erythroid differentiation in non-transplanted SCD patients using both *in vivo* and *in vitro* assay systems to critically assess the extent of ineffective erythropoiesis. We documented in both our *in vivo* and *in vitro* studies, the occurrence of ineffective erythropoiesis at late stages of terminal erythroid differentiation reflected by high cell death rates between the polychromatic and the orthochromatic stages. We explored the potential mechanistic basis for ineffective erythropoiesis in SCD patients and showed that the molecular mechanism responsible for cell death is likely related to HbS polymerization and its interaction with chaperone protein HSP70 leading to its cytoplasmic sequestration. Importantly, we documented that increased expression of fetal hemoglobin (HbF) can rescue differentiating erythroblasts from cell death.

Methods

Biological samples

The study was conducted according to the declaration of Helsinki with approval from the Medical Ethics Committee (GR-Ex/CPP-DC2016-2618/CNILMR01). All SCD patients were of SS genotype. Blood bags from SCD patients enrolled in an exchange transfusion program, bone marrow aspirates from five SCD patients undergoing surgery and bone marrow tissues from five non-anemic donors undergoing hip/sternum surgery, were obtained after informed consent, from Necker-Enfants Malades Hospital (Paris, France) and the North Shore-LIJ Health System (New York, USA) under Institutional Review Board (IRB) approval. Control blood bags from healthy donors were obtained from the Etablissement Français du Sang (EFS).

In vitro differentiation of human erythroid progenitors

Peripheral blood mononuclear cells were isolated from blood samples after Pancoll fractionation (PAN Biotech). $CD34^+$ cells were then isolated by a magnetic sorting system (Miltenyi Biotec CD34 Progenitor cell isolation kit) following the supplier protocol. $CD34^+$ cells were placed in an *in vitro* two-phase liquid culture system, as previously described.[10] For detailed protocols please refer to the *Online Supplementary Appendix*.

For cultures treated with pomalidomide, cells were incubated with 1 μM pomalidomide (Sigma) as previously described,[11] starting from day 1 (D1) of phase II of culture. For γ-globin derepression experiments using CRISPR/Cas9, patient $CD34^+$ cells were immunoselected and cultured for 48 hours (h) and then electroporated with ribonucleoprotein (RNP) complexes containing Cas9-GFP protein (4.5 μM) and the -197 guide RNA (gRNA) targeting both *HBG1* and *HBG2* γ-globin promoters (5' ATTGAGATAGTGTGGGGAAGGGG 3'; protospacer adjacent motif in bold) or a gRNA targeting the Adeno-associated virus integration site 1 (AAVS1; 5' GGGGCCAC-TAGGGACAGGATTGG 3'; protospacer adjacent motif in bold).[12] Cleavage efficiency was evaluated in cells harvested 6 days after electroporation by Sanger sequencing followed by tracking of indels by decomposition (TIDE) analysis.[13]

Imaging flow cytometry analysis of human bone marrow samples

Bone marrow samples were processed as previously described.[14] Detailed protocol are stated in the *Online Supplemental Appendix*.

Flow cytometry

Cells were analyzed using a BD FACScanto II flow cytometer and BD LSR Fortessa SORP flow cytometer (BD Biosciences) and acquired using the Diva software version 8 (BD Biosciences). Data was analyzed using FCS Express 6 software (DeNovo Software). Detailed protocols of cell staining are stated in the *Online Supplemental Appendix*.

Cell fractionation and western-blot

Cytoplasmic and nuclear protein fractions were extracted from erythroblasts at D7 of phase II of culture using the NE-PER nuclear and cytoplasmic kit (Pierce-Thermo Scientific). Ten μg of nuclear and cytoplasmic proteins were analyzed by SDS-PAGE, using 10% polyacrylamide gels, followed by immunoblotting. The antibodies used were rabbit anti-HSP70, mouse anti-actin and mouse anti-lamin A/C as a control for the nuclear extract. Proteins were revealed using electrochemiluminescence (ECL) clarity (Biorad) and the Chemidoc MP imaging system (Biorad). Analysis was performed using Image Lab (Biorad). Antibodies details are stated in the *Online Supplemental Appendix*.

Co-immunoprecipitation assays

Co-immunoprecipitation of HSP70 and hemoglobin was performed with lysates of 10 million RBC from SCD patients that were either exposed to hypoxia or not for one hour. HSP70 was immunoprecipitated by incubating the lysates with mouse anti-HSP70 antibody (Enzo Lifesciences) overnight at 4°C followed by a 45-minute incubation with protein-G sepharose beads (Cytiva-GE-Healthcare) at 4°C. Eluted proteins were analyzed by SDS-PAGE using a 4-12% polyacrylamide gel, followed by immunoblotting with mouse anti-α-globin (Santa Cruz Biotechnology) or rabbit anti-HSP70 (SANTA-CRUZ) antibodies. Proteins were revealed using ECL clarity and the Chemidoc MP imaging system.

Confocal microscopy and proximity ligation assay

Co-immunolocalization and proximity ligation assays (PLA) were performed with cells from D7 of phase II of culture. Acquisition was made on LSM700 Zeiss confocal microscope using Zen software. Analysis was performed using Fiji.[15] Detailed protocols are stated in the *Online Supplemental Appendix*.

Statistical analysis

Statistical analyses were performed with GraphPad Prism

(version 7). The data was analyzed using Mann-Whitney unpaired test and Wilcoxon paired test, as indicated in the figure legends.

Results

Hypoxia-induced cell death during *in vitro* terminal erythroid differentiation

The bone marrow environment has been well documented to be hypoxic (0.1-6% O_2).[16-18] As hypoxia induces HbS polymerization, we hypothesized that cell death may occur *in vivo* because of HbS polymer formation in the late stages of differentiation characterized by high intracellular hemoglobin concentration. In order to test our hypothesis, we performed *in vitro* erythroid differentiation using $CD34^+$ cells isolated from SCD patients and from healthy donors. A two-phase erythroid differentiation protocol was used and cultures were performed at two different oxygen conditions, i.e., normoxia and partial hypoxia (5% O_2), starting at D3 of the second phase, at which time hemoglobin synthesis begins to increase markedly (*Online Supplementary Figure S1*). The choice of 5% O_2 was made since it falls at the high end of the reported oxygen tension range of the hematopoietic niche (0.1-6% O_2),[17] and because it drives HbS polymerization and cell sickling, as we previously reported.[19] First, we performed video microscopy experiments with nucleated SCD erythroblasts at D9 of culture and confirmed their ability to sickle at 5% O_2 (Figure 1A; *Online Supplementary Video S1*). Differentiation of control erythroblasts showed no difference in the general waterfall pattern between normoxia and hypoxia (Figure 1B), although hypoxia translated into a consistently higher but not statistically significant increase in total cell count (Figure 1C). Under normoxia, SCD differentiation showed a mild deceleration till D9 as compared to control (Figure 1B), with a proliferation that was negatively impacted by hypoxia (Figure 1C). Under both oxygen conditions, cell proliferation was significantly higher in the control than in the SCD cultures, starting from D7 (Figure 1C). May Grünwald-Giemsa (MGG) staining confirmed the differentiation delay of SCD cells, especially under hypoxia where cells seemed to accumulate at the polychromatic stage when compared to control cells (Figure 1D). In addition, higher proportions of enucleated cells were found in control cells at D9 (Figure 1D) and D11 (Figure 1E). Enucleation was improved under hypoxia for control erythroblasts while it was significantly diminished for SCD cells (Figure 1E), indicating a negative impact of hypoxia at this critical maturation step in the context of SCD.

In order to assess if the decrease in proliferation in SCD was due to cell death, we measured the percentage of apoptotic cells in the cultures by staining the glycophorin A (GPA)-positive cells with annexin V (Figure 1F). The percentage of annexin V^+ cells was higher in SCD than in control cultures under both oxygen conditions at D7 and D9, with a greater variability among SCD than in control cells (Figure 1G). Furthermore, the extent of apoptosis of SCD cells was higher under hypoxia than under normoxia at both time points while no difference was noted for control cells (Figure 1G). Altogether, these findings imply that even under a conservative choice of 5% O_2 to mimic hypoxia in bone marrow there is increased cell death during the terminal differentiation stages in SCD cells only.

F-cells are enriched during sickle cell disease erythroid differentiation

Using flow cytometry, we measured the percentage of cells expressing HbF (F-cells) during *in vitro* differentiation (Figure 2A). The percentage of F-cells (%F-cells) in control cultures fell within the reported range of 20-40%,[20,21] while it was very variable for SCD cells reaching more than 70% at D9 (Figure 2B). Interestingly, there was no difference of %F-cells between normoxia and hypoxia for control cells, while for SCD, %F-cells was higher under hypoxia than under normoxia for all of the six independent primary cell samples (Figure 2B). Taken together with the apoptosis data, these findings imply that F-cells were positively selected under hypoxia in SCD. This inference was supported by flow cytometry data showing higher percentages of dead cells, based on the fixable viability stain (FVS), within the non-F-cell population as compared to the F-cell population for SCD cells (Figure 2C and D). In contrast, these percentages were similar between both cell populations in the control (Figure 2C and D), confirming preferential apoptosis of the cells with low/no HbF expression in the SCD context only.

HSP70 is sequestered in the cytoplasm of non-F-cells

As cytoplasmic sequestration of the chaperone protein HSP70 by α-globin aggregates is associated with cell death during erythropoiesis in β-thalassemia major,[5] we investigated if apoptosis of SCD erythroblasts might be due to cytoplasmic trapping of HSP70 by HbS polymers. We performed western blot analyses to quantify HSP70 in the cytoplasmic and nuclear extracts of erythroblasts at D7 of phase II of culture (Figure 3A). There was less HSP70 in the nucleus and more in the cytoplasm of SCD erythroblasts under hypoxia compared to normoxia (Figure 3A), indicating mislocalization of HSP70 in SCD cells under hypoxia. Importantly, these lower amounts of nuclear HSP70 were associated with lower amounts of GATA-1 (Figure 3A), suggesting that cell death under these conditions was likely due to altered protection of GATA-1 by HSP70.

The cells used in these assays were pools of live and apoptotic, F-cells and non-F-cells. In order to better address HSP70 localization in each of these subpopulations, we performed imaging flow cytometry experiments with cells stained for multiple markers. Only Hoechst-positive cells with high GPA expression were taken into consideration to exclude both reticulocytes and proerythroblasts. HSP70 fluorescence intensity was measured in the cytoplasm and the nucleus of live (FVS^-) and dead (FVS^+) cells at D7. HSP70 nuclear intensity was lower in dead than FVS^- cells, for both control and SCD cells under hypoxia (Figure 3B). Moreover, SCD FVS^+ cells showed higher HSP70 cytoplasmic levels than FVS^- cells, while no difference was detected between both subpopulations for control cells (Figure 3B). These results suggest that hypoxia-induced cell death in the SCD context is likely due to HSP70 entrapment in the cytoplasm. Next, we measured HSP70 intensity in F-cells and non-F-cells. Under hypoxia at D7, HSP70 nuclear intensity was higher in SCD F-cells than non-F cells, while there was no difference between both cell types in control (Figure 3C; *Online Supplementary Figure S2A*). We then measured the nucleus/cytoplasm (N/C) ratio of HSP70 intensity in polychromatic and orthochromatic cells. The

cell subtypes were identified based on morphological parameters of nuclear and cytoplasmic areas[22] (*Online Supplementary Figure S2B*; *Online Supplementary Table S1*) that discriminate between the basophilic, polychromatic and orthochromatic erythroblasts (Figure 3D; *Online Supplementary Figure S2C* and *D*). HSP70 N/C ratio was significantly higher in SCD F than non-F-cells (Figure 3E) which was not the case for control cells (*Online Supplementary Figure S2E*), indicating that increased HSP70 cytoplasmic entrapment is a feature of SCD non-F-cells. Although there was no significant difference of HSP70 N/C ratio between SCD F-cells and control, this ratio showed a broader distribution in SCD F-cells (*Online Supplementary Figure S2E*). We hypothesized that this heterogeneity might be linked to the variable intracellular levels of HbF in these cells. Using an analysis mask that quantifies the amount of HbF per cell, we classified F-cells as either low or high F-expressing cells, depending on the intracellular expression level of HbF (Figure 3F). We found that HSP70 N/C ratio was higher in high F-cells compared to low F-cells (Figure 3G), implying that the amounts of HSP70 trapped in the cytoplasm were inversely related to the cytoplasmic content of HbF and suggesting that high amounts of HbF protect SCD erythroblasts against apopto-

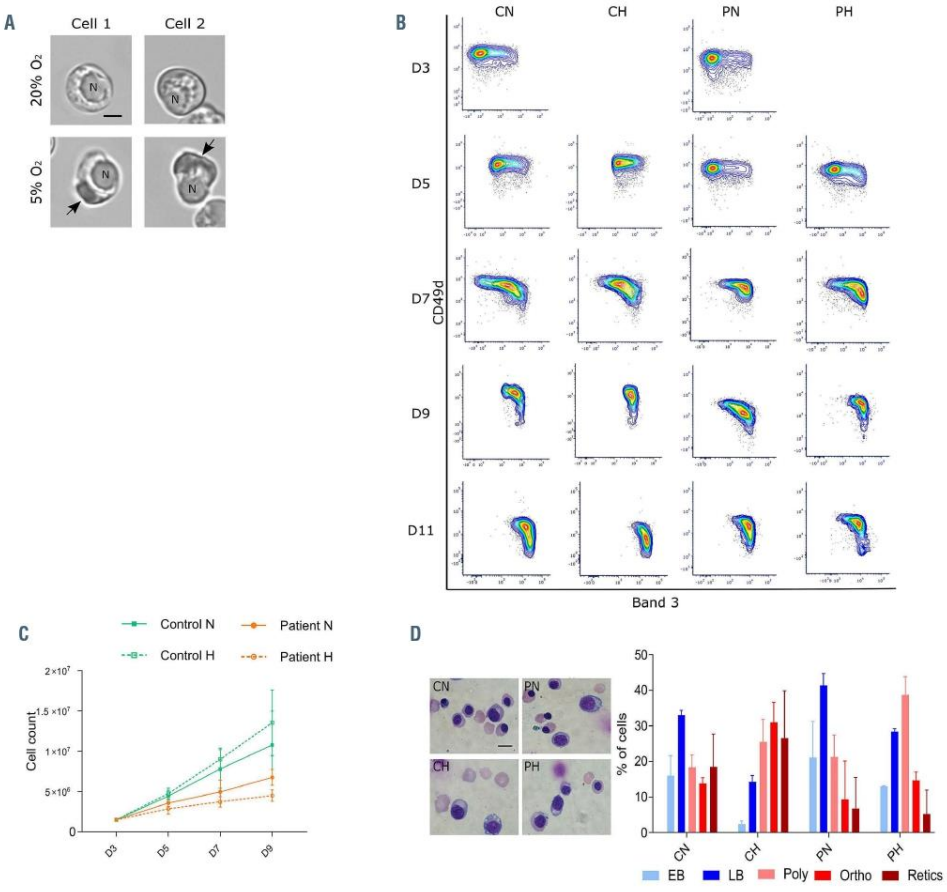

Figure 1. Cell proliferation and apoptosis during terminal erythroid differentiation *in vitro* under normoxia and partial hypoxia. (A) Microscopy images of two sickle cell disease (SCD) *in vitro* cultured erythroblasts incubated for 30 minutes at 20% (upper panel) and 5% (lower panel) oxygen. "N" represents the nucleus and the arrow points to the HbS polymers formed under 5% oxygen; scale bar: 5 µm. (B) A contour plot representing the distribution of glycophorin A (GPA)-positive cells with respect to the expression of Band 3 (x-axis) and CD49d (y-axis) at day (D) 3, D5, D7, D9 and D11 of phase II of culture in control erythroid precursors under normoxia (CN) or hypoxia (CH), and in patient erythroid precursors under normoxia (PN) or hypoxia (PH). (C) Cell count of erythroid precursors at D3, 5, 7 and 9 in control (n=4) and patient (n=6) under normoxia (N) and hypoxia (H) (means ± standard error of the mean [SEM]). (D) May Grunwald-Giemsa staining of erythroid precursors at D9 of phase II of culture (left panel; scale bar: 10 µm) and graph representing the cellular distribution as means ± SEM of early basophilic (EB), late basophilic (LB), polychromatic (Poly), orthochromatic (Ortho) and reticulocytes (Retics) at D9 of culture of control normoxia (CN), control hypoxia (CH), patient normoxia (PN) and patient hypoxia (PH). *(continued on next page)*

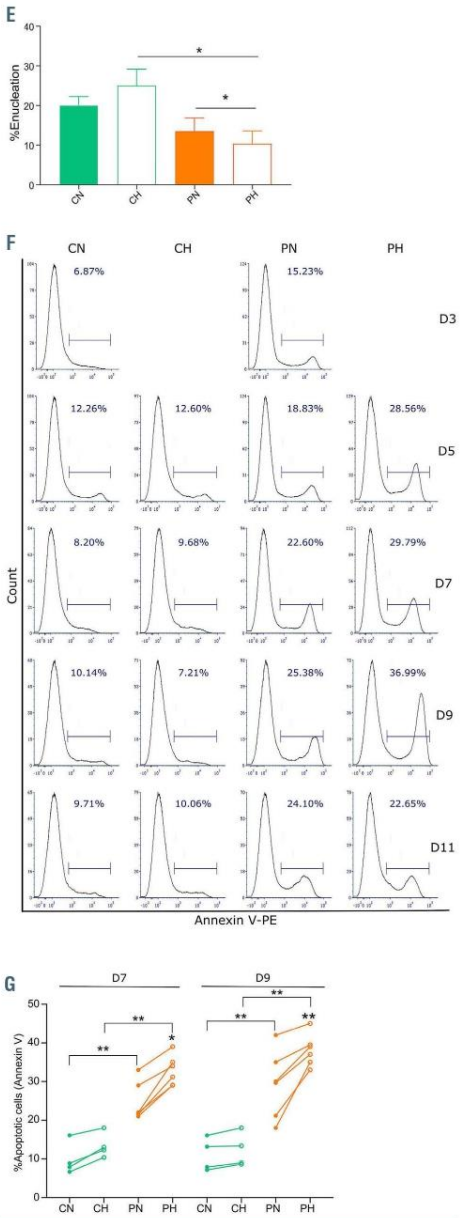

Figure 1. *(continued from previous page)* (E) Percentage of enucleation measured at D11 for CN, CH, PN and PH erythroblasts (means ± SEM; CN and CH: n=3; PN and PH: n=6). (F) Flow cytometry plots showing percentage of apoptotic cells (Annexin V-positive cells) measured at D3, D5, D7, D9 and D11. (G) Percentage of apoptotic cells in control (n=4) and patients (n=6) under normoxia (N) and hypoxia (H) at D7 and D9 of phase II of culture. *P<0.05, **P<0.01; Wilcoxon paired test and Mann-Whitney test (E and G).

sis. This inference was supported by our findings showing lower percentages of low F-cells in SCD cultures as compared to control, as well as lower percentages of SCD low F-cells under hypoxic than normoxic conditions (Figure 3H). On the other hand, the percentage of high F-cells was significantly higher in SCD erythroblasts as compared to control, with even higher percentages under hypoxia (Figure 3I). Of note, no difference in the percentage of low or high F-cells was observed between hypoxia and normoxia for control cells (Figure 3H and I), indicating that the differences observed for SCD cells are the result of differential cell death related to HbF expression levels.

HbS-HSP70 protein complex in sickle cell disease cells under hypoxia

In order to explore the molecular mechanism of cytoplasmic trapping of HSP70, we performed immunofluorescence assays using confocal microscopy and found co-localization of HSP70 and hemoglobin in both control and SCD cells (Figure 4A). We used Pearson's correlation coefficient[23,24] to assess the degree of co-localization and found no difference between both cell types (*data not shown*), probably because of the high abundance of hemoglobin in the cytoplasm. In order to overcome this limitation, we performed PLA, that show fluorescent spots when two proteins are at a distance <40 nm.[25] We detected SCD cells with fluorescent spots (PLA^+) under both normoxic and hypoxic conditions (Figure 4B) that were further quantified by imaging flow cytometry (Figure 4C). The percentage of PLA^+ cells was very low in control, with values close to background levels (1-1.5%) under both normoxia and hypoxia, while SCD cells showed higher values under normoxia (4.5-18.5%) with a systematic and significant increase under hypoxia (9.5-36%) (Figure 4D), indicating proximity between HSP70 and HbS but not HSP70 and HbA. Moreover, PLA^+ SCD cells showed higher mean fluorescence intensity under hypoxia than under normoxia (Figure 4D), indicating that hypoxia induces the formation of more potent HbS-HSP70 complexes that could account for cytoplasmic retention of HSP70.

In order to explore the potential of HbS polymers and HSP70 interacting within the same protein complex, we performed co-immunoprecipitation assays. SCD RBC suspensions were placed at normoxia or hypoxia then lysed, and HSP70 was immunoprecipitated. Using an anti-α-globin antibody we found co-immunoprecipitation of HSP70 and α-globin under hypoxia but not under normoxia (Figure 4E) supporting the presence of HbS-HSP70 protein complex. Of note, despite using the same amounts of RBC for both conditions, there was less immunoprecipitated HSP70 under hypoxia than normoxia likely due to decreased solubility of HbS polymer fibers under hypoxia as evidenced by the color of the lysates under both conditions and the presence of a small red colored precipitate under hypoxia (*Online Supplementary Figure S3*).

Cell death during the terminal stages of erythroid differentiation in bone marrow of sickle cell disease patients

In order to validate the direct relevance of the *in vitro* findings to *in vivo* conditions, we analyzed terminal erythroid differentiation using unmanipulated marrow samples from SCD patients. Bone marrow aspirates were obtained from five SCD patients and cells were stained for surface markers GPA, CD49d and Band 3 and analyzed by

flow cytometry. Differentiating erythroblasts were determined using the CD49d and Band 3 staining pattern within the GPA$^+$ population (Figure 5A), as previously described.[14] Imaging flow cytometry was used to confirm gating of all nucleated cells and cell homogeneity within each of the four gated populations by cellular features of size, morphology and nuclear size and polarization (Figure 5B). We quantified the cells at the early basophilic (EB), late basophilic (LB), polychromatic and orthochromatic stages. Considering the GPA positive population as 100%, the mean percentages of EB, LB, polychromatic and orthochromatic cells were 5.1%, 10.2%, 20.4% and 25.2% (Figure 5C), indicating loss of the expected cell doubling between the polychromatic and orthochromatic stages (1.24+/-0.1, P<0.01; Figure 5D). These results implied that cell death occurs between the polychromatic and orthochromatic stages in a significant proportion of erythroblasts, in accordance with our *in vitro* data. Similar analysis was performed with bone marrow aspirates of five controls (3% EB, 6.8% LB, 13% polychromatic cells and 24.6% orthochromatic cells, Figure 5C) that confirmed the expected doubling of cells with successive cell divisions without cell loss between development stages during normal erythropoiesis (Figure 5D). Next, we stained the cells with an anti-HbF antibody to measure the percentage of F-cells at the different stages. There was a significant increase in %F-cells between the polychromatic (16.4%±4) and orthochromatic stages (32.4%±4.79) (Figure 5E and F), concomitant with the cell loss observed between these stages (Figure 5C and D), indicating preferential survival of F-cells during late stages of erythroblast maturation *in vivo* and supporting our hypothesis for an anti-apoptotic role of HbF during *in vivo* erythropoiesis in SCD.

Induction of fetal hemoglobin protects against cell death

In order to confirm the anti-apoptotic role of HbF in SCD erythroblasts we induced its expression *in vitro* using pomalidomide (POM), an immunomodulatory drug previously shown to induce HbF expression during erythropoiesis,[11,26] and determined if higher HbF levels could rescue the cells from apoptosis. As we were interested in monitoring the stages during which hemoglobin is synthesized, POM was added at D1 of phase II of culture. As expected, POM-treated SCD cultures showed higher percentages of F-cells than untreated cultures (Figure 6A; *Online Supplementary Figure S4A*). HbF induction by POM was associated with significantly lower levels of apoptosis compared to untreated cultures under both hypoxia and normoxia (Figure 6B; *Online Supplementary Figure S4B*). Importantly, there was no significant difference in the apoptosis levels between normoxic and hypoxic conditions of POM-treated cells indicating that the higher F-cell levels protected SCD cells from apoptosis under hypoxia.

In order to specifically address the role of HbF, we used a CRISPR-Cas9 approach that we have recently developed to mimic the effect of hereditary persistence of fetal hemoglobin (HPFH) by disrupting the binding site for HbF

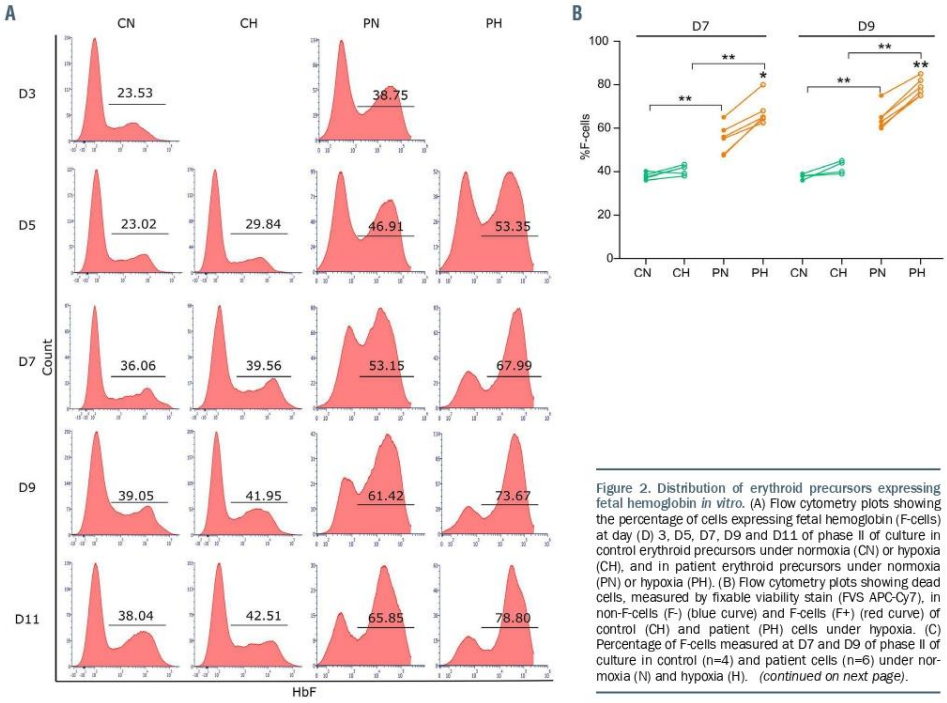

Figure 2. Distribution of erythroid precursors expressing fetal hemoglobin *in vitro*. (A) Flow cytometry plots showing the percentage of cells expressing fetal hemoglobin (F-cells) at day (D) 3, D5, D7, D9 and D11 of phase II of culture in control erythroid precursors under normoxia (CN) or hypoxia (CH), and in patient erythroid precursors under normoxia (PN) or hypoxia (PH). (B) Flow cytometry plots showing dead cells, measured by fixable viability stain (FVS APC-Cy7), in non-F-cells (F-) (blue curve) and F-cells (F+) (red curve) of control (CH) and patient (PH) cells under hypoxia. (C) Percentage of F-cells measured at D7 and D9 of phase II of culture in control (n=4) and patient cells (n=6) under normoxia (N) and hypoxia (H). *(continued on next page).*

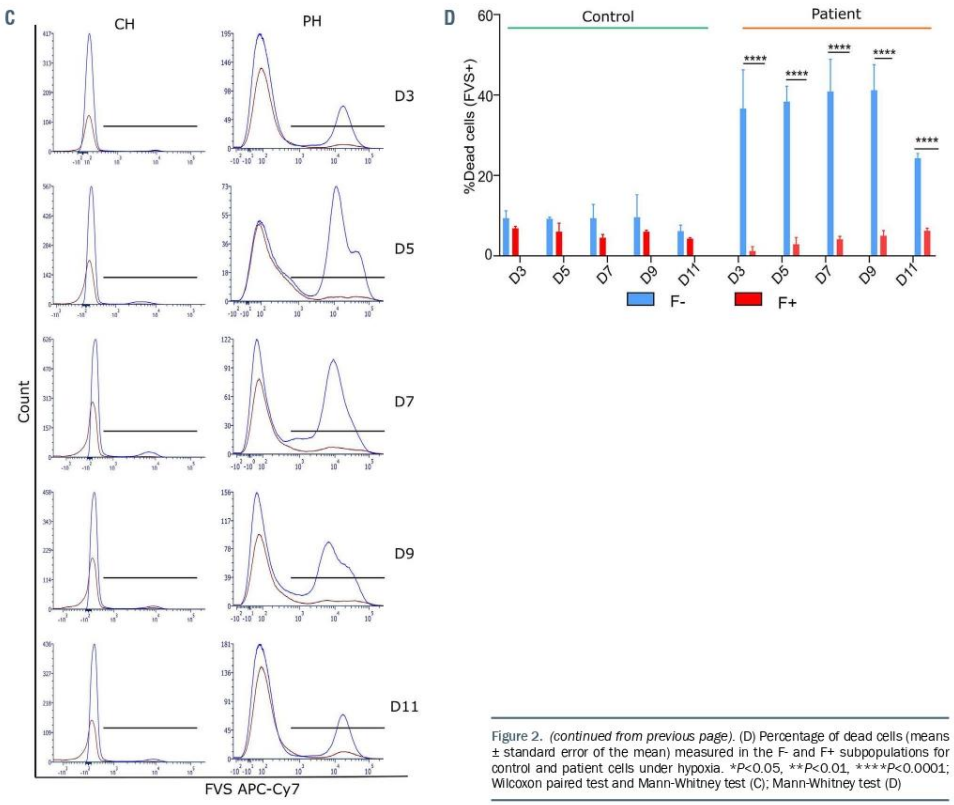

Figure 2. *(continued from previous page).* (D) Percentage of dead cells (means ± standard error of the mean) measured in the F- and F+ subpopulations for control and patient cells under hypoxia. *P<0.05, **P<0.01, ***P<0.0001; Wilcoxon paired test and Mann-Whitney test (C); Mann-Whitney test (D)

repressor LRF in the fetal γ-globin promoters (*HBG1* and *HBG2*)[12] (*Online Supplementary Figure S4C*). CD34$^+$ cells were transfected either with a gRNA targeting the LRF binding site (-197) or a gRNA targeting an unrelated locus (AAVS1). Genome editing efficiency at the γ-globin promoter ranged between 23.2% and 73.5%, as determined by Sanger sequencing at D6 of phase I of culture. Cells were grown and differentiated under normoxia or hypoxia. As expected, the disruption of the LRF binding site resulted in HbF induction as shown by higher %F-cells compared to AAVS1 control (Figure 6C; *Online Supplementary Figure S4D*). These higher levels of F-cells resulted in decreased apoptosis, under both normoxic and hypoxic conditions (Figure 6D; *Online Supplementary Figure S4E*), clearly demonstrating the positive and selective effect of HbF on SCD cell survival.

Discussion

Ineffective erythropoiesis has been previously suggested to be a feature of SCD[7,9,27] but it has not been critically evaluated and documented. Our present findings provide direct evidence for ineffective erythropoiesis in SCD patients, with significant cell death occurring at the late stages of terminal erythroid differentiation *in vivo*.

Among previous reports, the study by Wu and collaborators has highlighted abnormalities during erythropoiesis in the bone marrow of transplanted SCD patients by showing progressive intramedullary loss of SCD erythroblasts and relative enrichment of donor erythroid precursors at the onset of hemoglobinization in a small cohort of patients.[9] Our results further demonstrate significant cell death between the polychromatic and the orthochromatic stages, when cellular HbS concentration reaches sufficiently high levels to promote polymer formation under partial hypoxia. Our *in vivo* data unequivocally document the occurrence of ineffective erythropoiesis in non-transplanted SCD patients, in the absence of confounding factors like conditioning drugs and exogenous donor-related factors that can impact the hematopoietic niche and interfere with the survival of patient's erythroblasts.

This study also reveals a new role for HbF in SCD by showing that it protects a subpopulation of differentiating erythroblasts from apoptosis, both *in vivo* and *in vitro*. HbF is a known modulator of disease severity in SCD as it inhibits HbS polymerization at the molecular level, preventing or attenuating RBC sickling and alleviating disease complications.[28,29] In healthy adults, HbF accounts

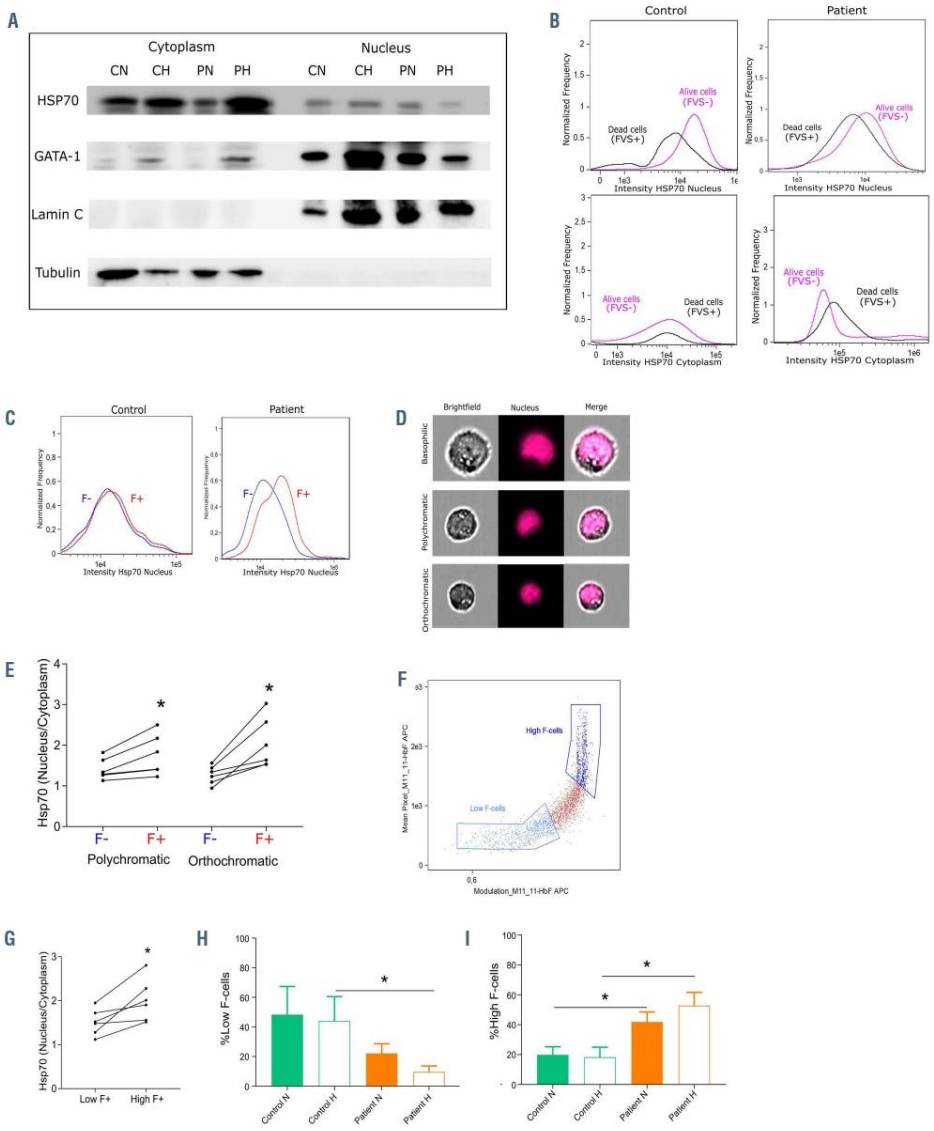

Figure 3. HSP70 cytoplasmic and nuclear distribution. (A) Western blot analysis of HSP70, GATA-1, lamin C and tubulin performed on cytoplasmic and nuclear extracts of erythroid precursors at day 7 (D7) of phase II of culture from control normoxia (CN), control hypoxia (CH), patient normoxia (PN) and patient hypoxia (PH). (B) Distribution of the nuclear intensity (upper panel) and cytoplasmic intensity (lower panel) of HSP70 at D7 of phase II of culture in dead cells (FVS+) and live cells (FVS-) of control and patient cells under hypoxia. (C) Distribution of the nuclear intensity of HSP70 at D7 of phase II of culture in the F- and F+ subpopulations of control (left) and patient (right) cells under hypoxia. (D) Images of basophilic, polychromatic and orthochromatic subpopulations obtained by imaging flow cytometry. (E) HSP70 nucleus/cytoplasm ratio in F- and F+ polychromatic and orthochromatic patient erythroblasts at D7 of phase II of culture (n=6). (F) Dot plot representing the modulation mask of fetal hemoglobin (HbF) (x-axis) and mean pixel HbF values (y-axis) used to discriminate between low and high F-cells. (G) HSP70 nucleus/cytoplasm ratio in low and high F-cells of patients' orthochromatic erythroblasts at D7 of phase II of culture under hypoxia (n=6). Percentage of (H) Low F-cells and (I) High F-cells in control (n=3) and patient (n=6) cells at normoxia and hypoxia at D7 of phase II of culture (means ± standard error of the mean). **P*<0.05. Wilcoxon paired test (E and G) and Mann-Whitney unpaired test (H and I). FVS: fixable viability stain; F-cells: cells expressing fetal hemoglobin.

for less than 1% of total hemoglobin[30] and is restricted to a small subset of RBC (2%) called F-cells.[31-33] In SCD, the expression of HbF is higher than in healthy individuals and varies considerably among patients. Although the mechanisms underlying increased expression of HbF are not completely elucidated, stress erythropoiesis and preferential survival of F-cells in the circulation are suggested contributing factors.[34-38] Our findings show that high HbF levels not only increase survival of circulating red cells but also play a role in the preferential survival of erythroblasts under physiologically relevant hypoxic conditions in the bone marrow.

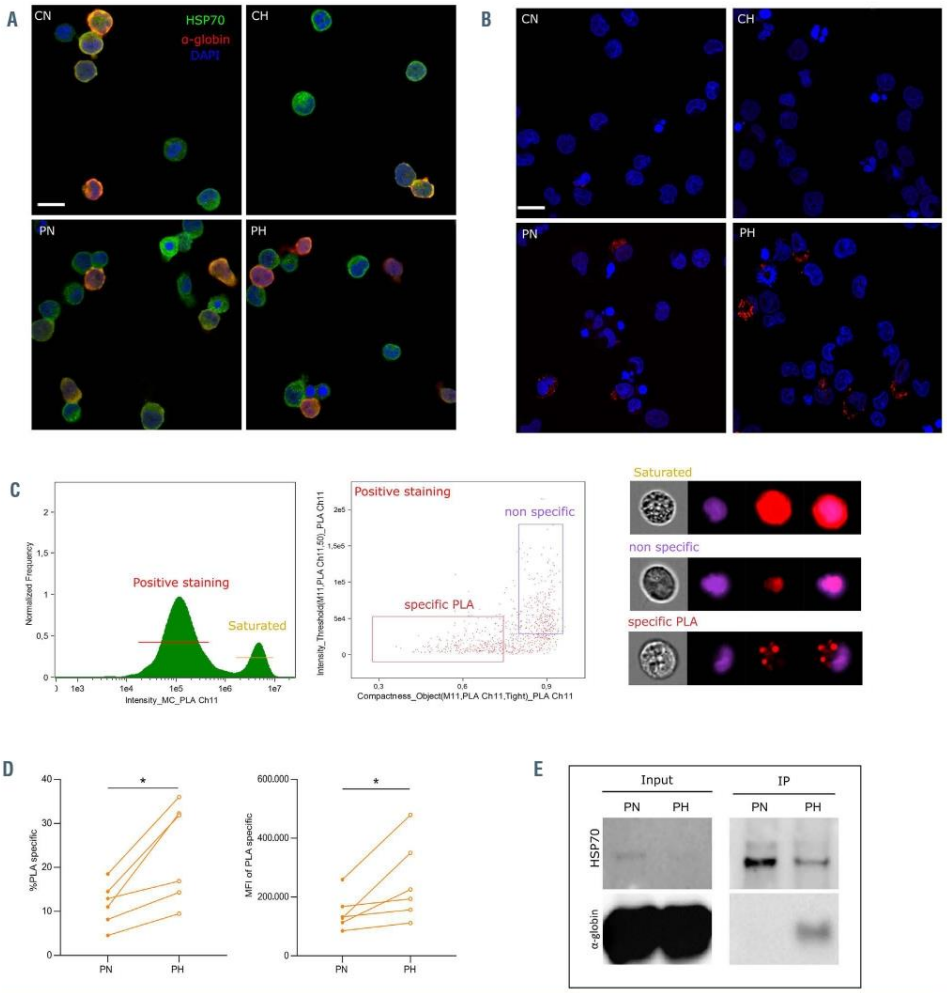

Figure 4. HSP70 and α-globin colocalization and co-immunoprecipitation. (A) Confocal microscopy images of control erythroid precursors under normoxia (CN) or hypoxia (CH), and of patient erythroid precursors under normoxia (PN) or hypoxia (PH) at day 7 (D7) of phase II of culture showing colocalization (in yellow) of HSP70 (green) and α-globin (red); nucleus is in blue (n=3); scale bar: 10 µm. (B) Proximity ligation assay (PLA) between HSP70 and α-globin at D7 of phase II of culture. Red spots indicate proximity (<40 nm) between both proteins. Spots were observed in PN and PH cultures, while no spots were seen in CN and CH. A representative image of each culture is shown (n=3); scale bar: 10 µm. (C) (Left) A histogram representing the intensity of APC signal generated by PLA, a gating of positive staining and saturated staining is indicated. (Middle) A dot plot representing an analysis mask using the compactness feature (x-axis) and intensity feature (y-axis) to discriminate between PLA-specific staining and non-specific staining. (Right) Representative images of each gate. (D) Percentage of cells (left) and mean fluorescence intensity (right) of PLA-specific staining in erythroid precursors of patient normoxia (PN) and patient hypoxia (PH) at D9 of phase II of culture (n=6). (E) Co-immunoprecipitation assay of HSP70 with α-globin using circulating sickle cell disease (SCD) red blood cells incubated under normoxia (PN) or hypoxia (PH) for 1 hour. HSP70 and α-globin bands are detected in the lysates (left panel) and after HSP70 immunoprecipitation (right panel). *P<0.05, Wilcoxon paired test (D).

Our findings show that *in vitro* induction of HbF by pomalidomide rescues SCD erythroblasts from cell death and improves their differentiation, in accordance with improved efficiency of erythropoiesis *in vivo* in treated SCD mice.[39] Furthermore, results using genetically modified CD34+ cells strongly imply that overexpression of HbF and concomitant down-regulation of HbS[12] in a specific and selective manner corrects the apoptosis observed during erythroid differentiation, which is therefore presumably a feature of HbS.

HSP70 is a chaperone protein that plays an important role during erythropoiesis by protecting GATA-1 from cleavage by caspase-3 in the presence of Epo,[40] thus promoting normal terminal differentiation. From a mechanistic perspective, sequestration of HSP70 in the cytoplasm through interaction with HbS polymers is therefore a possible mechanism for ineffective erythropoiesis in SCD. Co-immunoprecipitation of HSP70 and HbS under hypoxia is indeed highly suggestive of such interactions between these proteins. Furthermore, specific HSP70

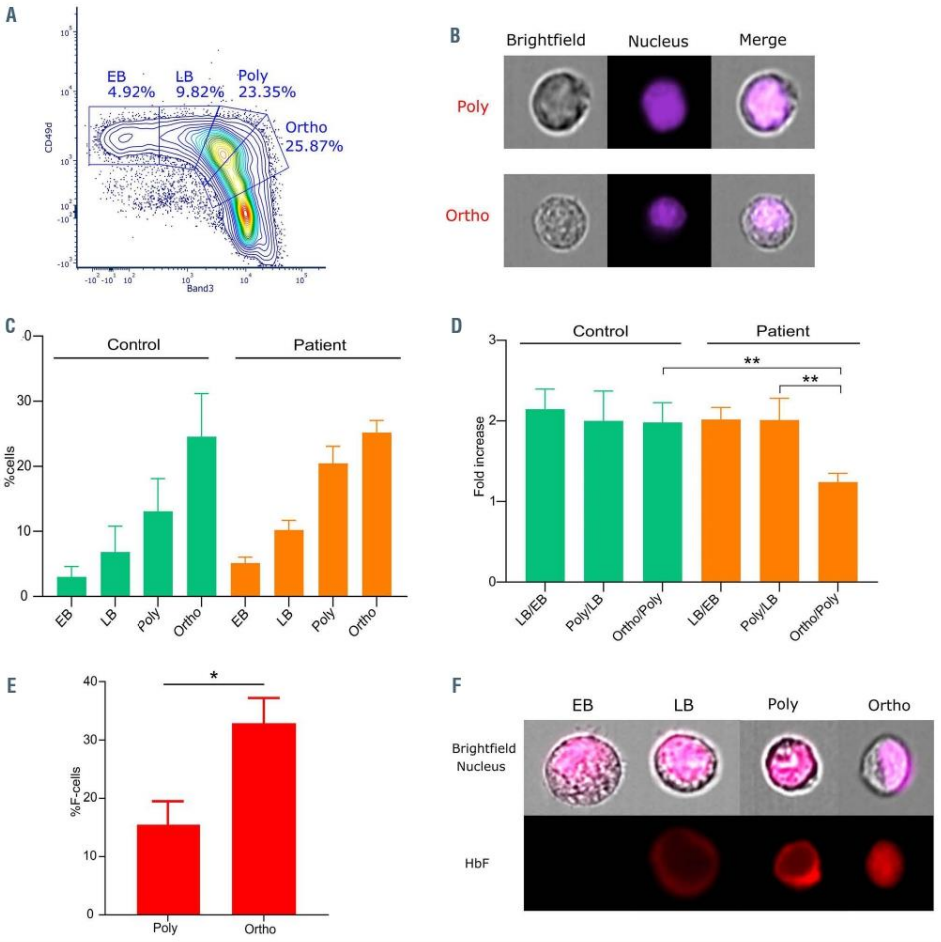

Figure 5. Analysis of human terminal erythroid differentiation *in vivo*. (A) A contour plot representing the distribution of glycophorin A (GPA)-positive cells with respect to Band 3 (x-axis) and CD49d (y-axis) from a bone marrow sample of a sickle cell disease (SCD) patient. (B) Images obtained using imaging flow cytometry from the gating of polychromatic (Poly) and orthochromatic (Ortho) erythroblasts. Nucleus was stained with Hoechst. (C) Percentage of cells at the early basophilic (EB), late basophilic (LB), polychromatic (Poly) and orthochromatic (Ortho) stages in five bone marrow samples of controls (green) and SCD patients (orange) (means ± standard error of the mean [SEM]). (D) The fold increase of cells between the EB and LB (LB/EB), LB and Poly (Poly/LB), Poly and Ortho (Ortho/Poly) stages in five controls and five SCD patients (means ± SEM). (E) Percentage of cells expressing fetal hemoglobin (F-cells) *in vivo* in the polychromatic (Poly) and orthochromatic (Ortho) subpopulations of the patient bone marrow samples (n=5) (means ± SEM). (F) Imaging flow cytometry images of early basophilic (EB), late basophilic (LB), polychromatic (Poly) and orthochromatic (Ortho) precursors. Upper images are a merge of brightfield and nucleus, lower images are for fetal hemoglobin (HbF) staining (red). **P*<0.05, ***P*<0.01; Mann-Whitney test (D and E).

sequestration in the pool of SCD dead cells under hypoxia could account for the lower HSP70 nuclear content of these cells and the subsequent lower GATA-1 nuclear levels. As the molecular event that initiates HSP70 trapping in SCD, namely HbS polymerization, occurs in cells with high cellular concentration of HbS, required for polymer formation, our results show the absence of cell death in the early stages of differentiation where the intracellular concentration of HbS is likely insufficient to induce sickling. Likewise, low levels of HbF are less protective against cell death, since a minimal threshold of intracellular HbF is needed for a protective polymer-inhibiting effect.[41] At physiological levels of hypoxia, there is however not an exclusive selection of F-cells, as significant amounts of cells with no/low HbF were found to complete erythroid differentiation. Further studies are needed to fully address the biological mechanisms underlying this observation and the commitment of erythroid progenitors to the F lineage in SCD.

Finally, this study sheds light on the importance of applying partial hypoxia during erythroid differentiation *in vitro* in order to mimic *in vivo* conditions in SCD. In our view, this together with cell proliferation and apoptosis are important parameters to consider in assessing the beneficial impact of therapeutic approaches in SCD such as HbF induction,[10,20,42] anti-sickling molecules such as voxelotor[43,44] or gene therapy aiming at expressing a therapeutic β-globin.[45] In addition, specific targeting of ineffective erythropoiesis should presumably have a major beneficial clinical impact.

In summary, our study shows that HbF has a dual beneficial effect in SCD by conferring a preferential survival of F-cells in the circulation and by decreasing ineffective erythropoiesis. These findings thus bring new insights into the role of HbF in modulating clinical severity of anemia in SCD by both regulating red cell production and red cell destruction.

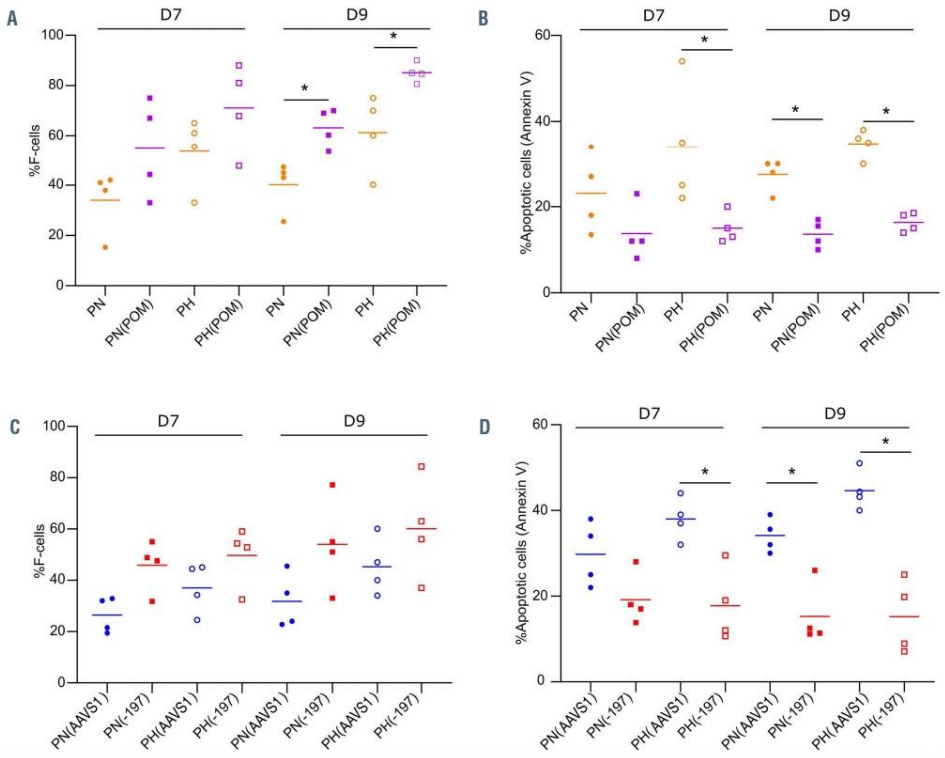

Figure 6. Effect of fetal hemoglobin induction by pomalidomide or CRISPR/Cas9 on terminal erythroid differentiation of sickle cell disease erythroblasts. (A) Percentage of cells expressing fetal hemoglobin (F-cells) at day (D) 7 and D9 of phase II of culture of culture in patient erythroblasts under normoxia (PN), hypoxia (PH), normoxia with POM [PN(POM)] and hypoxia with POM [PH(POM)] (n=4). (B) Percentage of F-cells at D7 and D9 of phase II of culture in patient erythroblasts under normoxia (PN) and hypoxia (PH) treated with guide RNA (gRNA) targeting the LRF binding site (-197) or an unrelated locus as control (AAVS1) (n=4). Genome editing efficiency was 56.1 ± 9.6% and 79.2± 2.8% for -197 and AAVS1 samples, respectively. (C) Percentage of apoptotic cells measured by flow cytometry in PN, PH, PN(POM) and PH(POM) at D7 and D9 of phase II of culture of culture (n=4). (D) Percentage of apoptotic cells at D7 and D9 of phase II of culture in patient erythroblasts under normoxia (PN) and hypoxia (PH) treated with gRNA targeting the LRF binding site (-197) or an unrelated locus as control (AAVS1) (n=4). Horizontal bars represent the mean of each group; *P<0.05, Mann-Whitney test (A, B and D).

Disclosures

No conflicts of interest to disclose.

Contributions

SEH designed and conducted experiments, acquired and analyzed data and wrote the manuscript; SC, AG, HY, MD, GF and SL conducted experiments, acquired and analyzed data; BBF and LJ provided biological samples; OR and AM supervised experiments and analyzed data; VB provided biological samples and discussed data; NM discussed data and wrote the manuscript, WEN designed research, analyzed data and wrote the manuscript. All authors read and edited the manuscript.

Acknowledgments

We thank the patients and their families for accepting to be part of this study. We thank Dr. Jean-Philippe Semblat, Dr. Maria Alejandra Lizarralde-Iragorri and Ms Sandrine Genetet for technical support, Dr. Flavia Guillem, Dr. Thiago Trovati Maciel and Dr. Olivier Hermine for helpful discussions, Dr. Slimane Allali and the nursing staff of Hôpital de jour Pédiatrie Générale of Hôpital Necker Enfants Malades for patient management. We thank Dr. Lionel Blanc for providing non-anemic bone marrow samples.

Funding

The work was supported by the Institut National de la Santé et de la Recherche Médicale (INSERM), Institut National de la Transfusion Sanguine, and grants from Laboratory of Excellence GR-Ex, reference ANR-11-LABX-0051, EUR G.E.N.E., reference ANR-17-EURE-0013, and NIH grant DK32094. The labex GR-Ex is funded by the IdEx program "Investissements d'avenir" of the French National Research Agency, reference ANR-18-IDEX-0001. PICT-IBiSA is part of the France-BioImaging infrastructure funded by ANR-10-INBS-04. SEH was funded by the Ministère de l'Enseignement Supérieur et de la Recherche (Ecole Doctorale BioSPC) and received financial support from, addmedica, the Club du Globule Rouge et du Fer and the Société Française d'Hématologie.

References

1. Pauling L, Itano HA, Singer SJ, Wells IC. Sickle cell anemia, a molecular disease. Science. 1949;110(3):543-548.
2. Piel FB, Steinberg MH, Rees DC. Sickle cell disease. N Engl J Med. 2017;376(16):1561-1573.
3. Ware RE, de Montalembert M, Tshilolo L, Abboud MR. Sickle cell disease. Lancet. 2017;390(10091):311-323.
4. Arlet JB, Dussiot M, Moura IC, Hermine O, Courtois G. Novel players in beta-thalassemia dyserythropoiesis and new therapeutic strategies. Curr Opin Hematol. 2016;23(3):181-188.
5. Arlet JB, Ribeil JA, Guillem F, et al. HSP70 sequestration by free alpha-globin promotes ineffective erythropoiesis in beta-thalassaemia. Nature. 2014;514(7521):242-246.
6. Rivella S. Ineffective erythropoiesis and thalassemias. Curr Opin Hematol. 2009;16(3):187-194.
7. Hasegawa S, Rodgers GP, Dwyer N, et al. Sickling of nucleated erythroid precursors from patients with sickle cell anemia. Exp Hematol. 1998;26(4):314-319.
8. Blouin MJ, De Paepe ME, Trudel M. Altered hematopoiesis in murine sickle cell disease. Blood. 1999;94(4):1451-1459.
9. Wu CJ, Krishnamurti L, Kutok JL, et al. Evidence for ineffective erythropoiesis in severe sickle cell disease. Blood. 2005;106(10):3639-3645.
10. McArthur JG, Svenstrup N, Chen C, et al. A novel, highly potent and selective phosphodiesterase-9 inhibitor for the treatment of sickle cell disease. Haematologica. 2020;105(3):623-631.
11. Dulmovits BM, Appiah-Kubi AO, Papoin J, et al. Pomalidomide reverses gamma-globin silencing through the transcriptional reprogramming of adult hematopoietic progenitors. Blood. 2016;127(11):1481-1492.
12. Weber L, Frati G, Felix T, et al. Editing a gamma-globin repressor binding site restores fetal hemoglobin synthesis and corrects the sickle cell disease phenotype. Sci Adv. 2020;6(7):eaay9392.
13. Brinkman EK, Chen T, Amendola M, van Steensel B. Easy quantitative assessment of genome editing by sequence trace decomposition. Nucleic Acids Res. 2014;42(22):e168.
14. Hu J, Liu J, Xue F, et al. Isolation and functional characterization of human erythroblasts at distinct stages: implications for understanding of normal and disordered erythropoiesis in vivo. Blood. 2013;121(16):3246-3253.
15. Schindelin J, Arganda-Carreras I, Frise E, et al. Fiji: an open-source platform for biological-image analysis. Nat Methods. 2012;9(7):676-682.
16. Mantel CR, O'Leary HA, Chitteti BR, et al. Enhancing hematopoietic stem cell transplantation efficacy by mitigating oxygen shock. Cell. 2015;161(7):1553-1565.
17. Mohyeldin A, Garzon-Muvdi T, Quinones-Hinojosa A. Oxygen in stem cell biology: a critical component of the stem cell niche. Cell Stem Cell. 2010;7(2):150-161.
18. Yeo JH, Cosgriff MP, Fraser ST. Analyzing the formation, morphology, and integrity of erythroblastic islands. Methods Mol Biol. 2018;1698:133-152.
19. Lizarralde Iragorri MA, El Hoss S, Brousse V, et al. A microfluidic approach to study the effect of mechanical stress on erythrocytes in sickle cell disease. Lab Chip. 2018;18(19):2975-2984.
20. Antoniani C, Meneghini V, Lattanzi A, et al. Induction of fetal hemoglobin synthesis by CRISPR/Cas9-mediated editing of the human beta-globin locus. Blood. 2018;131(17):1960-1973.
21. Zhang Y, Paikari A, Sumazin P, et al. Metformin induces FOXO3-dependent fetal hemoglobin production in human primary erythroid cells. Blood. 2018;132(3):321-333.
22. Kalfa T, McGrath KE. Analysis of erythropoiesis using imaging flow cytometry. Methods Mol Biol. 2018;1698:175-192.
23. Bolte S, Cordelieres FP. A guided tour into subcellular colocalization analysis in light microscopy. J Microsc. 2006;224(Pt 3):213-232.
24. Manders EM, Stap J, Brakenhoff GJ, van Driel R, Aten JA. Dynamics of three-dimensional replication patterns during the S-phase, analysed by double labelling of DNA and confocal microscopy. J Cell Sci. 1992;103 (Pt 3):857-862.
25. Schallmeiner E, Oksanen E, Ericsson O, et al. Sensitive protein detection via triple-binder proximity ligation assays. Nat Methods. 2007;4(2):135-137.
26. Moutouh-de Parseval LA, Verhelle D, Glezer E, et al. Pomalidomide and lenalidomide regulate erythropoiesis and fetal hemoglobin production in human CD34+ cells. J Clin Invest. 2008;118(1):248-258.
27. Finch CA, Lee MY, Leonard JM. Continuous RBC transfusions in a patient with sickle cell disease. Arch Intern Med. 1982;142(2):279-282.
28. Powars DR, Weiss JN, Chan LS, Schroeder WA. Is there a threshold level of fetal hemoglobin that ameliorates morbidity in sickle cell anemia? Blood. 1984;63(4):921-926.
29. Sewchand LS, Johnson CS, Meiselman HJ. The effect of fetal hemoglobin on the sickling dynamics of SS erythrocytes. Blood Cells. 1983;9(1):147-166.
30. Boyer SH, Margolet L, Boyer ML, et al. Inheritance of F cell frequency in heterocellular hereditary persistence of fetal hemoglobin: an example of allelic exclusion. Am J Hum Genet. 1977;29(3):256-271.
31. Boyer SH, Belding TK, Margolet L, Noyes AN. Fetal hemoglobin restriction to a few erythrocytes (F cells) in normal human adults. Science. 1975;188(4186):361-363.
32. Boyer SH, Belding TK, Margolte L, Noyes AN, Burke PJ, Bell WR. Variations in the frequency of fetal hemoglobin-bearing erythrocytes (F-cells) in well adults, pregnant women, and adult leukemics. Johns Hopkins Med J. 1975;137(3):105-115.
33. Wood WG, Stamatoyannopoulos G, Lim G, Nute PE. F-cells in the adult: normal values and levels in individuals with hereditary and acquired elevations of Hb F. Blood. 1975;46(5):671-682.
34. Stamatoyannopoulos G, Veith R, Galanello R, Papayannopoulou T. Hb F production in stressed erythropoiesis: observations and kinetic models. Ann N Y Acad Sci. 1985;445:188-197.
35. Dover GJ, Boyer SH, Charache S, Heintzelman K. Individual variation in the production and survival of F cells in sickle-cell disease. N Engl J Med. 1978;299(26):1428-1435.
36. Franco RS, Lohmann J, Silberstein EB, et al. Time-dependent changes in the density and hemoglobin F content of biotin-labeled sick-

le cells. J Clin Invest. 1998;101(12):2730-2740.
37. Franco RS, Yasin Z, Palascak MB, Ciraolo P, Joiner CH, Rucknagel DL. The effect of fetal hemoglobin on the survival characteristics of sickle cells. Blood. 2006;108(3):1073-1076.
38. Maier-Redelsperger M, Noguchi CT, de Montalembert M, et al. Variation in fetal hemoglobin parameters and predicted hemoglobin S polymerization in sickle cell children in the first two years of life: Parisian Prospective Study on Sickle Cell Disease. Blood. 1994;84(9):3182-3188.
39. Meiler SE, Wade M, Kutlar F, et al. Pomalidomide augments fetal hemoglobin production without the myelosuppressive effects of hydroxyurea in transgenic sickle cell mice. Blood. 2011;118(4):1109-1112.
40. Ribeil JA, Zermati Y, Vandekerckhove J, et al. Hsp70 regulates erythropoiesis by preventing caspase-3-mediated cleavage of GATA-1. Nature. 2007;445(7123):102-105.
41. Noguchi CT, Rodgers GP, Schechter AN. Intracellular polymerization. Disease severity and therapeutic predictions. Ann N Y Acad Sci. 1989;565:75-82.
42. Paikari A, Sheehan VA. Fetal haemoglobin induction in sickle cell disease. Br J Haematol. 2018;180(2):189-200.
43. Howard J, Hemmaway CJ, Telfer P, et al. A phase 1/2 ascending dose study and open-label extension study of voxelotor in patients with sickle cell disease. Blood. 2019;133(17):1865-1875.
44. Vichinsky E, Hoppe CC, Ataga KI, et al. A phase 3 randomized trial of voxelotor in sickle cell disease. N Engl J Med. 2019;381(6):509-519.
45. Ribeil JA, Hacein-Bey-Abina S, Payen E, et al. Gene therapy in a patient with sickle cell disease. N Engl J Med. 2017;376(9):848-855.

REVIEW 1

CE: D.C.; MOH/280305; Total nos of Pages: 7;

MOH 280305

REVIEW

Ineffective erythropoiesis in sickle cell disease: new insights and future implications

AQ2

Wassim El Nemer[a,b,c], *Auria Godard*[c,d,e], *and Sara El Hoss*[c,d,e]

Purpose of review
Sickle cell disease (SCD) is a hemolytic anemia caused by a point mutation in the β globin gene leading to the expression of an abnormal hemoglobin (HbS) that polymerizes under hypoxic conditions driving red cell sickling. Circulating red cells have been extensively characterized in SCD, as their destruction and removal from peripheral blood are the major contributors to anemia. However, few reports showed cellular abnormalities during erythropoiesis in SCD, suggesting that anemia could also be influenced by defects of central origin.

Recent findings
El Hoss *et al.* demonstrated ineffective erythropoiesis (IE) in SCD and deciphered the molecular mechanism underlying cell death during the hemoglobin synthesis phase of terminal differentiation. They showed that HbS polymerization induces apoptosis of differentiating erythroblasts and that fetal hemoglobin rescues these cells through its antipolymerization function.

Summary
IE is the major cause of anemia in β-thalassemia patients, and it is generally surmised that it contributes little to anemia of SCD. Recent reports demonstrate the occurrence of IE in SCD patients and show important alterations in the hematopoietic and erythroid niches, both in SCD patients and in the humanized Townes SCD mouse model. This implies that therapeutic strategies initially designed to improve red cell survival in the circulation of SCD patients would also positively impact erythropoiesis and bone marrow cellularity.

Keywords
erythropoiesis, fetal hemoglobin, heat shock protein 70, sickle cell disease

INTRODUCTION

Sickle cell disease (SCD) is a genetic recessive inherited disease and one of the most common severe monogenic disorders worldwide. SCD is caused by a point mutation in the β globin gene that substitutes Glutamate into Valine at the 6th position of the β globin protein leading to the expression of an abnormal hemoglobin (HbS) that polymerizes under hypoxic conditions driving red blood cell (RBC) sickling [1]. The clinical expression occurs in childhood, few months after birth. SCD is a multisystem disease characterized by hemolytic anemia, high susceptibility to infections, recurrent painful vaso-occlusive crises, stroke, acute chest syndrome, and organ failure, with the spleen being the first organ to be affected [2,3]. RBCs in SCD are characterized by decreased deformability and increased rigidity because of dehydration and sickling, which results in alterations of the blood rheology and the microcirculatory flow [2–6]. These alterations in the mechanical properties shorten the life span of peripheral RBCs, which is a major contributor to anemia in SCD. Over the past years, a number of studies showed abnormalities during terminal erythroid differentiation in SCD, suggesting that anemia could also be impacted by defects of central origin in this pathology. The fact that such abnormalities take place during the terminal phase of differentiation is not surprising since the causal mutation in SCD affects hemoglobin, whose expression is initiated during this phase. In the 1980s, ferrokinetic studies suggested the existence of

[a]Etablissement Français du Sang PACA-Corse, [b]Aix Marseille Univ, EFS, CNRS, ADES, 'Biologie des Groupes Sanguins', Marseille, [c]Laboratoire d'Excellence GR-Ex, [d]Université de Paris, UMR_S1134, BIGR, Inserm and [e]Institut National de la Transfusion Sanguine, Paris, France AQ3

Correspondence to Wassim El Nemer, UMR 7268, 27 boulevard Jean Moulin, 13005 Marseille, France. Tel: +33491170376; fax: +33491170370; e-mail: wassim.el-nemer@efs.sante.fr AQ4

Curr Opin Hematol 2021, 27:000–000
DOI:10.1097/MOH.0000000000000642

CE: D.C.; MOH/280305; Total nos of Pages: 7;
MOH 280305

KEY POINTS

- Ineffective erythropoiesis is a clinical feature in sickle cell disease (SCD), with a significant proportion of differentiating erythroblasts undergoing apoptosis between the polychromatic and the orthochromatic stages.
- Fetal hemoglobin (HbF) plays an important antiapoptotic role during terminal erythroid differentiation in SCD.
- Antisickling therapeutic strategies designed to improve red cell survival in SCD would positively impact erythropoiesis and bone marrow cellularity.

ineffective erythropoiesis (IE) in SCD [7,8]. Later, erythroblasts differentiated *in vitro* or isolated from bone marrow (BM) of SCD patients were shown to sickle under hypoxic conditions [9], bringing evidence of cellular abnormalities occurring during the erythroid differentiation phase. Such sickling was also reported in the BM of the SAD mouse model, in which late-stage erythroid precursors have altered morphology and high levels of hemoglobin polymers, with increased fragmentation of reticulocytes during medullary endothelial migration [10]. In 2005, the study by Wu *et al.* showed evidence of IE in transplanted SCD patients, with an imbalance favoring the survival of the donor erythroid progenitor cells [11].

In 2020, the study by El Hoss *et al.* demonstrated the occurrence of IE in nontransplanted SCD patients, both *in vivo* and *in vitro*, and identified the transition between the polychromatic and orthochromatic stages as the critical timepoint where cell death takes place. They showed that IE is tightly linked to the partial hypoxic environment of the BM that drives HbS polymerization leading to the cytoplasmic sequestration of heat shock protein 70 (HSP70) preventing it from transiting to the nucleus to protect GATA-1. They revealed and demonstrated a new role for fetal hemoglobin (HbF) in rescuing erythroid precursors from apoptosis through its antipolymerization function [12▪▪].

ERYTHROPOIESIS AND HEMOGLOBINOPATHIES

Human erythropoiesis is a complex multistep process that takes place in the BM in adults, starting from a multipotent hematopoietic stem cell (HSC) and ending with an enucleated reticulocyte that exits the BM and matures in the circulation to become an erythrocyte [13]. Erythropoiesis starts with an engagement phase, where HSCs give rise to the common myeloid progenitors (CMPs) [13]. The CMPs differentiate into the bipotent megakaryocytic-erythroid progenitors (MEPs) [14]. Burst-forming unit-erythroid (BFU-E) are the first committed progenitors to the erythroid lineage downstream of the MEPs that further differentiate into colony forming unit-erythroid (CFU-E) [14]. The CFU-E then enter the second phase of differentiation, also called terminal differentiation, where the proerythroblast sequentially divides and differentiates into early basophilic, late basophilic, polychromatic, and orthochromatic erythroblast, with a cell doubling between two consecutive stages and a total number of 4 mitoses (1 proerythroblast giving rise to 16 orthochromatic erythroblasts). During the terminal phase, hemoglobin is synthesized and nucleus condensation occurs, thus facilitating the enucleation process [15].

Over the last decade, considerable technical progress has been made to isolate and characterize erythroid progenitors and erythroblasts at different stages of development. A key step forward was achieved by the group of Narla Mohandas by developing a flow cytometry method based on the analysis of fluorescently labeled membrane proteins to distinguish between erythroblasts in the four-terminal differentiation stages. They showed that during erythroid differentiation, the expression of the major red cell proteins increased whereas the expression of adhesion molecules decreased. This led them to set a combination of three critical fluorescent markers [Glycophorin A (GPA), Band 3, and α4 integrin] to precisely follow and determine the terminal differentiation stages [16]. This staining strategy became the gold standard technique in the field, and today it is considered essential in studies investigating IE, like in hemoglobinopathies where the major defects occur during the terminal stages of differentiation.

In hemoglobinopathies, abnormal or altered expression of hemoglobin can directly impact the terminal differentiation phase, like in β thalassemia major (β-TM), where the absence of β globin drives massive apoptosis at the polychromatic stage, which indirectly impacts the early differentiation phase leading to the expansion of early erythroid precursors and erythroid progenitors [17,18]. The molecular mechanism underlying this cell death was uncovered when the critical role of HSP70 in protecting GATA-1 from cleavage by Caspase-3 was reported [19], followed by the demonstration of HSP70 sequestration in the cytoplasm of erythroid precursors in β-TM, preventing it from transiting to the nucleus to protect GATA-1 and thus leading to apoptosis [20].

CE: D.C.; MOH/280305; Total nos of Pages: 7;
MOH 280305

INEFFECTIVE ERYTHROPOIESIS IN SICKLE CELL DISEASE, FETAL HEMOGLOBIN, AND HEAT SHOCK PROTEIN 70

In El Hoss *et al.*, apoptosis of SCD erythroid precursors was shown to take place under normoxic conditions *in vitro* and to be exacerbated by partial hypoxia that mimics the BM environment. Significant levels of apoptosis under normoxia suggest that HbS polymerization is not a prerequisite for cell death and that other mechanisms can also contribute to IE in SCD. One mechanism could be related to oxidation because HbS is known to exhibit accelerated spontaneous auto-oxidation, 1.7-fold higher than HbA [21]. Future studies should focus on investigating the potential role of oxidative stress in apoptosis and cell senescence of SCD erythroblasts, as ROS production may alter the cell cycle by activating a PML/p53 signaling cascade [22].

AQ5

Under both oxygen conditions, and to different extents, imaging assays showed proximity between HSP70 and hemoglobin, suggesting a role for hemoglobin in HSP70 trapping even in the absence of HbS polymers. Such trapping could be due to the pool of free α chains in the cytoplasm [23] subsequent to the imbalance between α and β^S chains because of the lower affinity of β^S chain to α chain as compared to β^A [24]. This is supported by the fact that co-inheritance of α-thalassemia is a modulator of disease severity in SCD [25], and based on El Hoss *et al.*, one would expect a positive impact of α-thalassemia in SCD as early as the erythroid differentiation stage.

Although HbF was shown to play an antiapoptotic role by rescuing differentiating erythroblasts from cell death, there is a significant number of cells with no HbF that complete the differentiation process, both *in vitro* and *in vivo*. One explanation could reside in different kinetics between HbS expression/polymerization and HSP70 nuclear transit. This can be due to a relatively less hypoxic microenvironment for a number of erythroid clones slowing down the polymerization process of HbS, thus enabling enough HSP70 to transit to the nucleus before being trapped in the cytoplasm. A differential kinetics involving HSP70 nuclear transit can also explain the differences between IE of β-TM and SCD, the latter being less severe. As a matter of fact, in β-TM, lack of β globin drives aggregation of α globin chains shortly after they are expressed, trapping HSP70 in the cytoplasm early during the globin synthesis phase. In SCD, the molecular event that initiates HSP70 trapping occurs later as HbS tetramers are first soluble in the cytoplasm and need to reach high concentrations for polymer formation and subsequent HSP70 trapping (Fig. 1).

IMPACT OF INEFFECTIVE ERYTHROPOIESIS ON THE ERYTHROID AND THE HEMATOPOIETIC NICHES

Mammalian erythroid differentiation occurs in a specific niche in the BM known as the erythroblastic island (EBI). The EBI is constituted of one or two central macrophages surrounded by differentiating erythroblasts [26]. The central macrophage plays a critical role in erythropoiesis, acting as an anchor to the erythroblasts providing cellular interactions and nutrients required for differentiation and proliferation, in addition to a phagocytic function to eliminate and recycle the extruded nuclei of orthochromatic erythroblasts [27–29]. The erythroid niche is located in hypoxic microenvironments with an oxygen level of 1–7% [30,31]. EBI macrophages play an essential role in maintaining erythropoiesis both at steady-state and under acute stress conditions [32,33]. However, the limited access to these cells, as well as the lack of characterization of their precise phenotypic profile, has hampered progress in understanding their contribution to erythropoietic disorders.

The study of El Hoss *et al.* showed a loss of cell doubling between the polychromatic and the orthochromatic stages in the BM of 5 SCD patients, with a mean fold increase between these 2 stages of only 1.24 [12▪▪]. This indicates that around 40% of polychromatic erythroblasts are lost during the differentiation process. Considering that under physiological conditions the BM produces erythrocytes at a rate of approximately 2 million cells per second, this would mean that a minimum of 0.8 million cells is undergoing apoptosis every second in SCD erythropoiesis. As the closest cells with a phagocytic function, one would expect that the central macrophages of the EBIs would have to rapidly engulf very high numbers of apoptotic erythroblasts, which would negatively impact their other functions and potentially disturb erythroid differentiation.

Defects of the central macrophages could be reflected by the presence of circulating nucleated erythroblasts (CNEs) in peripheral blood. Damage or stress to the BM is known inducers of CNEs. This is especially the case in pathologies characterized by IE, such as SCD or β-thalassemia, where the percentage of CNEs is correlated with disease severity [34]. These CNEs may result from impaired interaction between macrophages and erythroblasts, which would then be released prematurely in the circulation. Thus, high numbers of CNEs in some SCD patients could reflect altered EBI structures.

Furthermore, IE could also have an impact on the overall BM environment in SCD. The autoxidation of HbS can promote excessive ROS production

CE: D.C.; MOH/280305; Total nos of Pages: 7;
MOH 280305

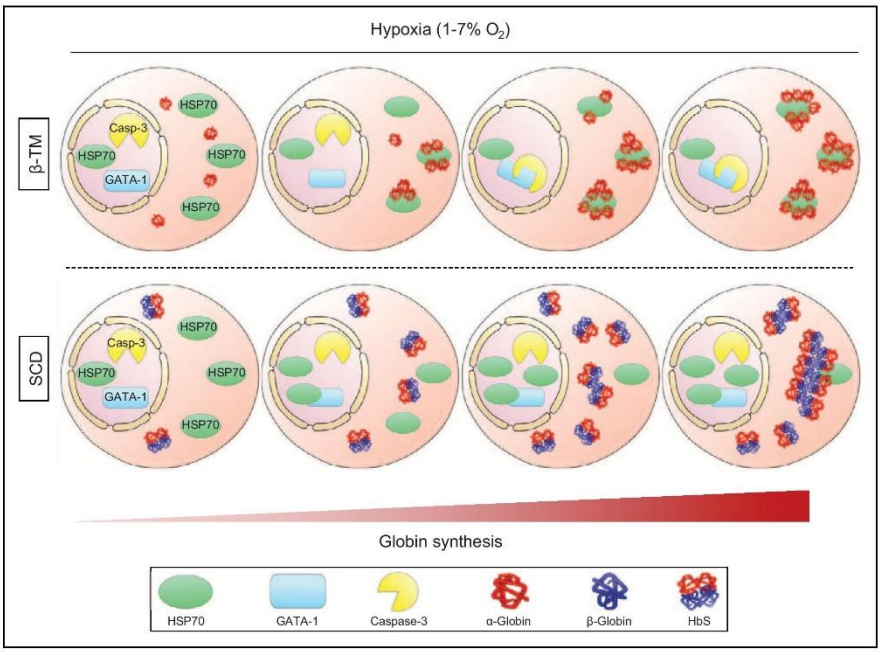

FIGURE 1. Trapping of HSP70 in the cytoplasm of differentiating erythroblasts: illustration of differential kinetics of HSP70 cytoplasmic trapping in β-thalassemia major (β-TM) and sickle cell disease (SCD) erythroblasts as a function of globin synthesis. In this example, 4, 8, 14 and 20 molecules of α-globin are gradually present in β-TM erythroblasts, corresponding to 2, 4, 7 and 10 molecules of HbS in SCD cells. α-globin chains form aggregates as early as they are expressed, trapping HSP70 in the cytoplasm, whereas it takes longer time for HbS to form polymers, as polymerization depends on the hypoxic levels of the bone marrow microenvironment and on the intracellular concentration of HbS. HbS, abnormal hemoglobin.

that might contribute to creating a pro-oxidant environment in the BM [35]. This is supported by a recent study on SS Townes mice showing increased oxidative stress during SCD erythropoiesis associated with disorganized and structurally abnormal marrow vascular structure [36▪▪]. The study also showed defects of perivascular CXCL12-abundant reticular mesenchymal stromal cells (CARs) in the BM, suggesting alterations of the hematopoietic niche, as CARs play a key role in the homeostatic maintenance of HSCs and hematopoietic progenitor cells within the BM. This is supported by another recent study showing that the hematopoietic niche of SCD patients is highly perturbed compared to that of healthy individuals, with increased circulating $CD34^+$ cells, depletion in committed erythroid progenitors, and increased concentration of hematopoietic cells [37▪]. In addition, chronic inflammation and continual oxidative stress may lead to a decrease in the numbers of Long Term-HSCs and impede the potential of proliferation and transduction of BM stem cells in patients with SCD [38]. A direct consequence of this aberrant vascular niche is an impairment of HSPC homing and engraftment during HSC transplantation (HCT), particularly in older SCD patients, where we expect BM defects to be more pronounced than in younger ones. As a matter of fact, the age at the performance of HCT is the strongest predictor of event-free survival in HLA-identical sibling donor HCT [39–41].

IMPACT OF TREATMENTS ON INEFFECTIVE ERYTHROPOIESIS IN SICKLE CELL DISEASE

The demonstration of IE in SCD raises the question of the impact of treatments on cell survival during the terminal phase of erythroid differentiation. It is

CE: D.C.; MOH/280305; Total nos of Pages: 7;
MOH 280305

tempting to speculate that treatments targeting HbS expression or polymerization would inhibit apoptosis and increase the reticulocyte count. Such treatments can be classified into three categories: (1) treatments inducing HbF expression, either by the use of pharmacological agents, such as hydroxycarbamide (HC) [42], 5-aza-2′-deoxycytidine [43], or the PDE9 inhibitor IMR-687 [44▪], or by gene therapy [45], (2) treatments using inhibitors of HbS polymerization such as Voxelotor [46,47], and (3) gene therapy aiming at expressing a therapeutic β globin, either in a gene addition approach [48], or by correcting the endogenous mutation [49,50]. To date, there are no studies investigating the impact of such treatments on terminal erythropoiesis in SCD patients, but the few data available in the literature support our hypothesis. As a matter of fact, Sauntharajah *et al.* reported that SCD patients treated with 5-aza-2′-deoxycytidine to induce HbF maintained BM cellularity and increased the proportion of erythroid cells [43], which we believe is a consequence of erythroblast rescue from cell death at the terminal stages of differentiation mediated by HbF induction. Future studies should investigate the impact of treatments on terminal erythropoiesis in SCD by focusing on the apoptosis and proliferation rates of differentiating erythroblasts. Such studies can be conducted *in vivo* using the Townes mouse model, and *in vitro* with the condition of applying partial hypoxia during the terminal differentiation phase to mimic the BM environment. Furthermore, in the particular case of gene therapy, we believe that monitoring erythroid differentiation in the BM of treated patients before and after therapy is crucial in order to evaluate the impact of the corrective therapy at a central level by correlating the data with the number of reticulocytes released in the circulation.

CONCLUSION

The study of El Hoss *et al.* highlights a novel anti-apoptotic role for HbF that positively impacts cell survival as early as the erythroid differentiation stage. This is consistent with high HbF expression levels in circulating reticulocytes of SCD patients that we expect to be higher than in patients with hemolytic anemia other than hemoglobinopathies, such as hereditary spherocytosis (HS), where HbF expression does not bring a selective advantage during the terminal erythroid differentiation stage. It would be interesting to compare the levels of F-reticulocytes between SCD and HS patients, for example, as it would help assessing the proportion of F-cells driven by stress erythropoiesis and the proportion resulting from the positive selection of F-poly/orthochromatic erythroblasts. Efforts should also be made to investigate early erythroid differentiation in SCD and the commitment of erythroid clones to the F lineage.

Acknowledgements

None.

Financial support and sponsorship

Work in the author's laboratory is supported by Etablissement Français du Sang (EFS), Aix Marseille Université, Inserm, the Laboratory of Excellence on Red Cells Labex GR-Ex (reference ANR-11-LABX-0051; GR-Ex is funded by the IdEx program 'Investissements d'avenir' of the French National Research Agency, reference ANR-18-IDEX-0001), the European Union's Horizon 2020 Research and Innovation Program, and generous funding from addmedica, Ministère de l'Enseignement Supérieur et de la Recherche (Ecole Doctorale BioSPC), the Club du Globule Rouge et du Fer (CGRF) and the Société Française d'Hématologie (SFH).

Conflicts of interest

There are no conflicts of interest.

REFERENCES AND RECOMMENDED READING

Papers of particular interest, published within the annual period of review, have been highlighted as:
▪ of special interest
▪▪ of outstanding interest

1. Pauling L, Itano HA, Singer SJ, Wells IC. Sickle cell anemia, a molecular disease. Science 1949; 110:. AQ6
2. Piel FB, Steinberg MH, Rees DC. Sickle cell disease. N Engl J Med 2017; 376:1561–1573.
3. Ware RE, Montalembert MD, Tshilolo L, Abboud MR. Sickle cell disease. Lancet 2017; 6736:1–13.
4. Barabino GA, Platt MO, Kaul DK. Sickle cell biomechanics. Annu Rev Biomed Eng 2010; 12:345–367.
5. Connes P, Lamarre Y, Waltz X, *et al.* Haemolysis and abnormal haemorheology in sickle cell anaemia. Br J Haematol 2014; 165:564–572.
6. Stuart MJ, Nagel RL. Sickle-cell disease. Lancet 2004; 364:1343–1360.
7. Cazzola M, Pootrakul P, Huebers HA, *et al.* Erythroid marrow function in anemic patients. Blood 1987; 69:296–301.
8. Finch CA, Lee MY, Leonard JM. Continuous RBC transfusions in a patient with sickle cell disease. Arch Intern Med 1982; 142:279–282.
9. Hasegawa S, Rodgers GP, Dwyer N, *et al.* Sickling of nucleated erythroid precursors from patients with sickle cell anemia. Exp Hematol 1998; 26:314–319.
10. Blouin MJ, De Paepe ME, Trudel M. Altered hematopoiesis in murine sickle cell disease. Blood 1999; 94:1451–1459.
11. Wu CJ, Krishnamurti L, Kutok JL, *et al.* Evidence for ineffective erythropoiesis in severe sickle cell disease. Blood 2005; 106:3639–3645.
12. El Hoss S, Cochet S, Godard A, *et al.* Fetal hemoglobin rescues ineffective erythropoiesis in sickle cell disease. Haematologica 2020. AQ7
▪▪ Demonstration of ineffective erythropoiesis in SCD, with the description of the underlying molecular mechanism.
13. Orkin SH. Diversification of haematopoietic stem cells to specific lineages. Nat Rev Genet 2000; 1:57–64.
14. Gregory CJ, Eaves AC. Human marrow cells capable of erythropoietic differentiation in vitro: definition of three erythroid colony responses. Blood 1977; 49:855–864.
15. Granick S, Levere RD. Heme Synthesis in Erythroid Cells. Prog Hematol 1964; 4:1–47.
16. Hu J, Liu J, Xue F, *et al.* Isolation and functional characterization of human erythroblasts at distinct stages: implications for understanding of normal and disordered erythropoiesis in vivo. Blood 2013; 121:3246–3253.

CE: D.C.; MOH/280305; Total nos of Pages: 7;

MOH 280305

AQ8
17. Ribeil JA, Arlet JB, Dussiot M, *et al.* Ineffective erythropoiesis in beta-thalassemia. ScientificWorldJournal 2013; 2013:394295.
18. Arlet JB, Dussiot M, Moura IC, *et al.* Novel players in beta-thalassemia dyserythropoiesis and new therapeutic strategies. Curr Opin Hematol 2016; 23:181–188.
19. Ribeil JA, Zermati Y, Vandekerckhove J, *et al.* Hsp70 regulates erythropoiesis by preventing caspase-3-mediated cleavage of GATA-1. Nature 2007; 445:102–105.
20. Arlet JB, Ribeil JA, Guillem F, *et al.* HSP70 sequestration by free alpha-globin promotes ineffective erythropoiesis in beta-thalassaemia. Nature 2014; 514:242–246.
21. Hebbel RP, Morgan WT, Eaton JW, Hedlund BE. Accelerated autoxidation and heme loss due to instability of sickle hemoglobin. Proc Natl Acad Sci USA 1988; 85:237–241.
22. Niwa-Kawakita M, Ferhi O, Soilihi H, *et al.* PML is a ROS sensor activating p53 upon oxidative stress. J Exp Med 2017; 214:3197–3206.
23. Vasseur C, Domingues-Hamdi E, Ledudal K, *et al.* Red blood cells free alpha-haemoglobin pool: a biomarker to monitor the beta-thalassemia intermedia variability. The ALPHAPOOL study. Br J Haematol 2017; 179:142–153.
24. Shaeffer JR. Evidence for a difference in affinities of human hemoglobin beta A and beta S chains for alpha chains. J Biol Chem 1980; 255:2322–2324.
25. Embury SH, Dozy AM, Miller J, *et al.* Concurrent sickle-cell anemia and alpha-thalassemia: effect on severity of anemia. N Engl J Med 1982; 306:270–274.
26. Lee SH, Crocker PR, Westaby S, *et al.* Isolation and immunocytochemical characterization of human bone marrow stromal macrophages in hemopoietic clusters. J Exp Med 1988; 168:1193–1198.
27. Bessis MC, Breton-Gorius J. Iron metabolism in the bone marrow as seen by electron microscopy: a critical review. Blood 1962; 19:635–663.
28. Seki M, Shirasawa H. Role of the reticular cells during maturation process of the erythroblast. 3. The fate of phagocytized nucleus. Acta Pathol Jpn 1965; 15:387–405.
29. Skutelsky E, Danon D. On the expulsion of the erythroid nucleus and its phagocytosis. Anat Rec 1972; 173:123–126.
30. Mohyeldin A, Garzon-Muvdi T, Quinones-Hinojosa A. Oxygen in stem cell biology: a critical component of the stem cell niche. Cell Stem Cell 2010; 7:150–161.
31. Yeo JH, Cosgriff MP, Fraser ST. Analyzing the formation, morphology, and integrity of Erythroblastic Islands. Methods Mol Biol 2018; 1698:133–152.
32. Chow A, Huggins M, Ahmed J, *et al.* CD169(+) macrophages provide a niche promoting erythropoiesis under homeostasis and stress. Nat Med 2013; 19:429–436.
33. Ramos P, Casu C, Gardenghi S, *et al.* Macrophages support pathological erythropoiesis in polycythemia vera and beta-thalassemia. Nat Med 2013; 19:437–445.
34. Danise P, Amendola G, Di Concilio R, *et al.* Nucleated red blood cells and soluble transferrin receptor in thalassemia syndromes: relationship with global and ineffective erythropoiesis. Clin Chem Lab Med 2009; 47:1539–1542.
35. Rifkind JM, Mohanty JG, Nagababu E. The pathophysiology of extracellular hemoglobin associated with enhanced oxidative reactions. Front Physiol 2014; 5:500.
36. Park SY, Matte A, Jung Y, *et al.* Pathologic angiogenesis in the bone marrow of ■■ humanized sickle cell mice is reversed by blood transfusion. Blood 2020; 135:2071–2084.
Demonstration of abnormal angiogenesis in the bone marrow of the humanized SCD mouse model and of the positive effect of transfusion in correcting the pathological phenotype.
37. Tolu SS, Wang K, Yan Z, *et al.* Characterization of hematopoiesis in sickle cell ■ disease by prospective isolation of stem and progenitor cells. Cells 2020; 9:.
Detailed characterization of HSCs in the bone marrow of SCD patients demonstrating important abnormailites of the hematopoitic niche.
38. Leonard A, Bonifacino A, Dominical VM, *et al.* Bone marrow characterization in sickle cell disease: inflammation and stress erythropoiesis lead to suboptimal CD34 recovery. Br J Haematol 2019; 186:286–299.
39. Bernaudin F, Verlhac S, Peffault de Latour R, *et al.* Association of matched sibling donor hematopoietic stem cell transplantation with transcranial Doppler velocities in children with sickle cell anemia. JAMA 2019; 321:266–276.
40. Cappelli B, Volt F, Tozatto-Maio K, *et al.* Risk factors and outcomes according to age at transplantation with an HLA-identical sibling for sickle cell disease. Haematologica 2019; 104:e543–e546.
41. Gluckman E, Cappelli B, Bernaudin F, *et al.* Sickle cell disease: an international survey of results of HLA-identical sibling hematopoietic stem cell transplantation. Blood 2017; 129:1548–1556.
42. Maier-Redelsperger M, de Montalembert M, Flahault A, *et al.* Fetal hemoglobin and F-cell responses to long-term hydroxyurea treatment in young sickle cell patients. The French Study Group on Sickle Cell Disease. Blood 1998; 91:4472–4479.
43. Sauntharajah Y, Hillery CA, Lavelle D, *et al.* Effects of 5-aza-2'-deoxycytidine on fetal hemoglobin levels, red cell adhesion, and hematopoietic differentiation in patients with sickle cell disease. Blood 2003; 102:3865–3870.
44. McArthur JG, Svenstrup N, Chen C, *et al.* A novel, highly potent and selective ■ phosphodiesterase-9 inhibitor for the treatment of sickle cell disease. Haematologica 2019.
A novel pharmacological selective inducer of fetal hemoglobin under current clinical trial.
45. Brendel C, Negre O, Rothe M, *et al.* Preclinical evaluation of a novel lentiviral vector driving lineage-specific BCL11A knockdown for sickle cell gene therapy. Mol Ther Methods Clin Dev 2020; 17:589–600.
46. Howard J, Hemmaway CJ, Telfer P, *et al.* A phase 1/2 ascending dose study and open-label extension study of voxelotor in patients with sickle cell disease. Blood 2019; 133:1865–1875.
47. Vichinsky E, Hoppe CC, Ataga KI, *et al.* A Phase 3 randomized trial of voxelotor in sickle cell disease. N Engl J Med 2019.
48. Ribeil JA, Hacein-Bey-Abina S, Payen E, *et al.* Gene therapy in a patient with sickle cell disease. N Engl J Med 2017; 376:848–855.
49. Dever DP, Bak RO, Reinisch A, *et al.* CRISPR/Cas9 beta-globin gene targeting in human haematopoietic stem cells. Nature 2016; 539:384–389.
50. Park SH, Lee CM, Dever DP, *et al.* Highly efficient editing of the beta-globin gene in patient-derived hematopoietic stem and progenitor cells to treat sickle cell disease. Nucleic Acids Res 2019; 47:7955–7972.

RESUME SUBSTANTIEL EN FRANÇAIS

La drépanocytose est une maladie héréditaire autosomique récessive, caractérisée par des épisodes douloureux de crises vaso-occlusives (CVO), une anémie hémolytique chronique et une défaillance progressive des organes. Elle est connue comme l'une des maladies monogéniques les plus courantes dans le monde (Weatherall et al., 2004). Dans cette pathologie, une mutation ponctuelle du 6ème codon du gène de la β-globine entraîne la synthèse d'une hémoglobine anormale, l'hémoglobine S (HbS), qui polymérise en condition désoxygénée, provoquant la falciformation des globules rouges (GRs) (Odièvre, Elion et al., 2011). Bien que l'anémie soit considérée comme périphérique dans la drépanocytose, nos travaux récents démontrant l'existence d'une dysérythropoïèse dans cette pathologie suggèrent une contribution centrale. Cette dysérythropoïèse est caractérisée par la mort d'une proportion importante d'érythroblastes lors de la différenciation terminale, plus spécifiquement entre les stades polychromatique et orthochromatique (El Hoss et al., 2021).

Les objectifs de ma thèse sont : 1) D'identifier les mécanismes moléculaires à l'origine de cette dysérythropoïèse dans la drépanocytose, 2) Sélectionner le protocole de culture *ex vivo* le plus adapté pour étudier la différenciation érythroïde terminale, 3) D'explorer l'impact de cette dysérythropoïèse sur le macrophage central de l'îlot érythroblastique.

La séquestration cytoplasmique de la protéine chaperonne HSP70 par les agrégats d'α-globine est associée à l'érythropoïèse inefficace ayant lieu chez les patients atteints de β-thalassémie majeure (Arlet et al., 2014). En effet, l'absence de HSP70 dans le noyau des cellules en cours de différenciation a pour conséquence la destruction de GATA-1, entraînant ainsi l'arrêt de maturation et la mort des cellules au cours de l'érythropoïèse terminale dans cette pathologie. Nous avons émis l'hypothèse qu'un mécanisme similaire pouvait également être à l'origine d'une dysérythropoïèse chez les patients drépanocytaires. Afin d'étudier cette hypothèse, nous avons effectué des expériences de différenciation érythroïde *in vitro* en utilisant des progéniteurs $CD34^+$ de patients ou de donneurs sains, cultivés en condition de normoxie ou d'hypoxie partielle (5%). Nous avons ensuite réalisé des expériences de western blot pour quantifier HSP70 dans des extraits cytoplasmiques et nucléaires de cellules aux stades de différenciation tardifs. Dans ces expériences, nous avons observé qu'il y avait moins de HSP70 dans le noyau et plus de HSP70 dans le cytoplasme des érythroblastes de patients sous hypoxie par rapport à la normoxie, ce qui n'était pas le cas dans des échantillons provenant de donneurs sains. Ces résultats indiquent que HSP70 est partiellement séquestré dans le cytoplasme des cellules de patients drépanocytaires en conditions hypoxiques.

Afin de déterminer si cette séquestration était due à une interaction anormale de HSP70 avec les polymères de HbS présents en conditions hypoxiques, nous avons réalisé des expériences de « Proximity Ligation Assay » (PLA). Ce test, basé sur des approches de microscopie, permet de détecter les interactions entre les protéines grâce à l'utilisation d'anticorps secondaires marqués par des oligonucléotides (sonde PLA) qui émettent un signal fluorescent lorsqu'ils sont à proximité l'un de l'autre (< 40 nm). Dans ces expériences, nous avons observé un faible pourcentage de cellules PLA^+ dans les cultures de donneurs sains (1-1,5%) à la fois en normoxie et en hypoxie, tandis que les cultures de patients présentaient des valeurs plus élevées sous normoxie (4,5 – 18,5%) qui étaient systématiquement et significativement augmentées sous hypoxie (9,5 – 36%). Ces résultats mettent en évidence une proximité forte entre HbS et HSP70, suggérant leur interaction dans les cellules de patients drépanocytaires, contrairement à l'hémoglobine adulte (HbA) et HSP70 dans les cellules de donneurs sains. De plus, les cellules PLA+ chez les patients avaient une intensité moyenne de fluorescence plus élevée sous hypoxie que sous normoxie, indiquant que l'hypoxie peut induire la formation de complexes HbS-HSP70 plus conséquents, ce qui pourrait expliquer la séquestration

cytoplasmique de HSP70 observée dans ces conditions. Nous avons ensuite effectué des expériences de co-immunoprécipitation à partir de GRs de patients, et observé la co-immunoprécipitation de HSP70 et de l'α-globine uniquement lorsque les GRs avaient été placés sous hypoxie, confirmant ainsi la présence de complexes formés par l'interaction des polymères de HbS et HSP70. Nos résultats mettent en évidence l'un des mécanismes moléculaires qui pourraient être à l'origine de la dysérythropoïse dans la drépanocytose, ouvrant ainsi de nouvelles perspectives dans la compréhension et le traitement de cette pathologie. Ces résultats ont fait partie d'un article publié dans Haematologica en 2021, que je signe en deuxième position, ainsi que d'une revue publiée dans Current Opinions in Hematology en 2021 que je signe en deuxième position.

Parallèlement, nous avons utilisé la cytométrie en flux pour étudier l'érythropoïèse chez des patients présentant des niveaux élevés d'érythroblastes circulants, qui sont considérés comme des marqueurs de stress médullaire. Nos observations ont révélé que les érythroblastes circulants chez ces patients se trouvaient à différents stades de différenciation terminale et reflétaient les proportions que l'on peut trouver dans la moelle osseuse. De plus, les cellules de ces patients, une fois différenciées *ex vivo*, présentaient une maturation accélérée par rapport à celles de patients drépanocytaires ne présentant pas d'érythroblastes circulants. Ces résultats soulignent la complexité et la variabilité de la différenciation érythroïde dans la drépanocytose et nécessitent une étude plus approfondie pour caractériser les mécanismes moléculaires pouvant expliquer la présence de ces cellules dans la circulation de certains patients.

Dans la deuxième partie de ma thèse, nous avons comparé deux protocoles d'érythropoïèse *ex vivo* couramment utilisés dans les laboratoires : un système de culture liquide à 2 phases (2P-LC) et un système de culture liquide à 4 phases (4P-LC). Nous avons constaté que les deux protocoles pouvaient reproduire les différentes étapes de l'érythropoïèse. Cependant, le système 4P-LC permettait une meilleure différenciation érythroïde avec un taux plus élevé de réticulocytes, le rendant plus adapté pour l'étude de la différenciation terminale. Ces résultats ont fait partie d'un article soumis dans Experimental Hematology & Oncology en 2023, que je signe en première position.

Dans la dernière partie de ma thèse, nous avons étudié l'impact de l'érythropoïèse inefficace dans la drépanocytose sur le macrophage de l'îlot érythroblastique. En effet, nos résultats suggèrent que dans la moelle osseuse des patients drépanocytaires, seulement 60 % des érythroblastes parviennent à se différencier jusqu'au stade orthochromatique, tandis que le reste des cellules entre en apoptose au stade polychromatique (El Hoss et al., 2021). Dans ce contexte, nous postulons que le macrophage central de l'IE, qui est une cellule phagocytaire et en contact direct avec les érythroblastes, pourrait être amené à phagocyter continuellement un nombre élevé d'érythroblastes apoptotiques riches en hémoglobine, et à avoir par conséquent une concentration intracellulaire très importante en fer. Cet excès de fer dans les phagosomes pourrait perturber le fonctionnement normal du macrophage central et entraîner son dysfonctionnement par un processus de mort cellulaire dépendant du fer, appelé "ferroptose". Afin d'étudier cette hypothèse, nous avons isolé des monocytes circulants du sang périphérique de donneurs sains et les avons différenciés avec de la dexaméthasone et du M-CSF pour générer des macrophages "IE-like" de type M2, exprimant les marqueurs de surface caractéristiques du macrophage central de la moelle osseuse (CD14, CD16, CD163, CD206, CD169, MerTK). Nous avons ensuite utilisé des GR comme source d'hémoglobine et montré qu'une phagocytose importante de ces cellules entraînait chez ces macrophages une mort cellulaire accrue, ainsi qu'une augmentation de la production d'espèces réactives à l'oxygène et de la peroxydation lipidique, marqueurs caractéristiques de la ferroptose. Cette mort cellulaire s'est également accompagnée d'une augmentation de l'expression de HMOX1 et SLC7A11, ainsi que d'une diminution de ACSL4, deux protéines impliquées

dans le processus de ferroptose. De plus, l'utilisation d'inhibiteurs de ferroptose, tels que la liproxtatin-1 et la ferrostatin-1, a entraîné une diminution significative du phénotype ferroptotique observé chez ces macrophages. Nous avons également montré que la phagocytose d'érythroblastes matures apoptotiques induisait un phénotype ferroptotique dans les macrophages "IE-like" qui serait lié à la présence d'hémoglobine dans ces érythroblastes, puisque la phagocytose de cellules plus précoces et sans hémoglobine, telles que des progéniteurs érythroïdes GPA-, n'avait pas d'impact sur la viabilité des macrophages. Nous avons également confirmé ces résultats en répétant ces expériences avec des cellules provenant de patients drépanocytaires.

De plus, nous avons réalisé des tests de RT-qPCR et d'ELISA, afin de caractériser le profil de libération des cytokines et la polarisation des macrophages dans le temps. A la suite de nos expérience d'érythrophagocytose, les macrophages « EI-like » présentaient une diminution des marqueurs anti-inflammatoires, tel que le CD163, CD206, et le TGF-β, avec une augmentation concomitante des marqueurs pro-inflammatoires, tels que le CD86, le CD80, le TNF-α et l'IL-6. Ces résultats suggèrent que, en plus d'induire la mort des macrophages, un excès de fer à la suite d'une érythrophagocytose accrue peut également entraîner un changement de profil inflammatoire de ces cellules. Cela pourrait entrainer la création et le maintien d'un environnement pro-inflammatoire dans la moelle osseuse qui pourrait empirer l'érythropoïèse inefficace présente chez les patients drépanocytaires.

Enfin, nous avons approfondi nos résultats par une approche *in vivo* en utilisant le modèle transgénique humanisé de souris Townes drépanocytaires. Dans ce modèle, nous avons observé une augmentation de la fluorescence de C11-BODIPY dans les macrophages de la moelle osseuse des souris SS, par rapport aux souris AS et AA. Ces résultats indiquent donc qu'il y a une augmentation de la peroxydation lipidique chez les macrophages des souris drépanocytaires, qui est une caractéristique de la ferroptose. De plus, le pourcentage de macrophage F4/80^{+}, CD169^{+}, VCAM^{+}, considérés comme étant les macrophages des îlots érythroblastiques chez les souris, étaient diminué dans la moelle des souris SS comparées aux souris AA et AS. Ces résultats préliminaires suggèrent que la niche érythropoïètique est perturbée dans la drépanocytose. De plus, nos résultats semblent indiquer que l'utilisation du modèle Townes est pertinente pour l'étude de la niche érythropoïètique dans le contexte de la drépanocytose. La caractérisation approfondie de l'érythropoïèse dans ce modèle permettra de compléter ces résultats. A l'avenir, ce modèle murin nous permettra de tester l'effet de plusieurs traitements sur l'amélioration du caractère drépanocytaire.

En conclusion, cette étude met en évidence un mécanisme contribuant à l'érythropoïèse inefficace dans la drépanocytose, tout en soulignant la grande variabilité existante entre les patients, suggérant l'implication d'autres facteurs. De plus, notre recherche met en évidence les répercussions que pourrait avoir l'érythropoïèse inefficace sur la niche érythroïde. Notamment, elle pourrait entraîner la mort des macrophages des îlots érythroblastiques et les pousser à adopter un profil pro-inflammatoire, ce qui pourrait davantage entraver l'érythropoïèse et contribuer à l'anémie dans cette pathologie.